OHIO STATE UNIVERSITY
DEC 14 1961
LIBRARY

BULLETIN
OF THE
CHEMICAL SOCIETY OF JAPAN

Vol. 34 No. 8 August 1961

CONTENTS

General and Physical

Photoreduction of Methylene Blue by Visible Light in the Aqueous Solution Containing Certain Kinds of Inorganic Salts. I. General Features of the Reaction . . . . . Y. USUI, H. OBATA and M. KOIZUMI 1049

Photoreduction of Methylene Blue by Visible Light in the Aqueous Solution Containing Certain Kinds of Inorganic Salts. II. Photobleached Product. . . . . H. OBATA 1057

A. C. Polarography of Thiamine Hydrochloride in Weakly Acidic Buffer Solutions. . K. OKAMOTO 1063

A Theoretical Treatment of Molecular Complexes. I. Silver-Aromatic Hydrocarbon Complexes . . . . . K. FUKUI, A. IMAMURA, T. YONEZAWA and C. NAGATA 1076

Infrared Spectra of Cyclohexanoxime and Cyclohexanoxime-*d*. . . . . M. KIMURA, Y. KURODA, O. YAMAMOTO and M. KUBO 1081

Dye-sensitized Photopolymerization of Vinyl Compounds. Polymerization of Acrylonitrile by Stannous Chloride and Acriflavine. I. . . . . A. WATANABE and M. KOIZUMI 1086

The Photovoltaic Behavior in Organic Compounds . . . . . H. INOKUCHI, Y. MARUYAMA and H. AKAMATU 1093

A New Quantum-mechanical Reactivity Index for Saturated Compounds . . . . . K. FUKUI, H. KATO and T. YONEZAWA 1111

Mercury Photosensitized Decomposition of Carbon Dioxide by 1849 Å (Hg 6^1P_1) . . . Y. MORI 1128

Abnormal Acceleration of the Rate of Bulk Polymerization of Styrene . . . . . N. NISHIMURA 1158

On the pd Hybridization of the Sulfur Atom in Thiothiophten. II. The Contraction of the d Orbital . . . . . K. MAEDA 1166

An Attempt to Discuss Reactivities of Excited Molecules by the Molecular Orbital Method. . . . . K. FUKUI, K. MOROKUMA and T. YONEZAWA 1178

Polarography of Narcotine-*N*-oxide. . . . . Y. ASAHI 1185

Analytical and Inorganic

Study on Metal Complexes of Analytical Importance. I. Vanadium Complexes of 8-Quinolinol and 2-Methyl-8-quinolinol . . . . . H. NAKAMURA, Y. SHIMURA and R. TSUCHIDA 1143

Organic and Biological

Studies on the Silk-platinum Catalyst. I. Its Preparation and Activity. . . . . A. AKAMATSU, Y. IZUMI and S. AKABORI 1067

Reduction of Organic Compounds with Urushibara Catalysts under High Pressure. VIII. Reduction of Acetophenone, Especially with Urushibara Nickel Catalyst Prepared by Various Modified Methods . . . . . S. TAIRA 1072

Isolation of 2,3-Cyclopenteno-5-methylpyridine from Coal Tar Bases. . . . . H. SUZUMURA 1097

Organoboron Compounds. I. On the Reaction of *n*-Butylboronic Acid with Polyvinylalcohol. . . . . S. KATO, Y. TSUZUKI and S. KITAJIMA 1107

(Continued on inside cover)

Published by the Chemical Society of Japan

THE CHEMICAL SOCIETY OF JAPAN
(NIPPON KAGAKUKAI)

Founded in 1948

Successor to the former Chemical Society of Japan founded in 1878 and to the Society of Chemical Industry, Japan founded in 1898.

OFFICERS

San-ichiro MIZUSHIMA, *President*, Director of Tokyo Research Institute Yawata Iron and Steel Co., Ltd.
Yoshikazu HACHIHAMA, *Vice-President*, Osaka University
Kenji IWAMOTO, *Vice-President*, The University of Gunma
Yonezo MORINO, *Vice-President*, The University of Tokyo
Sojiro OKA, *Vice-President*, The University of Tokyo
Hiroshi SOBUE, *Vice-President*, The University of Tokyo

BULLETIN OF THE CHEMICAL SOCIETY OF JAPAN

Editor: Tadao SHIBA, Tokyo Institute of Technology, Tokyo
Assistant Editor: Tadashi SUEHIRO, Gakushuin University, Tokyo
Editorial Board:

Yoshié BANSHO	Hidehiro GOTÔ	Keniti HIGASI
Yoshimasa HIRATA	Hiroo INOKUCHI	Tatsujiro ISHIMORI
Tadashi KAMIKUBO	Michio KOBAYASHI	Ichiro MIYAGAWA
Masazumi NAKAGAWA	Shigeru OAE	Shigeru OHASHI
Kazuo SATAKE	Syûzô SEKI	Osamu SIMAMURA
Yoshitada TOMODA	Iwao YASUMORI	Koshiro YOSHIOKA

(Continued from outside cover)

Polyterpenes. III. The Structure of Thujopsene . . . . . H. KOBAYASHI, S. NAGAHAMA and S. AKIYOSHI 1123
Kinetic Studies on Solvolysis. VI. Kinetic Evidence of the Distinct Rôle of the Hydrogen Atom of Hydroxylic Solvent Molecules as an Attacking Center at the First Ionization Stage. . . . . K. OKAMOTO and H. SHINGU 1131
Kinetic Studies on Solvolysis. VII. On the Kinetic Resolution at the First Stage of the S_N1-type Solvolysis of α-Phenethyl Chloride in Optically Active Carboxylic Acid Solvents . . . . . K. OKAMOTO, K. TAKEUCHI and H. SHINGU 1137
Studies on the Thiocarbamoylthiocarbonates. II. Synthesis and Thermal Decomposition of Aryl Thiocarbamoyltrithiocarbonates . . . . . A. KAJI 1147
Benzylideneaniline. III. Anils of Substituted Benzaldehydes . . . . . N. EBARA 1151
Studies on Organophosphorus Compounds. II. On Phosphite Cuprous Halide Complex Compounds. . . . . Y. NISHIZAWA 1170
A Novel Synthetic Route of 3,6-Dimethyl-2,3-dihydro-1*H*-cyclopent[*a*]anthracene and 6-Methyl-2,3-dihydro-1*H*-cyclopent[*a*]anthracene . . . . . M. NAKAZAKI, K. YAMAGAMI and S. ISOE 1189

Applied

Fischer-Tropsch Synthesis with Tubular Reactor of 18.11. Catalyst Bed. II. Reactor with Temperature Gradient along Out-side Wall . . . . . M. KURAISHI, M. KURITA, T. HOSOYA, H. ICHINOKAWA, K. OGAWA and H. UCHIDA 1101
Studies on the Diacylaminoanthraquinone Dyes . . . . . T. HAYASHI and R. SHIBATA 1116

Short Communications

Manganese(III) Complexes with Ethylenediaminetetraacetic Acid . . . . . Y. YOSHINO, Y. TSUNODA and A. OUCHI 1194
The Electron Spin Resonance Absorption of Vanadium Pentoxide Catalysts . . . . . K. TARAMA, S. TERANISHI, S. YOSHIDA and H. YOSHIDA 1195
Synthesis of D-Threosamine and D-Erythrosamine. . . . J. YOSHIMURA, Y. OHGO and T. SATO 1197
The Preparation of Carrier-free ^{234}Th(UX) by Anion Exchange from Nitric Acid-Alcohol Mixed Solution of Uranyl Nitrate. . . . . J. AKAISHI 1198

Photoreduction of Methylene Blue by Visible Light in the Aqueous Solution Containing Certain Kinds of Inorganic Salts. I. General Features of the Reaction

By Yoshiharu Usui, Hiroshi Obata and Masao Koizumi

(Received January 10, 1961)

In connection with the study of photoreduction of methylene blue with aliphatic amines, we did some experiments on the irreversible photodecomposition of the dye in the aerated aqueous solution[1]. It was our plan at that time to investigate systematically, varying pH of the solution, about the effect of the oxygen concentration upon the rate of this irreversible photodecomposition. But it happens that we had found the reversible photobleaching to take place with an appreciable rate in the degassed solution containing certain kinds of inorganic salts commonly used for buffering. Here "reversible" means that the dye is recovered when the air is introduced into the solution and the colorless product was confirmed to be the leuco compound of the dye. This fact which we have found seems to be of foundamental importance for the chemistry of dye in general, since the buffered solution which was found to be effective in promoting this novel photoreduction, is usually used for the dye solution. The object of this paper is to report some reults of our experiments undertaken to clarify the general nature of this extraordinary photoreduction which proceeds without any addition of particular reducing agent.

Experimental

Sample. — *Methylene Blue.* — Grübler's dye was recrystallized from *n*-butyl alcohol three times and was dried in vacuum.

$$\varepsilon_{\lambda=665\ m\mu} = 6.0 \times 10^4$$

Inorganic Reagents.—Sodium borate, sodium monohydrogen phosphate, potassium dihydrogen phosphate, sodium sulfate, sodium chloride, sodium iodide, hydrochloric acid, sodium hydroxide. All of the salts were of special grade and they were recrystallized from the redistilled water 2 or 3 times. Hydrochloric acid of special grade was distilled twice at the azeotropic point. Sodium hydroxide of special grade was used without further purification.

Apparatus and Procedure. — Degassing of the solution was performed in a suitable ampule by repeating freezing and evacuation 5~7 times. The solution then was poured into a reaction cell which is a spectrophotometer cell $1 \times 1 \times 4$ cm., connected to the evacuation apparatus via the tube fused to the upper part of the cell. The reaction was performed in a thermostat of 30 ± 0.5°C. The light source was a 500 W-75 V. projection lamp. It was used at 55.0 ± 0.5 V. and the intensity was checked by a photocell (PT 17 V 2) during the course of the reaction. At various time intervals, the cell was taken out and the absorption spectrum was measured by a Hitachi or a Kotaki spectrophotometer.

Results

1. The Irreversible Bleaching by Oxygen and the Reversible One in the Evacuated Solution. — The feature of the photobleaching of methylene blue in the borate buffer solution containing various amounts of oxygen was examined.

The composition of the solution was as follows; methylene blue 1.2×10^{-5} M, borate, 7.8×10^{-2} M, hydrochloric acid 1.4×10^{-1} M, pH = 7.62.

In case of the dye solution saturated with air, the irradiation causes a gradual decrease of the absorption spectra of methylene blue without any noticeable change of the maximum position.

When the concentration of oxygen is decreased down to 1.41×10^{-5} M, the bleaching caused by irradiation is still irreversible, the introduction of air not causing any recovery of dye. It was found that the absorption maximum shifts towards violet more and more, when the oxygen concentration is decreased.

When the solution is completely degassed, the bleaching still occurs and with a much greater rate than that of the oxygen-containing solution. However, the shift of the absorption maximum is somewhat less than in the case in which the oxygen concentration is small. The notable fact in this case is that the color appreciably recovers when the air is introduced after the irradiation. The position of the absorption maximum of the aerated solution exactly coincides with that of the partially bleached solution before aeration.

The rate of bleaching is proportional to the quantity of light absorption, that is

$$k't = -\ln(e^{acd} - 1) + \text{const.} \qquad (1)$$

1) H. Obata, K. Kogasaka and M. Koizumi, This Bulletin, **32**, 125 (1959).

except the two cases, i. e., the completely evacuated solution and the one dissolving the least amount of oxygen.

In evaluating the value of k' from Eq. 1, α-value was conventionally chosen as ε-value in order to compare the results with those of the pure aqueous solution[1], and the remaining quantity of methylene blue was obtained by use of Blaisdell's[2] method. The above equation does not hold for the two exceptional cases mentioned above, the rate in these cases decreasing more rapidly than calculated by Eq. 1. In Table I are given the values of k' and the shift of maximum absorption ($\Delta\lambda$) after 50 min. k' for the two exceptional cases were tentative as they were calculated from the initial slope of the curve drawn according to Eq. 1.

The concentration of oxygen was analyzed by a specially designed apparatus.

Table I

Concn. of O_2, M	k', min^{-1}	$\Delta\lambda$, mμ
0	(2.0×10^{-1})	5
$3.2_0 \times 10^{-5}$	(1.4×10^{-2})	9
6.76×10^{-5}	1.14×10^{-2}	8
8.58×10^{-5}	1.08×10^{-2}	5
1.13×10^{-4}	1.14×10^{-2}	3
1.53×10^{-4}	1.32×10^{-2}	3
3.40×10^{-4}	1.66×10^{-2}	0

As seen from Table I the value of k' is not affected so much by the concentration of oxygen. The results conform well with those of the pure aqueous solution, where it was found that the rate is almost constant down to about 4×10^{-5} M of oxygen whence the rate begins to decrease. The order of the k' value is also the same as that of the pure aqueous solution, in view of the difference of the light intensity[1].

2. Bleached Product of Methylene Blue in the Deaerated Solution.—In order to make clear the cause for photobleaching in the evacuated solution and the recovery of color by aeration, the absorption spectra of the solution irradiated for various times were examined from 200 to 700 mμ. Figure 1 shows the results obtained when the phosphate buffer solution of methylene blue was irradiated.

It is evident that accompanied with a decline of the main absorption of methylene blue, a new absorption appears in the ultraviolet region with the maximum at 255 mμ. Further it is observed that the change in ultraviolet region takes place with an isosbestic point at about 273 mμ. The absorption at 255 mμ coincides essentially with that of the leuco methylene blue chemically prepared, and it was almost

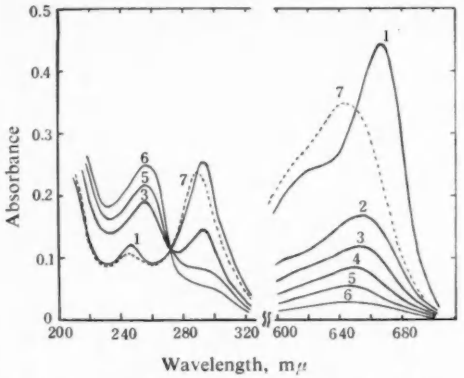

Fig. 1. The absorption spectra of the irradiated solution of methylene blue in deaerated phosphate buffer. $[Na_2HPO_4] = 1.2 \times 10^{-2}$ M, $[KH_2PO_4] = 2.8 \times 10^{-3}$ M, pH = 7.57.

1. Initial
2. 5 min.-irradiation
3. 10 min.-irradiation
4. 20 min.-irradiation
5. 50 min.-irradiation
6. 80 min.-irradiation
7. Aeration

definitely established by Obata[3] that the bleached product is nothing but the leuco form of dye which is but partially demethylated. It is to be added here that the dotted line in Fig. 1 which represents the absorption spectra of the recovered dye after aeration, has exactly the same maximum position as that of the partially bleached solution (see Sec. 6).

In connection with the formation of leuco dye, it seems to be worthy of reconfirming and studying further what Lewis[4] et al. formerly observed. Thus they perceived a slight fall of the absorption at 660 mμ with the rise of temperature ($\Delta D/\Delta T = 0.03/40°C$) in the aqueous solution of methylene blue at three different concentrations, 9.0×10^{-6}, 1.9×10^{-6}, 6.3×10^{-7} M, and they attributed this change to the formation of a colorless form according to the equilibrium; $D^+ + H_2O \rightleftarrows (DOH)H^+$. They, however, did not study about the change in the ultraviolet region. Hence we carefully examined the absorption spectra of the aqueous dye solution 6.3×10^{-7} M, at various temperatures from 20 to 75°C in the region 200 ~700 mμ, using a long path cell (10 cm.).

At first the aerated solution was examined at several temperatures, varying the temperature from low to high and then in the inverse direction. Three such independent experiments were done but no change beyond experimental

2) B. E. Blaisdell, *J. Soc. Dyers & Colorists*, **65**, 619 (1949).
3) Part II of this series.
4) G. N. Lewis et al., *J. Am. Chem. Soc.*, **65**, 1150 (1943).

error was observed. In some cases rather opposite changes were observed; thus ε_{max} increased with the rise of temperature and decreased to its original value with the fall of the temperature. This would perhaps be due to the adsorption and desorption of dye on the cell wall. Thus the aerated solution did not show any sign of the phenomenon that Lewis et al. had claimed to perceive.

Next, the three analogous experiments were performed using the evacuated solution, and this time, a small depression beyond the experimental error was observed in the visible region with the rise of temperature. In addition to this change a clear reversible change was observed in the neighborhood of 250 mμ. A typical result is shown in Fig. 2. It is seen that a new peak appears when the temperature is raised. Thus the formation of the colorless form that Lewis had postulated seems to be substantiated in the case of the degassed solution.

This colorless form might somehow be related to the formation of leuco dye, but there is no doubt that the change of spectra in the irradiated solution is not due to what Lewis et al. supposed to be, as was confirmed by Obata[3].

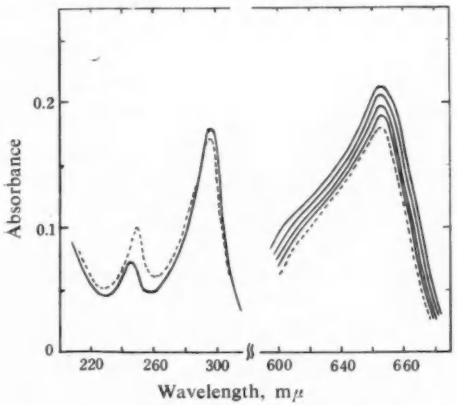

Fig. 2. Reversible temperature dependence of the absorption spectrum of methylene blue in aqueous solution degassed. (6.3×10^{-7} M)
Visible region; from upper to lower 20, 30, 40, 50 and 60°C (dotted line)
Ultraviolet region; 20, 60°C (dotted line)

3. Studies about the Solution Containing Various Kinds of Salts.—Since it has become established in Sec. 2 that methylene blue is photoreduced in the presence of certain salts, the next problem is to examine whether the similar phenomena be observed for other salts and how the rate will depend upon the type of salts, including the plain aqueous solution. The salts examined were sodium borate, sodium hydrogen phosphate, potassium dihydrogen phosphate, sodium sulfate, sodium chloride, sodium iodide, hydrochloric acid and sodium hydroxide.

The results obtained were quite similar at least qualitatively in all respects, thus in regards to the spectral change, recovery of color by aeration and the maintainance of the maximum position when recovered. But the rate depends very much upon the types of salts and a quite large difference is also observed in the magnitude of the spectral shift.

In Fig. 3 some typical cases are shown.

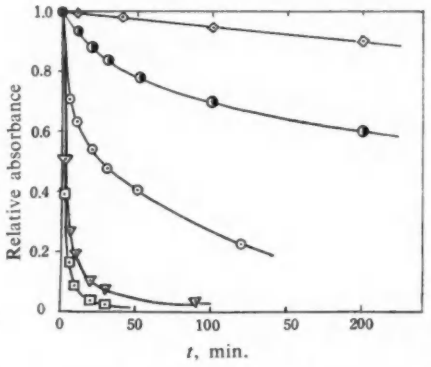

Fig. 3. Photobleaching of methylene blue in deaerated aqueous solutions containing various inorganic compounds at 30°C.

- HCl 1.0×10^{-3} M (pH=3.0)
- Na_2SO_4 1.0×10^{-2} M (pH=6.1) (NaI, NaCl and the plain aqueous solution are similar to Na_2SO_4)
- Borate buffer (pH=7.55)
- NaOH 1.0×10^{-3} M (pH=10.9)
- Phosphate buffer (pH=7.57)

In the case of phosphate buffer and sodium hydroxide the rate is far greater in the order of magnitude, next comes the borate buffer and in the case of other salts and plain aqueous solution, the rate is less than one hundredth of the first class. The rate is still slower in the case of hydrochloric acid.

Experimental results are given in Table II in which ΔD and $\Delta\lambda_{max}$ are respectively the depression and the shift of the absorption maximum per twenty minutes. As for the shift, details will be described further in Sec. 6. All these solutions are of course stable in the dark.

It is well-known that methylene blue is very weak against alkali, and for caution's sake, the spectral change of methylene blue in

Table II

Condition	D_0	ΔD	$\Delta\lambda_{max}$ mμ
Phosphate buffer soln.	0.550	0.515	17
Borate buffer soln.	0.621	0.304	2
NaOH (1×10^{-3} M) aq. soln.	0.619	0.543	8
NaI (1×10^{-2} M) aq. soln.	0.910	0.062	0
NaCl (1×10^{-2} M) aq. soln.	0.830	0.075	0
Na_2SO_4 (1×10^{-2} M) aq. soln.	0.580	0.070	0
Plain aq. soln.	0.986	0.088	1
HCl (1×10^{-3} M) aq. soln.	0.774	0.010	0

sodium hydroxide alkaline solution in the dark was examined.

In the case of 1 N solution, the absorption spectra in the visible region rapidly change into broader ones with a maximum near 590 mμ, whether the solution was degassed or not. When not deareated, this band remains constant after 41 hr. standing in the dark. But under the degassed condition the band gradually declines accompanied with a growth of a new peak at 250 mμ, and upon introduction of air it almost recovers its original height. When the concentration of sodium hydroxide is 10^{-3} N, there is no marked change observed in either aerated or deaerated solutions at room temperature. But when the temperature of the deaerated solution is raised to 60°C, a similar spectral change as in the case of 1 N sodium hydroxide (deaerated) takes place.

From the above observations it looks as if the spectral changes in the alkaline solutions are somewhat related to those in the neutral solutions caused by the temperature change. They may deserve further study but here it is enough to say that at 10^{-3} N sodium hydroxide scarcely any spectral changes occur in the dark at room temperature.

4. Scrutiny about any Possible Effect of Impurity.—In view of the rather unusual character of the present reductive reaction which proceeds without any reducing agent in the ordinary sense, it seems essential to scrutinize cautiously about the possible effect of any contaminating impurity which might act as a reducing agent, especially in cases of phosphate and borate where the rate is appreciably great. For this purpose the following experiment was performed.

Air was introduced to the nearly completely photobleached solution and the recovered dye was eliminated from the solution by adsorbing it on charcoal and filtering the solution through glass wool. Into the buffer solution thus pretreated, methylene blue was newly dissolved and the reaction was once more repeated. The rate proved to be almost the same as that of the preceeding experiment. From the above experiment any possible effect of impurity which might be contained in the buffer solution can be neglected.

Since it is very difficult to prepare a very pure sample of dye, the following special method was adopted in order to scrutinize the possible effect of any impurity contained in the dye.

According to Oster[5] the irradiation of the solution containing methylene blue, EDTA, *o*-phenanthroline and ferric salt, produces the complex between Fe^{2+} and *o*-phenanthroline and the reaction persists as long as ferric salt exists in the solution. This is because the leuco form of methylene blue produced by the photochemical reaction between EDTA and dye, reduces the ferric salt, the dye being recovered by this reaction. The similar reaction should necessarily be expected in our case since the leuco dye is produced by the irradiation. Accordingly the solution containing methylene blue, borate buffer, Fe^{3+} (6.0×10^{-4} M) and *o*-phenanthroline (2.3×10^{-3} M) was degassed and then irradiated. The result was that an absorption spectrum of Fe^{2+}-phenanthroline complex ($\lambda_{max}=510$ mμ) did appear and that the concentration of the complex produced, attained more than ten times than that of the dye. Hence it can safely be concluded that most part of the reaction is not due to any impurity contained in the dye sample. The details of this experiment will be described in Part III.

5. Search for other Reaction Products.—Since the dye is reduced to the leuco compound, it is naturally expected that some oxidizing substances be produced. Hence it was undertaken to detect hydrogen peroxide and oxygen.

After the reaction was performed using a cell with a breakable joint, the solvent was distilled in vacuum through the joint upon the mixed powder of ferric salt (12 mg.) and potassium ferricyanide (16 mg.). In case of borate buffer, the existence of hydrogen peroxide was in fact ascertained by a green tint, while in case of phosphate buffer no change was observed.

In case of phosphate buffer, a very small amount of gas collected (about 30% of the employed dye) after the irradiation was examined by a mass-spectrometer*. Oxygen was detected but it was interpreted to be due to the air since nitrogen and argon were also detected and the ratio of the three patterns practically coincided with that of the air. The

5) G. K. Oster and G. Oster, ibid., **81**, 5543 (1959).

* We are indebted to Professor T. Titani of Tokyo Metropolitan University for this analysis.

gas in question might have been due to the leak in the gas collection apparatus.

Thus according to this analysis no oxygen was detected. But this negative result does not necessarily deny the formation of oxygen. Because if oxygen be produced, there is no doubt that part of it must be consumed in the irreversible photo-decomposition of dye mentioned in Sec. 1. Moreover, when the phosphate buffer solution of dye partially bleached was kept in the dark for a long time, it recovered its color very gradually and this perhaps may be attributed to the existence of a very small quantity of oxygen produced during the irradiation.

6. Relation between the Quantity of Demethylation and That of the Produced Leuco Dye.—The shift of absorption spectra accompanied with the photobleaching can be attributed most certainly to the dimethyl amino groups[3]. Now to know the relation between these two quantities, the ratio D/D_0 (D and D_0 are respectively, the optical density of maximum absorption at time t and at $t=0$) is conventionally plotted against the position of maximum absorbance for all the results so far obtained. Figure 4 shows the plots for the phosphate buffer. In this case shift and bleaching apparently proceed in a parallel way and the position of absorption maximum in the final stage seems to tend toward the neighborhood of 640 mμ. When the absorption spectra of a partially bleached solution is divided by Blaisdell's method into two parts, i.e. the part due to the remaining methylene blue and that of other compounds, then the absorption of the latter always has its maximum near 640~645 mμ as shown in Fig. 5.

This strongly suggests that throughout irradiation or in most periods of irradiation except

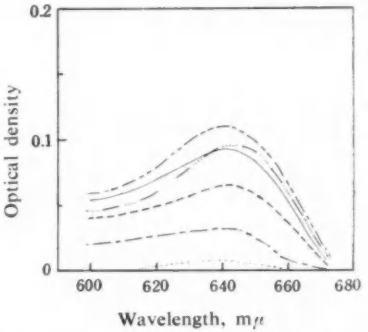

Fig. 5. The absorption spectra of the demethylated component separated by Blaisdell's treatment (in phosphate buffer pH=7.58).

	Irradiation time, min.	Opt. density remaining methylene blue at 665 mμ
a)	0	0.550
b)	1	0.278
c) ———	2	0.173
d)	4	0.090
e) - - - -	6	0.065
f) —·—	11	0.035
g) ·····	20	(0.028)

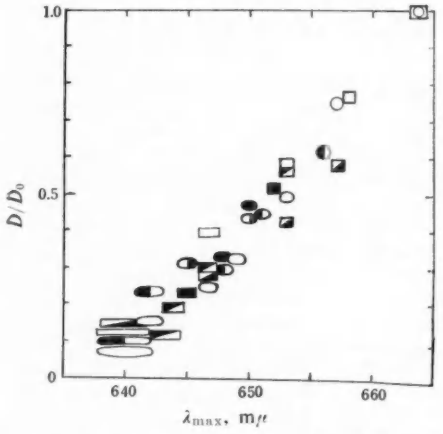

Fig. 4. Plot of D/D_0 against λ_{max} for the various conditions in phosphate buffer.

●	[Dye] 4×10^{-6} M	■	pH=8.81
◑	8×10^{-6}	◩	8.07
◐	1.2×10^{-5}	◪	7.71
○	1.6×10^{-5}	□	6.94

all pH=constant all [Dye]=constant

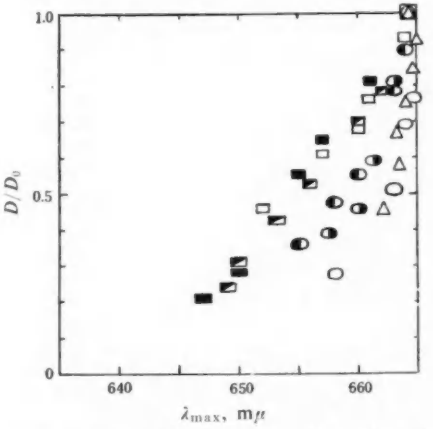

Fig. 6. Plot of D/D_0 against λ_{max} for the various conditions in borate buffer.

●	[Dye] 4×10^{-6} M	■	pH=9.14
◑	8×10^{-6}	◩	8.30
◐	1.2×10^{-5}	□	7.85
○	1.6×10^{-5}		

all pH=constant all [Dye]=constant

the last stage, a single molecular species is predominantly formed as a result of demethylation. In case of other salts, the relation between bleaching and shift is somewhat different from that of the phosphate buffer, as shown in Fig. 6.

There are many cases in which demethylation is appreciably delayed than bleaching. In case of borate buffer, demethylation seems to be accelerated by the increase of pH. Summarizing all the results, demethylation apparently takes place with a rate about equal to bleaching at most, or with a much smaller rate. But in all cases the band maximum of demethylated compound lies near 640~650 mμ as in the case of phosphate buffer, suggesting again the formation of a single molecular species through demethylation. An example of borate buffer is shown in Fig. 7.

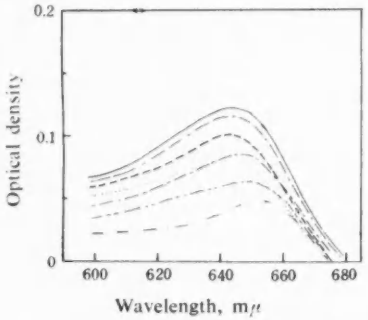

Fig. 7. The absorption spectra of the demetylated component separated by Blaisdell's treatment (in borate buffer pH 8.30).

	Irradiation time, min.	Opt. density remaining methylene blue at 665 mμ
a)	0	0.563
b)	4	0.472
c) ------	10	0.409
d) ------	20	0.340
e) ------	50	0.209
f)	80	0.153
g) ------	152	0.093
h)	212	0.078

Now correct data for the absorption maximum of mono-, di-*N*, *N'*-, di-*N*, *N*- and trimethylthionine can not be found in the literature, so that the number of demethylation can not be decided from Figs. 5 and 7, though the latter two seem rather plausible.

Suspecting the possibility that a small amount of hydrogen peroxide produced might cause demethylation to occur, the effect of the addition of hydrogen peroxide was examined. Such an investigation is also desirable from the standpoint of examining the effect of the reaction product upon the entire reaction.

The experiment was done using the aqueous solution of methylene blue and the intensity of the illuminating light was chosen so great that about 90% bleaching took place in about 10 hr. Plots of D/D_0 against λ_{max} are given in Fig. 8.

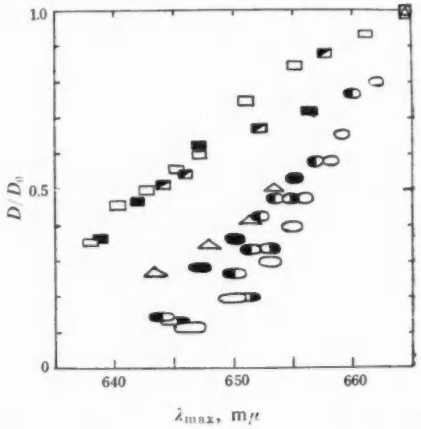

Fig. 8. Plot D/D_0 against λ_{max} for the various concentrations of H_2O_2 in plain aqueous solution.

- ◩ 5.15×10^{-4} M
- ■ 1.03×10^{-4} M
- □ 1.03×10^{-4} M
- ● 7.20×10^{-5} M
- △ 3.09×10^{-5} M
- ◐ 2.58×10^{-5} M
- ◑ 2.06×10^{-5} M
- ○ 0

It is evident that demethylation is much accelerated when the added hydrogen peroxide exceeds 7.22×10^{-5} M. But when the concentration of hydrogen peroxide is 3.9×10^{-5} M or 2.5×10^{-5} M, there is no noticeable effect observed. Accordingly, it is clear that demethylation occurring without added hydrogen peroxide is not due to hydrogen peroxide produced during the reaction. In the presence of a large quantity of hydrogen peroxide irreversible photodecomposition becomes marked and at 5.15×10^{-4} M of the added hydrogen peroxide, the reaction consists only of the irreversible photodecomposition. But the contribution of such an irreversible decomposition is negligible when the concentration of hydrogen peroxide is $\sim10^{-5}$ M.

Of course, it was ascertained that the addition of hydrogen preoxide in the above order of magnitude does not cause any dark reaction. In connection with the above experiments, the effect of the addition of pyruvate was examined and it was found that the recovery of dye exceeds 85~90% of the original dye (measured by D/D_0) when it is added, as against 80% when it is not added.

Discussion

The present reaction as a whole is very complicated and as to the dye, there occur simultaneously three types of reaction; demethylation, formation of leuco compound and the irreversible decomposition. The magnitude of the dye decomposed irreversibly is estimated at most to be about 20~30% of the entire dye disappearing (irreversible decomposition plus leuco formation), but the correct value can not be obtained since the extinction coefficient of the demethylated compound is unknown.

The fact that the magnitude of recovered dye when pyruvate is added to the plain aqueous solution (in this case no shift occurs) reaches about 90%, strongly supports the view that the greater part of the irreversible decomposition is due to some oxidative substance produced during the photoreduction. At the present stage it is not certain whether and how much the irreversible decomposition is essentially connected with the formation of leuco compound but 10% or less would be plausible from the above data.

As for the relation between demethylation and leuco formation, the following conclusions can be drawn from the experimental results. Thus the two reactions are not directly interrelated with each other but rather take place seemingly at least, as two independent simultaneous reactions; because the addition of pyruvate can almost completely suppress demethylation without essentially affecting the rate of leuco formation.

From the absorption spectra of the oxidized form of demethylated dye, the number of demethylation is perhaps one or two. The spectrum as seen in Figs. 5 and 7, rises at first and reaches a maximum when the optical density of the remaining methylene blue falls near one third of the original value and then declines gradually. The absorption spectra of the solutions which have been partially photobleached and then recolored by the introduction of air, have almost the same maximum position as that of the solution before aeration. The latter fact indicates that the ratio between methylene blue and demethylated dye in the oxidized form is quite similar to that in the reduced form. This conforms well with the fact that oxidation potential of the demethylated compound is almost the same as that of methylene blue[6]. The variation of the concentration of the oxidized form of demethylated dye, as judged from its absorption spectra, can well be interpreted, if one assumes that an equilibrium is rapidly attained between the oxidized and reduced form of methylene blue and the corresponding forms of the demethylated dye. If one further assumes that demethylation and leuco-formation have about the same rate (this situation perhaps corresponds to the case of phosphate buffer approximately) then the concentration of the oxidized form of demethylated dye will simply be given as follows.

Putting the mole fractions of the oxidized and reduced form of methylene blue as y_1 and x_1 respectively and the corresponding quantity for the demethylated dye as y_2 and x_2, then the total mole fraction of reduced form is $x = x_1+x_2$, and the total mole fraction of demethylated dye is x_2+y_2. From the assumption, $x_2+y_2=x_1+x_2$ or $y_2=x_1$.

If one assumes, to simplify the matter, that there is no irreversible decomposition, then $x_1+x_2+y_1+y_2=1$.

Since the percentage of the demethylated compound is the same in oxidized and reduced form, the following formula can easily be obtained, utilizing the above relations.

$$x_1/y_1=y_2/y_1=x_2/y_2=(1-y_1-y_2)/(y_1+y_2) \quad (2)$$

Hence

$$y_2=-y_1+\sqrt{y_1}$$

From the following figures calculated by Eq. 2 one can see how the changes in y_1 and y_2 are related with each other.

y_1	0.81	0.49	0.25	0.16	0.09	0.04	0.01
y_2	0.09	0.21	0.25	0.24	0.21	0.16	0.09

For the sake of completeness, the numerical figures will be given below when the rate of demethylation is 0.7 and 0.5 times that of bleaching, i.e. $x_2+y_2=0.7(x_1+x_2)$ and $x_2+y_2=0.5(x_1+x_2)$.

$x_2+y_2=0.5(x_1+x_2)$

y_1	0.8	0.6	0.5	0.4	0.3	0.2	0.1	0.04
y_2	0.06	0.104	0.118	0.125	0.122	0.106	0.070	0.034

$x_2+y_2=0.7(x_1+x_2)$

y_1	0.8	0.6	0.5	0.4	0.3	0.2	0.1	0.04
y_2	0.076	0.135	0.157	0.172	0.174	0.162	0.12	0.10

The real situation is that the irreversible decomposition always takes place more or less, but it is evident from the above data that the changes of absorption spectra of methylene blue and the demethylated dye in most cases (Figs. 5 and 7) correspond to the case that demethylation has roughly the same rate as that of bleaching.

The result that a small quantity of dissolved oxygen increases the degree of demethylation,

6) L. Rapkin, A. P. Struky and R. Wurmser, *J. Chim. Phys.*, **76**, 340 (1926); See also Part II of this series.

can be accounted for as due to the repeated reoxidation of leuco dye, since this process retards the leuco-formation, increasing the relative magnitude of demethylation.

In some cases demethylation is found to proceed noticeably at a later stage and this strongly suggests, as already mentioned, that the reduced dye is more susceptible to demethylation. Thus it is plausible that demethylation and bleaching are in this sense related with each other although they are in fact independent simultaneous reactions.

A brief structural discussion will be added at the end.

Since demethylation is related with the amino group of a side chain while the formation of leuco dye is connected with the ring nitrogen, it is natural that the two reactions take place independently. In general demethylation is considered to take place oxidatively so that it is plausible in the present case that the (transient) removal of the lone pair electrons participates in the course of demethylation. This view seems to account for the difference of salts in suppressing demethylation. Thus according to the results so far obtained less demethylation seems to occur in the presence of SO_4^{2-}, Cl^-, I^-, OH^- when compared with borate and phosphate, and this might be due to the attachment of such simple anions to the amino group which hinders the removal of lone pair electrons. The anticipation that the leuco form is more susceptible to demethylation is compatible with the above view, since the leuco dye is electroneutral and can not combine with an anion. This might be the reason why demethylation becomes more pronounced at a later stage.

As for the formation of leuco dye, it is most plausible to consider that the primary process for the reaction consists in the acceptance of an electron by the excited dye, but it is not known at the present stage what kind of molecular species acts as an electron donor. It is conceivable that the amino group of the dye molecule plays this role, but there seems to be another possibility that hydroxide ion loosely attached to or existing in the neighborhood of ring nitrogen behaves as an electron donor. The latter possibility might be supported by the existence of a colorless form $(DOH)H^+$ which Lewis first postulated and which the present paper further supports.

At any rate there is scarcely any doubt that the ultimate fission of water by the visible light is taking place in this case. Such a possibility was formerly considered as a very unlikely event from the standpoint[7] of energy, but recently experimental evidence for such a process to occur, seems to be rather strengthened[8]; the present result, we believe, demonstrates unequivocally that it can really occur though the mechanism is still entirely unknown and is to be solved in future.

Summary

It was discovered that the irradiation of the aqueous solution of methylene blue containing various kinds of salts, produces the leuco form of dye; accompanied with this reaction, irreversible photodecomposition of dye and demethylation occurs to some extent. Hydroxide, phosphate and borate were found to be most effective in promoting this photoreduction. Careful studies were performed to counteract the possible effect of impurity. Since the present reaction was considered most certainly to be due to the ultimate fission of water, the analysis for Oxygen and hydrogen peroxide was undertaken. The former was not detected by means of a mass-spectrograph in case of phosphate, but the latter was chemically detected in case of borate buffer. The connection between the quantity of demethylation and that of the formation of leuco dye was investigated and clarified to some extent.

Department of Chemistry
Faculty of Science
Tohoku University
Katahira-cho, Sendai

7) E. I. Rabinowitch, "Photosynthesis and Related Process", Vol. I, New York (1945), p. 78.

8) I. Fridovich and P. Handler, *J. Biol. Chem.*, 235, 1835 (1960); W. J. Nickerson and G. Strauss, *J. Am. Chem. Soc.*, **82**, 5008 (1960).

Photoreduction of Methylene Blue by Visible Light in the Aqueous Solution Containing Certain Kinds of Inorganic Salts. II. Photobleached Product

By Hiroshi OBATA

(Received January 10, 1961)

Koizumi, Usui and the present author have discovered[1] that the deaerated aqueous solution of methylene blue undergoes photobleaching by visible light, and they have clarified the general features of the phenomenon. The bleached solution has a well-defined absorption spectra with a new peak at 256 mμ and the color is recovered when air is introduced into the solution. It was further established that the absorption peak of the remaining oxidized form gradually shifts accompanied with the bleaching reaction. Also the recovered dye has its maximum at about 640 mμ, which is essentially the same as the ultimate position of the remaining oxidized form before aeration.

As regards the photobleaching it seems most probable to attribute it to the formation of leuco dye, but if so, one has perhaps to assume the ultimate fission of water by visible light, which occurs with great difficulty for the energetic reason. If the photobleached product be some substance other than the leuco dye, this difficulty may be avoided. In connection with such a possibility it seems necessary to pay some attention to Lewis' suggestion[2] that a certain colorless form of methylene blue with the structure $(Mb^+\cdots OH^-)H^+$ (OH^- is attached to ring nitrogen) exists in the aqueous solution. In case the photobleached product be such a substance or some others related with it instead of the leuco dye, then its chemical behavior would be expected to be quite different from that of the chemically prepared leuco dye which is believed to be MbH.

Secondly, as to the cause for the shift of the absorption maximum, Yoshida's work seems to be noteworthy[3]. He concludes that in the alcoholic solution methylene blue is demethylated by exposure to the visible light accompanied with the photoreduction. It seems natural to expect that the same reaction occurs in the aqueous solution, but as another possibility, the photo-hydrolysis of the dimethylamino group cannot be neglected a priori since it is well-known that in the alkaline aqueous solution, methylene blue is converted into methylene violet[4].

The present paper concerns the elucidation of the above two problems, and the investigation consists mainly of the comparison between the chemically prepared leuco dye and the photobleached product from the following three standpoints.

1) Comparison of the absorption spectra of the photobleached product with those of leucomethylene blue, benzoylleucomethylene blue and acetylleucomethylene blue. The latter two substances are considered to have a structure related with MbOH.

2) Comparison of the oxidative and reductive behavior of the photobleached product with that of leucomethylene blue.

3) Comparison of the pH dependence of the absorption spectrum of the photobleached product and that of leucomethylene blue.

The results lead to the conclusion that the photobleached product is most certainly a leuco dye partially demethylated.

Experimental

Materials.—*Methylene Blue.*—Grübler's reagent was recrystallized twice from water and then once more from butanol. The molar extinction coefficient was 62000. Most experiments were done with the solution of 2×10^{-5} mol./l.

Leucomethylene Blue.—The deaerated solution of methylene blue was reduced to the leuco form by warming the solution to about 60 C with a small amount of zinc powder. The maximum of the absorption spectrum of this solution is 256 mμ and the value agrees with that of the solution reduced by sodium hydrosulfite or hydrogen with palladium asbestos. This result ensures that the solution reduced by adding zinc powder is leucomethylene blue. The solution reduced by passing hydrogen in the presence of palladium asbestos was used for a few experiments.

Benzoylleucomethylene Blue and Acetylleucomethylene Blue[5].—*Leucomethylene Blue.*—A solution of 25 g. of methylene blue in 500 ml. of water was heated almost to boiling, 25 g. of zinc powder was

1) Y. Usui, H. Obata and M. Koizumi, This Bulletin, **34**, 1049 (1961).
2) G. N. Lewis, O. Goldschmid, T. T. Magel and J. Bigeleisen, *J. Am. Chem. Soc.*, **65**, 1150 (1943).
3) Z. Yoshida and S. Kazama, *J. Chem. Soc. Japan, Ind. Chem. Sec.* (*Kogyo Kagaku Zasshi*), **59**, 1418 (1956).
4) A. Bernthsen, *Ann.*, **230**, 211 (1885).
5) G. Cohn, *Ber.*, **33**, 1567 (1900); L. Chalkley, *J. Am. Chem. Soc.*, **47**, 2057 (1925).

added and then, during vigorous stirring, 70 ml. of pure concentrated hydrochloric acid was added as quickly as possible. After a few minutes, the color of this solution changed to pale greenish yellow. The filtrate was allowed to stand in the nitrogen atmosphere overnight; it was then cooled in an ice-bath and filtered. The precipitate obtained was well dried in a vacum desiccator. This precipitate was greenish and stable in the air for several days; yield 30 g.

Benzoylation.—The 4.5 g. of dry zinc salt obtained was dissolved in 9 ml. of dry pyridine, previously deoxygenated by flashing with nitrogen gas, and the solution was treated with 5 ml. of benzoyl chloride, heated for one hour in the nitrogen gas, and then allowed to stand overnight. The reaction mixture was poured into a large volume of cold water, the tarry substance that separated off was washed with 10% sodium carbonate solution and with water until it became a white powder, and then it was extracted with 10% hydrochloric acid. The acidic solution was made alkaline with aqueous ammonia and the white precipitate was collected and dried. The dried substance was recrystallized twice from alcohol. The crystalline substance obtained was pale yellow and melted at 190.5~192°C. The molar extinction coefficient was 55000.

Acetylation.—Acetylation was done with acetic anhydride by the same method as benzoylation. The melting point was 180.3~180.5°C, pale green. The molar extinction coefficient was 51000.

$K_3Fe(CN)_6$, $K_4Fe(CN)_6$ —G. R reagents were recrystalized from water three times.

$SnCl_4 \cdot 5H_2O$, $SnCl_2 \cdot 2H_2O$—G. R. reagents were used without further purification.

Apparatus for Photobleaching and Procedures.—Figure 1 shows the main part of the apparatus for bleaching the aqueous solution of methylene blue. As a light source, two tungsten lamps for spot light (500 W) were employed and the range of wavelength was chosen by means of a filter (Mazda VR2) and any shorter wavelength than 600 mμ was cut off completely. The reaction cell was a glass rectangular type for Beckman spectrophotometer and could be degassed. Absorption spectra were measured by a Kotaki or Hitachi spectrophotometer according to the visible or ultraviolet region. The photobleaching reaction of methylene blue was carried out in the aqueous solution without any buffered reagents at 30°C.

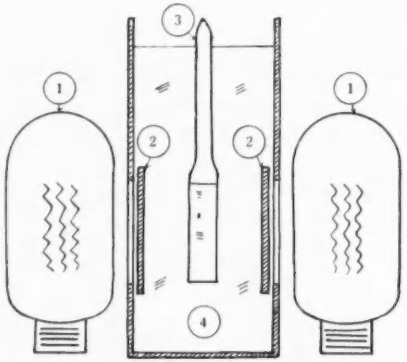

Fig. 1. Apparatus for photobleaching.
① Tungstene lamp for spot light (500 W)
② Filter
③ Reaction cell
④ Thermostatt

Results

Photobleaching of Aqueous Methylene Blue Solution in Vacuo.—It required more than ten hours for the aqueous methylene blue solution to be bleached in vacuo. After the irradiation of 10 hr., there remained about ten per cent of the oxidized form and the wavelength of absorption maximum (667 mμ) moved to about 640~650 mμ. Further, when the bleached solution was exposed to the air, the solution regained the blue color and the position of the absorption peak was practically the same as in the case of the above value. The optical density of the recolorized solution was about 70 per cent that of the original methylene blue solution. Thus the general features of the spectral change is quite similar to that in the case of the buffered solution[1].

Comparison of the Absorption Spectra of the Photobleached Product with Those of the Related Compounds.—If there should exist any difference in the absorption spectra of leucomethylene blue (DH) and those of DOH, the photobleached product would easily be identified spectroscopically. But the fact is that nothing has been reported about DOH, except Lewis' proposal so far as the author knows and still less about its absorption spectra. For the purpose of getting knowledge about the absorption spectra of DOH, those of the synthesized benzoylleucomethylene blue and acetylleucomethylene blue were measured.

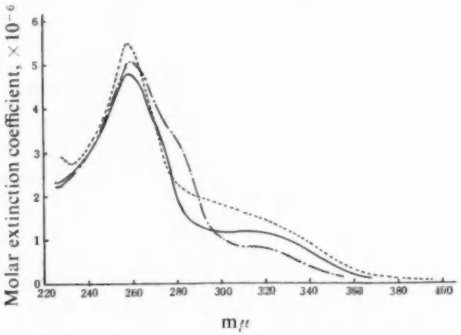

Fig. 2. Absorption spectra of leucomethylene blue and its derivatives.
——— Leucomethylene blue
– – – – Benzoylleucomethylene blue
—·— Acetylleucomethylene blue

These were fairly stable in the aerated condition and were expected to have the absorption band similar to that of DOH, because they are closely related with DOH in structure. The absorption spectra of benzoylleucomethylene blue and acetylleucomethylene blue were compared with that of leucomethylene blue in alcoholic solution. Figure 2 shows the absorption spectra of these three substances. They are similar in shape and the wavelengths of the maxima agree fairly completely. These results suggest that the absorption bands of DH and DOH resemble each other, hence one can not decide spectroscopically whether the photobleached product be DH or DOH.

Comparison of the Oxidative and Reductive Behavior between Photobleached Product and Leucomethylene Blue.—The reactivity of the photobleached product was compared with that of leucomethylene blue. The outline of the principle for this comparison is as follows. Two solutions containing respectively about equal amounts of leucomethylene blue and the photobleached product are added in vacuo, each to the same amount of solution containing a definite quantity of a suitable oxidation reduction system. Then the quantity of dye which has been oxidized is determined spectroscopically. The comparison of the ratio of the colored and colorless species in the equilibrium state for the two cases would be useful for the identification of the photobleached product. The reagents chosen are (1) $K_3Fe(CN)_6$–$K_4Fe(CN)_6$ system, (2) $SnCl_4$–$SnCl_2$ system and (3) thionine-leucothionine system.

(1) *The Reaction with $Fe(CN)_6^{3-}$—$Fe(CN)_6^{4-}$ System.*—The mixture of $K_3Fe(CN)_6$ and $K_4Fe(CN)_6$, each 1.6×10^{-5} mol., was added in vacuo to 7 ml. of the solution containing the dye system (leucomethylene blue or the photobleached product). The calculated concentration of $K_3Fe(CN)_6$ and $K_4Fe(CN)_6$ in the solution thus prepared, being 2.3×10^{-3} mol./l., was about 100 times that of the dye-system. As expected from the values of E_0' at pH 7 (0.43 V. for $Fe(CN)_6^{3-}$–$Fe(CN)_6^{4-}$, 0.011 V. for methylene blue-leucomethylene blue)[6] the addition of $K_3Fe(CN)_6$–$K_4Fe(CN)_6$ system to the solution of methylene blue rapidly produced a blue color of the oxidized dye; but the solution gradually changed its color and turned to a green tint after a few minutes. As to the photobleached solution, a change quite similar to that above was observed.

6) M. Clark, "Oxidation Reduction Potential in Organic System", Williams & Wilkins Co., Balimore (1960), p. 132; L. F. Hewitt, "Oxidation-Reduction Potential in Bacteriology and Biochemistry", 6th Ed., Livingstone Ltd., Edinburgh (1950), p. 21.

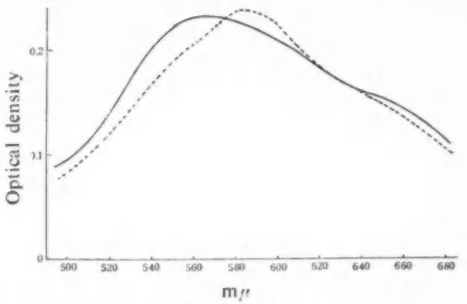

Fig. 3. Absorption spectra of the complex with $K_3Fe(CN)_6$.
—— Oxidized form of the photobleached product
---- Oxidized form of leucomethylene blue

In Fig. 3 the absorption spectra of these two solutions are shown and in addition, that of the aqueous methylene blue solution containing $K_3Fe(CN)_6$. A large shift of λ_{max} of methylene blue suggests the formation of a certain complex between the dye and $K_3Fe(CN)_6$. A further shift for the photobleached product, ca. 15 mμ corresponds, without doubt, to that of the component dye.

(2) *The Reaction with Sn^{4+}—Sn^{2+} System.*—In this case a more quantitative comparison can be done. Thus when a large quantity of the solution containing $SnCl_4$ and $SnCl_2$, 1:1 in mole ratio, is added to the solution of the reduced dye, the latter will be oxidized to such an extent that its potential attains the value of Sn^{4+}-Sn^{2+} system, which on account of its great excess, maintains practically its original value. The concentration of oxidized form (X_o) and that of reduced form (X_r) of dye in the equilibrium state can easily be obtained spectroscopically by measuring the optical density of the above solutions in both deaerated and aerated conditions, the former providing the value of X_o and the latter X_o+X_r. In this way the value of X_o/X_r in two cases, leucomethylene blue and the photobleached product can be compared at a constant oxidation reduction potential determined by Sn^{4+}/Sn^{2+} ratio.

In practice the experiment was done as follows. The stock solutions of stannic chloride and stannous chloride both in 1 N hydro chloric acid were neutralized by sodium acetate to adjust the pH value to 5. Two milliliters of 1:1 stannic chloride-stannous chloride solution was added to 5 ml. of reduced dye solution, the concentration of stannic chloride and stannous chloride having been suitably selected to make their ultimate concentration 0.02 mol./l. Upon mixing, the blue color immediately

appeared and its optical density was measured at 660 and 645 mμ respectively for the case of leucomethylene blue and the photobleached dye. Aerating the system the optical density was measured once more at the above wavelengths. Typical results are shown in Table I.

TABLE I. OPTICAL DENSITY OF LEUCOMETHYLENE BLUE AND THE PHOTOBLEACHED PRODUCT AFTER ADDING $SnCl_4$-$SuCl_2$ SYSTEM

	Leucomethylene blue	Photobleached product
Deaerated state	0.201	0.286
Aerated state	0.352	0.380
X_o/X_r	1.331	3.04

E_o' value of the photobleached product may be evaluated in the following way. The oxidation-reduction potential of the solution which is practically decided by the Sn^{4+}/Sn^{2+} ratio is expressed as follows.

$$E_h = E'_{oSn} + \frac{RT}{2F} \ln \frac{[Sn^{4+}]}{[Sn^{2+}]}$$

$$= E'_{oMb} + \frac{RT}{2F} \ln \frac{X_{oMb}}{X_{rMb}}$$

$$E'_{oph} + \frac{RT}{2F} \ln \frac{X_{oph}}{X_{rph}}$$

where E'_{oSn}, E'_{oMb} and E'_{oph} are respectively the midpoint potential (the potential when the concentration of oxidant and reductant is the same) of Sn^{4+}/Sn^{2+}, methylene blue, and the photobleached system at pH 5. Using the value of E'_{oMb} (0.101 V.)[6] in the literature and the value of X_{oMb}/X_{rMb} in Table I, one can determine the E_h value, which was found to be 0.1048 V. Since E_h has the same value for the photobleached system, one can easily get E'_{oph} from X_{oph}/X_{rph}. The value obtained is 0.090 V. which is close to the value of methylene blue.

(3) *The Reaction with Thionine-Leucothionine System.*—E_o' of thionine is only a little higher than that of methylene blue and the light absorption by thionine is almost negligible in the concentration 10^{-5}~10^{-6} mol./l. at a wavelength of the absorption maximum of methylene blue. But, if the concentration of the thionine solution was chosen above 10^{-3} mol./l. in order to keep the value of E_h approximately constant after mixing, then the absorption of thionine at 665 mμ would become so great that it would prevent a simple spectroscopic analysis of the methylene blue system. Moreover it is troublesome to prepare a solution containing a definite amount of thionine and leucothionine and to add it to the solution to be tested in vacuo. For this reason the analogous experiment as in the case of Sn^{4+}-Sn^{2+} system was not undertaken in this case and the following procedure was adopted. A suitable amount of thionine solution ~10^{-6} mol./l. in concentration is added to the solution to be examined in order to oxidize about a half of the existent leuco form. In case of leucomethylene blue, the concentration of oxidized form produced by the addition of thionine can easily be obtained spectroscopically. The total sum of oxidized and reduced form is also determined by measuring the optical density of the solution after aeration. From these two values the concentration of the oxidized and reduced forms of methylene blue as well as thionine in the equilibrium can easily be calculated. The use of E_o' value of thionine[6] (0.068 V. at pH 6.8) enables one to decide the E_o' value of methylene blue and vice versa. After having checked the above method by leucomethylene blue, it was applied to the photobleached product in order to estimate its E_o' value. But in this case the exact value for the concentration of oxidized and reduced form can not be decided spectroscopically because of the lack of the molar absorbancy. As an approximation the value of the molar extinction coefficient of methylene blue at 665 mμ was provisionally used.

To illustrate by an example, the absorption spectra when 3 ml. of thionine solution was added to the solution of 5 ml. of photobleached product are shown in Fig. 4. Curves ② and

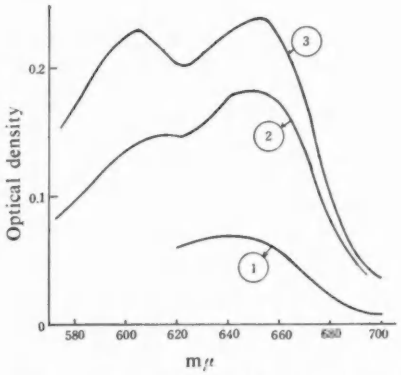

Fig. 4. Absorption spectra of the photobleached product when thionine solution added.

③ refer respectively to the deaerated and aerated solution and ① is the absorption spectrum due to the remaining oxidized form in the original photobleached solution (after having been corrected for dilution). From these data the concentration of each species in the equilibrium state was calculated and shown in Table II.

Table II. Concentration in the equilibrium state between thionine and the photobleached product

	Oxidized form	Reduced form	E_h
Thionine	0.08×10^{-6}	2.04×10^{-6}	0.0257
Photobleached product	3.64×10^{-6}	1.10×10^{-6}	

(The oxidized form remaining in the original photobleached solution: 1.6×10^{-6} mol./l.)

From the data in Table II E_0' of the photobleached product was calculated to be 0.0101 V. Two other similar experiments gave the values, 0.0090 and −0.0122 V. The average is 0.0023 V. It is to be added that when 10% less value is used for the extinction coefficient of the photobleached product, E_0' value in the above case varies from 0.0101 to 0.028 V.; thus the value itself is not so exact, but it is certain that it is close to that of methylene blue.

Comparison of the pH Dependence of the Absorption Spectra between Methylene Blue and the Photobleached Product.—Leucomethylene blue ionizes in two steps at pH 4.5 and 5.9, that is, there are three species of leucomethylene blue in respective pH regions as shown below.

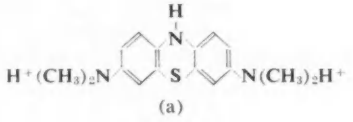

(a)

pH<4.5

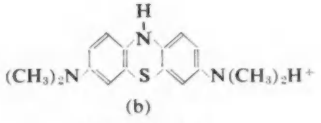

(b)

4.5<pH<5.9

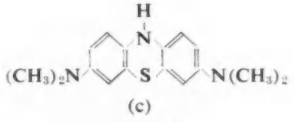

(c)

pH>5.9

Accordingly, the absorption spectra of leucomethylene blue in three pH regions may be different from each other. This was examined and the analogous experiment was done also for the photobleached product. Five milliliters of the solution of leucomethylene blue or the photobleached product was poured into 2 ml. of the acetate buffer solution in vacuo. The pH values chosen were 3.54, 4.02, 5.00, 6.62 and 8.25 each successively corresponding to the region where the species a, a, b, c, and c are predominant.

One could find, however, no differences between methylene blue and the photobleached product both in shape and in the position of the maximum wavelength at all pH values, the latter always being at 256 mμ. But some difference was found in the molar extinction coefficient at 256 mμ, with the highest value at pH 5 and decreasing both in larger and smaller pH regions. The results are shown in Table III and Fig. 5. In Table III the optical

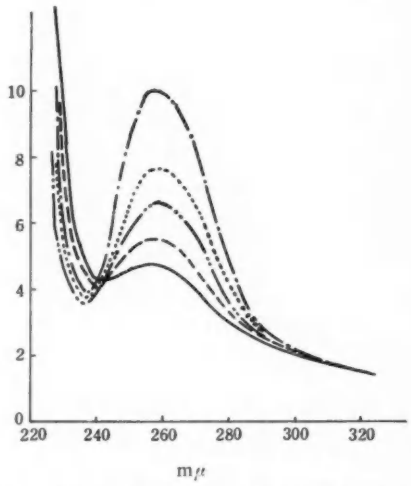

Fig. 5. Absorption spectra of the photobleached product in respective pH value.
(Absorption bands in shorter wavelength than 240 mμ are caused by acetic acid.)

——— pH 3.54 ····· pH 6.62
– – – pH 4.02 —·—· pH 8.62
—·— pH 5.50

density of the leuco form at the maximum absorption (256 mμ) (denoted as B), that of the oxidized form produced by aeration of the respective solution of leuco form (at 665 mμ for methylene blue and 645 mμ for the photobleached product) (denoted as A), and the ratio B/A are tabulated. The value of B/A or its relative value standardized to that at pH 5 would be a measure of the molar extinction coefficient at 256 mμ of leuco dye, because the absorption spectrum of methylene blue is essentially the same in the above pH region and the same would perhaps apply to the photobleached product.

In evaluating the data in Table III it must be noted that a certain correction was made for a small amount of coexisting oxidized form in the solution of leuco dye, by making use

TABLE III. OPTICAL DENSITIES IN VARIOUS pH VALUES

		pH				
		3.54	4.02	5.00	6.62	8.25
Photobleached product	A	0.442	0.335	0.186	0.380	0.372
	B	0.610	0.561	0.405	0.463	0.384
	B/A	1.447	1.675	2.18	1.22	1.033
	Relative value	0.663	0.768	1	0.559	0.474
Leucomethylene blue	A	0.340	0.243	0.230	0.160	0.164
	B	0.284	0.367	0.254	0.168	0.161
	B/A	0.836	0.992	1.045	0.730	0.636
	Relative value	0.798	0.947	1	0.698	0.606

of the fact that the ratio of the optical density at 256 mμ to that of 665 mμ or 645 mμ, as the case may be, in the oxidized form is approximately 1 : 3.

From the above results it is certain that as regards the pH dependence of the absorption spectrum there is no marked difference between leucomethylene blue and the photobleached product.

Discussion

From the results obtained in the present paper which demonstrate clearly the marked resemblance between the photobleached product and leucomethylene blue both in oxidative and reductive behavior as well as acid base character, there scarcely remains any doubt that the photobleached product is a leuco form dye. Lewis' colorless species $(DOH)H^+$ [2], for which the oxidative and reductive behavior as observed would never be expected, can safely be rejected as a photoproduct. But here another conceivable substance which is speculative but somewhat fascinating will be mentioned in connection with this colorless form. This is a compound supposed to be formed, should OH^- be photochemically split into H^- and O (I). It may happen that this is oxidized to II by aeration. If such a compound as I were

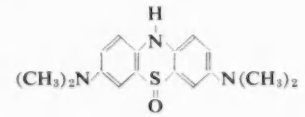

(I)

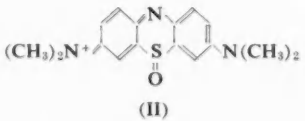

(II)

formed, there might be a possibility that the photofission becomes more feasible and that such a reaction is accompanied by the product of neither oxygen nor hydrogen peroxide. Although there are no such substances cited in the literature, but some *S*-oxides are really known in the derivatives of phenthiazines, which are hypsochromic than their mother compounds, for example, such compounds as 2, 7 - dinitrophenthiazine - *S* - oxide[7] (yellow against dark brown of 2, 7-dinitrophenthiazine) and benzothiazino tropone-*S*-oxide[8] (380 mμ against 440 mμ of benzothiazino-tropone). Hence the compound I does not contradict the present result so far as the shift of the absorption peak is concerned.

Apart from such a speculation one may conclude that the photobleached product is a leuco dye of a certain kind.

Next, there will be discussion as to whether the accompanying photoreaction is demethylation or hydrolysis of dimethylamino group. Substances to be taken up as possible photobleached products would be the following four; methylene azur A (*N*, *N*-dimethylthionine), methylene azur B (trimethylthionine), or thionol (III), methylene violet (*N*, *N*-dimethylthionolin) (IV). Unfortunately there are few reliable data available either for the absorption spectra or for the oxidation-reduction potential of such substances, and comparison with the present results are not always possible. According to Kehrmann[9] the absorption maximum of methylene azur A and methylene azur B are respectively 638 mμ and 656 mμ and the former is rather close to this observed value. As for the reduction potential on the other hand, Rapkin et al.[10] reported that E_o' of methylene azur B is about the same as that of methylene blue but their data have seemingly

7) F. Kehrmann, *Ber.*, **46**, 2809 (1913); F. Kehrmann and H. Goldstein, *Helv. Chim. Acta.*, **4**, 27 (1921).
8) Unpublished result in Prof. Nozoe's Laboratory in our Faculty.
9) F. Kehrmann, *Ber.*, **46**, 2136 (1913).
10) L. Rapkin, A. P. Struky and R. Wurmser, *J. Chim. Phys.*, **26**, 340 (1926).

to be reexamined according to a recent investigation[11].

(III)

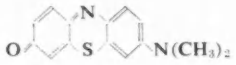

(IV)

Thionol was reported to have the absorption maximum at 590 or 595 mμ[4,12], which does not agree with the present value, while methylene violet has an absorption maximum at 635 mμ in the aqueous solution[4] (or 597.4 mμ in alcoholic solution[13]). As for the E_0' value of the latter compounds there is evidence that it is much lower than that of methylene blue, although its reliable value is not found in the literature. Thus the E_0' value of thionolin, the demethylated analogue of methylene violet, was reported to be −0.22 V. (at pH 7.11)[14], which is much lower than that of thionine (0.062 V. at pH 7.0), the demethylated analogue of methylene blue (0.011 V. at pH 7.0). From these data it would be natural to expect that the E_0' value of methylene violet is smaller than −0.22 V. at pH 7. Thus the possibilities of photohydrolysis which lead to III or IV, can be denied altogether.

11) For example, as regards toluidin blue, compare Rapkin's data with B. P. Nikol'skŭ and V. V. Pal'chevskŭ, *Zhur. Fiz. Khim.*, **32**, 1280 (1958).
12) S. Granick and L. Michaelis, *J. Am. Chem. Soc.*, **69**, 2883 (1947).
13) M. Althausse und G. Krüss, *Ber.*, **22**, 2065 (1889).
14) S. Granick, L. Michaelis and M. Schubert, *J. Am. Chem. Soc.*, **62**, 1802 (1940).

To sum up the above discussion, a photobleached product is most certainly a partially demethylated methylene blue, which is perhaps methylene azur A.

Summary

In order to identify the photobleached substances which are produced when the aqueous solution of methylene blue is irradiated with visible light, the following three kinds of experiments were carried out.

1) Comparison of the absorption spectra of the photobleached product with those of leucomethylene blue, benzoylleucomethylene blue and acetylleucomethylene blue.

2) Comparison of the oxidative and reductive behavior of the photobleached product with that of leucomethylene blue.

3) Comparison of the pH dependence of the absorption spectrum of the photobleached product and that of leucomethylene blue.

It was concluded that the photobleached product is the leuco form dye and its oxidized form is most certainly a partially demethylated methylene blue, perhaps methylene azur A.

The author wishes to express his thanks to Professor Masao Koizumi for his suggestions and criticism throughout this investigation.

Department of Chemistry
Faculty of Science
Tohoku University
Katahira-cho, Sendai

*A. C. Polarography of Thiamine Hydrochloride in Weakly Acidic Buffer Solutions**

By Koichi Okamoto

(Received August 31, 1960)

A number of polarographic investigations on thiamine hydrochloride have been reported[2]. Most of these studies have been carried out in highly acidic or basic solutions or in unbuffered solutions, because their D. C. reduction waves were not well-defined in weakly acidic or in neutral buffer solutions owing to the overlapping of hydrogen discharging currents or pre-sodium waves.

The stability of thiamine under such extreme conditions was not sufficient to carry out the polarographic measurements and in unbuffered solutions the real pH-values at the surface of D. M. E. could not be defined experimentally. Therefore, the investigations have to be done in buffered solutions in order to know the real polarographic reduction waves of thiamine in weakly acidic solutions.

When the A. C. polarographic method was applied, thiamine hydrochloride was found to show one or two well-defined peak currents in weakly acidic and in neutral buffer solutions. Especially the behavior of the first wave

* Polarographic Studies of some Organo-sulfur Compounds, Part II[1].
1) Part I. K. Okamoto, This Bulletin, **34**, 920 (1961).
2) M. Brezina and P. Zuman, "Polarography in Medicine, Biochemistry and Pharmacy", Interscience Publishers, New York (1958), p. 382.

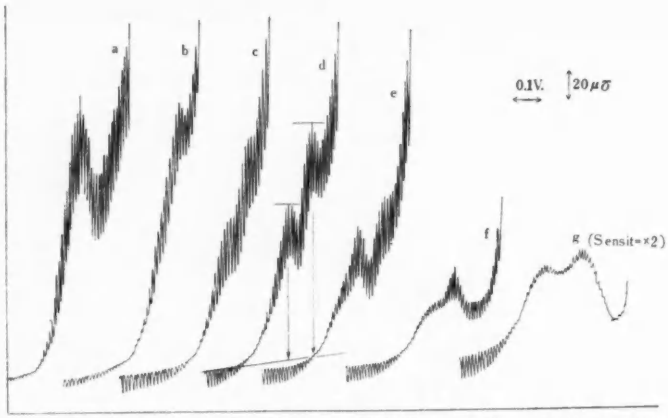

Fig. 1. Typical polarograms of B_1-HCl. a: pH 3.00, b: 4.75, c: 5.50, d: 6.00, e: 7.00, f: 7.90, g: 8.95. The applied voltage starts from −1.0 V. vs. S. C. E. $[B_1\text{-HCl}]=1\times10^{-3}$ mol./l. The solutions were air-free. Parallel capacitance is zero.

was distinctly observed in the solutions of pH 4.75~7.0. These two waves were considered to be attributed to the reduction of two species of thiamine hydrochloride in a solution.

In this paper, these A.C. polarographic behaviors of thiamine hydrochloride will be reported.

Experiments and Results

The polarograph used was the same as that reported in the previous paper[1]. The characteristics of the dropping mercury electrode were: $m=0.917$ mg. sec^{-1}, $t=4.68$ sec. (open circuit), 3.92 sec. (at −1.30 V. vs. S. C. E.), 3.85 sec. (at −1.40 V.).

The thiamine hydrochloride and other reagents used were of reagent grade.

Experiments were carried out 2 or 3 times on the same kind of sample at 25°C and the values obtained were averaged in general. All potentials and peak currents were expressed in V. vs. S. C. E. and μa, respectively.

Table I. The variation of the summit potentials E_s and the peak currents i_s with pH
$[B_1\text{-HCl}]=1\times10^{-3}$ mol./l., 25°C

pH	Buffer	$-E_s$, V. vs. S.C.E.		i_s, μa	
		$-E_s^1$	$-E_s^2$	i_s^1	i_s^2
3.00	A	N.W.	1.273	N.W.	234.6
4.00	A	N.W.	1.275	N.W.	233.2
4.25	A	N.W.	1.299	N.W.	227.0
4.50	A	N.W.	1.316	N.W.	209.0
4.75	A	N.W.*	1.320	N.W.	199.2
5.00	A	1.275	1.335	ca. 120	185.6
5.25	A	1.290	1.357	114.9	178.8
5.50	A	1.300	1.370	111.3	165.0
5.75	A	1.307	1.390	102.8	157.7
6.00	B	1.310	1.392	94.0	147.0
7.00	B	1.351	1.445	85.4	82.0
7.90	B	1.320	1.399	45.0	61.9
8.95	C	1.317	1.453	28.0	29.3
10.00	D	N.W.	N.W.	N.W.	N.W.

A: 0.5 M acetate buffer
B: 0.5 M phosphate buffer
C: 0.1 M borate buffer+KH_2PO_4
D: 0.1 M borate buffer+NaOH
N. W.: No wave * Shoulder

The Influences of pH to i_s and E_s. — In the buffer solutions of pH 3.0~10.0, containing 1×10^{-3} mol./l. thiamine hydrochloride (B_1-HCl), the variation of the wave forms with pH was observed, especially in the region of pH 4.00~6.00.

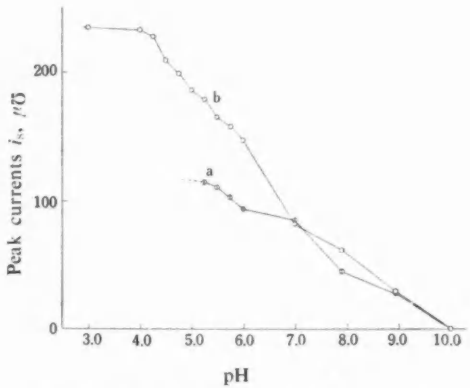

Fig. 2. The relation of the peak currents to pH.
a: 1st wave b: 2nd wave
$[B_1\text{-HCl}]=1\times10^{-3}$ mol./l., 25°C

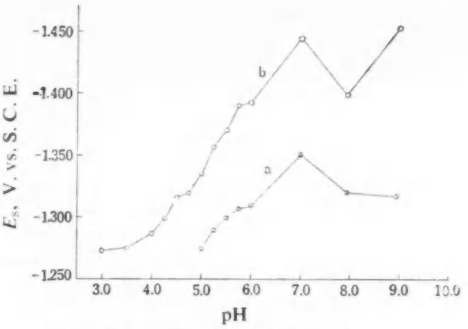

Fig. 3. The relation of E_s to pH.
a: first wave b: second wave
$[B_1\text{-HCl}] = 1\times10^{-4}$ mol./l., 25°C

Some of the typical polarograms were shown in Fig. 1 and the relations of peak currents i_s or of summit potentials E_s to pH were summarized in Table I, Figs. 2 and 3.

Wave heights were measured following the method shown in Fig. 1.

Only one peak current was obtained in the region of pH 3.0~4.75, two peak currents were observed in the region of pH 4.75~9.0. They had the same wave heights at pH 7.0. In basic solutions of pH 7.0~10.0, these two waves changed irregularly and completely disappeared at pH 10.0.

As shown in Figs. 1 and 2, the 1st wave began to be separated at pH about 4.75 and decreased gradually with pH-increase in the same manner as the second.

Gradual negative shifts of E_s of the first and the second waves with pH-increase were found, certain irregularities, however, being observed in basic solutions as shown in Fig. 3.

The Relations of the Concentrations of B_1-HCl to i_s and E_s.—In order to know whether these two peak currents were both due to the reduction of B_1-HCl itself, the relation between the concentrations and i_s was investigated in 0.5 M phosphate buffer of pH 6.00.

The results obtained were shown in Table II and Fig. 4. Good linearities were found for

Table II. The variations of i_s and E_s with the concentrations of B_1-HCl
Supporting electrolyte; 0.5 M phosphate buffer (pH 6.00), 25°C

Concn. ($\times10^{-4}$ mol./l.)	i_s, μA		$-E_s$, V. vs. S.C.E.	
	i_s^1	i_s^2	$-E_s^1$	$-E_s^2$
0.20	16.2	33.6	1.295	1.361
0.40	41.5	74.7	1.300	1.369
0.60	68.2	105.2	1.307	1.386
0.80	93.2	137.0	1.307	1.384
1.00	119.0	174.5	1.309	1.390

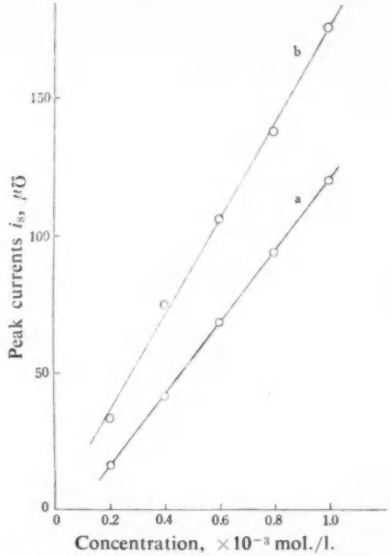

Fig. 4. The relation between the concentrations and the peak currents in 0.5 M-phosphate buffer of pH 6.00.
a: first wave b: second wave

two waves and the saturation tendencies occurred usually in cases where adsorption or desorption waves were not recognized at all.

Therefore, both of the waves seemed to be the real reduction waves of B_1-HCl itself.

The summit potential E_s fairly shifted to negative potentials with the increase of the concentrations of B_1-HCl.

Temperature Coefficients of i_s.—Temperature coefficients of the first and the second wave heights were obtained as 1.64 and 1.56% respectively on 0.5 M phosphate buffer solutions of pH 6.0 containing 1×10^{-3} mol./l. of B_1-HCl.

These coefficients coincided with the theoretical value of 1.6% of the diffusion currents.

The Influence of Mercury Heights H to i_s.—The relationship of H to i_s was studied using the method of the plotting $\log H$ (corrected with the reverse pressure of mercury height) against $\log i_s$. The sample offered was 1×10^{-3} mol./l. of B_1-HCl dissolved in 0.5 M phosphate buffer of pH 6.00.

The following equations were obtained:

$$\text{first wave;} \quad i_s^1 = H^{0.34} + K_1$$

$$\text{second wave;} \quad i_s^2 = H^{0.29} + K_2$$

where K_1 and K_2 are constants.

The peak currents were not proportional to the square root of H.

Electrocapillary Curve.—When strong adsorption-desorption phenomena occurred at the

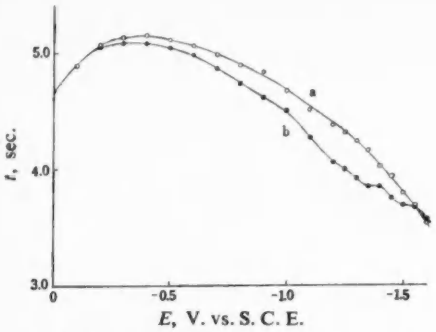

Fig. 5. Electrocapillary curves.
a: Reference; 0.5 M-phosphate buffer pH 6.00
b: 1 mmol B_1–HCl in reference soln. a.

surface of D. M. E., the electrocapillary curve was known to show certain irregularities.

The electrocapillary curve of B_1–HCl in pH 6.00 phosphate buffer solution was shown in Fig. 5.

In a very wide potential range $-0.20 \sim -1.55$ V., the drop time t was smaller in a solution of B_1–HCl than in a solution without it, and two small minima were observed at potentials -1.35 and -1.50 V. corresponding to the slightly negative potentials of each two peak current.

Weak adsorption seemed to take place at the surface of D. M. E., but it could have no remarkable effects upon A. C. polarographic waves; therefore, two A. C. waves were both considered to be not entirely so-called tensammetric waves.

Discussion

As described in the above section, comparatively-well defined two A. C. polarographic waves of B_1–HCl observed in weakly acidic buffer solutions, were not the simple tensammetric, but the reduction waves with a few tensammetric properties.

When the aqueous solution of B_1–HCl was titrated with sodium hydroxide solution, two equivalent points were observed[3], the first point corresponding to 1 mol. equivalent of sodium hydroxide and to the process I→II (Fig. 6), another to 3 mol. equivalent of sodium hydroxide and to the process V→VI, while no point corresponding to 2 mol. of sodium hydroxide was detected. The values of pK_1 and pK_2 were 4.70~4.80 and 9.30~9.37, respectively at 25°C[2].

On the other hand, a new polarographic wave began to be observed at about pH 4.75; therefore, this (first wave) was considered to correspond to a reduction of species II that would increase from pH about 3.5 up to neutral range, then the second wave was to correspond to a reduction of species I that gradually decreased with pH-increase.

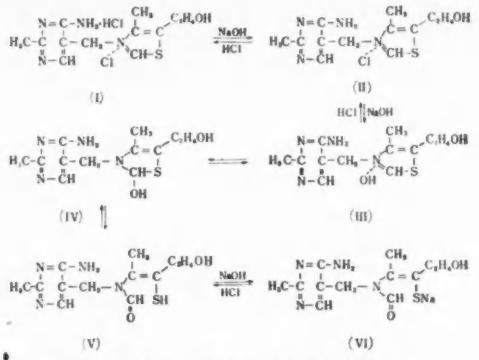

Fig. 6. The variation of B_1–HCl when titrated with HCl or NaOH solutions[3].

The first wave seemed to overlap with the second in the region of pH smaller than 4.75, but as the negative shift of the second was larger than of the first, it came to appear at pH 4.75.

At pH 4.70~4.80 the ratio of the polarographic wave heights of the first and the second should be 1:2 and at pH 7.0 should be 1:1 theoretically. Similar results were obtained experimentally as shown in Fig. 2.

The gradual decreasing of both wave heights with pH-increasing was explained as follows by the above dissociation processes (Fig. 6). If the polarographic reduction of thiamine took place at the double bond >N=C– in thiazole ring, IV, V and VI could not be reduced at D. M. E. Although these formes were not detected in the titration curve, they were considered to exist together in the solutions of pH about 5~9, so that the gradual decrease of wave heights were mainly due to this gradual increase of non-reductive IV or V.

The difference between the summit potentials of the first and second waves was up to about 100 mV., the influence of hydrochloric acid combining to pyrimidine ring or in other words to whole molecule of B_1, might produce this difference.

Summary

Although in ordinary D. C. polarography no well-defined polarographic reduction waves of thiamine in weakly acidic or in neutral buffer solutions have been reported, it was found that A. C. polarographic methods would be suitable for these studies.

3) A. Watanabe and Y. Asahi, *J. Pharm. Soc. Japan* (*Yakugaku Zasshi*), 75, 1046 (1955).

A. C. polarographic waves of thiamine appeared at $-1.27\sim-1.35$ V. in buffer solutions of pH 3.0~4.75, and in the region of pH 4.75~7.0 a new wave began to be observed at more positive potentials than $-1.27\sim1.35$ V., while another wave was observed at $-1.32\sim-1.44$ V. in the same pH region. The heights of two waves decreased with the increase of pH.

In basic buffer solutions the wave forms varied irregularly and the waves disappeared completely at pH 10.0.

According to the relation of i_s to temperature, mercury heights and concentrations, these two waves were both recognized as diffusion currents with a few tensammetric properties.

The nature of the first and second waves were attributed to the reductions of thiamine with Cl^-, and with hydrochloric acid and Cl^- to each dihydrothiamine, respectively.

The author is very much indebted to Director M. Matsui of our Laboratory for affording facilities for this investigation.

Physicochemistry Section
Research Department
Sankyo Co., Ltd.
Shinagawa-ku, Tokyo

Studies on the Silk-platinum Catalyst. I. Its Preparation and Activity

By Akira Akamatsu, Yoshiharu Izumi and Shiro Akabori

(Received January 19, 1961)

Recently, Izumi[1] reported on an entirely new type of palladium hydrogenation catalyst, which is unique in that its carrier is fibers of silk-fibroin. Parlladium chloride was easily coordinated with the silk-fibroin protein and then the resulting silk-palladium chelate was hydrogenated to give the catalyst. It is assumed that the metal in the catalyst is highly dispersed and tightly fixed to the micelle structure of silk-fibroin in a finely devided state, and consequently the active surface of the metal is considerably increased. Furthermore, the catalyst has a number of characteristics due to the nature of the carrier silk-fiibroin fibers.

In addition to these characteristics, other interesting properties were expected to be found, when palladium was replaced by platinum. A brown hair-like silk-platinum chelate was successfully formed, when silk-fibroin fibers were boiled with an aqueous solution of potassium tetrachloroplatinate (K_2PtCl_4). Activation of this chelate by hydrogenation gave the black-colored silk-platinum catalyst.

This catalyst was found to catalyze the hydrogenation of various compounds, as will be reported in the following papers of this series[2]. In general it showed the highest hydrogenation activity for aromatic nitro compounds. In the hydrogenation of nitrobenzene to aniline, its activity was about two hundred and fifty times as high as that of a platinic oxide catalyst containing the same amount of platinum metal. Further advantages of this catalyst, as of a silk-palladium catalyst, are the facility with which it can be mixed with reactants and separated from the reaction mixture without detachment of the metal from the carrier, and the fact that it can be stored for a long period in air-dried conditions without undergoing spontaneous combustion.

The present paper describes the conditions used for the preparation of this catalyst, and its activity and stability.

Results and Discussion

Conditions for Preparation of the Chelate.— In order to obtain a catalyst with high activity, as well as to minimize expensive loss of platinum, the platinum content of the chelate preparation must be increased. In the previous paper[1] Izumi reported on an "easily detachable form" of metal in the silk-palladium catalyst, which did not contribute to the activity. It is probable that this "easily detachable form" is free metal which has been reduced without forming a chelate. Similarly, platinum in the chelate is assumed to consist of "coordinated" and "not coordinated" platinum. The latter is simply deposited on the silkfiboin fibers as the free metal. It is possible that the former is readily soluble in concentrated hydrochloric acid while the latter is insoluble. Optimal conditions not only for "the

1) Y. Izumi, This Bulletin, 32, 932 (1959).
2) A. Akamatsu, Y. Izumi and S. Akabori, in preparation.

total platinum content", but also "the coordinated platinum content" were studied; the latter estimated as the concentrated hydrochloric acid soluble part. The results are shown in Fig. 1. (a) Four hundred milligrams of silk-fibroin fibers were boiled with an aqueous solution of potassium tetrachloro-platinate. The ratio of crystalline potassium tetrachloro-platinate to silk-fibroin in the solution, and the boiling time were constant. The concentration of the solution was varied by changing the volume of the solvent. Thus, the optimum concentration was found to be about 0.75%. (b) The boiling time was also kept constant and the volume of the 0.75% aqueous solution of potassium tetrachloro-platinate was varied. Comparatively high contents of platinum were obtained using more than 20 ml. of solution. (c) An adequate boiling time was found to be 14 to 20 min. Thus, the most desirable result was obtained when 400 mg. of silk-fibroin fibers were boiled with 20 ml. of a 0.75% aqueous solution of potassium tetrachloro-platinate for 14 to 20 min. This preparation was used for the work described in the following sections of this paper. Prolonged boiling of more than 20 min. only resulted in an increase in the "not coordinated part". Another good result was obtained, when a suspension of silk-fibroin in potassium tetrachloro-platinate solution was heated at 55°C in an air bath for 17 hr., instead being boiled.

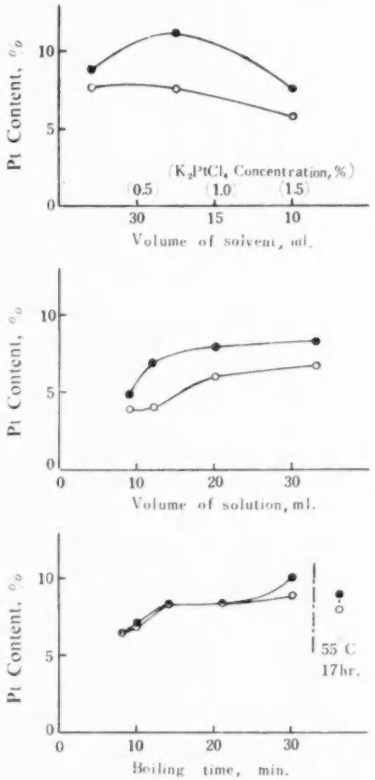

Fig. 1. Platinum content of chelate prepared under various conditions.

● Total platinum content, ○ Coordinated platinum

400 mg. of silk-fibroin was boiled (a) in an aq. solution containg 150 mg. of K_4PtCl_4 for 14 min., (b) in a 0.75% K_2PtCl_4 aq. solution for 14 min., and (c) in 20 ml. of a 0.75% K_2PtCl_4 aq. solution.

In the preparations described above, about 50% of the platinum in solution was used up in formation of the chelate. The remainder in the mother liquor was recovered and used for subsequent preparations.

Conditions for Activation of the Chelate.—The above chelate was converted to the active catalyst by reducing it with ca. 90 kg./cm² of hydrogen in an autoclave. To find the optimal conditions for activity, the hydrogenation reaction was carried out in various solvents at various temperatures for different periods. Representative experiments are summarized in Tables I to IV, in which the activity of the resulting catalysts are represented by their reaction velocity (v) during the hydrogenation of nitrobenzene to aniline using the same amount of catalyst in each case, and by their activity yield ($y \cdot v$.) which means their activity on the basis of the same amount of the metal in the catalyst. v was calculated according to the equation; $v = 100/t$, where t is the time in minutes required for 70% hydrogen uptake. $y \cdot v$ was calculated as the product of the reacion velocity (v) and the gravity yield*1 (y). The decrease in the gravity yield is due to destruction of the carrier fibroin fibers. In general, activation at high temperatures resulted in a high activity yield and low gravity yield. The former is not due only to an increase in the metal content resulting from destruction of the carrier.

When water was used as solvent during activation (Table I), carrier fibers were broken to pieces at above 150°C, and almost completely destroyed and dissolved in the solvent at 200°C. Activation for two hours gave a comparatively active catalyst. The most active catalyst was obtained at 160°C.

With diethyl succinate or methanol, less active catalysts were obtained with the silk-platinum catalyst (Table II), though in the

*1 For example, when 100 mg. of the chelate is hydrogenated to give 50 mg. of the active catalyst, the gravity yield is 50%.

Table I. Activation of the chelate in 50 ml. of water

Cat. No.	Precursor chelate, mg.	Temp. °C	Time hr.	Grav. yield y, %	React. vel. at 32 °C, v	Act. yield $y \cdot v$
1	250	80	1	88	2.1	1.8
2			2	91	2.5	2.3
3		100	1	84	2.6	2.2
4			2	84	2.7	2.3
5	200	150	1	73	5.4	3.9
6			2	69	5.9	4.1
7			3	62	4.5	2.9
8		178	2	44	11.5	5.0
9		200	1	—	—	—
10	100	160	2	61	9.5	5.8

Table II. Activation of the chelate (200 mg.) for 2 hr. in methanol and diethyl succinate

Cat. No.	Solvent 50 ml.	Temp. °C	Grav. yield y, %	React. vel. at 32 °C, v	Act. yield $y \cdot v$
11	Methanol	100	90	2.9	2.6
12		150	83	3.4	2.8
13	diEt. Succ.	100	95	0.4	0.4
14		150	94	1.8	1.7
15		200	81	4.0	3.2

Table III. Activation of the chelate at 160 °C for 2 hr. in dilute acetic acid

Cat. No.	Solvent 50 ml.	Precursor chelate, mg.	Grav. yield $\cdot$ v, %	React. vel. at 32 °C, v	Act. yield $y \cdot v$
16	1% AcOH	100	52	19.3	10.0
17	2.5% AcOH		55	11.8	6.5
18	5% AcOH		54	17.9	9.7
19	1% AcOH	2000	56	3.6	2.0

Table IV. Repeated activation of catalyst No. 19 for 1 hr.

Cat. No.	Method	Solvent ml.	Precursor catalyst, mg.	Grav. yield $y \cdot y'$	React. vel. at 32 °C, v	Act. yield $y \cdot y' \cdot v$
20	Reduction at 160 °C	1% AcOH (30)	300	31	60.0	18.8
21	Heating at 160 °C	1% AcOH (50)	100	35	34.9	12.5
22	Boiling in flask	1% AcOH (50)		51	3.0	1.5
23	Reduction at 160 °C	1% NH_3 (50)		25	7.5	1.9

Table V. Stability of catalyst

Storage time weeks	React. vel. at 32 °C, v
0	60.7
2	50.5
5	89.0
12	85.8

case of the silk-palladium catalyst, an exceedingly active catalyst was obtained with diethyl succinate (Table VI).

However, the use of dilute acetic acid as a solvent (Table III), increased the activation. One per cent acetic acid was the most effective among the other solvents tested. But increasing the amount of the precursor chelate in proportion to that of the solvent, failed to give satisfactory results (Cat. No. 19). So, for the repeated activation of this catalyst, the various conditions shown in Table IV were tested. Repeated hydrogenation under the same conditions resulted in an extremely high activity. Heating in an autoclave without hydrogen also gave a very active catalyst though it was less

Table VI. Reaction velocity in hydrogenation of alkyl nitrobenzenes

Substrate				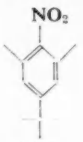	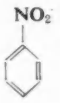
	4 g.	5.4 g.	5.9 g.	6.3 g.	4 g.
Solvent	Dioxane				Methanol
Silk-Pt 40 mg.	13.0 (52°C)	11.4 (52°C)	6.90 (55°C)	0.18 (50°C)	37.7 (23°C)
[Ratio]	[1.00]	[0.86]	[0.53]	[0.01]	
PtO_2 15 mg.	0.15 (50°C)	0.15 (50°C)	0.11† (50°C)	0.03† (100°C)	0.15 (17°C)
[Ratio]	[1.00]	[1.00]	[0.73]	[0.18]	
Silk-Pd 140 mg.	3.30 (100°C)	0.90 (100°C)	0.65 (100°C)	0	3.42 (18°C)
[Ratio]	[1.00]	[0.27]	[0.20]	[0.00]	
Silk-Pd-DES 54 mg.	5.03 (52°C)	1.07 (50°C)	—	—	15.6 (18°C)
[Ratio]	[1.00]	[0.21]			

† Calculated value

active than the former. However, boiling in a flask with 1% acetic acid was not effective. Repeated hydrogenation with 1% aqueous ammonia was not effective for increasing the total activity yield ($y \cdot y' \cdot v$), but it did increase the reaction velocity.

The present results show that the activity of the catalyst is influenced very much by the solvent used, and the temperature and time of activation. The destruction of the carrier and the increase in the metal content of the catalyst are evidently effected by these conditions, and indeed might contribute to some extent to the activity represented by the activity yied. But a low gravity yield was not always accompanied by a high actvity yield as shown by comparison of catalysts Nos. 9 and 16. It may be that these conditions directly and independently influence the activity. The solvent especially is an important factor in the activation, as Hartung et al.[3] reported concerning the effect of certain organic anions on the preparation of the palladium-charcoal catalysts. It was proved in this work that regardless of the extent of the gravity yield, use of acetic acid resulted in a very good activity, while methanol, diethyl succinate, and aqueous ammonia were not effective.

It does not seem unreasonable, as Hartung pointed out, to attribute these solvent effects on the arrangement of the crystalline structure or the spacing of the active centers on the catalyst. It should also be noted that the ratio of the volume of solvent to the amount of the precursor-chelate used influenced the activity to a large extent, though such a phenomenon was not seen in the case of the silk-palladium catalyst.

3) W. H. Hartung et al., *J. Org. Chem.*, **21**, 999 (1956).

Stability of the Catalyst. — In Table V are shown the reaction velocities observed in the hydrogenation of nitrobenzene to aniline, using the final catalyst*2 both immediately after its activation and after storage of the dry catalyst for several weeks in a stoppered bottle. The results clearly show the silk-platinum catalyst can be stored for a long period without loss and even with some increase of activity. No spontaneous combustion took place during the storage period.

Activity with Aromatic Nitro Compounds. — The activity of the silk-platinum catalyst*2 in the hydrogenation of various alkyl derivatives of nitrobenzene to the corresponding amines was compared with that of platinic oxide catalyst, silk-palladium catalyst (activated in methanol) and silk-palladium-DES catalyst (activated in diethyl succinate)*3. Table VI shows the reaction velocities for the hydrogenation of the same amount (1/30 mol.) of the various compounds, using catalysts, each of which contains the same amount (13 mg.) of metal. The silk-platinum catalyst showed the highest activity of all the catalysts with all the compounds tested. Notably in the hydrogenation of nitrobenzene in methanol, the reaction velocity was 254 times as fast as that with the platinic oxide catalyst. When methanol was used as a solvent, the reaction velocity for the silk-platinum and the silk-palladium-DES catalyst was faster than when dioxane was used, in spite of the low reaction temperature.

The ratios of the reaction velocity of alkyl nitrobenzenes to that of non-substituted nitrobenzene were calculated and are shown in

*2 This catalyst was prepared under the same conditions as that for catalyst No. 20 in Table IV. See Experimental.
*3 See Experimental.

brackets in Table VI. In the series of alkyl nitrobenzenes the ratios decreased as the alkyl groups increased in substituents and branching. This decrease is distinguishable with catalysts in which the carrier is silk-fibroin fibers. It is possible that, not only the bulkiness of the reactants, but also the characteristic structure of carrier silk-fibroin[4] exerts some steric hindrance retarding the hydrogenation.

Experimental

Determination of Platinum. — Platinum was measured by the iodine method[5], after the chelated sample had been treated as follows;

1) For Estimation of the Total Platinum Content. —About 15 mg. of the chelated sample were accurately weighed in a crucible and heated with 0.5 ml. of concentrated nitric acid on a steam bath for 20 min. The mixture was evaporated to dryness and the residue was strongly heated to ash over a burner. After the ash had been dissolved in 0.5 ml. of aqua-regia, the soluion was evaporated to dryness. One milliliter of concentrated hydrochloric acid was added to the residue and evaporated off twice to remove the nitrate. The residue was then dissolved in water and the solution diluted to 50.0 ml. Exactly 5.00 ml. of the solution was used for each determination.

2) For Estimation of Coordinated Platinum. — About 15 mg. of the chelated sample were accurately weighed in a test tube and heated with 2.0 ml. of 30% hydrochloric acid on a steam bath for 30 min. The mixture was filtered through filter paper and the filter paper was washed with water. The combined filtrates were transferred to a crucible and ashed by evaporation and strong heat. Then the ash was treated in the same way as described above for the estimation of the total platinum content.

Reaction Vessel.—The same autoclave as described in the previous paper[1] was used for activation of the chelate and for hydrogenation reactions.

Measurement of the Reaction Velocity. — One thirtieth of a mole of the substrates (for nitrobenzene, 4 g.) dissolved in 50 ml. of methanol and the catalysts to be tested (for silk-platinum catalyst, 40 mg.) were placed in the autoclave, into which hydrogen was then introduced to a pressure of 90 kg./cm². The initial pressure was read after shaking to allow equilibration, and then the shaking was continued until 70% of the theoretical amount of hydrogen had been taken up.

Preparation of Catlysts.—*1) Silk-platinum Catalyst.*—The catalyst, used in investigations of stability and activity, was prepared by the following method; a) Twenty grams of sik-fibroin fibers previously washed with boilng water were mixed with 1 l. of an 0.75% aqueous solution of potassium tetrachloroplatinate and the mixture was boiled for 18 min. The silk-platinum chelate obtained was filtered off, washed with water, methanol and then ether, and finally dried in vacuo. b) Twenty grams of the chelate were suspended in 500 ml. of 1% acetic acid reduced with hydrogen (80 kg./cm²) at 160°C for 2 hr. in a 1 l. autoclave. The catalyst obtained was filtered off, washed with water, methanol and ether, and dried in vacuo (12 g., 60%). The reaction velocity (v) with nitrobenzene at 16°C was 1.8. Repeated hydrogenation of 4 g. of this catalyst by the same method for 1 hr. gave the final catalyst (2.6 g., 66%). The reaction velocity (v) of this catalyst at 32°C was 60.7.

2) Platinic Oxide Catalyst.—This was prepared by the method of Ref. 6.

3) Silk-palladium Catalyst.—This was prepared as described in the previous paper[1].

4) Silk-Palladium-DES Catalyst. — Two hundred milligrams of the silk-palladium chelate[1] were suspended in 50 ml. of diethyl succinate and reduced with hydrogen (80 kg./cm²) at 220°C for 2 hr. in a 100 ml. autoclave. The resulting catalyst was washed with methanol and dried in vacuo.

Isolation of Products. — The products on the hydrogenation of nitrobenzene and of its alkyl derivatives were isolated as follows:

Aniline. — This was isolated as described previously[1].

p-Aminoisopropylbenzene, p-Amino-tert-butylbenzene. —The reaction mixture was filtered and the filtrate distilled in vacuo. The amines obtained were acetylated and the crude acetyl derivatives were recrystallized from alcohol: *p*-Aminoisopropylbenzene; b. p. 112°C/19 mmHg (lit.[7] 225°C/760 mmHg). *p*-Amino-*tert*-butylbenzene; b. p. 117~119°C/15 mmHg (lit.[8] 120~132°C/15 mmHg). *p*-Acetaminoisopropylbenzene; m. p. 105°C (lit.[9] 105~106°C). *p*-Acetamino-*tert*-butylbenzene; m. p. 171°C (lit.[8] 171~172°C).

3,5-Dimethyl-4-amino-tert-butylbenzene.—The crude amine was converted to its 2-nitro derivative and this was recrystallized; m. p. 86°C (lit.[10] 88~89°C).

Summary

1. A silk-platinum chelate, which had the highest platinum content, involving both the total platinum content and the coordinated platinum, was obtained when 400 mg. of silk-fibroin was boiled with 20 ml. of a 0.75% aqueous solution of potassium tetrachloroplatinate for 14 to 20 min.

2. The most active silk-platinum catalyst was obtained when reduction of the chelate was pepeated twice in 1% acetic acid with 90 kg./cm² of hydrogen at 160°C. The activity was much influenced by the solvent, temperature and time used for its activation.

3. The catalyst could be stored for a long

4) S. Akabori, S. Sakurai, Y. Izumi and Y. Fujii, *Nature*, **178**, 323 (1956); S. Akabori, Y. Izumi, Y. Fujii and S. Sakurai, *J. Chem. Soc. Japan, Pure Chem. Sec.* (*Nippon Kagaku Zasshi*), **77**, 1374 (1956); S. Akabori, Y. Izumi and Y. Fujii, ibid., **78**, 886 (1957); Y. Izumi, This Bulletin, **32**, 942 (1959).

5) E. B. Sandell, "Colorimetric Determination of Traces of Metals", Interscience Publishers, New York (1950), p. 493.

6) "Organic Synthesis", Coll. Vol. 1, 463 (1948).

7) M. S. Carpenter et al., *J. Org. Chem.*, **16**, 586 (1951).

8) B. M. Wepster et al., *Rec. trav. chem.*, **71**, 321 (1952).

9) B. M. Wepster et al., ibid., **71**, 348 (1952).

10) M. S. Carpenter et al., *J. Org. Chem.*, **19**, 77 (1954).

period in the dry state and even showed some increase in activity during storage.

4. The most active catalyst had about two hundred and fifty times as much activity as that of a platinic oxide catalyst in the hydrogenation of nitrobenzene to aniline.

5. The characteristic structure of the carrier seems to exert some steric hindrance on the hydrogenation of highly branched aromatic nitro compounds.

The authors wish to express their gratitude to Dr. S. Yamada for his suggestion concerning the platinum complex, to Mr. S. Watarai for supplying various alkyl nitrobenzene derivatives and to Mr. T. Kojima for his technical assistance in this investigation. They are also greatly indebted to the Gunze Seishi Co., Ltd. for supplying the silk fibers.

Division of Organic Chemistry
Institute for Protein Research
Osaka University
Nishi-ku, Osaka

Reduction of Organic Compounds with Urushibara Catalysts under High Pressure. VIII[1]*. Reduction of Acetophenone, Especially with Urushibara Nickel Catalyst Prepared by Various Modified Methods*

By Shin-ichi TAIRA

(Received December 27, 1960)

In the preceding paper[1] of this series, catalytic reduction of benzophenone with various Urushibara catalysts under various conditions was reported, and activities of Urushibara nickel, Urushibara cobalt and Urushibara copper, prepared by various methods were compared with each other.

The procedure for preparing Urushibara nickel catalyst has been successively modified since its discovery and some varieties of this catalyst were reported. The preparation of the Urushibara nickel catalyst is divided into two steps; namely, the preparation of precipitated nickel and the digestion of the precipitated nickel with acid or alkali. Varieties of the Urushibara nickel catalyst originate in methods of preparing the precipitated nickel and succesive treatment with acid or alkali. The precipitated nickel, prepared from nickel chloride or nickel acetate solution with zinc dust, gives Urushibara nickel B (U-Ni-B)[1,2] or Urushibara nickel CB (U-Ni-CB)[1] by digestion with caustic alkali. The same precipitated nickel gives Urushibara nickel A (U-Ni-A)[1,3] or Urushibara nickel CA (U-Ni-CA)[1] by treatment with acetic acid in place of caustic alkali. The U-Ni-CB and U-Ni-CA are prepared from the precipitated nickel which was obtained from nickel chloride solution and zinc dust at a low temperature. The precipitated nickel, prepared from nickel chloride solution with aluminum grains, gives Urushibara nickel BA (U-Ni-BA)[1,5] by treatment with sodium hydroxide solution, and Urushibara nickel AA (U-Ni-AA)[6] by treatment with acetic acid and sodium chloride.

In the present paper, reduction of acetophenone with various Urushibara nickel catalysts is investigated. In this connection, the possibility of preservation of the precipitated nickel retaining the activity of the catalyst therefrom was examined. The renewal of used catalyst was also examined, and it was found that a highly active catalyst can be regenerated from a used catalyst by a simple procedure.

Experimental

Apparatus.—Reduction was carried out in the same autoclave (Sakashita SE-20; electro-magnetically stirring type autoclave having a capacity of 200 ml.) used in the experiments reported in the preceding paper[1].

Materials.—Commercially available acetophenone was purified by repeated crystallization.

General Procedure for Reduction.—Any catalyst, prepared so as to contain 1 g. of nickel, was carefully transferred with ethanol into the autoclave. Then the air present in the autoclave was replaced

1) Part VII: S. Taira, This Bulletin, **34**, 261 (1961).
2) Y. Urushibara and S. Nishimura, ibid., **27**, 480 (1954).
3) Y. Urushibara, S. Nishimura and H. Uehara, ibid., **28**, 446 (1955).
4) K. Hata, S. Taira and I. Motoyama, ibid., **31**, 776 (1958).
5) I. Motoyama, ibid., **33**, 232 (1960).
6) K. Hata, K. Watanabe and H. Watanabe, ibid., **32**, 6 (1959).

by hydrogen gas four times. All operations were carried out under the following condition: (1) acetophenone: 30 g. (0.25 mol.), (2) ethanol: 60 ml., (3) pH: 9~11 (It has been recognized[1,7,8] that the catalytic reduction of carbonyl group with Urushibara catalyst was accelerated by a trace of alkali. When U-Ni-A or U-Ni-CA was used, 1 ml. of 10% sodium hydroxide solution was added.), (4) agitation: 40~45 strokes per minute, (5) reaction temperature: as a remarkable hydrogen uptake was found to begin at about 60°C in reduction of carbonyl group[7], agitation was started when the temperature in the autoclave reached about 60°C, and the temperature was kept between 60 and 70°C throughout the operation, (6) pressure: as it had been found that, in the case of the reduction of carbonyl group under high pressure, the velocity of reduction was only slightly affected by the initial pressure under 100 kg./cm^2[1,7], the effect of the initial pressure was ignored and (7) when the pressure in the autoclave dropped to 20~30 kg./cm^2, supplementary hydrogen gas was charged two or three times in every course of the operation, and the reduction was continued until the hydrogen uptake ceased. Pressure was observed at intervals of five minutes.

After the reduction was finished, the catalyst was filtered off and washed with ethanol. From the combined filtrate, the major part of the ethanol was removed by distillation on a water bath, and the residual liquid was distilled under reduced pressure. The fraction, distilling at 89~91°C/15 mmHg, was collected. The yield of methylphenylcarbinol was 91~95 per cent of the theoretical amount.

Preparation of Catalysts.—The U-Ni-B[1,2], U-Ni-CB[1], U-Ni-BA[4,5], U-Ni-A[3] and U-Ni-CA[1] were prepared by the methods described in the references cited. Regenerated Urushibara nickel catalyst was prepared from any used catalyst by the following methods. The used catalyst was recovered by filtration after the previous reaction, and dried at about 100°C and stored.

(A) To well-mixed zinc dust (5 g.) and recovered U-Ni-A (1.3 g.) with water (3 ml.) was added 80 g. of 10% sodium hydroxide solution. The mixture was occasionally stirred for 20 min. at 50~55°C and then 5 min. at 75~80°C. At the end of this process, generation of hydrogen gas ceased and grayish white zinc compounds were deposited. The upper liquor was removed by decantation and the residual solid was washed with 200 ml. of hot water and then with two 50 ml. portions of ethanol. Every washing was decanted.

(B) Recovered U-Ni-A (1.3 g.), used in Exp. No. 113 and left standing for 55 days, was well mixed with zinc dust (10 g.) and water (5 ml.). The mixture was treated with 160 g. of 13% acetic acid for about 5 min. As hydrogen gas was vigorously generated at first, good agitation by hand was required to prevent the contents from running over. In this case the solid did not come up to the surface of the solution which was green in color. The solid was collected on a glass filter and washed with 200 ml. of water and then with 100 ml. of ethanol.

(C) To a mixture of the recovered U-Ni-A (1.1 g.) used in Exp. No. 32, zinc dust (5 g.) and water (3 ml.) was added 80 g. of 13% acetic acid. The following procedure was similar to that described in B, and a very fine catalyst was obtained.

(D) To a mixture of recovered U-Ni-A (1.4 g.), zinc dust (2.5 g.) and water (2.5 ml.) was added 40 g. of 13% acetic acid. The following procedure was similar to that described in B.

(E) The recovered U-Ni-B (7.3 g.) used in Exp. No. 11 was treated with 160 g. of 13% acetic acid until the solid came up to the surface of the solution which had turned green. Since the major part of the zinc dust had been removed in the previous preparation of the U-Ni-B, only a small quantity of hydrogen gas was evolved in this process. The solid was collected on a glass filter, and washed with 200 ml. of water and then with 100 ml. of ethanol.

(F) The recovered U-Ni-CB (7 g.) used in Exp. No. 19 was treated with 160 g. of 13% acetic acid. Generation of hydrogen gas was hardly observed, and the solution turned black owing to the suspension of fine solid. After about 8 min. the solid was separated by centrifuge from the solution which was green in color. The solid was washed with two 200 ml. portions of water and then two 50 ml. portions of ethanol in the centrifugal tube. The washings were decanted.

(G) To a mixture of recovered U-Ni-A (1.4 g.) and water (2 ml.) was added 50 g. of 20% acetic acid. The mixture was then digested at 70~75°C for one minute on a boiling water bath. The U-Ni-A reacted vigorously with acetic acid at this temperature. Then solid, adsorbing hydrogen gas, came up to the surface of the solution which was green in color. The solid was collected on a glass filter and washed with 200 ml. of water and then with 100 ml. of ethanol.

(H) The weight of recovered U-Ni-A, prepared so as to contain 1 g. of nickel, being ordinary 1.3~1.4 g., the recovered U-Ni-A (0.9 g.) used in Exp. No. 37 was supplemented by 0.5 g. of recovered and stored U-Ni-A. To this was added 2 ml. of water and the mixture was treated as is described in G.

(I) To a mixture of recovered U-Ni-A (1.4 g.) and water (2 ml.) was added 50 g. of 10% acetic acid. The mixture was digested at 75~80°C for one minute on a water bath. The following procedure was similar to that described in G.

In all procedures, distilled water was used for washing, and the obtained catalyst was protected from contact with air as far as possible.

Results and Discussion

As reported in the preceding paper[1] on the reduction of benzophenone, the activity of various Urushibara nickel catalysts in the reduction of acetophenone was studied by comparing the time required for the completion

7) K. Hata, S. Taira and T. Higase, *J. Chem. Soc. Japan, Pure Chem. Sec.* (*Nippon Kagaku Zasshi*), **78**, 186 (1957).

8) S. Nishimura, ibid., **79**, 56 (1958).

TABLE I. REDUCTION OF ACETOPHENONE WITH VARIOUS URUSHIBARA NICKEL CATALYSTS

Exp. No.	Catalyst[a]	pH	Total weight of catalyst g.[b]	Initial pressure kg./cm²	Total pressure depression kg./cm²[c]	Initial temp. °C	Reaction temp. °C	Time min.
11	U-Ni-B	10	7.3	45	56.5	22	61~70	125
12	U-Ni-B	9.7	8.6	50	54.5	23	60~70	90
13	U-Ni-B	9.3	7.4	47	57	22	61~70	80
14	U-Ni-B	9	7.5	46	52	21	62~70	70
15	U-Ni-B[d]	10.6	10.5	42	59	25	62~70	105
16	U-Ni-B[d]	10.5	10.8	45	55	21	60~70	105
17	U-Ni-BA	9.4	1.2	40.5	51	25	61~70	120
18	U-Ni-BA	10.4	1.1	45	50	23	62~70	95
19	U-Ni-CB	9.7	7	49.5	56.5	22	63~66	65
110	U-Ni-CB	10.4	9.2	50	63	21	61~66	60
111	U-Ni-CB	10.7	8.4	49	71	30	64~69	50
112	U-Ni-A	9.5[e]	1.3	47	54.5	24	60~68	40
113	U-Ni-A	10[e]	1.3[f]	45	51.5	24	60~68	35
114	U-Ni-A	9.8[e]	1.3	46	50	24	61~68	35
115	U-Ni-A	9.2[e]	1.3[f]	49	55.5	24	62~70	25
116	U-Ni-CA	9.5[e]	0.9[g]	42	49.5	20	62~69	50
117	U-Ni-CA	9.6[e]	0.8[g]	47.5	55.5	20	62~66	50
118	U-Ni-CA	9.4[e]	0.6	49	51	17	65~70	40
119	U-Ni-CA	9.4[e]	0.7	44	46.5	22	61~69	40

a) Each catalyst was prepared so as to contain 1 g. of nickel.
b) The figures were obtained by weighing the recovered and dried catalysts.
c) Supplementary hydrogen gas was charged two or three times in course of the operation. Every depression of the pressure was sumed up.
d) The catalyst was prepared from the precipitated nickel, obtained from nickel acetate solution and zinc dust.
e) 1 ml. of 10% sodium hydroxide solution was added.
f) About 0.83 g. of nickel was found to be contained by analysis.
g) About 0.57 g. of nickel was found to be contained by analysis.

TABLE II. REDUCTION OF ACETOPHENONE WITH URUSHIBARA NICKEL CATALYSTS PREPARED FROM PRESERVED PRECIPITATED NICKEL[a]

Exp. No.	Catalyst[b]	pH	Total weight of catalyst g.[c]	Initial pressure kg./cm²	Total pressure depression kg./cm²[d]	Initial temp. °C	Reaction temp. °C	Time min.
21	U-Ni-B	9.2	9	48	57	32	60~69	85
22	U-Ni-B	9.3	8.6	47	55	24	60~68	50
23	U-Ni-A	9.4[e]	1.2	48	53.5	27	60~68	35
24	U-Ni-A	9.7[e]	1.3	50	52.5	25	61~65	40

a) All catalysts were prepared from precipitated nickel, obtained from nickel chloride solution and zinc dust, washed with water, dried at about 100°C and left standing for a week in the air.
b) Each catalyst was prepared so as to contain 1 g. of nickel.
c) The figures were obtained by weighing the recovered and dried catalysts.
d) Supplementary hydrogen gas was charged twice in course of the operation. Every depression of the pressure was sumed up.
e) 1 ml. of 10% sodium hydroxide solution was added.

of reduction under nearly the same condition.

A series of experiments shown in Table I was carried out to confirm the activity of each catalyst and to offer the standard of reference for the subsequent experiments. The reduction of acetophenone was effectively achieved with U-Ni-B, U-Ni-BA, U-Ni-CB, U-Ni-A and U-Ni-CA, among which U-Ni-A proved to be the most useful. The U-Ni-B, prepared from nickel acetate and zinc dust, which had been found to be similarly active in the reduction of benzophenone, was also effective for the reduction of acetophenone though somewhat less active (Exp. Nos. 15 and 16). The U-Ni-BA, which had been proved to be specially useful for hydrogenation of aromatic nucleus[4,5], was not so particularly active (Exp. Nos. 17 and 18) as it was in the reduction of

TABLE III. REDUCTION OF ACETOPHENONE WITH REGENERATED URUSHIBARA NICKEL CATALYSTS

Exp. No.	Catalyst (regenerated)	Original catalyst	Method of regeneration[a]	Total weight of catalyst g.[b]	Initial press. kg./cm²	Total press. depression kg./cm²[c]	Initial temp. °C	Reaction temp. °C	Time min.
31	U-Ni-B	U-Ni-A	A	5.7	49.5	59	21	60~64	130
32	U-Ni-A	U-Ni-A	B	1.1	50.5	50	14	65~69	30
33	U-Ni-A	U-Ni-A	C	0.9[d]	45.5	51.5	20	61~64	45
34	U-Ni-A	U-Ni-A	D	1.1	47	52	18	60~64	40
35	U-Ni-A	U-Ni-B	E	1.1[e]	46	55.5	21	60~68	45
36	U-Ni-A	U-Ni-CB	F	0.8[d]	46.5	52.5	26	63~69	60
37	U-Ni-A	U-Ni-A	G	0.9	47.5	55.5	26	60~64	40
38	U-Ni-A	U-Ni-A	H	0.9	48	55.5	22	61~63	40
39	U-Ni-A	U-Ni-A	I	0.8	48.5	54.5	20	60~65	45

In all operations excepting Exp. No. 31, 1 ml. of 10% sodium hydroxide solution was added.
a) The marks A, B, C and etc. indicate the paragraphs in Experimental part.
b) The figures were obtained by weighing the recovered and dried catalysts.
c) Supplementary hydrogen gas was charged twice in course of the operation. Every depression of the pressure was sumed up.
d) About 0.5 g. of nickel was found to be contained by analysis.
e) About 0.7 g. of nickel was found to be contained by analysis.

benzophenone[1]. The activities of U-Ni-CB and U-Ni-CA were found to be fairly high, though they were somewhat inferior to that of U-Ni-A.

The usual Urushibara nickel catalysts B and A can be prepared by a simple operation in only one hour or less. Supposing the relation of the precipitated nickel to Urushibara nickel catalyst is similar to that of Raney alloy to Raney nickel catalyst, the operation of preparing Urushibara nickel catalyst is certainly more simplified when precipitated nickel can be stored in the state ready to use. It has been claimed that precipitated nickel is inherently provided with active nickel surfaces and acid or alkali is not effective to create any active state on the surfaces, and that the rôle of acid or alkali is to remove the basic zinc chloride which has been formed by the reaction of zinc dust with nickel chloride solution[3]. It is presumable in this view that exposure of precipitated nickel to air for a long time may cause the deactivation or lowering of activity of the catalyst prepared from it. Some experiments on the preservation of precipitated nickel have already been reported in regard to the preparation of U-Ni-BA[5]. Precipitated nickel prepared from nickel chloride solution with aluminum grains was preserved in distilled water, 99% ethanol or dry state under reduced pressure. The U-Ni-BA, prepared from the preserved precipitated nickel, was unexpectedly shown to have practically the same activity as that which the catalyst prepared from freshly prepared precipitated nickel has.

The present author tried reduction of acetophenone with the U-Ni-B and U-Ni-A obtained from precipitated nickel, which was prepared from nickel chloride solution with zinc dust by the ordinary methods[2,3], dried at about 100°C, and left standing for a week in the air. The results are shown in Table II. These results do not differ from those obtained with the normally prepared U-Ni-B and U-Ni-A. Therefore, contact with air is safely permitted for precipitated nickel. It may not be necessary for the water for washing to be distilled in the preparation of precipitated nickel.

One of the features of the Urushibara nickel catalyst is that it is not self-inflammable by contact with air under ordinary conditions. Consequently, nickel can be recovered from such waste catalyst as nickel chloride which can be used again for the preparation of the Urushibara nickel catalyst. But the operation may be troublesome and expensive. If recovered Urushibara nickel can be repeatedly used in place of the precipitated nickel, the time for preparing the precipitated nickel and the cost of nickel chloride will be saved. For the purpose of attaining this request a series of experiments was carried out to regenerate the active catalyst directly from recovered catalyst (Table III).

First, the U-Ni-B was prepared from the mixture of recovered U-Ni-A and zinc dust by treatment with sodium hydroxide solution. The regenerated catalyst was found to be useful enough for the reduction of acetophenone though it was somewhat less active (Exp. No. 31). The cause of this reactivation was considered to result from the removal of adsorbed substances on the surfaces of nickel particles by hydrogen gas generated from zinc dust with caustic alkali. Then the catalyst prepared from recovered U-Ni-A and zinc dust by

treatment with acetic acid was also expected to have considerable activity. In fact, such a catalyst proved to be highly active and gave a better result than that obtained with the original U-Ni-A (Exp. No. 32). To save the amount of zinc dust, the next catalysts were prepared by using one half or one fourth the amount of zinc dust as the quantity used for preparing the catalyst in Exp. No. 32. They had also high activities (Exp. Nos. 33 and 34), and gave practically the same results as those obtained with the normally prepared U-Ni-A (cf. Exp. Nos. 112–115 in Table I). If the existence of a small amount of zinc is enough to reactivate the recovered catalyst, the recovered U-Ni-B and U-Ni-CB may become active by being treated with acetic acid. Actually, each of the catalysts prepared from the recovered U-Ni-B and U-Ni-CB used in Exp. Nos. 11 and 19, gave a better result than those obtained with the original catalysts (Exp. Nos. 35 and 36). As the recovered U-Ni-B and U-Ni-CB contain only a small quantity of zinc, only a little hydrogen gas is evolved by the digestion with acetic acid. Accordingly, zinc dust is supposed to be excluded from the reagents necessary for the renewal of the catalyst. Thus some catalysts were prepared from recovered U-Ni-A by being treated with acetic acid only, and these catalysts were also found to be highly active (Exp. Nos. 37, 38 and 39). In these cases, however, nickel itself reacted vigorously with hot acetic acid, and solid, adsorbing hydrogen gas, came up to the surface of the green solution. In consideration of the results described above, acetic acid must have, in case of preparing the U-Ni-A, some activating effect on the surfaces of nickel particles besides the chemical function of generating hydrogen gas and removing deactivating substances (basic zinc chloride and others). Probably one important function of acetic acid may consist in eroding the surfaces of nickel particles and creating new ones. This assumption accounts for the reactivation of recovered catalysts and also for the fact that the U-Ni-A has not high activity, when the digestion with acetic acid is interrupted before the solution turns green by the formation of nickel ion[1]. The discussion as to whether or not the precipitated nickel has inherently active nickel surfaces seems not to be important.

Summary

Catalytic reduction of acetophenone with various Urushibara nickel catalysts was studied under high pressure. The U-Ni-A with a small amount of alkali was found to be the most useful. The U-Ni-CB and U-Ni-CA were also highly active as they were in case of the reduction of benzophenone. The activity of the U-Ni-A and U-Ni-B, prepared from preserved precipitated nickel, was the same as that of the catalysts obtained from the freshly prepared precipitated nickel. In addition, it was found that the recovered Urushibara nickel catalyst could be repeatedly used after a simple regeneration process especially in the form of U-Ni-A. Such a regenerated catalyst had practically the same activity as that of the normally prepared U-Ni-A.

The author wishes to express his thanks to Professor Kazuo Hata for his continuous encouragement throughout this work.

Department of Chemistry
Faculty of Science
Tokyo Metropolitan University
Setagaya-ku, Tokyo

A Theoretical Treatment of Molecular Complexes. I. Silver-Aromatic Hydrocarbon Complexes

By Kenichi FUKUI, Akira IMAMURA, Teijiro YONEZAWA and Chikayoshi NAGATA

(Received January 11, 1961)

Theoretical researches of molecular complexes have become active since Mulliken combined the old concepts of molecular compound and established a new theory[1]. Prior to this research many qualitative discussions on molecular complexes had been presented. These are the covalent bond theory by Bennett and Willis[2], the polarization aggregate theory by Briegleb[3], the ionic complex theory by

1) R. S. Mulliken, *J. Am. Chem. Soc.*, **74**, 811 (1952).

2) G. M. Bennett and G. H. Willis, *J. Chem. Soc.*, **1929**, 256.

3) G. Briegleb, *Z. physik. Chem.*, **B16**, 249 (1932).

Weiss[4], and the complex resonance by Brackmann[5]. Weiss had pointed out that molecular complexes have an ionic structure B^+A^-, so that the lower the ionization potential for an electron donor is, and the higher the electron affinity for an electron accceptor is, the more easily the molecular complex is formed. Brackmann regarded the structure of complex as a resonance hybrid to which no-bond and dative structures contribute.

$$D:A \leftrightarrow D^+:A^-$$

Based upon these concepts, Mulliken presented a quantum mechanical theory on the charge transfer spectra of molecular complex[1]. Further, Mulliken predicted the configuration of benzene-iodine complex, benzene-silver complex and BF_3–$N(CH_3)_3$ complex, and his assumption was proved to be correct except in the case of benzene-iodine complex. With regard to benzene-iodine complex, Aono discussed Mulliken's model and presented a corrected one[6]. It may be true that in spite of these successes, Mulliken's procedure is not very useful to discuss the relative ease of complex formation among different molecules. There are often found some trials of discussing this problem by comparing the magnitude of ionization potentials of electron donors. For example, with respect to the silver-aromatic molecular complex, a correlation between the magnitude of ionization potential of methyl derivatives of 1,2-benzanthracene and their equilibrium constants in complex formation was pointed out by Nakajima[7]. However, this treatment has only a limited application since the ionization potential is not the sole factor relating to the ease of complex formation, and is hence not suitable in discussing the configuration of complex.

In the present paper we make use of the delocalization method in order to approach the conformation of molecular compound, finding a clear correlation between the equilibrium constant and the calculated value of the delocalization energy for silver-aromatic hydrocarbon complexes.

Model and Formulation

In this paper the delocalization method was applied to silver-aromatic hydrocarbon complexes. Since it has been confirmed by X-ray diffraction that in silver-benzene complex silver cation is located above the middle of a carbon-carbon bond of benzene plane[8], we assume that silver cation approaches from above the molecular plane to the middle of a carbon-carbon bond of a benzene ring in aromatic hydrocarbons to form the molecular complex. The π electronic stabilization energy due to delocalization from the occupied orbitals of the aromatic hydrocarbon to the lowest vacant orbital of the silver cation is calculated by the perturbation theory. This procedure is quite similar to the one which has been used in the frontier electron theory presented by some of the present authors[9]. When the aromatic molecule is confined to alternant hydrocarbons and their derivatives, and the silver cation is combined with the rth and the sth carbon atoms of the aromatic hydrocarbon by a weak bond, the secular equation of the π part of the total system which includes the silver cation and the aromatic molecule is written in the simple LCAO MO treatment (overlap neglected) as follows:

$$D(\lambda)=\begin{vmatrix} h-\lambda & 0 & 0 & \cdots & 0 & \gamma & \gamma & 0 & \cdots & 0 \\ 0 & a_{11}-\lambda & a_{12} & \cdots & & a_{1r} & a_{1s} & & \cdots & a_{1n} \\ 0 & a_{21} & a_{22}-\lambda & \cdots & & a_{2r} & a_{2s} & & \cdots & a_{2n} \\ \vdots & & & & & & & & & \\ 0 & & & & & & & & & \\ \gamma & a_{r1} & a_{r2} & \cdots & & a_{rr}-\lambda & a_{rs} & & \cdots & a_{rn} \\ \gamma & a_{s1} & a_{s2} & \cdots & & a_{sr} & a_{ss}-\lambda & & \cdots & a_{sn} \\ 0 & & & & & & & & & \\ \vdots & & & & & & & & & \\ 0 & a_{n1} & a_{n2} & \cdots & & a_{nr} & a_{ns} & & \cdots & a_{nn}-\lambda \end{vmatrix}$$

$$=(h-\lambda)\Delta(\lambda) -\gamma^2\{\Delta_{rr}(\lambda)+\Delta_{ss}(\lambda)-2\Delta_{rs}(\lambda)\} \quad (1)$$

where

$$\Delta(\lambda)=\begin{vmatrix} a_{11}-\lambda & a_{12} & \cdots & a_{1n} \\ a_{21} & a_{22}-\lambda & \cdots & a_{2n} \\ \vdots & \vdots & & \vdots \\ a_{n1} & a_{n2} & \cdots & a_{nn}-\lambda \end{vmatrix} \quad (2)$$

is the secular determinant for the isolated aromatic molecule, and $\Delta_{rr}(\lambda)$, $\Delta_{ss}(\lambda)$, and $\Delta_{rs}(\lambda)$ are the minors of $\Delta(\lambda)$ corresponding to (rr), (ss) and (rs) elements, respectively; a_{ii} and $a_{ij}(i\neq j)$ are the Coulomb and the resonance integrals, respectively; and h and γ are the Coulomb integral of the silver cation and the resonance integral between the silver cation and the rth and the sth atoms of the aromatic molecule at which the delocalization of π electron takes place, respectively. In presenting the value of energies, we make the zero point equal to the Coulomb integral of

4) J. Weiss, *J. Chem. Soc.*, **1942**, 245; **1943**, 462.
5) W. Brackmann, *Rec. trav. chim.*, **68**, 147 (1949).
6) S. Aono, *Progr. Theoret. Phys. Japan*, **22**, 313 (1959).
7) T. Nakajima, *The Science Reports of the Tôhoku Univ. Ser. I*, **41**, 171 (1957).
8) R. E. Rundle and J. H. Goring, *J. Am. Chem. Soc.*, **72**, 5337 (1950).
9) K. Fukui, T. Yonezawa and C. Nagata, This Bulletin, **27**, 423 (1954).

benzene carbon and express them in units of $(-\beta)$ which is the resonance integral of the benzene C–C bond. If we designate the roots of $\Delta(\lambda)=0$ and $D(\lambda)=0$ as

$$\lambda_1, \lambda_2, \cdots\cdots \lambda_n\ ;\ \lambda^{(1)}, \lambda^{(2)} \cdots\cdots {}^{(n)}, \lambda^{(h)}$$
$$(\lambda_1 > \lambda_2 > \cdots\cdots > \lambda_n)$$

respectively, among which $\lambda^{(h)}$ will be very close to the value of h and $\lambda^{(j)}$ to λ_j $(j=1,2 \cdots\cdots n)$ since γ is small. Namely $\lambda^{(j)}$ and $\lambda^{(h)}$ can be written as $\lambda^{(j)}=\lambda_j+\delta_j$, $\lambda^{(h)}=h+\delta_h$ in which $|\delta_j|$ and $|\delta_h|$ are small. For simplicity, we exclusively treat the following two cases in which $\Delta(\lambda)$ has no multiple root.

Case 1: When h is not equal to any λ_j, we can obtain δ_j as

$$\left.\begin{aligned}\delta_j &= 2\left\{\frac{\Delta_{rr}(\lambda_j)}{(h-\lambda_j)\Delta'(\lambda_j)} + \frac{\Delta_{ss}(\lambda_j)}{(h-\lambda_j)\Delta'(\lambda_j)} - \frac{2\Delta_{rs}(\lambda_j)}{(h-\lambda_j)\Delta'(\lambda_j)}\right\}\gamma^2 + [\gamma^4] \\ &\qquad (j=1,2\cdots\cdots n) \\ \delta_h &= -\sum_{j=1}^{n}\left\{\frac{\Delta_{rr}(\lambda_j)}{(h-\lambda_j)\Delta'(\lambda_j)} + \frac{\Delta_{ss}(\lambda_j)}{(h-\lambda_j)\Delta'(\lambda_j)} - \frac{2\Delta_{rs}(\lambda_j)}{(h-\lambda_j)\Delta'(\lambda_j)}\right\}\gamma^2 \\ &\quad + [\gamma^4]\end{aligned}\right\} \quad (3)$$

where $[\gamma^4]$ denotes the higher terms. The delocalization energy, ΔE, is defined as follows:

$$\Delta E = 2\sum_{j=1}^{m}(\lambda^{(j)}-\lambda_j) \quad (4)$$

$$= 2\sum_{j=1}^{m}\left\{\frac{\Delta_{rr}(\lambda_j)+\Delta_{ss}(\lambda_j)-2\Delta_{rs}(\lambda_j)}{(h-\lambda_j)\Delta'(\lambda_j)}\right\}\gamma^2 + [\gamma^4]$$

$$= -2\sum_{j=1}^{m}\frac{(C_r^j+C_s^j)^2}{h-\lambda_j}\gamma^2 + [\gamma^4] \quad (5)$$

where $j=1,2\cdots\cdots m$ denote the occupied orbitals, and the rth and the sth carbon atoms are adjacent to each other. And C_r^j is the coefficient of the rth atomic orbital in the jth molecular orbital of the isolated aromatic molecule. When h is equal to zero, then the total delocalization energy becomes

$$\Delta E = \{S_r^{(E)} + S_s^{(E)} + 2S_{rs}^{(E)}\}\gamma^2 + [\gamma^4] \quad (6)$$

where $S_r^{(E)}$, $S_s^{(E)}$ are superdelocalizabilities at the rth and the sth carbon atoms for the electrophilic reaction[9], and $S_{rs}^{(E)}$ is given in Eq. 7 and may be named bond-delocalizability of the bond rs.

$$S_{rs} = \sum_{j=1}^{n}\frac{(\nu_j-\nu)C_r^jC_s^j}{\lambda_j} \quad (7)$$

where ν_j is the number of π electrons in the jth molecular orbital and ν is the number of π electrons in the approaching orbital to or from which the delocalization of electrons occurs. $S_{rs}^{(E)}$ designates S_{rs} in which $\nu=0$.

The formula obtained by Eq. 5 indicates that the magnitude of delocalization energy depends sensitively upon the local symmetry of the molecular orbital; that is to say, when C_r^j and C_s^j have same signs, the magnitude of delocalization energy is large, while it is small in case of different signs. It may be stressed that a conclusion similar to that of Mulliken has thus been derived by the present treatment.

Case 2: When h is equal to the energy of the highest occupied orbital of the isolated aromatic molecule λ_f,

$$\left.\begin{aligned}\delta_j &= 2\left\{\frac{\Delta_{rr}(\lambda_j)}{(h-\lambda_j)\Delta'(\lambda_j)} + \frac{\Delta_{ss}(\lambda_j)}{(h-\lambda_j)\Delta'(\lambda_j)} - \frac{2\Delta_{rs}(\lambda_j)}{(h-\lambda_j)\Delta'(\lambda_j)}\right\}\gamma^2 + [\gamma^4] \\ &\qquad (j=1,2,\cdots\cdots n) \\ \left.\begin{matrix}\delta_h \\ \delta_f\end{matrix}\right\} &= \pm\sqrt{-\frac{\Delta_{rr}(h)+\Delta_{ss}(h)-2\Delta_{rs}(h)}{\Delta'(h)}} \\ &\quad \times\gamma + [\gamma^2]\end{aligned}\right\} \quad (8)$$

and the delocalization energy depends dominantly upon the term of first order. Hence, we obtain

$$\Delta E = 2\sqrt{-\frac{\Delta_{rr}(h)+\Delta_{ss}(h)-2\Delta_{rs}(h)}{\Delta'(h)}}\gamma + [\gamma^2]$$
$$= 2|C_r^f + C_s^f|\gamma + [\gamma^2] \quad (9)$$

It may be remarked that in case 2, the magnitude of ΔE depends upon the local symmetry of the highest occupied orbital, the frontier orbital at the bond to be attacked.

Then the following conclusion can be derived. When h is not equal to any λ_j, the larger the value of $-\sum_j \frac{(C_r^j+C_s^j)^2}{h-\lambda_j}$ is, the easier the molecular complex formation is, and when h is equal to λ_f, the reactivity is proportional to $|C_r^f+C_s^f|$.

Results and Discussion

The easiness of the molecular complex formation depends upon many factors such as delocalization energy, dispersion energy, exchange repulsion energy and electrostatic energy. Therefore, the reactivity should be discussed under consideration of all these factors. In discussing the relative easiness of complex formation of a series of similar compounds, however, it is expected that the energies, other than delocalization energy, contributing to the activation energy, may be approximately constant or negligible. In such a case, the delocalization energy is considered to play a dominant role.

In the present paper, an attempt is made to

TABLE I. THE VALUES OF THE INDEX FOR COMPLEX FORMATION AND THE EQUILIBRIUM CONSTANT FOR THE COMPLEX BETWEEN SILVER CATION AND AROMATIC COMPOUNDS

Aromatic compound	K_1 (mol./l.)$^{-1}$	$S_r^{(E)}+S_s^{(E)}+2S_{rs}^{(E)}$	Energy of the highest occupied orbital
	2.41	1.333	−1.000
	2.63	1.402	−0.669
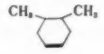	2.89	1.553	−0.707
	2.95	1.418	−0.823
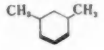	3.03	1.466	−0.763
	3.08	1.600	−0.618
	3.67	1.798	−0.605
	3.94	1.370	−0.705
	6.3	2.139	−0.504
	18.2	2.089	−0.662

Thick lines in the figure of aromatic compounds indicate the bonds with maximum value of the index, which are assumed to be the positions of attack by silver cations.

With regard to toluene and xylene, and carbon-carbon bond adjacent to the methyl group is not taken into account for the sake of steric circumstances.

K_1 is the equilibrium constant for the following reaction

$$Ag^+ + Ar = AgAr^+ \qquad K_1 = (AgAr^+)/(Ag^+)(Ar)$$

explain the reactivity of complex formation of a series of similar compounds by the consideration of the delocalization energy only. The delocalization energies calculated by the formulas stated above are tabulated in Table I together with the equilibrium constants of the first step of the molecular complex formation between silver cation and aromatic compound[10]. A clear parallelism is seen between the index and the equilibrium constant. The parameters used in calculation for methyl group are as follows.

α_{CH_3} (Coulomb integral for methyl group in Eq. 1) = 3

$\beta_{C\text{-}CH_3}$ (resonance integral for CH_3-C bond in Eq. 1) = 1

The energies of the highest occupied levels thus obtained are compared with the observed ionization potentials in Table II. At a glance at this table, a good parallelism is observed between the ionization potential and the energy of the highest occupied level. This implies that the adopted parameters should be appropriate.

TABLE II. RELATION BETWEEN THE IONIZATION POTENTIAL AND THE HIGHEST OCCUPIED LEVEL IN AROMATIC COMPOUNDS

Aromatic compound	Ionization potential eV.	Highest occupied level
Benzene	9.24[a]	−1.000
Toluene	8.82[b]	−0.823
m-Xylene	8.58[a]	−0.763
o-Xylene	8.58[a]	−0.707
p-Xylene	8.48[a]	−0.669
Naphthalene	8.12[a]	−0.618

a; From F. H. Field and J. L. Franklin, "Electron Impact Phenomena", Academic Press, Inc., New York (1957).

b; K. Watanabe, *J. Chem. Phys.*, **26**, 542 (1957).

The value of index for *o*-xylene seems too large. This discrepancy may partly be ascribed to the neglect of the effect of the steric hindrance between two methyl groups. With regard to biphenyl, the calculation is carried out with

10) L. J. Andrews and R. R. M. Keefer, *J. Am. Chem. Soc.*, **71**, 3644 (1949); **72**, 5034 (1950).

TABLE III. THE VALUES OF THE INDEX FOR COMPLEX FORMATION AND THE EQUILIBRIUM CONSTANT FOR THE COMPLEX BETWEEN SILVER CATION AND POLYCONDENSED AROMATIC HYDROCARBONS

Aromatic compound	K_1	$S_r^{(E)}+S_s^{(E)}+2S_{rs}^{(E)}$	Energy of the highest occupied orbital
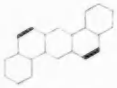	1.65	1.864	−0.474
	1.35	1.747	−0.414
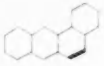	1.33	1.900	−0.452
	1.30	1.737	−0.568
	1.09	1.798	−0.605

Thick lines in the figure of aromatic compounds indicate the bonds with maximum value of the index, which are assumed to be the positions of attack by silver cations.

K_1 is the equilibrium constant for the following reaction.

$$Ag^+ + Ar \rightleftarrows AgAr^+ \qquad K_1 = (AgAr^+)/(Ag^+)(Ar)$$

the assumption that this compound has a plane structure. Experimental data show that this compound is not planar. If two benzene nuclei are but little conjugated with each other, the value of the equilibrium constant for this compound may reasonably be expected to be approximately twice as large as that of benzene as was pointed out by Andrews et al.[10] On the other hand, the index is scarcely affected by the degree of conjugation between two benzene nuclei. On the occasion of comparison with the value of the index, therefore, the observed value of equilibrium constant must be divided by a factor which is larger than unity and smaller than two. This is the reason why the observed value of the equilibrium constant seems too large in comparison with the magnitude of the index calculated.

It seems that also the value of energy of the highest occupied orbital can be a good measure for complex formation. This fact shows that the ionization potential is also useful as a rough index to discuss the easiness of complex formation, though it is impossible to predict the position of attack as stated above.

Furthermore, the complex formation in polycondensed aromatic hydrocarbons is treated in a similar manner and the results are shown in Table III. In this series the parallelism between the value of index and equilibrium constant[11] is not so good. In these polycondensed aromatic hydrocarbons their molecular size is not uniform. The coordination with silver cations may take place at more than one positions in a molecule which has more than one positions of equal or nearly equal reactivity. One silver cation which has already added to a position in a hydrocarbon molecule will not exert a substantial influence upon the later addition of another silver cation to another position in the same molecule, provided these two positions are sufficiently apart from each other. In such a case, in order to be compared with the calculated value of the theoretical index, the observed value of the equilibrium constant must be modified by considering the number of sites in one molecule as is stated above in the case of biphenyl.

Another factor influencing the easiness of the complex formation is the polarizability which may be different in various cases. This means that ion-induced dipole interactions are not uniform from molecule to molecule, and it is indispensable for the prediction of reactivity to take the ion-dipole interaction into account. This point will be discussed in future.

Faculty of Engineering
Kyoto University
Sakyo-ku, Kyoto

11) R. E. Kofahl and H. J. Lucas, *J. Am. Chem. Soc.*, 76, 3931 (1954).

Infrared Spectra of Cyclohexanoxime and Cyclohexanoxime-d

By Masao KIMURA, Yoko KURODA, Osamu YAMAMOTO* and Masaji KUBO

(Received January 17, 1961)

Although several studies have been made on the infrared spectra of oximes, most of them have dealt with OH and C=N stretching vibration. Other vibrational frequencies of the functional group of oximes such as those of the NO stretching, the OH bending, etc. have attracted less attention. The infrared spectra of diacetyl monoxime and isonitrosoacetone have already been reported[1]. The study was undertaken in an attempt to inquire into the character of the absorption spectra of oximes. However, each molecule of these compounds has a carbonyl group in conjugation with a C=N bond. Moreover, the type of hydrogen bondings in these compounds could not be determined uniquely, because both a nitrogen atom and an oxygen atom in an oxime group as well as the oxygen atom of a carbonyl group may take part in hydrogen bonds as a proton acceptor. In the present study, it is attempted to assign the observed bands of cyclohexanoxime and cyclohexanoxime-*d* to various modes of the functional group. These compounds are devoid of conjugate systems. In addition, the crystal structure of cyclohexanoxime has already been determined by X-ray analysis[2]. It is reported that the crystal consists of trimers linked by O–H···N hydrogen bonds. Accordingly, all absorption bands, at least those observed in the spectra of the solid, can be interpreted as arising from the vibrations of assciated molecules linked by hydrogen bonding of this type.

The infrared spectrum of cyclohexanoxime has been recorded by Cross and Rolfe[3], Palm and Werbin[4], Califano and Lüttke[5], Matsui[6] and Bredereck et al.[7], but no complete assignment of bands has been carried out as yet.

Experimental

A commercial preparation of cyclohexanoxime was purified by recrystallization from a solution in ligroin. A deuterated sample was prepared by exchanging hydrogen of OH groups with deuterium from heavy water. These samples were dried before use.

The spectra were taken with a Hilger H-800 spectrophotometer equipped with rock-salt and potassium bromide prisms, the region scanned covering 4000～500 cm^{-1}. Both potassium bromide disks and Nujol or hexachlorobutadiene mulls were employed for taking the spectra of solids. Solutions of various concentrations in carbon tetrachloride and carbon disulfide were also used in order to observe changes in absorption intensity with concentration. All the infrared spectra were recorded at room temperature.

Assignment and Discussion

All absorptions associated with the functional group –C=N–OH of oximes except for the C=N stretching vibration are expected to show an appreciable concentration dependence, just as is observed in the spectra of diacetyl monoxime and isonitrosoacetone[1]. On deuteration, new bands arising from OD groups should appear in place of all bands attributable to OH groups. Therefore, attention was paid especially to the concentration dependence of absorption intensity as well as to the disappearance of certain bands on deuteration. Bands involving changes in intensity with concentration are listed in Table I. The C=N stretching frequency is also given in Table I, since it is considered to be a frequency characteristic of the functional group of oximes.

OH and OD Stretching Frequencies, ν(OH) and ν(OD).—For the OH stretching vibration, a single sharp band and a composite broad band consisting of two sub-maxima were observed in the range 3600～3000 cm^{-1} (Fig. 1). The intensity of the latter band became strong with increasing concentration at the expense of that of the former. Only the broad band was present in the spectrum of the solid. These bands shifted towards much lower frequencies on deuteration (Table I). The band of the OD stretching vibration showed a general pattern and a concentration change almost identical with those of the OH stretching

* Present address: Kao Soap Company, Wakayamashi.

1) M. Kimura, Y. Kuroda, H. Takagi and M. Kubo, This Bulletin, **33**, 1086 (1960).

2) Y. Okaya, A. Shimada and I. Nitta, ibid., **29**, 210 (1956).

3) L. H. Cross and A. C. Rolfe, *Trans. Faraday Soc.*, **47**, 354 (1951).

4) A. Palm and H. Werbin, *Canad. J. Chem.*, **31**, 1004 (1953).

5) S. Califano and W. Lüttke, *Z. physik. Chem., N. F.* **5**, 240 (1955).

6) Y. Matsui, Symposium on Infrared and Raman Spectroscopy, Tokyo, September, 1959.

7) H. Bredereck, A. Wagner, D. Hummel and H. Kreiselmeier, *Ber.*, **89**, 1532 (1956).

TABLE I. FREQUENCIES OBSERVED FOR THE FUNCTIONAL GROUP OF CYCLOHEXANOXIME AND CYCLOHEXANOXIME-*d*

Frequency, cm^{-1} –CNOH	Frequency, cm^{-1} –CNOD	Intensity change on dilution	Assignment
3598*		increase	ν(OH), free
3250, 3115		decrease	ν(OH), assoc.
	2670*	increase	ν(OD), free
	2400	decrease	ν(OD), assoc.
1662	1652	no change	ν(C=N)
1480 A**		decrease	δ(OH), assoc.
1372* B		increase	δ(OH), free
1237* C		increase	δ(OH), free
	1080 A'	decrease	δ(OD), assoc.
	1015* B'	increase	δ(OD), free
	971* C'	increase	δ(OD), free
961 D	955 D'	decrease	ν(NO), assoc.
948* E	944* E'	increase	ν(NO), free
933* F	930* F'	increase	ν(NO), free
795			γ(OH), assoc. (solid)
740*		decrease	γ(OH), assoc. (soln.)
	580		γ(OD), assoc. (solid)
	535*	decrease	γ(OH), assoc. (soln.)

* These bands were not found in the spectra of the solid.
** Some of the peaks in Figs. 2 and 3 are indicated by letters.

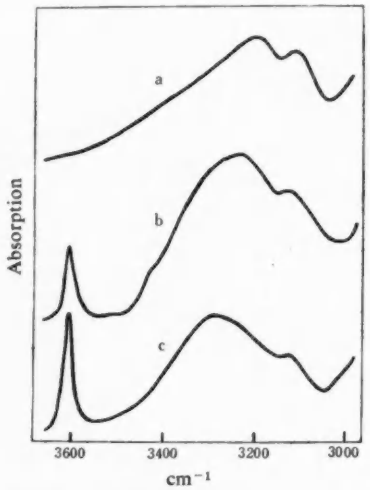

Fig. 1. Infrared absorption spectra of cyclohexanoxime. (a) Solid in a KBr disk, 2 mg./200 mg. KBr. (b) 0.24 mol./l. CCl_4 solution, 0.2 mm. cell. (c) 0.10 mol./l. CCl_4 solution, 0.53 mm. cell.

vibration. However they were masked by the absorption bands of carbon dioxide to such an extent that it was not feasible to locate them exactly. The single sharp band and the broad band were ascribed to the stretching vibrations of the OH or OD bond of free molecules and associated molecules, respectively.

The broad band of bonded OH groups at about 3200 cm^{-1} showed nearly the same appearance regardless of the state of the samples (Fig. 1), indicating that the type of hydrogen bonding formed in solution was –OH···N=C<. The appearance of the band was almost independent of the concentration of solutions. Accordingly, the presence of two sub-maxima in the bonded OH stretching band observed in solutions is not attributable to different kinds of hydrogen bondings or to various polymeric molecules involving hydrogen bondings of various extents. In the spectra of diacetyl monoxime and isonitrosoacetone, similar composite absorptions having few sub-maxima were observed for the bonded OH stretching vibrations. In the previous paper, the form of hydrogen bonding was presumed for these compounds to be of the –OH···O=C< type. However, unlike the behavior of the stretching band of bonded OH groups in cyclohexanoxime, the shape of the bands and the position of the sub-maxima in the spectra of diacetyl monoxime and isonitrosoacetone changed to some extent with the state of aggregation and also with the concentration of solutions. The frequency shift of the OH stretching vibration caused by association was about 240 cm^{-1} in diacetyl monoxime and isonitrosoacetone, whereas it was about 400 cm^{-1} in cyclohexanoxime. This suggests that the

hydrogen bonds in cyclohexanoxime are different from and stronger than those in diacetyl monoxime and isonitrosoacetone.

C=N Stretching Frequency, ν(C=N). — Only one absorption band of medium intensity could be observed in the range 1750～1500 cm^{-1} (Table I). Accordingly, this absorption was assigned to the C=N stretching vibration. The band showed no change in its intensity with concentration and state, although deuteration caused a slight lowering of the frequency.

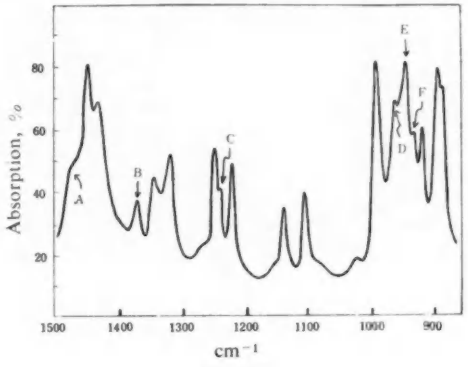

Fig. 2a.

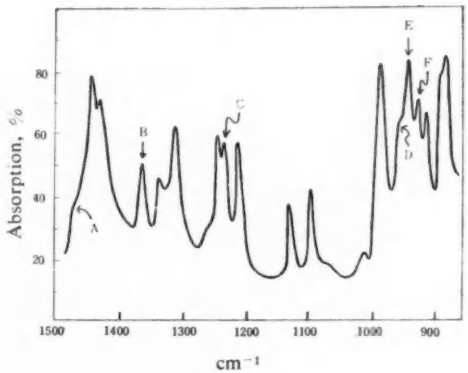

Fig. 2b.

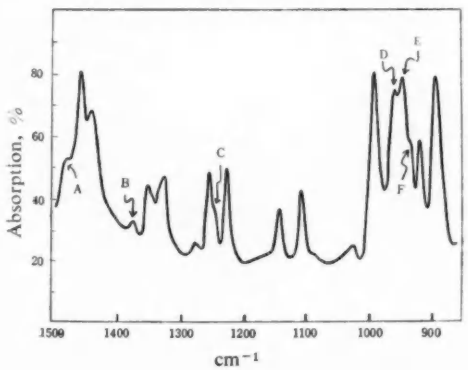

Fig. 2c.

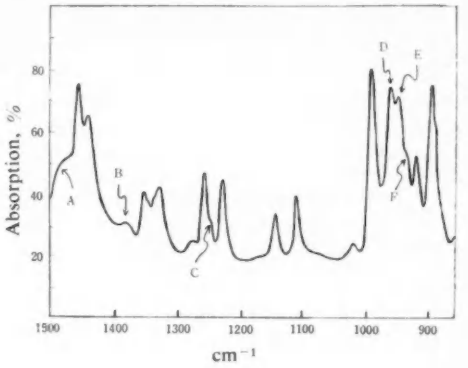

Fig. 2d.

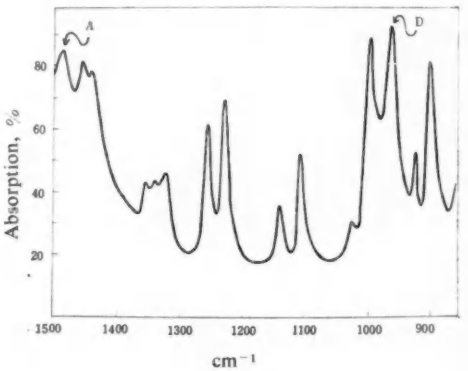

Fig. 2e.

Fig. 2. Infrared absorption spectra of cyclohexanoxime. (a) 0.055 mol./l. CCl_4 or CS_2 solution, 1.6 mm. cell. (b) 0.22 mol./l. CCl_4 or CS_2 solution, 0.4 mm. cell. (c) 0.88 mol./l. CCl_4 solution, 0.1 mm. cell. (d) 1.77 mol./l. CCl_4 solution, 0.05 mm. cell. (e) Solid in a KBr disk, 2 mg./200 mg. KBr.

The value of 1662 cm^{-1} for the C=N stretching vibration is in agreement with 1669 cm^{-1} reported by Cross and Rolfe[3], 1662 cm^{-1} by Palm and Werbin[4] and 1665 cm^{-1} by Bredereck et al.[7] These values are characteristic of unconjugated oximes such as acetaldoxime and formaldoxime and are higher than those of conjugated oximes such as diacetyl monoxime (1630 cm^{-1}) and isonitrosoacetone (1613 cm^{-1}). Since in cyclohexanoxime, diacetyl monoxime and isonitrosoacetone, association caused no frequency shift of the C=N stretching band while deuteration was accompanied by a shift of only about 10 cm^{-1}, a separation between the C=N stretching frequencies of conjugated and

unconjugated oximes is presumably due to the difference in the double bond character of the C=N bond. In fact, the C=N bond of *p*-benzoquinone monoxime involving a very strong conjugation absorbs at 1555 cm^{-1}, which is much lower than the corresponding wave number of diacetyl monoxime and isonitrosoacetone[8].

OH and OD In-plane Bending Frequencies, δ(OH) and δ(OD), and Out-of-plane Bending Frequencies, γ(OH) and γ(OD). — Bands disappearing on deuteration and the corresponding bands of the deuterated compound are associated with the absorptions by OH and OD groups, respectively (Table I). Such bands appearing below 1500 cm^{-1} can be classified into two groups on the basis of their frequencies and the widths. One of them includes bands showing a distinct absorption peak in the higher frequency region except for a band at 1480 cm^{-1}, which was partly masked by a strong absorption due to the CH_2 bending. The other is comprised of relatively diffuse bands appearing in the lower frequency region. Bands at 1480, 1372 and 1237 cm^{-1} and the corresponding bands of the deuterated compound at 1080, 1015 and 971 cm^{-1} belong to the former group and must be ascribed to the in-plane bending vibration of the OH and OD groups, respectively, because they are in a wave number range, in which this kind of vibration is usually expected (Figs. 2 and 3). The band of cyclohexanoxime near 750 cm^{-1} and that of the deuterated compound at about 550 cm^{-1} belong to the latter group and were assigned to the out-of-plane bending vibration of the OH and OD groups, respectively (Figs. 4 and 5). No absorption band arising from the OH out-of-plane bending vibration of free molecules will be observed in the potassium

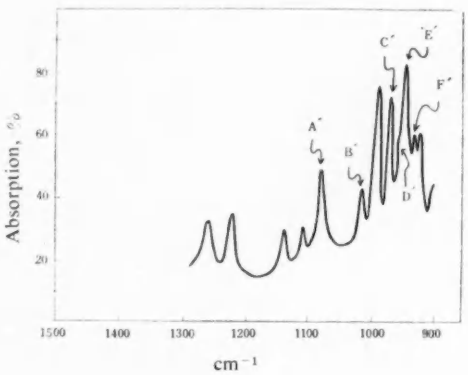

Fig. 3a.

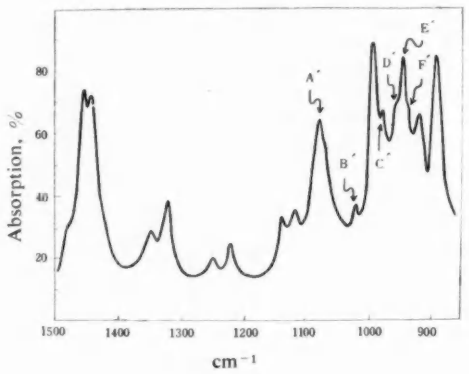

Fig. 3b.

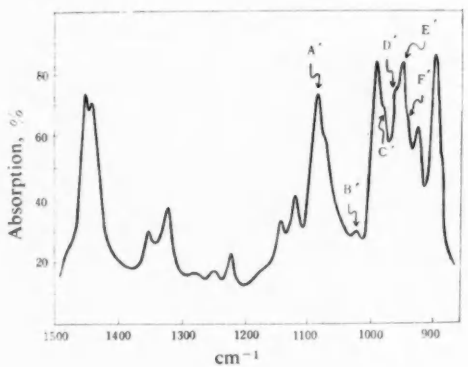

Fig. 3c.

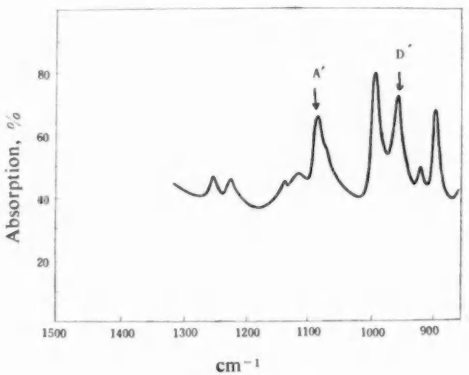

Fig. 3d.

Fig. 3. Infrared absorption spectra of cyclohexanoxime-*d*. (a) 0.035 mol./l. CS_2 solution, 1.5 mm. cell. (b) 0.22 mol./l. CCl_4 or CS_2 solution, 0.5 mm. cell. (c) 0.56 mol. CCl_4 solution, 0.2 mm. cell. (d) Solid in a Nujol mull.

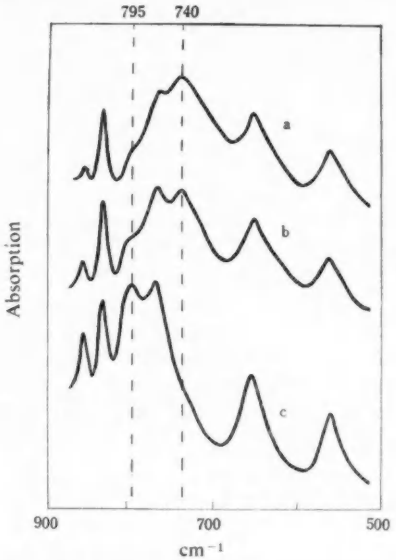

Fig. 4. Infrared absorption spectra of cyclohexanoxime. (a) 0.168 mol./l. CS_2 solution, 0.53 mm. cell. (b) 1.04 mol./l. CS_2 solution, 0.083 mm. cell. (c) Solid in a Nujol mull.

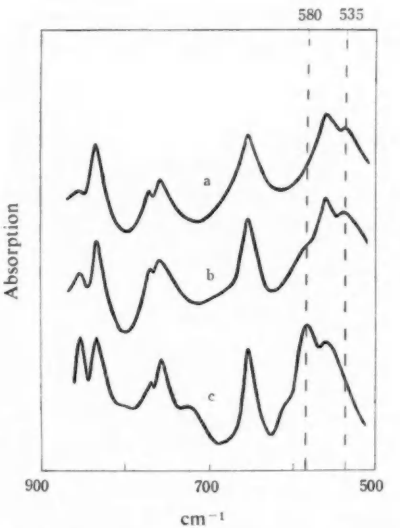

Fig. 5. Infrared absorption spectra of cyclohexanoxime-*d*. (a) 0.168 mol./l. CS_2 solution, 0.53 mm. cell. (b) 1.04 mol./l. CS_2 solution, 0.083 mm. cell. (c) Solid in a Nujol mull.

bromide region. Generally speaking, the OH or OD bending frequency of associated molecules of organic compounds is higher than that of free molecules. Bands arising from free molecules must be absent in the spectra of solids. Thus, the band of cyclohexanoxime at 1480 cm^{-1} and that of the deuterated compound at 1080 cm^{-1} were reasonably assigned to the vibration of associated molecules. This assignment is consistent with the change of intensity with concentration.

Two bands were found to be associated with the OH in-plane bending vibration of free molecules. A similar situation was observed in some alcohols by Tarte and Deponthière[9] and Maclou and Henry[10]. For instance, Tarte and Deponthière have reported two bands at 1243 and 1030 cm^{-1} for ethanol vapor and assigned them to the OH in-plane bending vibration of free molecules, because these bands were replaced by two bands at 890 and 790 cm^{-1} on deuteration. As was pointed out Tarte and Deponthière, two reasons are conceivable for the origin of the appearance of two bands: rotational isomerism about a C–O bond and some coupling such as Fermi resonance. Pritchard and Nelson[11] interpreted the bands of *tert*-butanol in solutions at 1329 and 1141 cm^{-1} as the coupled bands of the CH_3 rocking and the OH in-plane bending of free molecules. However, such coupling seems unlikely to exist in cyclohexanoxime. The ratio of the product of two frequencies for the OH in-plane bending vibration and that for the OD in-plane bending vibration is 1.72 rather than $\sqrt{2}$ as expected from the product rule. The value seems to favor an interpretation of the double band in terms of rotational isomerism about an N–O bond. Such double OH bending frequency was not observed for diacetyl monoxime and isonitrosoacetone. In these compounds, a lower frequency band due to free OH groups might be masked by other strong absorption bands, although it is conceivable that these compounds have a single OH in-plane bending band. Califano and Lüttke did not mention the double character of the free OH bending vibration in their study on acetaldoxime and formaldoxime. Further examination is required in order to elucidate this problem.

Bands at 795 and 580 cm^{-1} observed in the crystals of cyclohexanoxime and cyclohexanoxime-*d*, respectively, could not be observed even in concentrated solutions. However, new very broad bands appeared at 740 and 535 cm^{-1}. The frequency difference between crystals and solutions will be due to the different molecular environments.

8) D. Hadži, *J. Chem. Soc.*, **1956**, 2725.
9) P. Tarte and R. Deponthière, *J. Chem. Phys.*, **26**, 962 (1957).
10) M. Maclou and L. Henry, *Compt. rend.*, **244**, 1494 (1957).
11) J. G. Pritchard and H. M. Nelson, *J. Phys. Chem.*, **64**, 795 (1960).

NO Stretching Frequeny, ν(NO).—Bands at 961, 948 and 933 cm^{-1} and the corresponding bands of the deuterated compound at 955, 944 and 930 cm^{-1} can be assigned unequivocally to the NO stretching vibrations (Figs. 2 and 3). From their concentration dependence, it is evident that the band of cyclohexanoxime at 961 cm^{-1} and that of the deuterated compound at 955 cm^{-1} are due to the NO stretching vibration of associated molecules.

Two bands were assigned to the NO stretching vibration of free molecules. They can possibly be ascribed to the respective NO stretching absorptions of two isomers. This fact provides an indirect but additional evidence in favor of the presence of rotational isomers. Deuteration gave rise to a slight shift of the NO stretching frequency to a lower frequency, while association caused a shift to a higher frequency by about 13 cm^{-1}, which is nearly equal to the amount of shift observed in diacetyl monoxime and isonitrosoacetone[1]. The NO stretching frequency observed in the present study is lower than those of *p*-benzoquinone monoxime and naphthoquinone monoximes[8] at about 1000 cm^{-1}, but is much higher than those of alkyl nitrites[12] covering a range 814 ~751 cm^{-1}.

12) P. Tarte, *Bull. soc. chim. Belges*, **60**, 227 (1951); *J. Chem. Phys.*, **20**, 1570 (1952).

Summary

The infrared absorption bands due to the functional group of cyclohexanoxime and cyclohexanoxime-*d* were reasonably assigned by taking into account the concentration dependence of these bands in solutions. Cyclohexanoxime having no conjugate system showed a spectral feature different in many respects from that of diacetyl monoxime or isonitrosoacetone already studied. The type of hydrogen bonding is $-OH\cdots N-C<$ both in solutions and in the solid state. Consequently, the stretching frequency of bonded OH groups of cyclohexanoxime is different from those of diacetyl monoxime and isonitosoacetone. The doubling of absorption bands was observed for both the OH in-plane bending vibration and the NO stretching vibration of free molecules. This suggests the presence of rotational isomers. The wave numbers of the C=N stretching vibration is higher, while that of the NO stretching vibration is lower than those of the corresponding vibrations of diacetyl monoxime and isonitrosoacetone. This indicates that the double bond character of the C=N bond in cyclohexanoxime is greater than that in oximes having a conjugate system.

Department of Chemistry
Nagoya University
Chikusa-ku, Nagoya

---

*Dye-sensitized Photopolymerization of Vinyl Compounds. Polymerization of Acrylonitrile by Stannous Chloride and Acriflavine. I**

By Ai WATANABE and Masao KOIZUMI

(Received January 17, 1961)

The photochemical polymerization of vinyl compounds in the presence of a dye and a suitable reducing agent has been found by Oster[1], and it has been proposed that the initiation step is due to a certain kind of radical produced by the action of the oxygen upon leuco dye, which has been formed by the reduction of the original dye. It seems that most of the reactions can be well interpreted by this scheme, and yet there are only a few cases in which detailed kinetic studies have established the above scheme.

For example, the photopolymerization of acrylonitrile in the presence of a dye and a metallic ion such as Sn^{2+}, has not yet fully investigated, though it has been established by Oster that such systems are excellent for the preparatory purpose[2].

In the course of the preliminary investigations upon such systems which include more than twenty dyes and various reducing agents such as potassium thiocyanate, thiourea (TU), ascorbic acid (AA), sodium thiosulfate, stannous chloride etc., it was felt that a different scheme may occur in certain cases, especially in cases

* Partly presented at the 12th Annual Meeting of the Chemical Society of Japan, Kyoto, April, 1959.

1) G. Oster, *Nature*, **173**, 300 (1954).

2) G. Oster, *Chem. Abstr.*, **53**, 12747 (1959).

Table I. Some results of the preliminary experiments
[D] $=1.2\times10^{-4}$ M, [reducing agent] $=0.12$ M

		KSCN	TU	AA	$SnCl_2$**	$Na_2S_2O_3$	None
Thionine	P	+	+	−	+	−	−
	B	++	++	(+)	+++		
Methylene blue	P	+	+	−	++	−	−
	B	+	++	(+)	+++	++	
Uranine	P	−	±	−	±	−	−
	B		+	(+)	+		
Eosine	P	++	++	−	−	+	−
	B	+	+	+	++		
Erythrosine*	P	++	++	++	±	+	−
	B	++	+	++	++		
Acridine yellow	P	−	+	±	+++	−	−
	B					++	
Acriflavine	P	−	−	±	+++	−	−
	B						

* Concentration is less than 10^{-4} M.
** ca. 2.9×10^{-2} N HCl solution
P: Polymerization, B: Bleaching
+ and − represent respectively the occurrence and non-occurrence of the reaction. The number of + signs roughly gives the magnitude of the reaction. (+) shows that the bleaching takes place completely or nearly completely when mixed.

where stannous chloride is used as a reducing agent. Hence using acriflavine which was found to be most efficient in combination with stannous chloride, we have examined kinetically the effect of various factors upon the rate of photopolymerization. This paper pertains to the results obtained when the system containing dimethylformamide (DMF), water, acrylonitrile (AN), acriflavine (Af or D) and stannous chloride was irradiated in the presence of oxygen.

Preliminary Experiment

More than twenty dyes were tested preliminarily for examining their efficiency in promoting the polymerization, when they were added to the mixture of AN, water, methanol (2:1:1.2 in volume) containing potassium thiosulfate, TU, AA, sodium thiosulfate or stannous chloride as reducing agents. The samples in test tubes were irradiated by a 100 V.–500 W projection lamp (used at 80 V.) placed 10 cm. apart from the tubes for 1 hr. The magnitude of polymerization was visually judged from the quantity of the precipitate produced. The purpose of the experiments was to find extremely prominent cases, and the exact comparison of the result is of course impossible on account of crudeness in procedure, observation etc. In Table I are given the results obtained for the three types of dyes, about which the oxidative and reductive behavior have been examined to some extent. It is evident from the above table that there exists no parallelism between the magnitude of polymerization and the easiness in bleaching and recovery of color. For example, thiazine dyes which are easily reduced as well as rapidly reoxidized by oxygen, have rather a small power of initiating the polymerization. It is ture that the excess of oxygen will inhibit the polymerization since it has been confirmed by the suppression of polymerization by bubbling the air through the solution. But it is expected that the consumption of oxygen during the reoxidation of leuco dye will soon realize the situation in which the polymerization may take place rather smoothly. The above results in thiazine dyes contradict this expectation altogether. On the other hand xanthene dyes, of which the leuco form shows a great resistance against reoxidation by oxygen, can have some power of inducing polymerization when coupled with proper reducing agents. Acridine dyes, which lie between the above two classes as judged from our unpublished results which demonstrate that these dyes make reversible bleaching in the aqueous solution containing Sn^{2+} whether oxygen exists or not, show a very pronounced efficiency for promoting polymerization when used with stannous chloride.

All these facts suggest that the photopolymerization induced by dyes would some in cases go via a different scheme from Oster's, especially in case of acriflavine and stannous chloride.

From such a viewpoint the quantitative investigation upon the system acriflavine-stannous chloride was undertaken.

Experimental

Materials.—Acrylonitrile from American Cyanamide Co. was distilled after dehydrating with calcium chloride, b. p. 76.5°C. Dimethylformamide

(DMF) from Du Pont was dehydrated by potassium carbonate and then distilled, b. p. 151~151.5°C. $SnCl_2 \cdot 2H_2O$ (G. R) and $SnCl_4 \cdot 3H_2O$ (G. R) were used without further purification. Acriflavine from Merck was also used without purification.

Procedure.—As a light source a projection lamp 100 V.-500 W was used at 80 V. The distance between the light source and a reaction cell placed in a thermostat is 33 cm. Mazda Color Filter V-Y3C which cuts off $\lambda <$ ca. 420 mμ is set in front of the reaction cell. In the experiments for studying the effect of light intensity, neutral filters were used. A reaction cell is made of terex glass $1 \times 1 \times 4.5$ cm. and it is connected with a capillary utilized as a dilatometer. The drop of meniscus in the capillary due to polymerization was followed by use of a travelling microscope. All the experiments were done at 35°C except otherwise described.

To prepare the sample for reaction, (1) acrylonitrile, (2) the aqueous solution of dye and (3) DMF dissolving stannous chloride were mixed in a proper ratio. The concentration of dye and stannous chloride in the latter two solutions are adjusted to get a desired composition of the ultimate sample. In studying the effect of [AN], the ratio of 1 and 3 was changed keeping the quantity of 2 as constant, while for investigating the effect of [H_2O] the ratio of 2 and 3 was changed keeping the quantity of 1 as constant. It is to be noted that DMF solution of stannous chloride must be prepared prior to the experiment in order to get a good reproducibility.

In order to separate the polymer the sample, after the reaction, was poured into a large quantity of methanol and the precipitate was washed with methanol containing hydrochloric acid (concentrated hydrochloric acid : methanol = 0.0015 : 1 in volume) and after washing once more with methanol was dried at 40°C in vacuo. The molecular weight of the polymer thus obtained was determined by measuring the viscosity of the solution of DMF containing about 0.1% of polymer at 25°C. To calculate the intrinsic viscosity Schulz and Sing's formula[3] was employed.

$$[\eta] = \frac{\eta_{sp}/c}{1 + 0.28\eta_{sp}}$$

The average molecular weight was evaluated from the following relation[4].

$$[\eta] = 3.92 \times 10^{-4} \overline{M}^{0.75}$$

Results

When the sample containing stannous chloride and acriflavine is irradiated, the polymerization usually commences at once, but when the sample contains only either of the two the polymerization does not occur in fact. There is no dark reaction perceived even when a large quantity of stannous chloride and acriflavine are added. In Fig. 1, curve 1 represents the rate for the sample, AN : H_2O : DMF = 4 : 3 : 4.2 (in volume), [$SnCl_2$] = 2.73×10^{-2} M, [Acriflavine] = 2.73×10^{-4} M. Accompanied with the polymerization, the solution becomes turbid due to the precipitation of the polymer. When the concentration of stannous chloride is small a certain period of induction appears and after that the curve becomes linear (curve 2). As regards curve 3 mention will be made later. In case of a small concentration of dye the rate begins to decrease earlier than in other cases. In all cases the rate was evaluated from the initial linear portion of the curve. It is to be noted that when the same cell was used for a long period of time, the cell walls gradually became opaque and it had to be renewed occasionally. Therefore, it is not always possible to compare and to correlate the data of a different series of experiments described below.

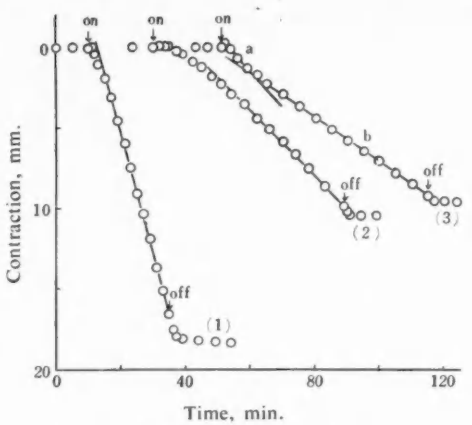

Fig. 1. The contraction-time curves.

	[D] 10^{-4} M	[$SnCl_2$] 10^{-3} M	AN : H_2O : DMF (in volume)
(1)	2.73	27.3	4 : 3 : 4.2
(2)	2.73	1.71	4 : 3 : 4.2
(3)	3.00	11.0	3.6 : 0.51 : 5.89

1. The Effect of Evacuation. — The relative rates of the cautiously degassed samples were 1.02, 1.16 as compared with 1.49, 1.52, 1.46 of the aerated ones ([Acriflavine] = 1.0×10^{-4} M, [$SnCl_2$] = 1.25×10^{-2} M, AN : H_2O : DMF = 3.3 : 2.0 : 4.7 (in volume)). It is evident that the polymerization does take place in the evacuated sample though the rate is somewhat smaller than the aerated solution. The ratio of the rates in two cases being about 1 : 1.4, it seems rather plausible to consider that the effect of oxygen is of the secondary importance (see Discussion). Tentatively assuming the above viewpoint and to orient the investigation, the effect of various factors upon the rate was examined in the first place using aerated solution. Another reason for this was to avoid

3) G. V. Schulz and G. Sing, *J. Prakt. Chem.*, **161**, 161 (1942).
4) P. F. Onyon, *J. Polymer Sci.*, **22**, 13 (1956).

the troublesome procedure for repeated evacuation. The results given below concern only with such aerated samples.

2. The Effect of Dye Concentration. — The variation of the rate when the concentration of acriflavine is changed from zero to 1.4×10^{-4} M is shown in Fig. 2. It is apparent from the

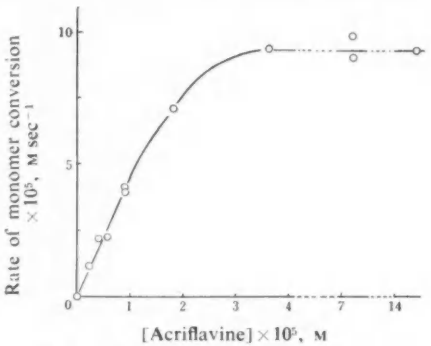

Fig. 2. Dependence of rate on acriflavine concentration.
$[SnCl_2]=1.8\times10^{-2}$ M; AN : H_2O : DMF = 4 : 3 : 4.2 (in volume)

figure that in the region of $\sim10^{-6}$ M of dye, the rate linearly increases with the dye concentration. This was further confirmed by log (rate)~log[AF] curve, which gave the slop of 0.9. When the concentration of dye exceeds ca. 3.5×10^{-5} M, the rate remains constant. From the above results it is concluded that, at a small concentration of dye, the rate is proportional to the dye concentration and it appears to be proportional also to the absorbed light but it will be shown below that it is not the fact (see Sect. 7).

3. The Effect of the Concentration of Stannous Chloride. — The effect of the concentration of stannous chloride on the rate is shown in Fig. 3. Although there exists some scattering of the experimental points, it is still evident that in the low concentration region ($<$ ca. 3.5×10^{-3} M) the linearity holds between the rate and $[SnCl_2]$, and this fact was also confirmed by the slope of 0.9 for log (rate)~log $[SnCl_2]$ plot. Above ca. 10^{-2} M of stannous chloride the rate remains constant. It is to be added that in the case of a high concentration of $[SnCl_2]$ the polymer deposits throughout the entire cell while in case of low concentration, the polymer adheres to the lower half of the front wall of the vessel.

4. The Effect of Monomer Concentration. — In Fig. 4, the rate is plotted against the square of the monomer concentration. It is apparent that the rate $\propto[AN]^2$. Another series of experiments gave a similar result. log(rate)~log[AN] plot gave a straight line of slope 1.9~2.05.

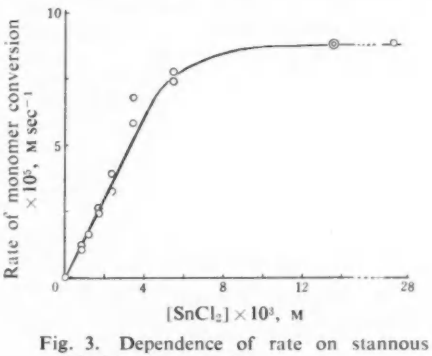

Fig. 3. Dependence of rate on stannous chloride concentration.
$[D]=2.73\times10^{-4}$ M; AN : H_2O : DMF = 4 : 3 : 4.2 (in volume)

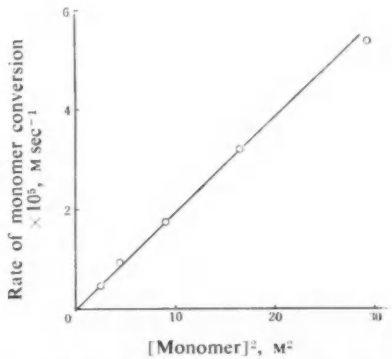

Fig. 4. Dependence of rate on acrylonitrile concentration.
$[D]=3.00\times10^{-4}$ M; $[SnCl_2]=1.37\times10^{-2}$ M; $[H_2O]=14.9$ M

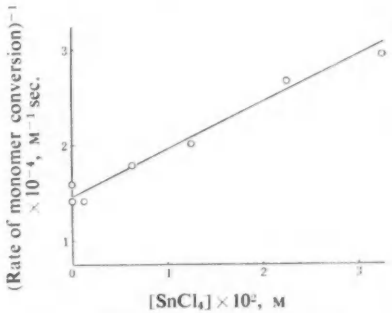

Fig. 5. Dependence of rate on stannic chloride concentration.
$[D]=2.00\times10^{-4}$ M; $[SnCl_2]=1.25\times10^{-2}$ M; AN : H_2O : DMF = 3.6 : 2.5 : 4.0 (in volume)

5. The Effect of the Concentration of Stannic Chloride. — When $SnCl_4$ is added, the rate is decreased. As shown in Fig. 5, there exists an approximate linearity between the reciprocal of the rate and the concentration of stannic chloride.

6. The Effect of Water Content. — It was found that the polymerization can occur without any water being added, and the effect of water content on the rate was investigated in some detail. Time plots in the case of a large quantity of water were simple as shown in Fig. 1 (1), but they were curved as shown in Fig. 1 (3) when the content of water was low. Corresponding to this anomaly the polymer did not appear at first; the above phenomenon may perhaps be connected with the precipitation of the polymer. In Fig. 6 the rate is plotted against $[H_2O]/[DMF]$; × and ○ represent respectively the rates evaluated from parts a and b of the curve. It is apparent from

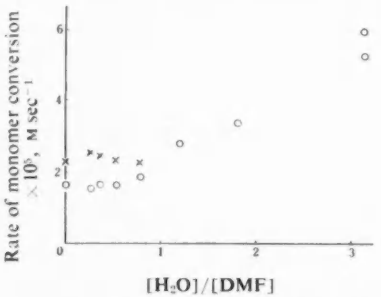

Fig. 6. Dependence of rate on $[H_2O]/[DMF]$.
$[AN]=5.4$ M; $[D]=3.0\times10^{-4}$ M; $[SnCl_2]=1.1\times10^{-2}$ M

the figure that the addition of water up to about $[H_2O]/[DMF]=1$ scarcely affects the rate but a larger quantity causes an increase to some extent. It is known that 1 : 1 complex is formed between DMF and water[5], and the above result might be correlated with this phenomenon.

7. The Effect of Light Intensity. — The intensity of the exciting light was changed to 50, 25 and 11% of the standard light by use of neutral filters. As seen from Fig. 7 the rate is nearly proportional to the root of light intensity. Although these experiments were done only for the samples containing such a large quantity of dye as to absorb almost all the effective light, there is scarcely any doubt that this relation also holds for the case of a small concentration of dye.

8. Average Degree of Polymerization. — The effect of the monomer concentration on the degree of polymerization was examined. As shown in Fig. 8, linear relation holds approximately between $\bar{P}$ and [AN]. The effect of the addition of stannic chloride on $\bar{P}$ was also

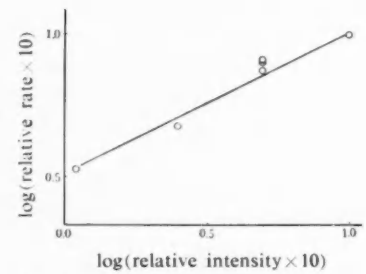

Fig. 7. The intensity exponent.
$[D]=2.00\times10^{-4}$ M; $[SnCl_2]=1.25\times10^{-2}$ M;
AN : H_2O : DMF = 3.6 : 2.5 : 4.0 (in volume)

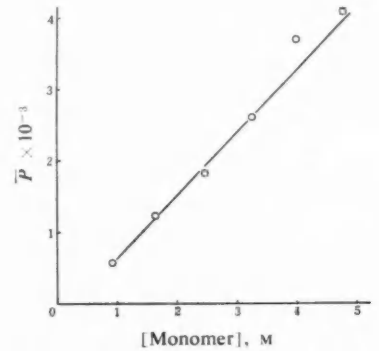

Fig. 8. Dependence of average degree of polymerization on acrylonitrile concentration.
$[D]=2.00\times10^{-4}$ M; $[SnCl_2]=1.25\times10^{-2}$ M; $[H_2O]=13.9$ M

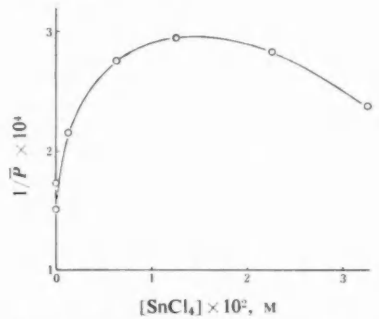

Fig. 9. Dependence of average degree of polymerization on stannic chloride concentration.
$[D]=2.00\times10^{-4}$ M; $[SnCl_2]=1.25\times10^{-2}$ M; AN : H_2O : DMF = 3.6 : 2.5 : 3.9 (in volume)

5) A. D. Jenkins and R. Johnston, ibid., **39**, 81 (1959).

examined. The result is shown in Fig. 9. If stannic chloride only takes part in the termination or chain transfer process, $1/\bar{P}$ should increase monotonously with $[SnCl_4]$, so that it is certain that stannic chloride interferes with other processes, particularly with the initiation step.

9. Activation Energy.—The temperature dependence of the rate was measured in the region from 16.5 to 40°C. The Arrhenius plot is shown in Fig. 10. The rate is almost independent of temperature between 25 and 40°C. But below about 25°C, the rate decreases with the fall of temperature. The apparent activation energy is evaluated to be 7±2 kcal./mol.

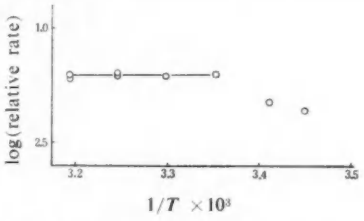

Fig. 10. Arrhenius plot.
$[D]=2.00\times10^{-4}$ M; $[SnCl_2]=1.25\times10^{-2}$ M; AN : H_2O : DMF = 3.6 : 2.5 : 4.0 (in volume)

Discussion

From the result that the polymerization takes place in the degassed solution and with the same order of rate as that of the aerated one, it is certain that the existence of oxygen is not of primary importance for the reaction to occur. Hence it is tentatively assumed that oxygen is not involved in the essential steps of the reaction, particularly in the early stages of the initiation. Then the molecular species which participate in the initiation step would be stannous chloride, acriflavine and AN, since both water and stannic chloride do not affect the rate so much. Thus the addition of stannic chloride as much as 3×10^{-2} M only decrease the rate to about a half and 15 M of water increases the rate only 3~4 times, a small amount scarcely affecting the rate. It may be certain that stannous chloride employed contains a small amount of stannic chloride, but its effect may be neglected from the experimental results. Hence attention will be paid only on the dependence of the rate upon $[SnCl_2]$, [D], [AN] and intensity of light I_0.

Now the overall rate of polymerization is in general expressed by the following equation if the condition of steady state is satisfied.

$$v=k_p[R][M] \qquad (I)$$

where [R] and [M] are the concentrations of growing polymer and monomer. [R] can be expressed by II or III according as the termination process is the first order or the second order in regard to [R].

$$[R]=v_i/k_t \qquad (II)$$

$$[R]=(v_i/k_t)^{1/2} \qquad (III)$$

The experimental rate formula satisfies the following condition

$$v \propto [D][SnCl_2][M]^2$$

and $$v \propto I_0^{1/2}$$

when [D] and $[SnCl_2]$ are small.

Hence v_i in this case must be expressed as follows:

case II, $v_i \propto [D]^{1/2}[D^*]^{1/2}[SnCl_2][M]$

case III, $v_i \propto [D][D^*][SnCl_2]^2[M]^2$

where D* is the excited dye. Case III however can be rejected since it was found experimentally that the following relation holds,

$$\bar{P} \propto [M]$$

and in general $\bar{P}$ may be equated to v/v_i at least approximately (unless the rate of chain transfer is quite appreciable). Thus the initiation processes must be those that satisfy the following relations.

When [D] and $[SnCl_2]$ are small

$$v_i \propto [D]^{1/2}[D^*]^{1/2}[SnCl_2][M] \qquad (IV)$$

When both [D] and $[SnCl_2]$ are large

$$v_i \propto [M]I_0^{1/2} \qquad (V)$$

The equations IV and V look rather unusual and these suggest the peculiar character of the reaction scheme.

Here we propose the following two schemes as plausible ones.

A. $D \xrightarrow[(1)]{h\nu} D^* \xrightarrow[(3)]{D} D^i \xrightarrow[(5)]{Sn^{2+}} (D^- \cdots\cdots Sn^{3+})$

D^* —(2)→ D; D^i —(4)→ D; $(D^- \cdots\cdots Sn^{3+})$ —(6′)→ $D+Sn^{2+}$; $(D^- \cdots\cdots Sn^{3+})$ —(6)→ Leuco + Sn^{4+}

$\xrightarrow[(7)]{Sn^{2+}} D + Sn^+ + Sn^{3+} \xrightarrow{(8)} D + 2Sn^{2+}$
(or $D^- + Sn^{3+}$) (or $D + Sn^{2+}$)

$Sn^{3+} + M \xrightarrow[(9)]{k_1} R$
(or $Sn^+ + M \longrightarrow R$)

B. $D + Sn^{2+} \underset{(0)}{\overset{K_0}{\rightleftharpoons}} (DSn^{2+}) \xrightarrow[(1)]{h\nu} (D^*Sn^{2+})$

(D^*Sn^{2+}) —(2)→ D

$\xrightarrow[(3)]{D} (D^iSn^{2+}) \longrightarrow (D^- \cdots\cdots Sn^{3+})$

(D^iSn^{2+}) —(4)→ D; $(D^- \cdots\cdots Sn^{3+})$ —(6′)→ $D+Sn^{2+}$; $(D^- \cdots\cdots Sn^{3+})$ —(6)→ Leuco + Sn^{4+}

$\xrightarrow[(7)]{Sn^{2+}}$ same as above

In scheme A, Sn^{2+} participates in the steps 5 and 7 while in scheme B a complex is formed between Sn^{2+} and D and the corresponding scheme to 5 in A is lacking. In both schemes it is assumed that the transition from singlet excited state (D^*) to triplet (D^t) is induced by the ground state dye molecule. Although this is plausible and in fact such a process has also been accepted by Oster for the case of acridine dyes[6], it is noteworthy that there is another possibility that the excimer[7] be formed between D and D^*. The discrimination may however be impossible only from the rate formula. ($D^- \cdots\cdots Sn^{3+}$) is supposed to be a charge transfer complex or the like.

For both schemes A and B the essential point is that two kinds of molecular species of radical nature produced by process 7, react almost exclusively in such a way as to produce stable molecular species and only a small fraction of them react with monomer to produce an initiator of polymerization 9. Thus when D^- and Sn^{3+} are produced by 7 electron transfer should rapidly occur between them, recovering D and Sn^{2+}, while when D, Sn^+ and Sn^{3+} are produced, the analogous electron transfer should take place between Sn^+ and Sn^{3+} (8), Sn^+, Sn^{3+}, D^- (this is rather unplausible) or all of them may initiate the polymerization. In fact such schemes as above seem almost indispensable to interpret the following relations consistently.

$$v_i \propto I_0^{1/2}, \qquad v \propto [M]^2, \qquad \bar{P} \propto [M]$$

From the above schemes, the following rate formulas can be derived.

Case A

$$v_i = \left\{\frac{k_1 I_0 k_3 [D]}{k_2 + k_3 [D]}\right\}\left\{\frac{k_5 [Sn^{2+}]}{k_4 + k_5 [Sn^{2+}]}\right\} \times \left\{\frac{k_7 [Sn^{2+}]}{k_6 + k_6' + k_7 [Sn^{2+}]}\right\}^{1/2} \frac{k_9}{k_8^{1/2}} [M] \qquad \text{(VI)}$$

Case B

$$v_i = \left\{\frac{I_0 k_1 K_0 [Sn^{2+}]}{1 + K_0 [Sn^{2+}]}\right\}\left\{\frac{k_3 [D]}{k_2 + k_3 [D]}\right\}\left\{\frac{k_5}{k_4 + k_5}\right\} \times \left\{\frac{k_7 [Sn^{2+}]}{k_6 + k_6' + k_7 [Sn^{2+}]}\right\}^{1/2} \frac{k_9}{k_8^{1/2}} [M] \qquad \text{(VII)}$$

Both VI and VII can express the experimental results satisfactorily as in the following way.

i) Large [D]: v is independent of [D].

$$v \propto I_0^{1/2}$$

ii) Small [D]: $k_1 I_0$ may be put approximately proportional to [D]. Hence

$$v \propto [D]$$

iii) Large $[Sn^{2+}]$: v is independent of $[Sn^{2+}]$.

iv) small $[Sn^{2+}]$: $v \propto [Sn^{2+}]$

v) In all cases, $v \propto [M]^2$

As for the effect of water, both hydration of D and the formation of a certain ion pair from Sn^{2+} and OH^- would favor the reaction. For example the formation of $(SnOH)^+$ would promote processes 5 and 7 in both case A and case B; moreover the hydration of D would also be favorable for these process and in addition, for 3 and 0 (in case B). All these effects together should cause the rate to increase with the content of water. But these effects are of secondary importance in the reaction scheme and to not affect the rate very much.

In connection with the above schemes, it may be worthy of adding here some discussions about the rate of dye bleaching in the absence of acrylonitrile. Provided that process 7 be neglected, the rate of bleaching of dye will be given as follows:

Case A

$$\frac{k_1 I_0 k_3 [D]}{k_2 + k_3 [D]} \cdot \frac{k_5 [Sn^{2+}]}{k_4 + k_5 [Sn^{2+}]} \cdot \frac{k_6}{k_6 + k_6'} \qquad \text{(VIII)}$$

Case B

$$\frac{k_1 I_0 K_0 [Sn^{2+}]}{1 + K_0 [Sn^{2+}]} \cdot \frac{k_3 [D]}{k_2 + k_3 [D]} \cdot \frac{k_5}{k_4 + k_5} \cdot \frac{k_6}{k_6 + k_6'} \qquad \text{(IX)}$$

Thus the similar relation in respect to [D] and $[Sn^{2+}]$ will hold for two cases. But when the process 7 participate in the reaction the rate would decrease when the concentration of Sn^{2+} exceeds a certain value. It may be possible to examine this effect experimentally.

If Oster's mechanism holds in the present case, which postulates the formation of leuco dye prior to the initiation process, the rate formula of initiation would be similar to VIII and IX which contradicts the experimental results altogether. Thus three relations $v \propto I_0^{1/2}$, $v \propto [M]^2$ and $\bar{P} \propto [M]$ can not be interpreted satisfactorily on this basis. Analogous discussion may be extended to the effect of oxygen on the rate, the increase amounting to about 40% of that of the evacuated solution. If this increase is due to the participation of the process $D + SnCl_2 \rightarrow Leuco + SnCl_4$, $Leuco + O_2 \rightarrow$ active radical, then the kinetic order in respect to $[SnCl_2]$ and [D] would be the average of the two simultaneous reactions and

6) F. Millich and G. Oster, *J. Am. Chem. Soc.*, **81**, 1357 (1959).
7) B. Stevens and E. Hutton, *Nature*, **186**, 1045 (1960).

would not be the whole number as experimentally obtained. Hence it seems more plausible that oxygen interferes with the intermediate ($D^-\cdots\cdots Sn^{3+}$) rather than its attack on leuco dye. The discrimination between cases A and B may perhaps be made by spectroscopic investigation. Further investigations are now under way to confirm the above schemes more definitely and to select case A or case B.

Summary

When the aerated solution of acrylonitrile, acriflavine and stannous chloride in the mixture of water and dimethylformamide is irradiated by the visible light, the polymerization of acrylonitrile immediately takes place. The presence of water and oxygen was found to be unnecessary for the reaction to occur. The dependence of rate on the concentration of each species and on the light intensity (I_0) can be summarized as follows.

Acriflavine	$<$ca. 1×10^{-5} M, 1st order;
	$>$ca. 3.5×10^{-5} M, const.
Stannous chloride	$<$ca. 3.5×10^{-3} M, 1st order;
	$>$ca. 1.2×10^{-2} M, const.
Acrylonitrile,	2nd order
I_0,	1/2th order

It was further found that the average degree of polymerization is proportional to the monomer concentration. The scheme involving the photoreduction of dye by stannous chloride and its recovery by the existent oxygen cannot explain the present result. It was proposed as a new mechanism that a transient metallic ion of tin with an odd valency is formed and this, interacting with acrylonitrile, initiates the polymerization.

The present research was mostly performed by Ai Watanabe at Osaka City University and was finished during her stay at Sendai as a visiting research fellow. The authors express their cordial thanks to Professor R. Fujishiro of Osaka City University for his interest and encouragement.

Department of Chemistry
Faculty of Science
Tohoku University
Katahira-cho, Sendai

The Photovoltaic Behavior in Organic Compounds

By Hiroo INOKUCHI*, Yusei MARUYAMA* and Hideo AKAMATU

(Received January 17, 1961)

The study on the photo-electrical behavior in organic semiconductors produced by excitation accompanying absorption of light, especially the investigation of the photoconduction, has been carried out by several workers[1]. However, relatively little is known about the photovoltaic phenomena of these organic compounds[2].

In one of the few articles on this subject, Nelson[3] reported a photovoltaic behavior of junctions between organic compounds and cadmium sulfide in association with optical sensitization in photography. The author proposed that the induced photovoltage is related to the difference in energy between the conduction band of the organics (dye) and that of cadmium sulfide. On the other hand, Calvin and Kearns[4] reported interesting results on photovoltaic organic junctions: Mg-phthalocyanine || tetramethyl-*p*-phenylene diamine and coronene || chloranil junctions.

In this paper, we show that the photovoltaic behaviors have been observed with a simple cell, consisting of a junction between aromatic compounds and metal or stannic oxide. Further, in comparison with other semiconductive behaviors of polycyclic aromatic compounds, the produced electromotive force will be discussed.

Experimental Procedures

For an observation of photo-electromotive force between organic semiconductor and metal or metal

* Present address: The Institute for Solid State Physics, The University of Tokyo, Azabu, Tokyo.

1) H. Inokuchi and H. Akamatu, "Solid State Physics", Vol. 12, Chapter 2, Academic Press. New York, (1961).

2) H. Baba, K. Chitoku and K. Nitta, *Nature*, **177**, 672 (1956).

3) R. C. Nelson, *J. Chem. Phys.*, **22**, 885, 890, 892 (1954), **29**, 388 (1958); *J. Opt. Soc. Am.*, **45**, 774 (1955); **46**, 13 (1956).

4) M. Calvin and D. Kearns, *J. Chem. Phys.*, **29**, 950 (1958).

oxide, a sandwich-type cell was applied. This cell was made by sandwiching aromatic compounds between two electrodes: The evaporated film of aromatic compounds was deposited onto a glass plate which had been coated in advance with a thin metal film or onto a stannic oxide conducting layer to provide a junction electrode. The specimen film was usually one or two microns in thickness. Further, the second electrode was evaporated onto the specimen film. The conducting path between these electrodes extended through the specimen film. The resulting construction of the cell was illustrated in Fig. 1 of the previous report[5].

For the preparation of alkali metal-aromatics junction, as shown in Fig. 1, the alkali metal, evaporated onto organic film as a second electrode under less than 10^{-5} mmHg, acted as a junction electrode. After the evaporation of alkali metal, all observations of their electromotive forces were carried out under a high vacuum to avoid a decomposition of the alkali metal by an action of moisture. However, a fluctuation was frequently introduced concerning the direction of electromotive force. For the elimination of this fluctuation, the construction of a more precise apparatus is in due course.

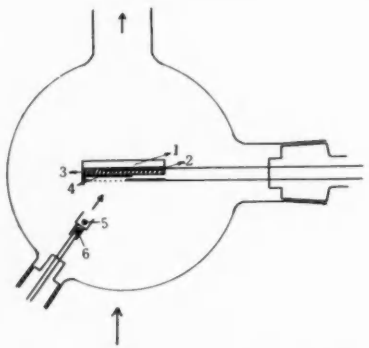

Fig. 1 The arrangement for preparation of alkali metal-aromatics junction. (1) Pyrex glass plate, (2) terminal electrode, (3) aromatic compound, (4) junction metal (alkali metal), (5) nickel dish, and (6) electric heater for evaporation.

The sandwich-type aromatics-aromatics junction was made by the successive evaporation of two sorts of aromatic compounds, kept in the vessel 5 of Fig. 1, onto a conducting glass plate without an intrusion of air into the contact area between these two compounds.

The illumination of white light was produced from a tungsten lamp onto the side of the junction metal. The measurement of induced photovoltage had to be associated with a vibration-reed electrometer because its produced electric power was extremely low. By means of a quartz-prism monochrometer and also of interference filters, a spectral response of photo-electromotive force in the range from 350 mμ to 1300 mμ was observed.

The applied aromatic compounds, perylene, violanthrene and violanthrone, were provided from Drs. T. Handa and also J. Aoki. Coronene, a seven membered aromatic hydrocarbon, was provided from Badisch Anilin und Soda Fabrik, Germany. These organic compounds were purified with a combination of three methods; recrystallization, sublimation and chromatography.

Results and Discussions

When the contact between an organic semiconductor and a metal was illuminated with white light from a tungsten lamp, the induced electromotive force reached immediately a saturated value and this was kept quite steadily for a long period. However, in the alkali metal-aromatics junction it was found that its electromotive force decreased to a value smaller than the original one. This behavior would be introduced from a high reactivity of alkali metal with moisture and/or from a formation of charge transfer complex between the metal and the aromatic compound.

For the noble metal-aromatics junction, the observed photoelectromotive force varied from a few millivolts to 10 mV. depending on the sorts of metals applied to the junction and also on the condition of preparation technique as illustrated in Table I. In all of these photocells, the junction metal acted as a negative electrode against the terminal electrode; thereby, at the junction, electrons flowed from the hydrocarbons to the junction metals under the illumination.

On the other hand, a quite stable photovoltage was produced at the contact between perylene and stannic oxide, and its saturated value reached 80 mV. when a light was incident on it through the transparent stannic oxide electrode (electrical conducting glass electrode). The spectral response of this electromotive force was a curve which is in good coincidence with the optical absorbance curve and also with the response curve of photoconduction for solid perylene as illustrated in Fig. 2.

Similar behavior of the photovoltaic effect was found in the junction between coronene, violanthrene or violanthrone and stannic oxide, whose electromotive forces were 20, 450 and 80 mV. respectively. These four hydrocarbons acted as electron acceptors with respect to stannic oxide under illumination of panchromatic light. However, the spectral response of photovoltage of violanthrone junction was a quite peculiar one as shown in Fig. 3. Its threshold value was found to be around 0.9 eV., which is in agreement with that of the photoconduction of its aromatic compound.

5) H. Inokuchi, H. Kuroda and H. Akamatu, This Bulletin, 34, 749 (1961).

TABLE I. THE PHOTOVOLTAGE OF METAL-AROMATICS JUNCTIONS

Photovoltaic junction		Photo-emf	
Aromatics (sign)	Metal (sign)	Voltage, mV.	Wattage, W.
Violanthrene (+)	Pt (−)	2∼ 3	$\sim 10^{-17}$
Violanthrene (+)	Au (−)	6∼ 9*	$\sim 10^{-16}$
Violanthrene (+)	Ag (−)	Detectable	
Violanthrene (+)	Sn (−)	2∼ 8	$\sim 10^{-16}$
Violanthrene (+)	Pb (−)	4∼14	$\sim 10^{-16}$

* As a special case, emf reached to 50 mV.

TABLE II. THE PHOTO-ELECTROMOTIVE FORCE OF ALKALI METAL-AROMATICS JUNCTIONS

Photovoltaic junction		Photo-emf		
Aromatics (sign)	Metal (sign)	Voltage, V.	Wattage, W.	$J\varepsilon/2$, eV.
Perylene (−)	Li (+)	0.3∼1.0	$\sim 10^{-10}$	1.0
Coronene (−)	Li (+)	0.3	$\sim 10^{-10}$	0.8
Violanthrene (−)	Li (+)	0.3∼0.8	$\sim 10^{-9}$	0.43
Violanthrone (−)	Li (+)	0.2∼0.9	$\sim 10^{-10}$	0.39
Perylene (+)	Na (−)	0.3∼1.0	$\sim 10^{-11}$	1.0
Violanthrene (+)	Na (−)	0.3∼0.8	$\sim 10^{-10}$	0.43
Violanthrone (±)	Na (∓)	0.1∼0.5	$\sim 10^{-5}$	0.39
Perylene (±)	K (∓)	0.2∼0.9	$\sim 10^{-10}$	1.0
Violanthrene (+)	K (−)	0.2∼0.8	$\sim 10^{-10}$	0.43
Violanthrone (−)	K (+)	0.2∼0.5	$\sim 10^{-9}$	0.39

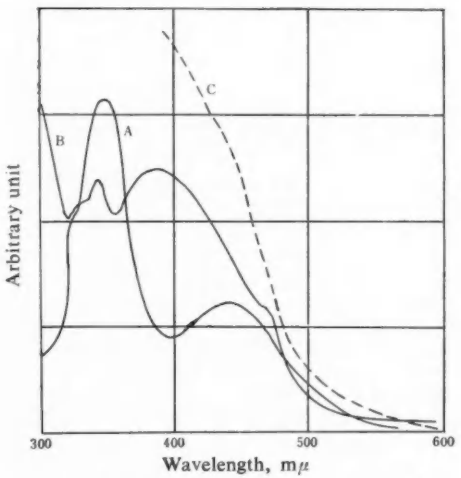

Fig. 2 The spectral response curves of photoconductivity (A), absorption spectrum (B) and photovoltage (C) for perylene in solid phase.

These results imply that the spectral responses of the photovoltage are predominated by the electronic structure of polycyclic aromatic compounds but not by that of stannic oxide. In this connection, no optical absorption in stannic oxide film was found in a visible region longer than 390 mμ.

In the alkali metal-aromatics junction, the induced photo-electromotive force reached to almost one volt as listed in Table II. Its

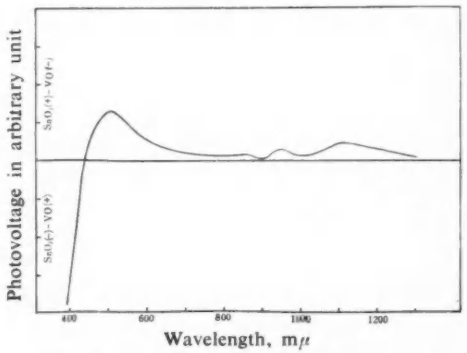

Fig. 3 The spectral response curve of photovoltage for the SnO_2-violanthrone (SnO_2-VO) junction.

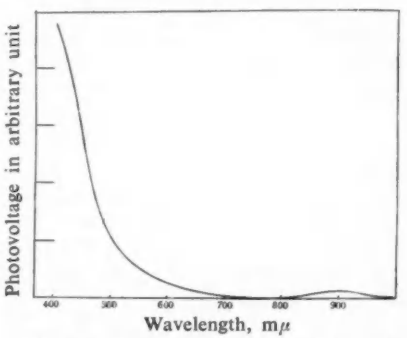

Fig. 4 The spectral response of photovoltage produced at the junction between sodium metal and violanthrene.

spectral response was a curve falling monotonously from short wavelength to long wavelength side. An extrapolation of this decrement found a tentative threshold value, which is sited in a range from 600 to 700 mμ as shown in Fig. 4.

A weak but definite response of photovoltage was found in a longer wavelength region than the extrapolation value. However, further investigations are restricted by fluctuation concerning the direction of electromotive force and also by the lack of stability of the force. In the lithium-aromatics junction, the metal acted as a positive electrode relative to the terminal electrode. Most of the aromatic compounds in the sodium-aromatics junction, however, acted as a positive electrode with respect to sodium; that is to say, electrons were transferred from the hydrocarbons to the junction metal at the junction and then the organic solids acted as electron donors. In the potassium-aromatics junction, the direction of photo-electromotive force was changed depending on the sorts of organic solids and also on the wavelength of incident light.

These values of photovoltage decreased to a small value in time. This decrease may be introduced from the complex formation between aromatic compound and alkali metal and/or may be produced by a decomposition of the junction. These fluctuations on the observed values may be eliminated by means of the application of ultra-high vacuum.

As a preliminary work of aromatics-aromatics junction, we have found that a fairly large electromotive force ($10\sim10^2$ mV.) was produced at the contact between two pure aromatic hydrocarbons; for instance, perylene and violanthrene, under illumination. The details of this work will appear elsewhere.

When a contact between semiconductive material (band gap: $\Delta\varepsilon$) and metal is made, it is believed that the flow of charge carrier, $I_o \exp[-\Delta\varepsilon/2kT]$, happended at the contact and a potential barrier occurs at the boundary layer. On illuminating the contact of junction, the flows of forward and backward currents, I_f and I_b, are expressed as

$$I_f = I_o \exp[-(\Delta\varepsilon/2 - eV_{op})/kT] \quad (1)$$

$$I_b = I_o \exp[-(\Delta\varepsilon/2)/kT] + I_L \quad (2)$$

respectively, where I_L is the excess flow of charge carrier under illumination and V_{op} is photo-electromotive force, measured for an open circuit condition. At an equilibrium condition, V_{op} is expressed as

$$V_{op} = \frac{kT}{e} \ln\left[1 + \frac{I_L}{I_o \exp[-(\Delta\varepsilon/2)/kT]}\right] \quad (3)$$

because of $I_f = I_b$.

When the induced current I_L under illumination of light is large, Eq. 3 is rewritten as

$$V_{op} \fallingdotseq \frac{\Delta\varepsilon}{2e} + \frac{kT}{e} \ln\frac{I_L}{I_o} \approx \frac{\Delta\varepsilon}{2e} \quad (kT \ll e) \quad (4)$$

$$V_{op} \fallingdotseq \frac{kT}{e} \frac{I_L}{I_o} \exp[-(\Delta\varepsilon/2)/kT] \ll 1 \quad (5)$$

For the alkali metal-aromatics junction, it is expected the produced photovoltage, V_{op}, follows Eq. 4 because the excess flow of illuminated current is great. On the contrary, the minute photovoltage for the noble metal-aromatics junctions is explained by Eq. 5 tentatively.

Summary

When a contact between a semiconductive material and a metal is made, it is expected that a potential barrier occurs at the boundary layer and the photovoltaic effect which is observed with illumination on this barrier. It has been found that this is the case for organic semiconductors. The photovoltaic cell was made with aromatic compounds sandwiched between two metal layers or metal and stannic oxide. One of them was a terminal electrode and the other, the junction electrode, was made with evaporated film of platinum, gold, silver, tin, lead or alkali metal. All observations of photovoltage were carried out in vacuo or in an atmosphere of inert gas.

With the illumination of white light from a tungsten lamp, the induced photovoltage varied from several millivolts to one volt, depending on the sorts of metals applied to the junctions. In most of these junctions, the organic solids acted as positive electrodes with respect to the junction metal.

In the alkali metal-aromatics system, a fluctuation was frequently observed concerning the direction of electromotive force, but the value of photovoltage was generally much higher than in the case of the other metals; thus the spectral response of the voltage was measurable. This response was less dependent on the sorts of organic solids but dependent on the sorts of metals. On the other hand, the spectral response in the junction between organic solid and stannic oxide, was a curve which is in good coincidence with the optical absorption curve for solid organics.

The cost of this research has been defrayed from the Grant in Aid for Fundamental Scientific Research from the Ministry of Education, to which the author's thanks are due.

Department of Chemistry
Faculty of Science
The University of Tokyo
Hongo, Tokyo

Isolation of 2,3-Cyclopenteno-5-methylpyridine from Coal Tar Bases

By Hajime SUZUMURA

(Received January 24, 1961)

It was previously reported that 3,4,5-collidine and 2,3-cyclopenteno-6-methylpyridine were isolated from the tertiary amine fraction boiling about 210°C in coal tar bases and their chemical structure were confirmed[1]. On further investigation, a $C_9H_{11}N$ base was isolated by solvent extraction and picrate formation from bases boiling about 220°C. This was identified as 2,3-cyclopenteno-5-methylpyridine, comparing the physical properties of the isolated base and its derivatives with those of the synthesized base[2].

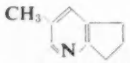

2,3-Cyclopenteno-5-methylpyridine

The presence of this base in coal tar and petroleum distillates has not hitherto been reported. In Table I is shown the comparison of the isolated base with the synthesized compound.

Experimental

Original Material. — The material used in the present investigation is a coal tar base fraction called "toluidine-xylidine fraction" (TX_n) furnished by Yawata Chemical Industry Co., Kyushu, Japan. The boiling point range of the material is shown in Table II. This sample contains 10% of neutral oil and 34% of primary amines determined as xylidines by diazotization-titration, therefore the content of the tertiary amines which constitute the rest of the sample is approximately 56%.

Separation of the Tertiary Amines.—A mixture of 6 kg. TX_n and 1350 cc. of concentrated sulfuric acid was steam-distilled and neutral oil and a small amount of tar acids were respectively removed as a distillate. By addition of sodium hydroxide to the residual acidic solution, 4.84 kg. of the base was recovered. Then, 2.9 kg. of acetic anhydride was added and refluxed to remove the primary amines. The reaction mixture was distilled through a 30 cm. column and the distillate up to 250°C was collected and made alkaline with sodium hydroxide and steam-distilled. The disillate, after being dried over solid sodium hydroxide, was distilled in vacuo through a fractionating column[1] with a reflux ratio of 20:1 and divided into the fractions shown in Table III.

In the fractions Nos. 5 and 6, which were to be examined, the primary amines were still present to a minor extent and the acetylation procedure was repeated.

TABLE I. 2,3-CYCLOPENTENO-5-METHYLPYRIDINE

Property	The isolated base	The synthesized base	
		By the author	Literature[2]
M. p.*, °C	38.5～41	38.7～41	39～41
B. p.*, °C	225 (756 mmHg)	225 (756 mmHg)	222 (752 mmHg)
M. p. of picrate, °C	205.2～206.2	204.8～205.8	204～206
D. p. of picrolonate, °C	211.5～212.5	211.5～212.5	210～212
Elementary analysis			(calcd.)
C, %	80.75	81.12	81.16
H, %	8.39	8.44	8.33
N, %	10.41	10.31	10.52
Neutralization equivalents	134	—	133.2

* M. p. and b. p. (micro method) are corrected values.

TABLE II

Distillate Vol. %	First drop	5	10	50	90	95	Dry point
B. p., °C	200.5	204.0	206.0	210.0	222.5	225.0	228.0

1) S. Jifuku, S. Nakayama, H. Suzumura and M. Uemura, *Coal Tar (Tokyo)*, **10**, 126 (1958).

2) H. L. Lochte and A. G. Pittman, *J. Am. Chem. Soc.*, **82**, 469 (1960).

TABLE III. FRACTIONATION OF THE TERTIARY AMINES

No. of fraction	B. p. (30 mmHg) °C	Distillate g.	n_D^{25}	B. p. (micro) °C	Xylidine %
1	FD~102	277.7	1.5160		
2	102~106	112.9	1.5207		
3	106~111	163.7	1.5348		
4	111~114	65.5	1.5319	213.1	12.1
5	114~117	135.3	1.5309	223.6	7.3
6	117~121	64.7	1.5387	227.6	3.6
7	121~125	109.1	1.5720	231.0	
8	125~	1941.0			
	Total	2869.9			

The properties of the fraction, after this treatment, are shown in Table IV.

TABLE IV

No. of fraction	4'	5'	6'
n_D^{25}	1.5277	1.5281	1.5345
Yield, g.	50	117	49

Isolation of 2, 3-Cyclopenteno-5-methylpyridine.—As the chromatographic separation using a column of cupric chloride-aluminum oxide and also the urea adduct method were ineffective, the separation by solvent extraction was carried out. As the solutes, the fractions Nos. 5' and 6' of Table IV were used. A countercurrent extraction apparatus of semiautomatic type equipped with one hundred distribution tubes was employed. The volume of each tube was 20 cc. Ligroin was introduced into the apparatus as the light phase and the acidic sodium phosphate buffer solution (pH 4.78) as the heavy phase. By a single withdrawal procedure, the ligroin layers were transferred successively, giving a series of fractions, and from those fractions the bases were collected as the picrates. Results of the extractions using Nos. 5' and 6' as the solutes are shown in Table V.

The melting points shown in the table were determined on the picrates once recrystallized from ethanol. From Table V, it was observed that the new component was, next to quinoline, not easily soluble in the buffer solution; the base had a relatively large distribution coefficient.

In order to obtain a large amount of the base to work with, the extraction whose scheme is shown in Table VI was carried out using a 300 cc. separating funnel. Twenty-five grams of the fraction No. 6' was diluted with ligroin to 100 cc., to which 100 cc. of the buffer solution was added, shaken for 3 min., then allowed to settle. The heavy phase

TABLE V. COUNTERCURRENT EXTRACTION

Light phase No.	No. 5' (0.6 g.) M. p. of picrate °C	No. 5' (0.6 g.) Yield and appearance	No. 6' (1.0 g.) M. p. of picrate °C	No. 6' (1.0 g.) Yield and appearance
1	187~189	Yellow needles	197 ~199	Orange yellow plates, 0.2 g.
2	160~167		198 ~200	
3	164~178		199 ~200	
4	189~194	Pale yellow needles	185 ~192	
5	191~194		168 ~171	
6	195~198		175 ~181	
7	192~198		193 ~196	
8	192~196		197 ~199	
9	191~195		199.5~200.5	Yellow needles, 0.1 g.
10	189~192		199 ~200	
11			199 ~200	
12			199.5~200	
13			198.5~199.5	
14			198 ~199	
15			197 ~198	
16			197 ~198	

Crude picrates from Nos. 5—9 were combined and after recrystallization from ethanol, 0.1 g. of picrate was obtained, m. p. 201~202°C.

Base from Nos. 1, 2 and 3 were identified as quinoline by their picrates and tartrates.

was drawn off and the new buffer solution was added; the extraction was repeated three more times in the same manner as described above. After the bulk of the solvent was removed by distillation, the raffinate was purified as a picrate. Recrystallization from ethanol yielded 1.7 g. of picrate, which melted at about 200°C. This picrate, when admixed with the picrate of quinoline, m. p. 198~200°C (uncorr.), showed a large melting point depression amounting to 20°C, hence it is obviously different from that of quinoline.

TABLE VI. EXTRACTION USING A SEPARATING FUNNEL

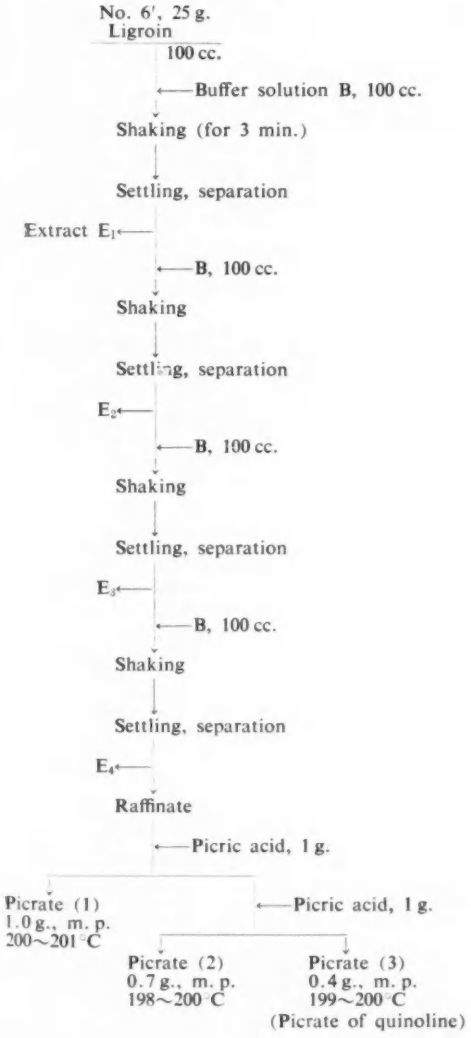

From 20 g. of fraction No. 5' by the same procedure, 0.9 g. of picrate, m. p. 196~198°C (uncorr.), was obtained. The picrate, recrystallized from ethanol melted at 201~202°C (uncorr.). This purified picrate was decomposed by addition of sodium hydroxide and the regenerated base was recovered by steam distillation followed by extraction with ether. The ether extract of the distillate was concentrated to give colorless plates, m. p. 38.5~41°C.

Properties, Derivative and Absorption Spectra of the Isolated Base.—*Neutralization Equivalents.*—The base (0.073 g.) was titrated by 0.1 N hydrochloric acid (F 0.999) using bromophenol blue as an indicator and measuring the pH of the solution. For the neutralization of the base, 5.45 cc. of 0.1 N hydrochloric acid was required.

Found: 134. Calcd. for $C_9H_{11}N$: 133.

The Picrate.—Several recrystallizations from ethanol yielded yellow needles, m. p. 205.2~206.2°C.

Found: N, 15.16. Calcd. for $C_{15}H_{14}N_4O_7$: N, 15.47%.

The Picrolonate.—It was prepared from equimolar quantities of picrolonic acid and the base in ethanol. Recrystallization from ethanol yielded yellow needles which decomposed at 211.5~212.5°C.

The Ultraviolet Absorption Spectrum.—The spectrum in cyclohexane is shown in Fig. 1.

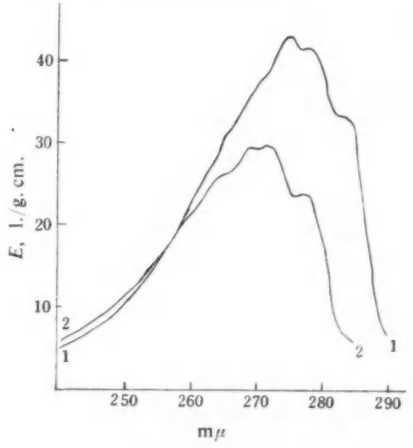

Fig. 1.
1, 2,3-Cyclopenteno-5-methylpyridine
2, 2,3,5-collidine

The ultraviolet spectrum of 2,3-cyclopenteno-5-methylpyridine (λ_{max} 276 mμ) has the same similarity to that of 2,3,5-collidine (λ_{max} 271 mμ) as the spectrum of 2,3-cyclopenteno-6-methylpyridine (λ_{max} 275 mμ) has to that of 2,3,6-collidine (λ_{max} 270 mμ)[1,2].

The Infrared Absorption Spectrum.—The spectrum in carbon disulfide is shown in Fig. 2.

Characteristic absorption bands at 13.7 μ and 14.1 μ are similar to those of 2,3,5-collidine. This similarity may well be explained by the relationship between absorption bands and the position of substituents of alkyl pyridines[3].

3) H. Shindo and N. Ikekawa, *Pharm. Bull. (Tokyo)*, **4**, 192 (1956).

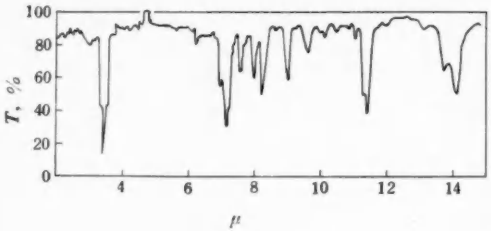

Fig. 2.

In Fig. 3 are shown the specific absorption bands appearing in the fingerprint region of cyclopentenopyridine, 2,3-dimethylpyridine, 2,3-cyclopenteno-6-methylpyridine and 2,3,6-collidine.

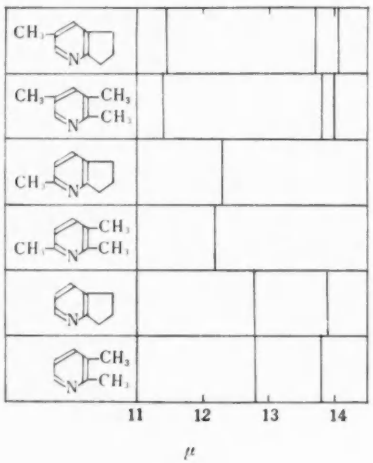

Fig. 3.

The Synthesis of 2,3-Cyclopenteno-5-methylpyridine.—In order to compare the isolated base from coal tar with the authentic sample of the base, a synthesis was carried out in the manner similar to that described by Lochte et al.[2]. The procedure is schematically shown below.

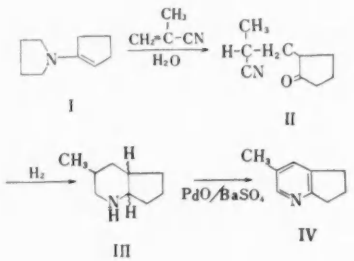

Cyclopentano-pyrrolidine Enamine (I).—A solution of 10 g. of cyclopentanone and 26 g. of pyrrolidine in 140 cc. of dry benzene was refluxed for 6 hr. in a flask fitted with an azeotropic water separator. The benzene and the excess of pyrrolidine were distilled off leaving a viscous liquid, 15.8 g., which was used without further purification in the subsequent reaciton.

2-(2-Methyl-2-cyanoethyl)-cyclopentanone (II).—Methacrylonitrile* (9.5 g.) was added to a solution of the enamine I in 100 cc. of dimethylformamide. The resulting solution was refluxed for 31 hr. in a flask fitted with a tower of calcium chloride. The bulk of the solvent was then removed by distillation and to the residue were added 57 cc. of water and 4 cc. of glacial acetic acid. This solution was refluxed for 2 hr. 40 min., cooled and extracted four times with benzene. The combined benzene extracts were washed three times with 10% hydrochloric acid, twice with 10% potassium carbonate solution, and once with water and dried over sodium sulfate. After removal of the benzene, the residue was distilled in vacuo giving 4.6 g. of a liquid boiling at 125~126°C (5 mmHg), n_D^{25} 1.4580 and 1.1 g., n_D^{25} 1.4709 (reported $n_D^{25.5}$ 1.4624). The semicarbazone prepared from the two fractions melted at 195.4°C and 189~190°C respectively (reported 195°C).

Hexahydro-2,3-cyclopenteno-5-methylpyridine (III).—Raney nickel** was added to a solution of II in absolute ethanol. This mixture was hydrogenated at an initial H_2 pressure of 34 kg./cm² and 120°C in a 100 cc. autoclave equipped with an elecromagnetic stirring device. The Raney nickel was filtered off and the solvent was removed by distillation in vacuo. The residual liquid was distilled in a Claisen flask yielding a corless liquid, b. p. 85°C (21 mmHg).

The experimental results are shown in Table VII.

2,3-Cyclopenteno-5-methylpyridine (IV).—In the present experiment, III was dehydrogenated in the liquid phase with palladium oxide/barium sulfate in place of palladium-carbon described in the literature cited. A mixture of equal amounts by weight of the base and the catalyst (palladium oxide/barium sulfate) was placed in a flask and refluxed in a nitrogen stream in an oil bath. The cooled mixture was extracted with ether and the ether extract was concentrated to give the crude base.

The experimental result was shown in Table VIII.

The pure base was obtained by the decomposition of the recrystallized picrate as described above.

Preparation of Palladium Oxide/Barium Sulfate[5].—Palladium chloride (0.3 g.) was dissolved in a mixture of 15 cc. of 2 N sulfuric acid and 120 cc.

* Preparation of methacrylonitrile—commercial methacrylamide (17.0 g.) and 20 g. of P_2O_5 were thoroughly mixed and heated in a flask over free flame. The distillate, after treatment with a small amount of K_2CO_3, was distilled to give a fraction, 8 g., boiling at 89~89.5°C, n_D^{22} 1.4001 (reported[4] n_D^{20} 1.4007).

4) Rohm and Haas, G. m. b. H., U. S. Pat. 2210320 (1940).

** Raney nickel—one gram of commercial alloy (Ni : Al = 50 : 50) was gradually added with stirring to 10 cc. of 20% sodium hydroxide solution in a beaker placed in a water bath maintained at 50°C, over a period of about 50 min. After the addition was complete, the resulting Raney nickel was washed with water to the neutral pH, then with 95% ethanol and finally with absolute ethanol.

5) R. Kuhn and H. J. Haas, *Angew. Chem.*, **67**, 785 (1955).

Table VII. Hydrogenation

Sample g.	Conditions				Product		
	H_0 kg./cm²	ΔP kg./cm²	Temp. °C	Period	Wt. g.	n_D^{25}	Yield %
2.9	33.8	10.8	108~120	4 hr. 35 min.	3.75	1.4820	63
3.4	34.1	15.7	108~118	5 hr. 30 min.			

Table VIII. Dehydrogenation

Hexahydrobase(III) g.	$PdO/BaSO_4$ g.	Conditions		Product	
		Temp., °C	Period	Yield, g.	M. p., °C
0.37	0.37	180	6 hr.	0.35	below 20
0.52	0.52	200~210	8 hr. 15 min.	0.35	35~37

of water which was kept at 80°C. After the solution was allowed to settle for 20 min., it was poured with vigorous stirring into 165 cc. of 0.2 N barium hydroxide yielding a precipitate. It was filtered off by suction, washed with 240 cc. of water and dried in vacuo. Pale brown powder was obtained; 3.7 g.

Derivatives of the Synthesized Base. — *The Picrate.* — Yellow needles, m. p. 204.8~205.8°C. From 900 mg. of the picrate, 250 mg. of the base, m. p. 38.7~41°C was regenerated by addition of sodium hydroxide followed by steamdistillation.

The Picrolonate.—It was prepared in the same manner as described in the case of the isolated base. Recrystallization from ethanol yielded yellow needles which decomposed at 211.5~212.5°C.

Confirmation. — The isolated 2,3-cyclopenteno-5-methylpyridine, the picrate and the picrolonate when admixed with the corresponding synthesized sample gave no melting point depression. The infrared absorption spectrum of the isolated base and that of the synthesized base were superimposable.

The author wishes to thank Professor Ryozo Goto, Kyoto University, for his helpful discussions and criticisms of this work.

The Laboratory of Research Centre
Yawata Chemical Industry Co., Ltd.
Chuo-ku, Tokyo

Fischer-Tropsch Synthesis with Tubular Reactor of 18.1 l. Catalyst Bed. II. Reactor with Temperature Gradient along Out-side Wall

By Michio Kuraishi*, Minoru Kurita, Tadasuke Hosoya, Hideo Ichinokawa, Kiyoshi Ogawa and Hiroshi Uchida

(Received January 18, 1961)

A previous paper[1] in this series described the Fischer-Tropsch synthesis with the reactor whose out-side wall temperature was kept constant along the whole length by means of a heat transfer medium of flowing oil. However, the catalyst bed temperature tended to rise very high, and the product yield remained below that to be expected from the synthesis results with the reactor of the same design but of a much smaller catalyst bed of 2 l. A closer investigation in this respect disclosed that the large magnitude of temperature rise was mainly due to a high heat transfer resistance across an oil film on the out-side wall of the reactor. For the better performance, therefore, the reactor ought to be modified in construction in order that the heat transfer efficiency across the oil film might be improved. By the use of the reactor which has been improved along this line, the present synthesis experiments are conducted.

The previous paper, in addition, dealt with

* Present address: Japan Gas Chemical Co., Enokicho, Niigata.

1) M. Kuraishi, M. Kurita, T. Hosoya, H. Ichinokawa, K. Ogawa and H. Uchida, This Bulletin, 34, 780 (1961).

the calculation of the temperature profile in the catalyst bed on the basis of the concentration gradient determined along the heights of the catalyst bed. Because of the temperature gradient already present in the oil surrounding the reactor, the method of the calculation, however, can be applied with difficulty to the result with the present reactor. In this paper the calculating method with the result is proposed.

Experimental

In an effort to improve the heat transfer efficiency across the oil film on the out-side wall of the previous reactor, the previous reactor system was subjected to some modifications. Fig. 1 shows a

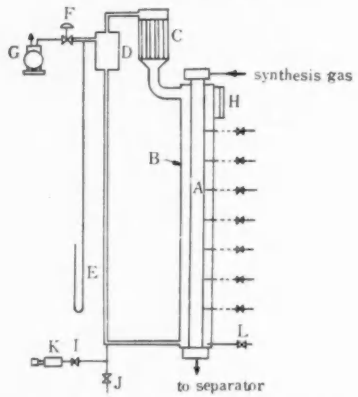

Fig. 1. Schematic diagram of reactor system.
A, Reactor
B, Cylinder for oil bath
C, Condenser
D, Reservoir
E, Contact manometer
F, Magnetic valve
G, Pump
H, Level indicator
I, J, L, Needle valves
K, Dowtherm feeder

schematic diagram of the system after the modifications. The main modification made was that the reactor (A, 10 m. high by 50 mm. I. D.) was placed in a cylinder (B) which was filled with oil (Dowthem) boiling under a reduced nitrogen pressure, whereas the previous reactor had been held in the oil under forced circulation at a fixed flow rate under an atmospheric pressure of nitrogen. A small amount (ca. 200 l./hr.) of nitrogen was always being introduced from a valve (L) into the oil bath by way of a number of openings (0.8 mm. diameter) perforated along two semi-circular tubes placed, opposite to each other, at the bottom of the cylinder. The nitrogen gas passed upwards through the oil, and could easily be controlled at a fixed pressure by means of a leak opened by a magnetic valve (F) which was coupled with a mercury contact manometer (E).

The top zone of the oil bath was equipped with a level indicator (H), by the aid of which the oil was maintained at a constant level by either introducing or withdrawing a small quantity of oil through a valve (I) or (J), respectively. A condenser (C) was placed directly above the top of the cylinder, in which the oil vapor accompanying the nitrogen stream was refluxed back into the oil bath. A reservoir (D) served to avoid a sudden change in the nitrogen pressure. After passing through C, D and F, the gas was finally drawn out by a pump (G).

In view of the kind of reactor type called rectification cooling type, which was originated by Dorschner[2], the present reactor may also be known as such, but it differs from Dorschner's reactor in some respects.

Besides the sintered catalyst (designated catalyst A hereafter) in the previous paper[1], a fused iron catalyst (designated catalyst B hereafter) of the same promoter-composition was employed in this study. Granules of the catalyst ranging from 5 to 2 mm. in size were used, and the catalyst bed of 18.1 l. contained 39.41 kg. of the granules after reduction. The technique of the catalyst pretreatment as well as of the synthesis was essentially the same as was described elsewhere[3] in detail.

Results and Discussion

Results. — Table I shows, together with the synthesis variables, results from a series of five experiments, among which two experiments were carried out by using catalyst A while the other three ones by using catalyst B. Numerals listed in the column of nitrogen pressure serve as a measure to estimate roughly the oil bath temperature: the higher the pressure is, the higher the temperature rises. Further, the axial temperature profiles in the catalyst bed as well as in the oil bath are exemplified in Figs. 2A, B, C and D for experiments Nos. 1, 2, 6 and 7, respectively.

It was after the experiment described in the previous paper[1] (hereafter simply called experiment A) had been made that the bed of catalyst A was used in this study, and hence the bed had already undergone an activity decrease to some extent. In this connection, a much higher yield of the product (oil plus wax) may have not been produced in experiment No. 1 as compared with the yield (14.14 kg./day) in experiment A, in spite of the improvement made for the heat transfer efficiency[4]. Nevertheless, one can yet recognize the effects of the improvement clearly. One of the effects is the axial temperature gradient

2) O. Dorschner, *Chem. Ing. Tech.*, **25**, 277 (1953).
3) M. Kuraishi, H. Ichinokawa et al., *J. Chem. Soc. Japan, Ind. Chem. Sec.* (*Kogyo Kagaku Zasshi*), **63**, 1588 (1960).
4) It is to be noted that in experiment No. 1 the temperature at the axial middle point of the oil bath was essentially the same as the oil bath temperature in experiment A.

TABLE I. RESULTS OF SYNTHESIS EXPERIMENTS

Exp.	Catalyst	Pressure kg./cm² (gauge)	Nitrogen pressure mmHg	Space velocity of inlet gas hr^{-1}	Space velocity of raw gas hr^{-1}	Volume contraction %	Oil plus wax kg./day	Aqueous product kg./day	Oil plus wax per m^3 $(CO+H_2)$ g.	Use ratio H_2/CO
No. 1	A	30	580	2250	668	41.1	15.91	21.94	105	1.10
No. 2	A	30	760	2270	816	44.6	21.21	27.45	106	1.11
No. 5	B	25	440	2080	582	41.5	16.83	20.09	131	1.06
No. 6	B	30	520	2125	790	48.1	24.39	32.82	118	1.06
No. 7	B	30	480	1670	785	49.8	26.03	30.96	125	1.10

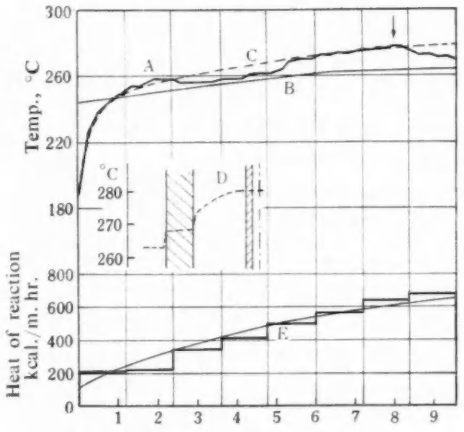

Fig. 2A. Experiment No. 1.

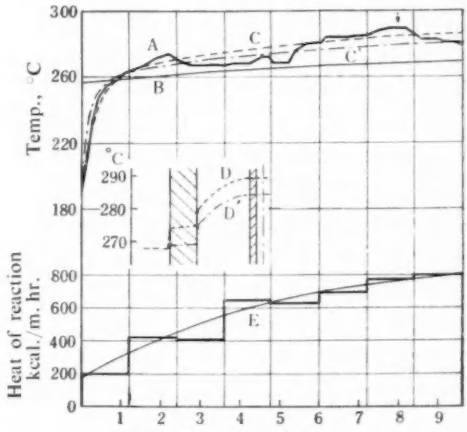

Fig. 2B. Experiment No. 1.
C, D, Temperature profile calculated by the use of $h'_L = 600$ kcal./m² hr. °C
C', D', Temperature profile calculated by the use of $h'_L = 4800$ kcal./m² hr. °C

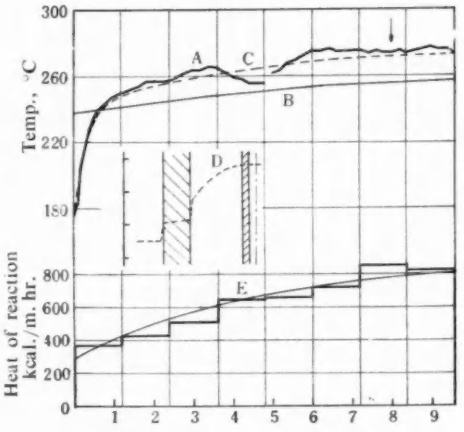

Fig. 2C. Experiment No. 6.

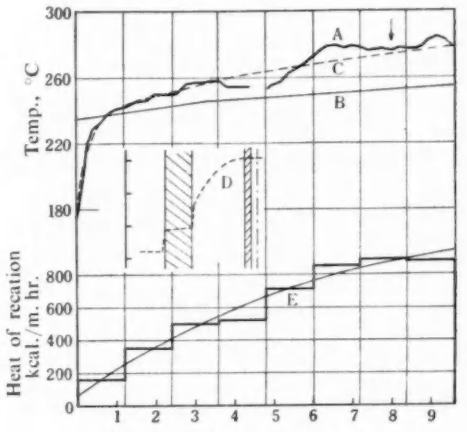

Fig. 2D. Experiment No. 7.

Figs. 2A–D. Experimental and calculated temperature profiles (above) and heat of reaction as function of x (below, E).
A, Experimental temperature profile
B, Oil bath temperature
C, Calculated axial profile
D, Calculated radial profile

in the oil bath, increasing continuously from top to bottom. The appearance of the gradient arises from the fact that the boiling temperature of oil is continuously increased with gravity of increasing amounts of oil in the oil bath cylinder from top to bottom. The temperature gradient thus produced along the oil bath may have helped the catalyst bed temperature to rise with the distance (x) from the top of the bed. In contrast to the above, the temperature profile in the bed of experiment A showed a downward tendency along the lower half of the bed. Another effect is the smaller magnitude of temperature difference between the oil bath and the reactor axis, in other words, the smaller magnitude of the bed over-temperature (hereafter denoted by $(t-t_b)$, where t and t_b are the temperatures measured along the axis of catalyst bed and along the oil bath, respectively), which was 15°C at a maximum for experiment No. 1 while 25°C for experiment A.

By using a fresh bed of catalyst B in place of the deteriorated one of catalyst A, much higher yields of the product, attaining from 24 to 26 kg./day, were produced (refer to the results of experiments Nos. 6 and 7), even though the nitrogen pressure was kept below that of experiment Nos. 1 and 2. Moreover, the magnitude of $(t-t_b)$ remained comparatively small: at the region of a maximum $(t-t_b)$, 22 and 30°C for experiments Nos. 6 and 7, respectively. The somewhat larger magnitude of $(t-t_b)$ observed with the latter experiment may be accounted for by a lower space velocity of the inlet gas, details of which will be stated later.

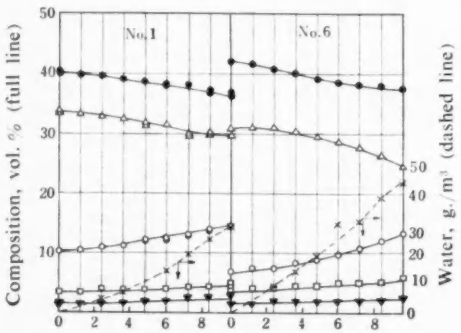

Fig. 3. Concentration gradient along catalyst bed.

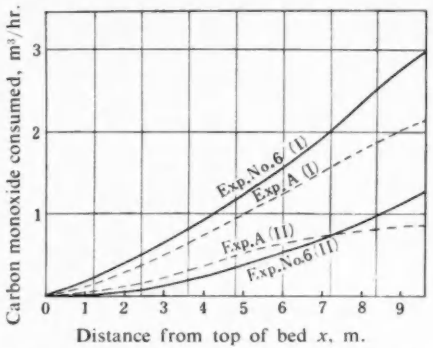

Fig. 4. Carbon monoxide consumed by either reaction (1) or (2) as a function of x.

The concentration gradient of the individual components along the reactor was determined in the same manner that was made in experiment A[1]. Among the results the gradient for experiment No. 6, for instance, is shown in the right half of Fig. 3, while the gradient for experiment A is given again in the other half. Starting with the results of Fig. 3 and following the procedure as reported in the previous paper[1], one can calculate amounts of carbon monoxide consumed with the progress of the synthesis either by $2H_2+CO \rightarrow >CH_2+H_2O\cdots$ (1) or by $CO+H_2O \rightarrow CO_2+H_2\cdots$(2). Fig. 4 illustrates plots of the amount vs. x, together with the recited ones for experiment A. The figure discloses that although the amounts of carbon monoxide consumed by the reaction 1 in the top zone of the catalyst beds differ slightly from each other the amount at the end of the bed in experiment No. 6 attains 3/2.1 times as large as the amount in experiment A. In view of the fact it can be seen that in experiment No. 6 better use was made of the lower half of the catalyst bed than that in experiment A.

Method of Calculating Temperature Profiles in Catalyst Bed.—Because of the presence of the temperature gradient along the oil bath, the solution to the heat balance equation, as cited in the previous paper[1], is to be made under the different boundary conditions from the previous ones. The equation is then given as follows.

$$C_pG\frac{\partial t}{\partial x}=\frac{1}{r}\left[\frac{\partial}{\partial r}\left(\lambda_r\cdot r\frac{\partial t}{\partial r}\right)+\frac{\partial}{\partial x}\left(\lambda_x\cdot r\frac{\partial t}{\partial x}\right)\right]+Q \quad (1)$$

with the following boundary conditions,

$$t=t_0 \quad \text{at} \quad x=0$$

$$\lambda_r\partial t/\partial r+U(t-t_b)=0 \quad \text{at} \quad r=r_2$$

and $\partial t/\partial r=0$ at $r=r_1$

where C_p is the heat capacity per unit mass of fluid, G is the mass velocity based on an empty tube, r is the distance in lateral direction, λ is the effective thermal conductivity of the catalyst bed system, Q is the reaction heat, U is the overall heat transfer coefficient, r_1 and r_2 are the inner and the outer radii of the catalyst bed, respectively.

A numerical solution of Eq. 1 may be possible. However, the calculation will be very time-consuming since t_b varies with x. As a compromise, it would be rather convenient for the present purpose to start with a more simplified equation of the heat balance, in which the temperature is assumed to be radially uniform at every cross section of the bed that an average temperature[5] (t_{av}) over the bed cross section may simply be taken into account. The solution then gives the axial temperature profile. Once the axial temperature profile has been drawn, Eq. 1 can be solved more easily with respect to a cross section, in the neighborhood of which the axial temperature is kept essentially constant. The solution gives the radial temperature profile.

Under the assumption of uniform temperature across the bed, the following equation of the heat balance can be established,

$$G_pGdt/dx+2\pi r_2U'(t-t_b)/S=Q \qquad (2)$$

with the boundary condition that $t=t_0$ at $x=0$. The symbol S in the equation is the cross sectional area of the bed, and the second term in the left-hand side of the equation concerns the heat transfer across the tube wall of the reactor held in the oil bath whose axial temperature gradient is assumed to be given by a linear function of x, namely $t_b=t_{bo}+ax$, where t_{bo} is the oil bath temperature at $x=0$. The constant a takes a value characteristic of the gradient in the oil bath. It should further be noted that U' is to be distinguished from U in Eq. 1. The calculation of U' is made by taking the tube wall coefficient of the heat transfer based on t_{av} (denoted by h') into account whereas U by taking the coefficient based on t at $r=r_2$ (denoted by h) into account. In this paper, h' with respect to the present annular shaped cylinderical bed was evaluated by making use of the formula[6] proposed by Maeda et al.[7] for h' with a cylindrical bed, while h by the aid of the formula[8] by the Hatta et al.[9] In the latter formula, λ_r is taken into consideration.

In Eq. 2, Q is again approximated to

$$Q=C_1e^{-Mx}-C_2e^{-Nx} \qquad (3)$$

where C_1, C_2, M and N are constants. Combination of 2 with 3, and subsequent rearrangement give

$$dt/dx+A(t-t_{bo}-ax)=G_1e^{-Mx}-G_2e^{-Nx} \qquad (4)$$

in which the following abbreviations are introduced.

$$A\equiv 2\pi r_2U'/C_pGS,\quad G_1\equiv C_1/C_pG$$
$$G_2\equiv C_2/C_pG \qquad (5)$$

The solution of Eq. 4 is given by

$$t=t_{bo}+e^{-Ax}\left[t_0-t_{bo}+\frac{G_1}{A-M}\left\{e^{(A+1)x}-1\right\}-\frac{G_2}{A-M}\left\{e^{(A-N)x}-1\right\}\right]+a\left\{x-\frac{1}{A}(1-e^{-Ax})\right\} \qquad (6)$$

On the other hand, under the assumption of $dt/dx=0$, Eq. 1 is reduced to a simpler form of

$$\lambda_r\{d^2t/dr^2+(1/r)(dt/dr)\}+Q=0 \qquad (7)$$

with the boundary conditions that $dt/dr=0$ at $r=r_1$, and $\lambda_r dt/dr+U(t-t_b)=0$ at $r=r_2$. The solution results in Eq. 8.

$$t=t_b+\frac{Qr_2^2}{4\lambda_r}\left[\left\{1-\left(\frac{r}{r_2}\right)^2\right\}+2\left(\frac{r_1}{r_2}\right)^2\ln\frac{r}{r_2}+\frac{2\lambda_r}{Ur_2}\left\{1-\left(\frac{r_1}{r_2}\right)^2\right\}\right] \qquad (8)$$

By the aid of Eqs. 6 and 8 both the axial and the radial temperature profiles can be drawn.

Let us make an approximate check on the accuracy of the present calculation method by performing a profile calculation. The calculation is carried out on the basis of the experimental data of experiment A, and the resulting profiles are shown in Fig. 5 with the dotted and dashed lines, of which the radial one is given for the cross section at $x=6$ m. In the neighborhood of the cross section, the axial temperature has been found nearly constant. For the sake of comparison, the figure is included with the previous profiles (dashed lines) calculated by using the solution with no simplification of Eq. 1. The respective profiles calculated by either one of the two

5) The average temperature (t_{av}) is defined by

$$t_{av}=\int_{r_1}^{r_2}t\cdot 2\pi r dr/\pi(r_2^2-r_1^2)$$

6) $h'D/k=4.90(R_{ep})^{0.60}e^{-2.2d_p/D}$, where D is the diameter of bed, k is the thermal conductivity of fluid, R_{ep} is the modified Reynolds number, and d_p is the diameter of catalyst granules (4 and 3.4 mm. for catalysts A and B, respectively). In the evaluation of h', D_{eq} defined by $D_{eq}=D_2-D_1$ is used in place of D.

7) S. Maeda and K. Kawazoe, *Chem. Eng. Japan* (*Kagaku Kogaku*), **17**, 276 (1953).

8) $\lambda_r/k=0.209(R_{ep})^{0.87}$ and $hD_{eq}/\lambda_r=127(R_{ep}\cdot d_p/D_{eq})^{-0.87}$.

9) S. Hatta and S. Maeda, *Chem. Eng. Japan* (*Kagaku Kikai*), **13**, 79 (1949).

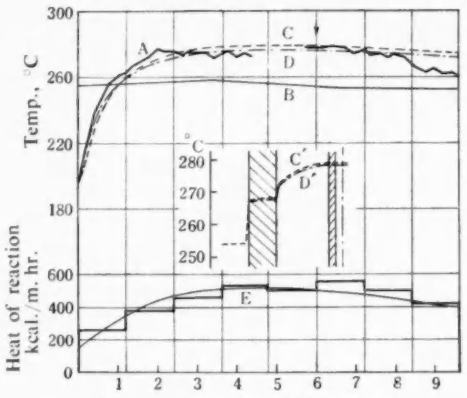

Fig. 5. Experimental and calculated temperature profiles (above) and reaction heat as a function of x (below, E) for experiment A.

A, Experimental temperature profile
B, Oil bath temperature
C, C', Profiles as cited in previous paper
D, D', Profiles calculated by the aid of Eqs. 6 and 8

different methods show a good approximation with each other. However, it should be noted that the present method of calculating the axial temperature profile is available only when λ is so high that the radial temperature gradient can be ignored. It otherwise may lead to errors, for instance, in such a case that the synthesis is made by the once-through operation where the mass velocity of the inlet gas, as a consequence, λ is usually much lower.

Calculation of Temperature Profile. — Before proceeding to the profile calculation, the coefficient (h_L) of heat transfer referred to the out-side wall of present reactor, over which the oil film is kept under nucleated boiling, has to be evaluated. Although there have appeared a few papers[10] dealing with the heat transfer phenomenon considered, none of them except for the paper by Nishikawa[11] is available for the calculation. Accordingly, a rough estimation of h_L is made for experiment No. 2 by means of Nishikawa's formula, which results in the value of 4800 kcal./m² hr. °C. By using this value the profile calculation is made[12]. The profiles thus drawn are shown in Fig. 2B with the dotted and dashed lines, which appear to be in a poor agreement with the experimental profiles: the calculated axial temperature profile rises more rapidly in the top zone while it lies below the experimental one in the lower half of the catalyst bed, and in addition the radial temperature profile at the cross section of $x=8$ m. shows a maximum temperature across the bed of 284.3°C, in contrast to the measured one of 289°C. The disagreement may probably be due to too high an estimated value of h'_L, consequently of U'.

The calculation is then repeated with other different values of h'_L for a better agreement between the measured axis-temperature in the bed and the calculated one, and finally $h'_L=600$ kcal./m² hr. °C, consequently $U'=391$ kcal./m² hr. °C, is conveniently chosen, by the choice of which the temperature of 289.5°C is attained. The value of h'_L has thus appeared only one eighth of the value afore-cited[13], but it is still 3.5 times as much as the value in the previous reactor. The axial profile calculations have then been made, and an improvement in the accordance between the calculated and the measured profiles is obtained (refer to the dashed line in Fig. 2B). The same calculations made on the basis of the data of the other experiments of Nos, 1, 6 and 7 results in the profiles as cited in Figs. 2A, C and D, respectively. The profiles are in a good agreement with measured ones, except for a small intermediate range where the measured profile lies somewhat below the calculated one. Moreover, the radial temperature profile is visualized by the calculation as shown in the figure, and a comparison of the profile with that in Fig. 5 is suggestive of the improving effect of the present procedure on the heat transfer efficiency across the out-side wall. In this study, however, no experimental evidence is available for the radial profile.

It should be noted that the present procedure of improving the heat transfer efficiency can effectively be applied only when the difficulty exists in the heat transfer resistance across the liquid film on the out-side wall of the reactor. In this respect, a comparison between the results of experiment Nos. 6 and 7 shows that the magnitude of $(t-t_b)$ is a

10) Y. Y. Hsu and J. W. Westwater, *Am. Inst. Chem. Engrs. J.*, **4**, 58 (1958); C. Corty and A. S. Foust, *Chem. Eng. Progr., Symposium Ser.* No. 17, **51**, 1 (1955). S. A. Guerrieri and R. D. Talty, ibid., No. 18, **52**, 69 (1956), et al.

11) K. Nishikawa, *Trans. Jap. Soc. Mech. Eng.*, No. 120, **22**, 551 (1956).

12) In fact, the temperature gradient in the oil bath is convex upwards instead of being a linear function of x, as shown in Figs. 2A, D. In the calculation of the profile, a few axial step lengths are chosen, and the solution is applied to each of the steps successively. Although the integration constant in the solution remains the same in the first step where the boundary condition is $t=t_b$ at $x=0$, it differs in value for the succeeding steps because the different boundary condition that t at the end of the first step is equal to t at the top of the second step, and so forth, are established.

13) We are not as yet certain of the accurate reason why the value of h'_L thus chosen is far smaller than that obtainable from Nishikawa's formula.

little smaller for experiment No. 6 which was conducted under the essentially same operating conditions, except for the greater G, than those in experiment No. 7. As regards the present two experiments where h'_L is as high as 600 kcal./m² hr. °C, the greater value of λ[14], which is necessarily accompanied by the increasing G, may therefore become rather responsible for the smaller magnitude of $(t-t_b)$. The effect of varying values of G on $(t-t_b)$ can be seen more clearly when the results of the once-through operation is considered[15].

Dorschner[2] has already pointed out that the outside wall temperature gradient increasing from top to bottom exerts an advantageous effect on an efficient use of the catalyst bed. For the purpose of producing such a temperature gradient, he employed a bath of an oil mixture consisting of hydrocarbons of different boiling points, whereas in the present procedure one kind of oil, Dowtherm, is simply used. In addition, the procedure has another advantage of providing a better means of temperature control: the oil bath temperature has to be increased successively to follow the deterioration of the catalyst activity, which can be done by a simple regulation of the nitrogen pressure. However, it suffered from the following limitation that a considerable magnitude of the temperature difference (for example, ca. 20°C from top to bottom in the present reactor) can not be produced until the reactor reaches as high as 10 m.

14) The values of λ for experiment Nos. 6 and 7 were 5.09 and 4.03 kcal./m.·hr. °C, respectively.
15) The results will be reported elsewhere.

Summary

The present experiments on the Fischer-Tropsch synthesis have been made with the reactor which was placed in a bath of oil boiling under a reduced nitrogen pressure. The heat transfer efficiency referred to the out-side wall of the reactor has been improved considerably, and, as a consequence, the magnitude of the bed over-temperature remains comparatively small, in spite of the high yield of the product attaining 24~26 kg./day.

The axial and the radial temperature profiles have been separately calculated on the basis of the concentration gradient determined along the heights of the reactor: first the calculation of the former profile under the assumption of uniform temperature across the bed, and secondly that of the latter profile at a cross section in the neighborhood of which the axial temperature is approximately constant. By the convenient choice of 600 kcal./m² hr. °C for the tube wall coefficient of heat transfer referred to the out-side wall of the present reactor, the calculated axial temperature profile is in good agreement with the experimental profile except for a small intermediate range.

The authors are grateful to Mr. M. Oba, Mr. A. Matsuda, Mr. H. Imai and Mr. K. Shimomura for their assistance in the synthesis experiments.

Government Chemical Industrial Research Institute, Tokyo
Shibuya-ku, Tokyo

Organoboron Compounds. I. On the Reaction of n-Butylboronic Acid with Polyvinylalcohol

By Seiji KATO, Yojiro TSUZUKI and Shigenobu KITAJIMA

(Received October 17, 1960)

It is well-known that boric acid reacts with various diols and sugars, giving more acidic complexes, and thus boric acid can be titrated with standard sodium hydroxide in the presence of mannitol. One of the authors[1] previously studied the reactions polarimetrically and showed that the formation of the complexes is a reaction of ionic nature. Boric acid, reacting with polyvinylalcohol, also forms polyvinyl borate ester. Owing to this reaction a remarkable change is observed on the viscosity of aqueous polyvinylalcohol on the addition of boric acid, hence boric acid is available as a modification agent of the viscosity of aqueous polyvinylalcohol when filaments are spum from it. In a similar manner esters of boronic acid with polyols can be formed, which have been known as arneboronates. Kuivila[2] prepared

1) Y. Tsuzuki, This Bulletin, **16**, 23 (1941).
2) H. Kuivila, *J. Org. Chem.*, **19**, 780 (1954).

them by the reaction of some arylboronic acid with numerous diols and sugars.

The present paper deals with the reaction of *n*-butylboronic acid with polyvinylalcohol, and discusses the experimental method, esterification grade, and some properties of the products.

Experimental

Preparation of *n*-Butylboronic Acid. — *n*-Butylboronic acid was prepared in an atmosphere of nitrogen, practically according to Johonson's method[3], in the following way:

$$n\text{-Bu-MgBr} + B(OCH_3)_3 \rightarrow n\text{-Bu-B}(OCH_3)_2 + MgBrOCH_3$$

$$n\text{-Bu-B}(OCH_3)_2 + H_2O \rightarrow n\text{-Bu-B}(OH)_2 + CH_3OH$$

From 80.6 g. (0.50 mol.) of *n*-butylmagnesiumbromide and the equivalent quantity of methylborate (52 g.) was obtained *n*-butylboronic acid as fine crystals, m. p. 92~94°C, yield ca. 50 g. (ca. 50% of the theory).

Esterification of Polyvinylalcohol with *n*-Butylboronic Acid. — Purified polyvinylalcohol (PVA) which has the polymerization grade of about 1500 and was reprecipitated by the usual method is dissolved in water, the concentration of which is always kept constant (2.5%). The concentration of boronic acid solutions varied from experiment to experiment. The solution of boronic acid is placed in a 500 ml. four-necked flask with a reflux condenser, and a 2.5% solution of PVA is dropped from a separating funnel at a temperature from 40 to 70°C during one hour, and stirring is continued for one more hour. An insoluble product appears as a white emulsion. On salting out this emulsion, a gum-like material is produced. This product is dried in vacuo and reprecipitated from benzene solution into cold methanol for purification.

Determination of Boron. — Although a number of methods for the analysis of boron have been proposed, they are for the most part troublesome. The present authors have modified the method of Martin in the following way[4], which is proved to be easier and more practical.

The sample is refluxed with a sodium peroxide solution for several hours until it is dissolved. The solution is exactly neutralized to pH 6.9 with hydrochloric acid by the help of a pH-meter and on adding mannitol the solution is titrated back until the pH-meter exactly indicates the mark of 6.9. The content of boron can be estimated from the data*.

Infrared Spectra. — *n*-Butylboronate ester is dissolved in carbon tetrachloride and a thin film is made on a mercury dish. The thickness was about 0.03 mm. The apparatus used was a Hitachi spectrophotometer EPI-2.

Results and Discussion

Polyvinylalcohol (PVA) reacts with *n*-butylboronic acid instantly in aqueous solution. The product is obtained in a state of emulsion, but after salting out, it can be obtained as a solid. If the concentration of *n*-butylboronic acid is varied against the constant concentration of PVA, the products are varied in form from gum-like to transparent white hard solids. The materials obtained are all insoluble in water, but dissolve in many organic solvents. These differences chiefly depend upon the boron content of the products. The solubility of the products increases with the increasing boron content. Table I shows the solubility in several organic solvents, of the product which contains the highest quantity of boron.

TABLE I. THE SOLUBILITY OF PVA-*n*-BUTYLBORONATE

Solvent	Solubility	Solvent	Solubilty
Methanol (in hot)	s	Chloroform	ss
Ethanol	s	Benzene	ss
Buthanol	s	Toluene	ss
Ether	ss	Nitrobenzene	sw
Tetrahydrofuran	ss	Phenol	sw
Petroleum-ether	sw	Chlorobenzene	s
Acetone	sw	Aniline	is
Ethylacetate	s	Pyridine	s
Carbon disulfide	ss	Formic acid	is
Carbon tetrachloride	ss	Acetic acid	sw

Note, s: soluble ss: very soluble
is: insoluble sw: swelling

It has been known that in acetalization of PVA, the product acetalized dissolves in various organic solvents, and that the solubility increases with the acetalization grade. In view of these phenomena, the authors have estimated the esterification grade of PVA-boronates by determining the boron content of the products, the formation of which is formulated as follows:

$$PVA + n\text{-Bu-B}(OH)_2 \rightarrow PVA\langle O_2B\text{-}n\text{-Bu} + H_2O$$

In the above reaction PVA is partially esterified with boronic acid; hence the product may be represented as consisting of the following two parts:

3) J. R. Johnson et al., *J. Am. Chem. Soc.*, **60**, 115 (1938).
4) J. R. Martin, *Anal. Chem.*, **24**, 182 (1952).
* While PVA-borate is produced as the result of oxidation and hydrolysis, it gives free PVA on adding mannitol as seen below:

$$PVA\langle O_2B\text{-}n\text{-Bu} \xrightarrow{Na_2O_2} PVA\langle O_2B\text{-O-}n\text{-Bu} \xrightarrow{H_2O} PVA\langle O_2B\text{-OH}$$

$$PVA\langle O_2B\text{-OH} + \text{Mannitol} \longrightarrow PVA + \text{Mannitol}\langle O_2BO^- + H^+$$

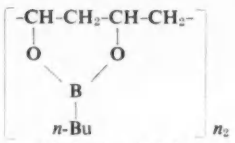

Mol. wt. = 153.8

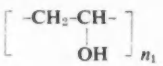

Mol. wt. = 44

Then,

$$N = 2n_2 + n_1$$

where N is the polymerization grade of PVA, and

$$B\% = (10.8\, n_2)/(153.8\, n_2 + 44\, n_1) \times 100$$

$$E_g = 2n_2/N \times 100$$

where E_g is the esterification grade.

From the above three equations, it follows that

$$E_g = (133.74 \times B\%)/(16.41 - B\%)$$

Flory[5] has shown from the statistical theory that the maximum grade of acetalization is 86.47%; that is to say, 13.53% of the hydroxyl groups in PVA remains unreacted. While Noma and his coworkers[6] obtained experimentally the maximum value of acetalization, they used the reaction of PVA with diethylchloroacetal, and by determining the chlorine content by the Carius method, they found that the acetalization grade is not affected by the concentration of diethylchloroacetal, and the maximum value is in reality less than 85%. As to the reaction of PVA with *n*-butylboronic acid, the esterification grade E_g increases with concentration of the latter. Table II shows the relation between the concentration of *n*-butylboronic acid and E_g, where the concentration of PVA is fixed to be 2.5%.

Table II. Relation between concentration of reactant and E_g

No.	*n*-Butylboronic acid	Molar ratio	B%	E_g, %
B-1	1.25	1/2	—*	—
B-2	2.50	1	5.97	75.4
B-3	5.00	2	6.17	80.6
B-4	7.50	3	6.31	83.6
B-5	10.00	4	6.39	85.6

* Not salted out.

As seen from Table II the molar ratio of PVA to *n*-butylboronic acid is varied from one half to four. Above this concentration *n*-butylboronic acid dissolves incompletely, and hence the reaction does not proceed normally.

It is, however, to be remarked that the maximum value of E_g agrees with the values obtained by Flory[5] and Noma[6]. The structure of PVA has been studied by many authors[7] and is generally considered to be of 1, 3-glycol form, but in the above equations the forms of 1, 2- and 1, 4-glycol, are not effective in estimating the value of E_g, because the molecular weight of the unit is equal.

Observing the fact that these esters in benzene as well as carbon tetrachloride can be spun into poor solvents and that the esters are very soluble in various solvents it may be considered that PVA reacts with boronic acid to form no didiol complexes II of so-called network structure but yields a monodiol I. This presumption is supported by the investigations of PVA-borate by Irany[8] and by Deuel[9]. Sakurada and Okada[10] previously reported on the reaction of PVA with boric acid, showing the structure of the product by means of X-ray diffraction, that the trivalent hydroxyl groups in boric acid form a cyclic structure such as III and when the relative concentration of boric acid to PVA becomes higher, a didiol structure II should also be taken into consideration.

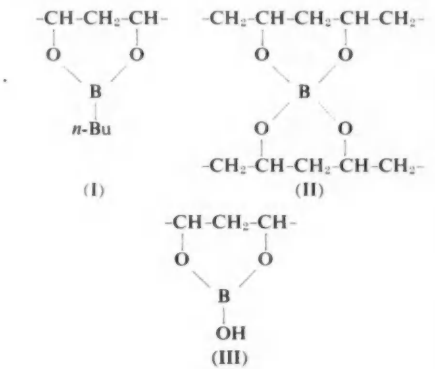

Fig. 1

In the case of *n*-butylboronic acid, however, a structure as II is not conceivable, for boronic acid is of divalent character and the boron atom is sterically hindered by the *n*-butyl group greater than the hydroxyl of boric acid.

The Effect of Catalyst and Temerature. — While in acetalization of PVA, an acid catalyst is fundamental for determining the reaction velocity[11], but the reaction of this esterification

5) P. J. Flory, *J. Am. Chem. Soc.*, **61**, 1518 (1939).
6) K. Noma et al., *High Polymer Chem.* (*Kobunshi Kagaku*), **6**, 439 (1939).
7) C. S. Marvell and C. E. Denoon, *J. Am. Chem. Soc.*, **60**, 1045 (1938).
8) E. P. Irany, *Ind. Eng. Chem.*, **35**, 1290 (1943).
9) H. Deuel und H. Neukom, *Makromol. Chem.*, **3**, 13 (1949).
10) I. Sakurada and A. Okada, *High Polymer Chem.*, (*Kobunshi kagaku*), **15**, 491 (1958).
11) G. Smets and B. Pett, *Makromol. Chem.*, **33**, 41 (1959). Y. Ogata et al., *J. Am. Chem. Soc.*, **78**, 2962 (1956).

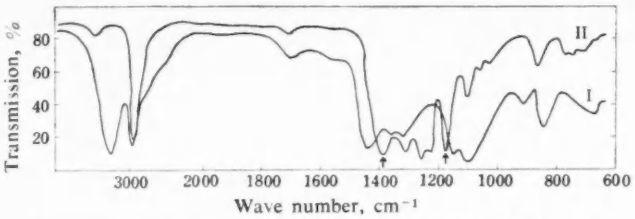

Fig. 2. Infrared spectra of polyvinylalcohol (I) and polyvinyl *n*-butylboronate (II).

proceeds instantly, and the determination of E_g showed that the influence of H^+ on the reaction was not noticeable. Of course in alkaline solution, esterification does not proceed; the ester, if produced, may be saponified as soon as it is formed.

The Effect of Temperature. — The effect of temperature on E_g is remarkable. In the range of 40 to 70°C, the values of E_g rise as the temperature is raised, as shown in Table III.

TABLE III

Temp., °C	40	50	60	70
E_g, %	69.3	71.9	80.3	85.6

Infrared Spectra. — In order to study the structure of the esterification products, deeper infrared spectra were taken in the form of films prepared from carbon tetrachloride solutions of the esters on a mercury dish, the results of the observation being shown in Fig. 2.

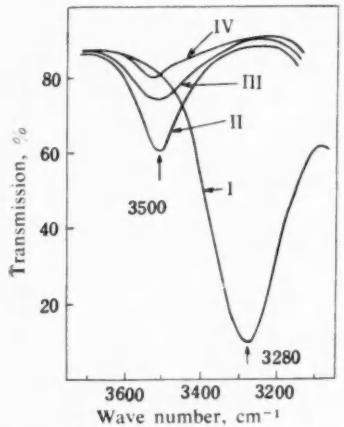

Fig. 3. Shifts of OH absorption band.
I: PVA II: B-2 III: B-4 IV: B-5

Curve I in Fig. 2 shows the spectrum of PVA unreacted. On treating with *n*-butylboronic acid it shows new absorption bands in the region of 1000 to 1500 cm^{-1}. In this region 1190 and 1390 cm^{-1} can be assigned respectively to –B–C and –B–O bonds[12-14]. At the same time the OH stretching absorption band at 3280 cm^{-1} of PVA shifts to a higher frequency by treatment with boronic acid and decreases in intensity with the increasing value of E_g as shown in Fig. 3.

As seen in Fig. 3, it is observed that the decrease in intensity is related to E_g qualitatively, and quantitative treatments will be reported in a later paper.

Summary and Conclusion

It has been shown that PVA is partially esterified with *n*-butylboronic acid, giving products of the form of PVA B-*n*-Bu.

The esterification grade, E_g, of the products is estimated from the boron content. E_g increases with the increasing concentration of *n*-butylboronic acid used, the maximum E_g being 85.6%. E_g rises from 69.3 to 85.6% as the reaction temperature is elevated from 40 to 70°C.

On treating with *n*-butylboronic acid PVA shows new absorption bands 1190 and 1390 cm^{-1} in deeper infrared spectra, which are assigned respectively to –B–C and –B–O bonds. At the same time the OH stretching absorption band at 3280 cm^{-1} of PVA shifts to a higher frequency, and decreases in intensity with the increasing E_g.

Tokyo College of Science
Shinjuku-ku, Tokyo

12) W. J. Lehmann, *J. Chem. Phys.*, **28**, 777 (1958).
13) Jeo Cazes, *Compt. rend.*, **247**, 2019 (1958).
14) H. R. Snyder et al., *J. Am. Chem. Soc.*, **80**, 3612 (1958).

A New Quantum-mechanical Reactivity Index for Saturated Compounds

By Kenichi FUKUI, Hiroshi KATO and Teijiro YONEZAWA

(Received January 24, 1961)

In our previous paper[1], the frontier electron density[2] was shown to become a good intramolecular index of the reactivity in a metathetical reaction of saturated compounds.

In the present paper, we treat several lower paraffins and halomethanes by using the same method as that used in the previous treatment[1], and attempt to derive a new intermolecular index of the reactivity, which is hereafter referred to as the delocalizability, D_r. This index is similar to the superdelocalizability[3] of conjugated molecules. It is found that the magnitude of D_r in these compounds has an intimate correlation with the value of activation energy observed in metathetical reactions.

Electronic Structure of *n*-Paraffins and Methyl Fluoride

The calculated values of orbital energies and electron distributions in methane, ethane, propane, *n*-butane and methyl fluoride are listed in Table I.

With regard to *n*-paraffins, we can point out the following characteristics:

(1) The bonding electrons tend to localize in the particular bonds in each molecular orbital. For example, the electrons in the highest occupied and the lowest vacant orbitals in these compounds except methane, have a general trend to localize in the central C-C bonds as shown in Fig. 1*.

(2) The electron distributions of occupied and unoccupied orbitals are almost symmetrical with respect to the energy equal to α (see below) as is seen in Fig. 1.

(3) The distances of levels of molecular orbital energy in these compounds are much larger than those of conjugated molecules. The excitation energy of the N-V transition in a simple LCAO MO sense is, therefore, estimated to be 9~10 eV. referring the presumed value

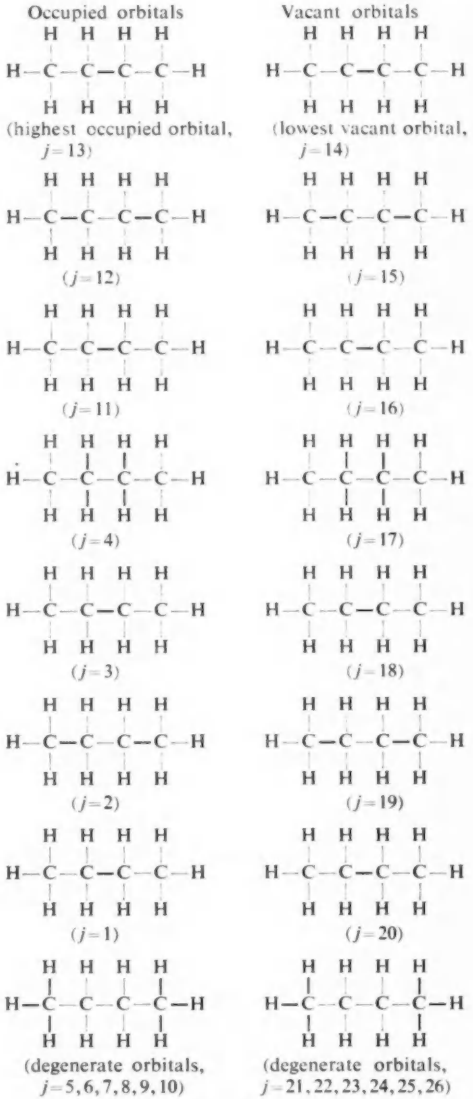

Fig. 1. The electron distributions of *n*-butane.
(Thick lines denote the most densely populated bonds of bonding electrons.)

1) K. Fukui, H. Kato and T. Yonezawa, This Bulletin, 34, 442 (1961).
2) See e. g. K. Fukui, T. Yonezawa, C. Nagata and H. Shingu, *J. Chem. Phys.*, 22, 1432 (1954).
3) K. Fukui, T. Yonezawa and C. Nagata, This Bulletin, 27, 423 (1954).
* This result suggests that in lower *n*-paraffins their first ionization can be attributed to the removal of one electron localized in C-C bonds.

TABLE I. THE ORBITAL ENERGIES AND ELECTRON DISTRIBUTIONS IN SEVERAL SATURATED COMPOUNDS

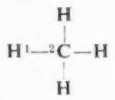

Orbital energy		Electron distribution	
j	ε_j	$(C^j_{H1})^2$	$(C^j_{C2})^2$
6,7,8	$\alpha-1.3722\beta$*	0.1171	0.1329
5	$\alpha-0.8478\beta$	0.1856	0.0644
2,3,4	$\alpha+0.8322\beta$*	0.1329	0.1171
1	$\alpha+1.6678\beta$	0.0644	0.1856

* threefold degenerate

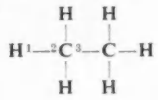

Orbital energy		Electron distribution		
j	ε_j	$(C^j_{H1})^2$	$(C^j_{C2})^2$	$(C^j_{C3})^2$
11,12,13,14	$\alpha-1.3722\beta$*	0.0781	0.0886	0
10	$\alpha-1.3527\beta$	0.0323	0.0355	0.2966
9	$\alpha-1.0019\beta$	0.1057	0.0561	0.0145
8	$\alpha-0.6881\beta$	0.0878	0.0173	0.1847
7	$\alpha+0.7254\beta$	0.0336	0.0238	0.3278
3,4,5,6	$\alpha+0.8322\beta$*	0.0886	0.0781	0
2	$\alpha+1.5208\beta$	0.0465	0.1139	0.0187
1	$\alpha+1.7566\beta$	0.0274	0.0867	0.1575

* fourfold degenerate

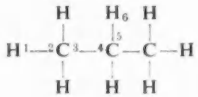

Orbital energy		Electron distribution					
j	ε_j	$(C^j_{H1})^2$	$(C^j_{C2})^2$	$(C^j_{C3})^2$	$(C^j_{C4})^2$	$(C^j_{C5})^2$	$(C^j_{H6})^2$
16,17,18,19,20	$\alpha-1.3722\beta$*	0.062	0.071	0	0	0.053	0.047
15	$\alpha-1.3576\beta$	0.011	0.012	0.105	0.106	0.115	0.104
14	$\alpha-1.3482\beta$	0.021	0.023	0.183	0.186	0	0
13	$\alpha-1.0614\beta$	0.058	0.036	0.035	0	0.070	0.113
12	$\alpha-0.8535\beta$	0.090	0.032	0.028	0.105	0	0
11	$\alpha-0.6169\beta$	0.045	0.006	0.144	0.100	0.013	0.089
10	$\alpha+0.6997\beta$	0.020	0.014	0.207	0.191	0	0
9	$\alpha+0.7548\beta$	0.013	0.009	0.117	0.128	0.081	0.108
4,5,6,7,8	$\alpha+0.8322\beta$*	0.071	0.062	0	0	0.047	0.053
3	$\alpha+1.4502\beta$	0.026	0.058	0.001	0.043	0.142	0.063
2	$\alpha+1.6419\beta$	0.035	0.099	0.079	0.020	0	0
1	$\alpha+1.7919\beta$	0.014	0.045	0.100	0.121	0.078	0.024

* fivefold degenerate

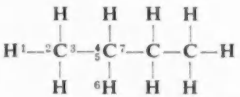

Orbital energy		Electron distribution						
j	ε_j	$(C^j_{H1})^2$	$(C^j_{C2})^2$	$(C^j_{C3})^2$	$(C^j_{C4})^2$	$(C^j_{C5})^2$	$(C^j_{H6})^2$	$(C^j_{C7})^2$
21,22,23,24,25,26	$\alpha-1.3722\beta$*	0.052	0.059	0	0	0.044	0.039	0
20	$\alpha-1.3612\beta$	0.005	0.006	0.047	0.048	0.074	0.066	0.092
19	$\alpha-1.3546\beta$	0.014	0.016	0.133	0.134	0.037	0.034	0
18	$\alpha-1.3436\beta$	0.012	0.013	0.104	0.101	0.005	0.005	0.200
17	$\alpha-1.0870\beta$	0.035	0.022	0.032	0.002	0.057	0.087	0.007
16	$\alpha-0.9473\beta$	0.070	0.032	0	0·032	0.012	0.027	0.083
15	$\alpha-0.7567\beta$	0.064	0.016	0.077	0.116	0.006	0.023	0.009
14	$\alpha-0.5822\beta$	0.026	0.003	0.099	0.058	0.008	0.063	0.114
13	$\alpha+0.6971\beta$	0.012	0.008	0.128	0.113	0.001	0.002	0.192
12	$\alpha+0.7339\beta$	0.016	0.011	0.151	0.155	0.024	0.033	0
11	$\alpha+0.7627\beta$	0.005	0.004	0.047	0.053	0.055	0.072	0.119
5,6,7,8,9,10	$\alpha+0.8322\beta$*	0.059	0.052	0	0	0.039	0.044	0
4	$\alpha+1.4135\beta$	0.014	0.031	0	0.037	0.107	0.050	0.014
3	$\alpha+1.5585\beta$	0.029	0.074	0.024	0.002	0.036	0.014	0.065
2	$\alpha+1.7073\beta$	0.023	0.070	0.094	0.064	0.022	0.007	0.004
1	$\alpha+1.8098\beta$	0.008	0.026	0.063	0.084	0.057	0.017	0.103

* sixfold degenerate

TABLE I (Continued)

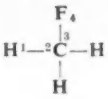

Orbital energy		Electron distribution			
j	ε_j	$(C^j_{H1})^2$	$(C^j_{C2})^2$	$(C^j_{C3})^2$	$(C^j_{F4})^2$
7,8	$\alpha-1.3722\beta$*	0.1561	0.1773	0	0
6	$\alpha-1.0729\beta$	0.1756	0.1112	0.1291	0.0083
5	$\alpha-0.2183\beta$	0.0656	0	0.6691	0.1338
3,4	$\alpha+0.8322\beta$*	0.1773	0.1561	0	0
2	$\alpha+1.0527\beta$	0.0188	0.0244	0.0724	0.7962
1	$\alpha+1.6184\beta$	0.0723	0.1978	0.1285	0.0618

* doubly degenerate

of $-\beta$ (6~7 eV.). This excitation energy is consistent with the spectroscopic data[4].

The characteristics of orbital energies and of the electron distribution stated above agree with the properties observed experimentally in saturated compounds and also with calculated results obtained by Lennard-Jones and Hall's equivalent orbital method[5].

In the doubly degenerate highest occupied orbitals of methyl fluoride, the bonding electrons localize dominantly in the methyl group. In the next highest occupied orbital, an exceedingly large density is observed on the fluorine atom in accordance with the facts pointed out by Frost and McDowell[6], who measured the ionization potentials of methyl halides.

The Coulomb and resonance integrals used in the present paper are summarized in the following table.

$\alpha_H=\alpha-0.2\beta$	$\beta_{cc}=0.34\beta$*
$\alpha_F=\alpha+0.9\beta$	$\beta_{CH}=1.1\beta$
$\alpha_{Cl}=\alpha+0.5\beta$	$\beta_{CF}=0.5\beta$
$\alpha_{Br}=\alpha+0.45\beta$	$\beta_{CCl}=0.65\beta$
$\alpha_I=\alpha+0.40\alpha$	$\beta_{CBr}=0.58\beta$
$\alpha_C=\alpha$	$\beta_{CI}=0.53\beta$

* β_{cc} refers to the resonance integral between two sp^3 orbitals attached to one and the same carbon atom.

A New Reactivity Index for Radical Reactions of Saturated Compounds, $D_r^{(R)}$

The radical reactions of alkyl compounds are covered by the general equation

$$R\text{-}X+Y\cdot\rightarrow[R\cdots X\cdots Y]\rightarrow R\cdot+X\text{-}Y \qquad (1)$$

where R is an alkyl group, X is the group to be extracted and Y is an attacking radical or atom. The bracket in the equation refers to the transition state.

The secular determinant for the activated complex, [R-X···Y], is written

$$\Delta_\sigma=\begin{vmatrix} \alpha_Y-\varepsilon & \gamma\beta & 0 & 0 & 0 & 0 & 0 \\ \gamma\beta & \alpha_X-\varepsilon & \beta_{CX} & 0 & 0 & 0 & 0 \\ 0 & \beta_{CX} & \alpha_C-\varepsilon & \beta_{CH} & \beta_{cc} & & \\ 0 & 0 & \beta_{CH} & \alpha_H-\varepsilon & 0 & & \\ 0 & 0 & \beta_{cc} & 0 & \alpha_C-\varepsilon & & \\ 0 & & & & & & \end{vmatrix}$$

(The secular equation for the R-X molecule)

where α_A refers to the Coulomb integrals of atom A, β_{AB} is the resonance integral between bonding orbitals of atom A and B, and γ is a parameter for the resonance integral of the X-Y incipient bond in the transition state.

By using the perturbation theory, we can derive a new reactivity index, named D_r, for metathetical radical reactions in saturated compounds, in place of the superdelocalizability (S_r) in our previous paper[3].

$$D_r^{(R)}=\sum_j^{occ}\frac{(C_r^j)^2}{\varepsilon_j-\alpha}\beta+\sum_j^{unocc}\frac{(C^j_r)^2}{\alpha-\varepsilon_j}\beta \qquad (3)$$

where C_r^j is the coefficient of the rth atomic orbital in the jth molecular orbital, ε_j is the jth molecular orbital energy, α is the Coulomb integral of a sp^3 orbital in a carbon atom, and β is the resonance integral between two sp^3 orbitals in a C-C bond.

In the derivation of Eq. 3, we assume that α_x is equal to α, and the values of α and β in the activated complex are the same as those of the isolated molecule.

It may be worthy of notice that $D_r^{(R)}$ represents the stabilization energy due to σ type interaction in a radical reaction, while $S_r^{(R)}$ denotes the stabilization energy which

4) P. G. Wilkinson and H. L. Jhonston, *J. Chem. Phys.*, **18**, 190 (1950); W. P. Potts, ibid., **20**, 809 (1952).
5) J. Lennard-Jones and G. G. Hall, *Disc. Faraday Soc.*, **10**, 18 (1951); *Trans. Faraday Soc.*, **47**, 581 (1952); K. Fueki and K. Hirota, *J. Chem. Soc. Japan, Pure Chem. Sec.* (*Nippon Kagaku Zasshi*), **81**, 212 (1960).
6) D. C. Frost and C. A. McDowell, *Proc. Roy. Soc.*, **A241**, 194 (1957).

TABLE II (a). THE CALCULATED VALUES OF $D_r^{(R)}$ AND OBSERVED ACTIVATION ENERGIES IN SEVERAL *n*-PARAFFINS

$$R\text{-}H + R'\cdot \rightarrow R\cdot + R'\text{-}H$$

Compound R-H		$D_r^{(R)}(H)$	E(kcal./mol.)[5] $CH_3\cdot$	$CH_3CH_2\cdot$	$CH_3CH_2CH_2\cdot$
CH_3-H		0.9926	11.5	15.0	16.5
CH_3CH_2-H	(prim-H)	1.0029	10.0	14.8	16.2
$CH_3CH_2CH_2$-H	(prim-H)	1.0032	9.5	14.2	15.5
$CH_3CH_2CH_2CH_2$-H	(prim-H)	1.0043	9.3	13.9	15.3
$(CH_3)_2CHCH_2$-H	(prim-H)	1.0049	—	—	—
$(CH_3)_2CH$-H	(sec-H)	1.015	8.7	13.3	14.5
$CH_3CH_2CH(CH_3)$-H	(sec-H)	1.016	8.2	12.7	14.1
$(CH_3)_3C$-H	(tert-H)	1.027	7.7	11.6	13.4

TABLE II (b). THE AVERAGE VALUES OF $D_r^{(R)}$ (H) AND RATE CONSTANTS CHARACTERISTICS OF VARIOUS TYPES OF HYDROGEN ATOM IN ALKANES

Type of hydrogen atom	$D_r^{(R)}(H)$	$k_C \times 10^{-6}$ at 182°C (mol^{-1} cc. sec^{-1}*[7])
H in methane	0.993	—
Primary H	1.003	0.3
Secondary H	1.016	2.1
Tertiary H	1.027	15

* k_C means the rate constant divided by the number of H atoms of the same kind.

arises from the hyperconjugation taking place between a reagent and a conjugated molecule.

Results and Discussions

In our previous paper[1], the magnitudes of the frontier electron densities at hydrogen atoms in several saturated hydrocarbons ran parallel with the experimental reactivities[7] of hydrogen atoms in metathetical reactions. The frontier electron density for radical attack was shown to be a good intramolecular index of reactivity. This index, however, does not indicate the correct order of reactivity in different molecules. Therefore, we adopt $D_r^{(R)}$ which is useful not only as an intramolecular index but also as an intermolecular index. The calculated values of $D_r^{(R)}$ in several saturated compounds are listed together with the observed values of activation energy[8,9] in various metathetical reactions in Tables II and III.

TABLE III. THE VALUES OF $D_r^{(R)}(H)$ AND ACTIVATION ENERGIES OF HALOMETHANES IN METATHETICAL REACTIONS

(a) $CH_nCl_{4-n} + CH_3\cdot \rightarrow CH_{n-1}Cl_{4-n}\cdot + CH_4$

Compound	$D^{(R)}(H)$	E(kcal./mol.)[9]
$CHCl_3$	2.181	5.8
CH_2Cl_2	1.237	7.2
CH_3Cl	1.058	9.4

(b) $CH_nF_{4-n} + CH_3\cdot \rightarrow CH_{n-1}F_{4-n}\cdot + CH_4$

Compound	$D_r^{(R)}(H)$	E(kcal./mol.)[9]
CH_3F	1.181	8.7
CH_2F_2	1.235	6.2

(c) $CH_nX_{4-n} + Br\cdot \rightarrow CH_{n-1}X_{4-n}\cdot + HBr$

Compound	$D_r^{(R)}(H)$	E(kcal./mol.)[9]
CH_4	0.993	17.8
CH_3Br	1.071	15.6
$CHCl_3$	2.181	10.0

Hydrogen Extraction Reaction.—In the case of reaction $RH + R'\cdot \rightarrow R\cdot + R'H$, results of calculation and experiments are cited in Table II (a) and (b), where R and R' are two different alkyl groups. The values of $D_r^{(R)}$ at hydrogen atoms in several lower paraffins indicate a tendency that the larger the molecule RH is, the smaller is the magnitude of activation energy, this being in accord with experiments[8]. Furthermore, these values of $D_r^{(R)}$ agree with the activities of various kinds of hydrogen atoms estimated by Trotman-Dickenson[7] as shown in Table II (b).

In Table III (a), (b) and (c), the calculated values of $D_r^{(R)}$ at hydrogen atoms in various halomethanes are listed together with the observed activation energies[9]. In Table III (a), the radical reactions between methyl radical and chlorine-substituted methanes are indicated. The greater the number of chlorine atoms in methane is, the smaller is the activation energy, and also the magnitude of $D_r^{(R)}$ at hydrogen atoms increases with the number of chlorine atoms. The results on fluorine-substituted methanes are shown in Table III (b), and

7) A. F. Trotman-Dickenson, *Quart. Revs.*, 7, 198 (1953).

8) N. N. Tikhomirova and V. V. Voevodski, *Chem. Abstr.*, 45, 9940 (1951).

9) E. W. R. Steacie, "Atomic and Free Radical Reactions", Reinhold Co., New York. (1946); ibid., Second Ed. Vol. II (1954).

the case where a bromine atom attacks methane derivatives is indicated in Table III (c). Also in the last two cases, although experimental data are few, a parallelism between the values of $D_r^{(R)}$ and the activation energies[9] is clearly observed.

Halogen Abstraction Reaction.—In Table IV (a), (b) and (c) are illustrated both the calculated values of $D_r^{(R)}$ at the halogen atom

TABLE IV. THE VALUES OF $D_r^{(R)}(X)$ AND ACTIVATION ENERGIES IN HALOMETHANES IN METATHETICAL REACTIONS

(a) $CH_3X + H\cdot \rightarrow CH_3\cdot + HX$

CH_3X	$D_r^{(R)}(X)$	E(kcal./mol.)[9]
CH_3I	1.851	5
CH_3Br	1.669	—
CH_3Cl	1.496	7~9
CH_3F	1.415	9

(b) $CH_nCl_{4-n} + H\cdot \rightarrow CH_nCl_{3-n}\cdot + HCl$

Compound	$D_r^{(R)}(Cl)$	E(kcal./mol.)[9]
CH_3Cl	1.496	7~9
CH_2Cl_2	1.756	6
$CHCl_3$	3.200	4.3
CCl_4	3.829	3.5

(c) $CH_nBr_{4-n} + Na\cdot \rightarrow CH_nBr_{3-n}\cdot + NaBr$

Compound	$D_r^{(R)}(Br)$	E(kcal./mol.)[9]
CH_3Br	1.669	5.9
CH_2Br_2	2.045	2.6
$CHBr_3$	4.889	0.3

in various halomethanes and the observed values of activation energy in the halogen extraction reactions[9]. In Table IV (a), a good agreement is observed between the values of $D_r^{(R)}$ and the activation energies of various monosubstituted halomethanes. In Table IV (b), the values of $D_r^{(R)}$ at chlorine atoms in various chlorine-substituted methanes and the activation energies in the hydrogen-atom reactions are indicated. In Table IV (c), the values of $D_r^{(R)}$ at bromine atoms in several bromomethanes are compared with the activation energies in the sodium-atom reaction.

In spite of the fact that this is the first attempt of the quantum-mechanical investigation of the reactivity of saturated compounds, the agreement of the theory with experience is almost satisfactory, and hence the new quantum-mechanical quantity $D_r^{(R)}$ can be a useful index for predicting the reactivity of saturated compounds, equally with S_r in conjugated molecules. There remain, however, some points to be checked in future. These are summarized as follows:

(1) We assume that α_x is equal to α to derive D_r. Meanwhile, a slight change in activation energy is experimentally observed according to the species of attacking reagents. Hence, if the values of α_x would be modified according to the change of the attacking reagent, this effect can be interpreted in the present procedure.

(2) In the present treatment, we do not take into account the stabilization energy due to the resonance in an attacking alkyl radical or the radical formed. It has been made clear that this resonance energy has a remarkable influence on the magnitude of the activation energy[10]. In this connection, the present treatment should be modified so as to involve the contribution of this kind of resonance to the activation energy.

(3) A disagreement between the values of $D_r^{(R)}$ in methyl halides and the experimental activation energies is observed. This is probaly because the energies of the vacant orbitals of some methyl halides are nearly equal to α. Thus, the values of the $D_r^{(R)}$ become extremely large. If carefully selected values of parameters for halogen atoms should be adopted, these disagreements may be avoidable.

Faculty of Engineering
Kyoto University
Sakyo-ku, Kyoto

10) M. G. Evans, *Disc. Faraday Soc.*, **10**, 1 (1951); C. A. Coulson, ibid., **2**, 9 (1947).

Studies on the Diacylaminoanthraquinone Dyes

By Takayuki HAYASHI and Reiko SHIBATA

(Received September 20, 1960)

In our previous papers[1-5], 1-acylamino-, 1,4-, 1,5- and 1,8-diacylaminoanthraquinones having NO_2, Cl, OMe, $SO_2N(Me)_2$ or NH_2 (X or Y)* as a substituent in the acyl group were prepared. Visible and infrared absorption spectra of these dyes were measured in solution and in solid, respectively, and cotton was dyed with them, and their light fastness on cotton was tested. On the basis of these results, the effects of X and Y substituent groups were discussed with their various properties, such as wavelengths of absorption maxima, relative difficulties of vatting, color tones of vat solutions, shades of dyed cotton, and light fastness. In this paper, the abovementioned properties have been discussed correlatively for all of these dyes.

Results and Discussion

Visible Absorption Spectra.—Visible absorption spectra of 1-acylamino-, 1,4- and 1,5-diacylaminoanthraquinone series were observed and discussed by Peters and Sumner[6]. In this paper, from the results of visible absorption for 1-acylamino-, 1,4-, 1,5- and 1,8-diacylaminoanthraquinones, the relation between wavelengths or intensities of the absorption maximum and positions of acyl groups has been discussed. Furthermore, for each series of 1-acylamino-, 1,4-, 1,5- and 1,8-diacylaminoanthraquinones the effect of the substituent (X or Y) in the acyl group upon the wavelength and intensity of the absorption maximum has been considered.

The absorption maxima[1-4] of 1-benzoylamino-, 1,4-, 1,5- and 1,8-dibenzoylaminoanthraquinones appeared at 421, 502, 448 and 455 mμ in *o*-dichlorobenzene with the peak molar extinction coefficient of 5900, 7600, 12000 and 11000, respectively. Since the molecule of the 1,5-derivative is divided into two halves diagonally as in III, simple additivity is established between two chromophoric systems within it, and one to three benzene rings in

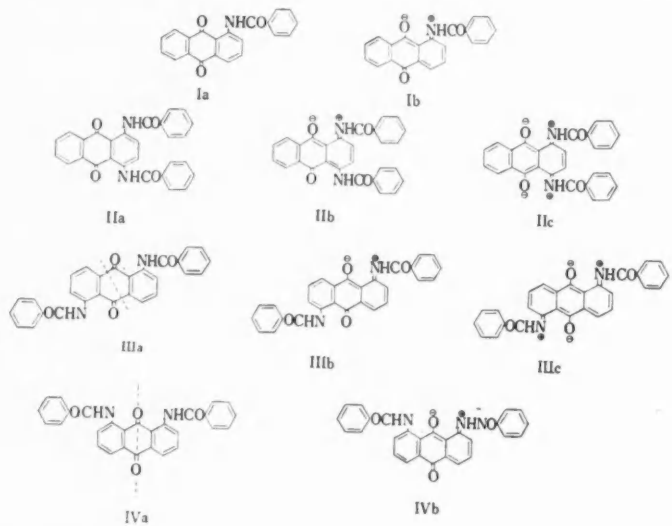

1) T. Hayashi and R. Shibata, *J. Chem. Soc. Japan, Ind. Chem Sec.* (*Kogyo Kagaku Zasshi*), **63**, 513 (1960).
2) T. Hayashi and R. Shibata, ibid., **63**, 840 (1960).
3) T. Hayashi, ibid., **63**, 1241 (1960).
4) T. Hayashi, ibid., **63**, 1395 (1960).
5) T. Hayashi, ibid., **63**, 1985 (1960).
* X or Y denotes a substituent in the acyl group of acylaminoanthraquinones.
6) R. H. Peters and H. H. Sumner, *J. Chem. Soc.*, 1953, 2101.

the anthraquinone nucleus increase their quinonoid character, thereby reducing the aromaticity, but the extent of the contribution of a structure IIIc to the resonance is exceedingly small. For the 1-derivative, on the other hand, one to two benzene rings in the anthraquinone nucleus increase their quinonoid character as in I, thereby reducing the aromaticity, and only one carbonyl group of the anthraquinone nucleus takes part in conjugation, this being different from the 1,5-derivative. The wavelength of the absorption maximum for the 1,5-derivative should therefore be somewhat longer than for the 1-derivative, but the intensity of the former should be approximately twice that of the latter. Since the molecule of the 1,8-derivative is divided into two halves vertically as in IV, simple additivity is established between two chromophoric systems within it as the 1,5-derivative, but one to two benzene rings in the anthraquinone nucleus increase their quinonoid character, thereby reducing the aromaticity, this being different from the 1,5-derivative. Though one carbonyl group is held by two chromophoric systems in common for the 1,8-derivative, mesomeric shifts of electrons within the chromophoric systems are suppressed, owing to cross conjugation of two systems, in which case the extent of the contribution of a structure IVb to the resonance should be a little greater than for a structure IIIb. The effective area of π-electron systems[7,8] for IV is also slightly smaller than for III. The wavelength of the absorption maximum for the 1,8-derivative should therefore be somewhat longer than for the 1,5-derivative, and the intensity of the former should be a little lower than for the latter but approximately twice that of the 1-derivative. For the 1,4-derivative one to two benzene rings in the anthraquinone nucleus increase their quinonoid character, thereby reducing the aromaticity, and the extent of the contribution of a structure IIc to the resonance is more marked. The 1,4-derivative shows no such simple additivity as indicated in III owing to interaction between their two chromophoric systems, probably producing a new one, and an effective area of π-electron systems for II is smaller than for III or IV. The wavelength of the absorption maximum for the 1,4-derivative should therefore be the longest among them and the intensity should lie between those of 1- and 1,8-derivatives. Such relations should be established similarly among 1-acylamino-, 1,4-, 1,5- and 1,8-diacylaminoanthraquinones with the same substituent in the acyl group.

From results[1-4] of the bands for each series, it was known that electron-attracting substituents mainly showed a +I effect and electron-donating substituents mainly a −T effect and the *p*-dimethylsulfamyl group showed a +I effect similar to a *p*-nitro group, this being different from the result of the *p*-sulfamyl group obtained by Zollinger[9]. For the bands of each series, it was shown that the shifts of the absorption maximum complied with Hammett's rule[10] and that the relationship between the wavelengths of the absorption maximum and Brown's σ^+ values[11,12] was

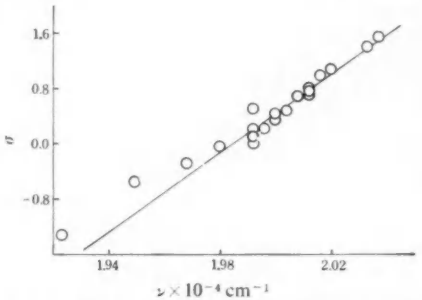

Fig. 1. The relationship between wave-number (ν) of the maximum absorption and Hammett's σ value on the 1,4-diacylaminoanthraquinone series.

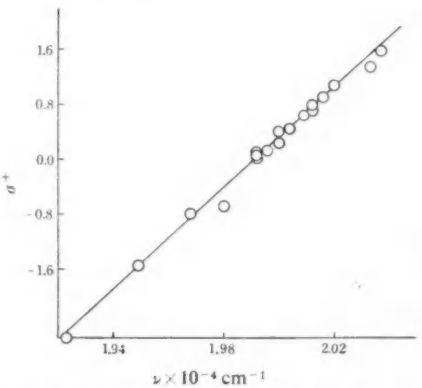

Fig. 2. The relationship between the wavenumber (ν) of the maximum absorption and Brown's σ^+ value on the 1,4-diacylaminoanthraquinone series.

7) E. A. Braude, ibid., **1950**, 379.
8) R. H. Peters and H. H. Sumner, *J. Soc. Dyers Colorists*, **71**, 130 (1955).
9) H. Zollinger and C. Wittwer, *Helv. Chim. Acta*, **39**, 347 (1956).
10) H. H. Jaffé, *Chem. Revs.*, **53**, 191 (1953).
11) H. C. Brown and Y. Okamoto, *J. Am. Chem. Soc.*, **80**, 4979 (1958).
12) G. W. Gray, "Steric Effects in Conjugated Systems", Butterworths Scientific Publications, London (1958), p. 100.

more linear than that between them and Hammett's σ values[10] as indicated in Figs. 1 and 2 for the 1,4-diacylaminoanthraquinone series. Accordingly it is possible to estimate a shift from Brown's σ^+ value of a substituent in the acyl group and obtain an expected shift of the absorption maximum by introduction of an adequate substituent with known Brown's σ^+ value to the acyl group. Hammett's σ value of *p*- and *m*-dimethylsulfamyl groups were 0.70 and 0.53, and Brown's σ^+ values of these were 0.86 and 0.68, respectivery, from Figs. 1 and 2.

For each series, dyes with *o*-chloro, *o*-methoxy or *o*-nitro groups, besides an *o*-amino group, as X and Y, showed a considerably hypsochromic shift and a decreasing intensity in their absorption maxima. Both the wavelengths and the intensities were almost independent of all combinations of substituents in two acyl groups for each series. As indicated in Table I, the absorption maximum of 1,5-diacetylaminoanthraquinone agreed with those of 1,5-di-*o*-substitutes. This fact was admitted on the other *o*-substitutes. The effect of the *o*-substituted phenyl group should therefore be much the same as that of the methyl group, and this fact shows that the benzene ring has been twisted around the C–C linkage between

Table I. Visible absorption bands of *o*-substituted benzoylamino- and acetylamino-anthraquinones[1-4]

	o-Substitute	Acetylamino-anthraquinone
1-Derivative	407~411 (5300~6000)**	415 (5300)
1,4-Derivative	483~486 (6950~7100)	487 (7550)
1,5-Derivative	437~439 (10500~11500)	438 (11000)
1,8-Derivative	438~441 (9700~10200)	440 (10400)

the *o*-substituted phenyl and the carbonyl group in the acyl group. The twisting may be attributed to the steric hindrance between the *o*-nitro and the carbonyl group or to the repulsion between the *o*-chloro or *o*-methoxy and the carbonyl group in the acyl group. The wavelengths of the absorption maximum of 1-*o*-amino-, 1,4-, 1,5- and 1,8-di-*o*-amino-substitutes were 436, 514, 460 and 463 mμ in *o*-dichlorobenzene, respectively. As these absorption peaks do not show a hypsochromic shift, they are different from the ones of the other *o*-substitutes, such the interesting twisting of the benzene ring as in *o*-substitutes may not arise.

** Wavelength, mμ (molar extinction coefficient).

Infrared Absorption Spectra.—Three and six μ bands of infrared absorption spectra for some acylaminoanthraquinones have been observed as powders suspended in Nujol on account of their limited solubility and were discussed by Flett[13]. In this work, infrared absorption spectra of 1-acylamino-, 1,4-, 1,5- and 1,8-dibenzoylaminoanthraquinones have also been observed as powders suspended in Nujol and information has been gained about their structures in the solid. This information may be, to some extent, similar to deduction for the structure of the dye molecule in cotton dyed with them.

As indicated in Table II, a C=O frequency in the peri-position of the benzoyl group for 1,4-dibenzoylaminoanthraquinone is lower than for the 1,5-isomer, and then the C=O bond of the former is more weakened than for the latter. This fact may generally suggest that the shade of the 1,4-diacylaminoanthraquinone series on cotton is more bathochromic than in the case of the 1,5-isomer. As 3 μ bands of 1,5-dibenzoylaminoanthraquinone almost agree with those of the 1,8-isomer, the effect of imino groups on the whole of the molecule is much the same in both cases. This fact may generally suggest that a shade of the 1,5-diacylaminoanthraquinone series on cotton is approximately the same with that of the 1,8-isomer.

Table II. 3 and 6 μ bands of solid benzoylaminoanthraquinones[a]

	3 μ bands cm^{-1}	6 μ bands cm^{-1} (C=O frequencies)
1-Derivative	3175	1681, 1669, 1637
1,4-Derivative	3125, 3086, 3058	1686, 1639
1,5-Derivative	3226, 3195, 3125[a]	1689, 1639
1,8-Derivative	3226, 3185, 3125[a]	1701, 1681, 1631

a) 3 μ bands obtained from KBr discs of 1,5- and 1,8-derivatives were all the same (3257, 3226, 3125 cm^{-1}).

Though it is known that the question, whether or not shifts of a C=O frequency comply with Hammett's rule, must be generally discussed in regard to the result obtained from the dilute solution of a nonpolar solvent, the results obtained from the solid of the 1-acylaminoanthraquinone series have been examined on account of its limited solubility in the present work. Shifts in the C=O frequency of the acyl groups were in harmony with Hammett's rule, as indicated in Fig. 3. Shifts in the C=O frequency of the peri-position of the acyl groups lay on the S-shaped curve against

13) M. S. C. Flett, *J. Chem. Soc.*, **1948**, 1441.

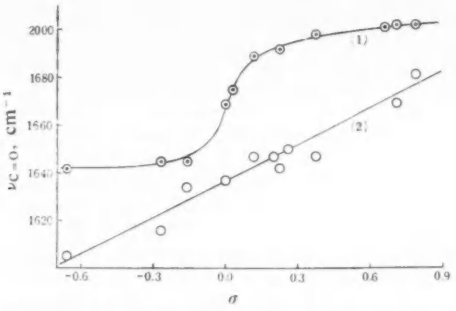

Fig. 3. The relationship between the C=O frequency ($\nu_{C=O}$) and Hammett's σ value on the 1-acylaminoanthraquinone series.
(1) The quinone-type C=O frequency in the peri-position of the acylamino group.
(2) The C=O frequency in the acyl group.

Hammett's σ value, as indicated in Fig. 3, and the latter C=O bond was therefore strengthened to much the same degree for the dyes with any of the electron-attracting substituents and the reverse was found to be true for the dyes with any of the electron-donating substituents. For the 1-derivative with a *p*- or *m*-dimethylsulfamyl group which is intensely electron-attracting, the C=O bonds of its molecule in solid have been strengthened to the extent indicated on the curve of Fig. 3.

As C=O frequencies[5] of (*o*-nitrobenzoyl)-aminoanthraquinone agree with those of 1-acetylaminoanthraquinone[13], the effect of the *o*-nitrophenyl group on them is thought to be of the same degree as that of the methyl group. This fact shows that the benzene ring of the former has been twisted around the C–C linkage between the *o*-substituted phenyl and the carbonyl group in the acyl group, and that the twisting may be attributed to steric hindrance between the *o*-nitro and the carbonyl group in the acyl group. For the *o*-nitro-substitute, this interpretation of its molecular structure in solid is the same as the deduction on that in solution on the basis of the results of the visible absorption. From shifts in the C=O frequency[5] of the acyl group for *o*-chloro- and *o*-methoxy-substitutes, however, it seems probable that such twisting of the benzene ring does not arise on the molecule in solid, this being different from the molecule in solution. Though the benzene ring of the *o*-chloro- or *o*-methoxy-substitute in solution has been twisted by repulsion between the *o*-chloro or *o*-methoxy and the carbonyl group in the acyl group, such twisting may be suppressed in a solid where the molecules are paked closely. From the result of infrared absorption, it seems likely that for the *o*-amino-substitute in solid the benzene ring also does not twist, this being identical with the deduction on its molecular structure in solution on the basis of the results of the visible absorption.

Relative Difficulties of Vatting.—It has been concluded that from the interpretation of visible absorption for the acylaminoanthraquinone series, an electron density of the quinone-type carbonyl group within the chromophoric system decreases in the order of 1, 4-, 1, 8- and 1, 5-isomers, and that it decreases in the order of 1, 4- and 1, 5-isomers from examinations of their infrared absorption. From both these bits of information and a reduction mechanism of anthraquinone[14], it is deduced that difficulty of reduction, namely difficulty of vatting, should naturally increase in the order of 1, 4-, 1, 8- and 1, 5-isomers. The result has also been obtained from our experiments[2-4] showing that difficulty of vatting increases in the order of 1, 4-, 1, 8- and 1, 5-isomers and vatting of the 1, 8-isomer is no more difficult than vatting of the 1, 4-isomer.

The result has been obtained from our experiments[2-4] that, for each seris of 1, 4-, 1, 5- and 1, 8-diacylaminoanthraquinones, the effect of X or Y on the difficulty of vatting increases in the order of *p*-$SO_2N(Me)_2$, *m*-$SO_2N(Me)_2$, *m*-OMe, *m*-Cl, *p*-OMe, *p*-Cl, *m*-NO_2, *p*-NO_2. But difficulties of vatting of *m*-methoxy-, *m*-chloro- and *p*-methoxy-substitutes have been of much the same degree as that of the non-substitute and those of dimethylsulfamyl-substitutes have been especially small[2-4]. It is known that the relative difficulty of vatting, namely the relative difficulty of reduction,

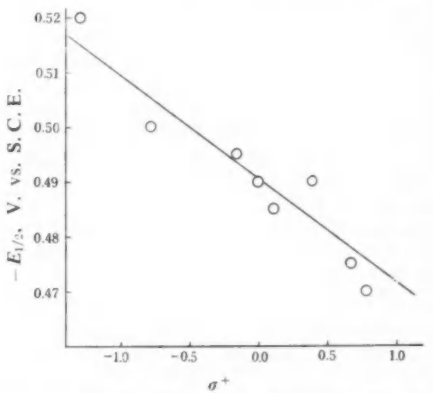

Fig. 4. The relationship between the first half-wave potential ($-E_{1/2}$) in ethanol and Brown's σ^+ value on the 1-acylaminoanthraquinone series.

14) T. Vickerstaff, "Physical Chemistry of Dyeing", Oliver & Boyd, London (1954), p. 282.

is dependent on both the magnitude of the reduction potential and the degree of the rate of reduction[14]. For the reduction potential, shifts of the reduction potential for 2-substitutes of 1,4-naphthoquinone or for 3-substitutes of phenanthrenquinone were in harmony with Hammett's rule[2], and a relationship between the first half-wave potentials of 1-acylaminoanthraquinone series and Brown's σ^+ values were also in accordance with Hammett's rule, as indicated in Fig. 4. From these results, there seems likely to be a correlation between the magnitude of the reduction potential and Hammett's σ or Brown's σ^+ value of the substituent for each series of acylaminoanthraquinones. On the contrary, from our results described above, it is evident that the effect of X or Y on the difficulty of vatting has been dependent not only on Hammett's σ or Brown's σ^+ value but also on the hydrophilic or hydrophobic property of X or Y. Therefore, it seems likely that for each series the relative difficulty of vatting is dependent on both the magnitude of the reduction potential and the degree of the rate of reduction, and that the rate of reduction bears a relation to the hydrophilic or hydrophobic property of X or Y.

Color Tones of Vat Solutions. — For leuco salts of these dyes, as two electron-donating substituents (O^-) occupy 9- and 10-positions where they have the maximum conjugation with the anthracene nucleus, the effect of these substituents is considerably greater than that of such substituents as acyl groups occupying the other positions. Therefore, the entire visible absorption curve, that is, color tones of vat solution for all of 1,4-, 1,5- and 1,8-diacylaminoanthraquinone series should be similar to one another. Such deduction has been consistent with our results[2-4], that is, the color tones of vat solution for all of them, except for di-*o*-substitutes, were from reddish violet-blue to reddish violet. Waters[15] and Venkataraman[16] also reported that for the vat solutions of anthraquinone, aminoanthraquinone, acylaminoanthraquinone and others the visible absorption curves with maximum absorption bands at 425 and 515 mμ were given, being approximately similar to one another.

Shades of Dyes. — The 1,4-diacylaminoanthraquinone series was a red dye, and 1,5- and 1,8-derivatives were yellow dyes but the shade of the latter on cotton was somewhat more bathochromic than that of the corresponding isomer of the former[2-4]. For all of the dyes with a nitro group as X or Y, the shades on cotton were from brown to intensly brownish on account of the amino group (reduction of the nitro group)[2-4]. The fact that the shade is hypsochromic in the order of 1,4-, 1,8- and 1,5-isomers, is explained in the same way by electronic interpretations on shifts in visible absorption bands for these dyes in solution. It was admitted that for each series of diacylaminoanthraquinones a shade of the XY type*** was in the middle between shades of the corresponding XX type and of the YY type, and this fact has shown that the effects of X and Y on the shift of the shade are additive. An electron-donating substituent in the acyl group causes the bathochromic shift of the shade and the reverse is found for electron-attracting substituents. Though *p*- and *m*-dimethylsulfamyl groups were found to be intensly electron-attracting from examinations of the visible absorption, the shades of dyes with these groups as X or Y have merely shown a change from the weak hypsochromic to the weak bathochromic shift. For 1,4- and 1,5-diacylaminoanthraquinone series, an effect of X or Y on enhancement of brilliance of the shade has been shown to be greater in the *m*- than in the *p*-position within the acyl group, as described in the PB Report[17], but such a difference has not been found for the 1,8-derivative. Generally speaking, the degree of brilliance on the shade of the XY type for each series of diacylaminoanthraquinones was higher than that of the corresponding XX or YY type.

It is known that adsorption of leuco vat dyes on cellulose is dependent on both their affinity and rate of diffusion[18], but as the rate of diffusion may be independent of a kind of X or Y for the acylaminoanthraquinone series, it seems likely that adsorption of leuco acylaminoanthraquinones is dependent on their affinity, and, therefore, the greater the affinity is, the greater is the depth of the shade. From affinities of some acylaminoanthraquinones for cotton, it has been concluded that for any one of these series there is little difference in affinity between the *m*- and *p*-substitutes but their affinities are greater than that of a non-substitute and a great reduction in affinity is shown on the *o*-substitutes[5,18]. From these bits of information, the depth of the shade of the non-substitute should be less than those of *m*- and *p*-substitutes and those of the *o*-substitutes should be especially small for each series. Such deductions have been consistent with our results[2-4] obtained from comparison

15) E. Waters, *J. Soc. Dyers Colorists*, **66**, 544 (1950).
16) M. R. Padhye, N. R. Rao and K. Venkataraman, *J. Sci. Ind. Research (India)*, **13B**, 759 (1954); *Chem. Abstr.*, **49**, 15836 (1955).

*** The XX or YY type denotes the diacylaminoanthraquinone with the same two acyl groups and the XY type that with two different acyl groups.
17) BIOS 987 (PB 75860) p. 185.
18) T. Vickerstaff, loc. cit., p. 299.

with the depth of the shade for many sets of the same shade. It is known that there is a definite correlation between affinity and molecular weight for these dyes, except for *o*-substitutes[8,18], but for dyes with a dimethylsulfamyl group as X or Y, the depth of the shade has been less in spite of the increase of molecular weight with the increasing surface area. This fact is due to a reduction of van der Waals force based on a decreasing coplanarity which is attributed to the bulky volume of the dimethylsulfamyl group.

***o*-Substitutes.**—It has been known from our experiments[2-4] that vatting of *o*-substitutes is more difficult than for *m*- and *p*-substitutes and the color tones of the vat solution for the former are more hypsochromic and pale than for the latter, and the former has dyed cotton with more difficulty.

From interpretations of visible absorption bands for *o*-substitutes, it has been concluded that mesomeric shifts of electrons within their chromophoric system are suppressed by the *o*-substituents, namely the *o*-substituents lower the electron density of the quinone-type carbonyl group. In consideration of both this fact and the vatting mechanism of *o*-substitutes, it is natural that these dyes have increasing difficulty in vatting, as described above. For leuco *o*-substitutes the hypsochromic shifts in the color tone of their vat solutions, described above, are attributed to the reduced conjugation between the anthracene nucleus and *o*-substituted benzoyl groups, and the palenen of vat solutions may be due to a decrease in an effective area of the π-electron system for *o*-substitutes. For *o*-chloro- and *o*-methoxybenzoylaminoanthraquinones, Valentin[19] has partially attributed their reduced affinities to internal chelation within acylamido groups, as indicated in Va and Vb, but the reduced affinity of *o*-methylbenzoylaminoanthraquinone[8,18] can not be explained satisfactorily from his suggestion, and the presence of the internal chelation is inconsistent with the information about the molecular structure obtained from their visible absorption. As *o*-substituents make it difficult for the *o*-substitutes to attain a planar configuration as indicated by this information, these dyes may dye cotton with difficulty, as described above, on account of the reduction of van der Waals force with the decreased affinity.

Va

Vb

Vc

From interpretations on their visible absorption, it seems likely that *o*-amino-substitutes (reduction of the *o*-nitro-substitutes) have maintained coplanarity of the molecule, but the *o*-aminosubstitutes have also dyed cotton with difficulty. These results may be taken to show that the *o*-amino group prevents the hydrogen bond formation between the amido group and the cellulose hydroxyl group on account either of the steric hindrance of the *o*-amino group or the internal chelation as indicated in Vc.

Light Fastness.—Several relations between chemical constitutions of 1,4-, 1,5- and 1,8-diacylaminoanthraquinone series and their light fastness have been drawn from the results[2-4] of the light fastness test for them. In the first place, grades of light fastness on cotton for 1,4-, 1,5- and 1,8-dibenzoylaminoanthraquinones were 7, 6 and 5, respectively. The light fastness of the diacylaminoanthraquinone series on cotton has generally become lower in the order of 1,4-, 1,5- and 1,8-isomers. The shades of these dyes on cotton, except for *p*-substitutes of the 1,4-diacylaminoanthraquinone series, have not shown fading, but have shown a sign of turning brown under sunlight. For 1,5- and 1,8-diacylaminoanthraquinone series the light fastness of *p*-substitutes was generally higher than that of corresponding *m*-substitutes, which was higher than that of corresponding *o*-substitutes for each series of 1,4-, 1,5- and 1,8-diacylaminoanthraquinones. For each series of them, in comparison with the light fastness of a non-substitute, the dyes with a chloro group as X have shown almost no lowering, but the dyes with a methoxy or dimethylsulfamyl group have shown slight lowering, and all of the dyes with a nitro group (an amino group on cotton) evident lowering.

It is know that for a group of dyes of the

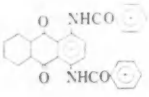

VIa

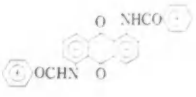

VIb

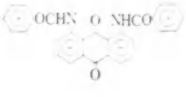

VIc

19) L. Valentin, *J. Soc. Dyers Colorists*, **72**, 286 (1956).

same type, for example simple azo dyes, in general, the greater the difference is of an electron density on two parts within a molecule of the dye, the higher the light fastness of the dye is. For dibenzoylaminoanthraquinones it seems likely that an electron density of the benzene ring in the benzoyl group is lower than that of the benzene ring within the anthraquinone nucleus, as indicated in VIa, VIb and VIc, from both pieces of information about mesomeric shifts of electrons within the chromophoric systems and examinations of some reactions of the dyes with reagents. For 1,4-dibenzoylaminoanthraquinone two chromophoric systems hold one benzene ring within the anthraquinone nucleus in common, but for 1,5- and 1,8-dibenzoylaminoanthraquinones two chromophoric systems bear relations with different benzene rings in the anthraquinone nucleus respectively. The difference between electron densities of the benzene ring in the benzoyl group and of the benzene ring in the anthraquinone nucleus for the 1,4-derivative should therefore be greater than for the 1,5- or 1,8-derivative. From interpretations of both visible and infrared absorption for 1,5- and 1,8-derivatives, it has been concluded that an electron density of the quinone-type carbonyl group on the peri-position of the benzoylamido group for the latter is somewhat higher than for the former. As two chromophoric systems of the 1,8-derivative holding one carbonyl group in common are cross conjugation, mesomeric shifts of electrons within them are suppressed by each other; but, on the other hand, two chromophoric systems of the 1,5-derivative bear almost no relation to each other. The extent of the mesomeric shift of electrons within one chromophoric system for the former is therefore less than for the latter, and then the difference between electron densities of the benzene ring in the benzoyl group and of the benzene ring in the anthraquinone nucleus for the former is less than for the latter. Finally, the difference between electron densities of two benzene rings decreases in the order of 1,4-, 1,5- and 1,8-isomers, and this order may be responsible for the lowering of light fastness in the order of 1,4-, 1,5- and 1,8-isomers, described above. An alternative possibility is that the 1,5-isomer being transform it probably packs more compactly than the 1,8-isomer which is in cis-form in the solid of the dye within the fiber, and also that the light fastness of the former may be higher than that of the latter.

The effects of Cl, OMe or NH_2 as X on light fastness, described above, were similar to the results[20] already known concerning many dyes. Though a dimethylsulfamyl group is intensely electron-attracting, shades of the dyes with this group as X or Y have only shown changes from weak bathochromic to weak hypsochromic shifts in comparison with the shade of the non-substitute, and further the dimethylsulfamyl group has an appearance of a weak electron-attracting or weak electron-donating group in these cases. This fact may bear some relation to the lowering of the light fastness of these dyes described above. The lowering of light fastness may be due to the fact that these dyes can not pack compactly in the solid of the dye within the fibre owing to the bulky volume of the dimethylsulfamyl group.

The authors wish to express their sincere thanks to Professor Yoshio Nagai and Dr. Shimpachiro Kato of Tokyo University for their helpful suggestions and encouragement in the course of this work. They also wish to thank the Tokuyama Research Laboratory of Idemitsu Kōsan Co. for infrared measurements.

Department of Chemistry
Faculty of Literature and Science
Yamaguchi University
Ushirogawara, Yamaguchi-shi

20) A. Gebhard, ibid., **25**, 305 (1909).

Polyterpenes. III[1]. *The Structure of Thujopsene**

By Hiroshi KOBAYASHI, Shizuo NAGAHAMA and Saburo AKIYOSHI

(Received November 19, 1960)

Thujopsene, the main component of Hiba wood oil, has attracted much attention in the last few years[2]. Hirose and Nakatsuka[3] pointed out that widdrene[4], which was later shown to be widely distributed in *Cupressaceae*[5], was identical with thujopsene. Erdtman and Norin[6] confirmed this identity and proposed structure Ia for this compound. Independently we also arrived at the same conclusion and proposed structure Ia and Ib[7], of which the former is preferred[5]. Subsequently Erdtman and Norin[9] presented further evidence and revised their structure to Ib. Sisido and Nozaki[10] proposed structure Ic for thujopsene, but later withdrew their suggestion[11] in favor of Erdtman and Norin's proposal. In view of the evidence presented[12] we also consider that the properties of thujopsene are best explained by the formula Ib.

We now wish to present our findings which have already been outlined in our short communication[8].

Thujopsene (I) possesses the molecular formula $C_{15}H_{24}$ and is a tricyclic hydrocarbon compound having an unsaturated bond. On the permanganate oxidation in acetone, it gives ketocarboxylic acid, $C_{15}H_{24}O_3$ (II), as a main product in addition to other by-products. Ozonolysis of thujopsene gives the same acid II. This acid II is therefore considered as the primary product to which thujopsene cleaves at the unsaturated bond without any other change. Thus, the purpose of the studies comes to determine the structure of acid II.

Hypobromite oxidation of II affords a dicarboxylic acid, $C_{14}H_{22}O_4$ (III), which shows the presence of the CH_3-CO- group in the keto acid II, and these results, when considered together with the preceding data, seem

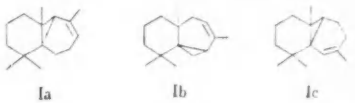

Ia Ib Ic

Fig. 1

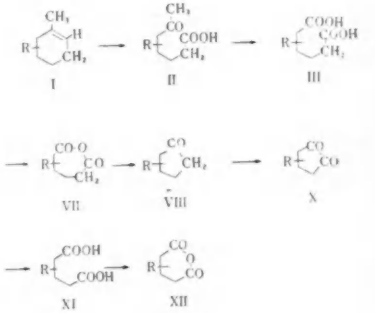

Fig. 2

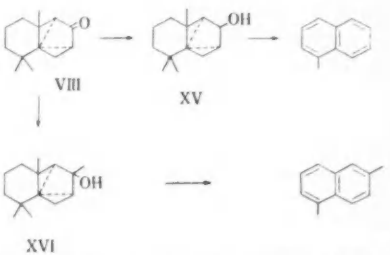

Fig. 3. In VIII, a cyclopropane ring is fused to a cyclopropanone ring in either of the ways which are showed above by the two broken lines.

The broken lines in XV and XVI present the same meaning as in VIII.

* Contribution No. 16 from the Department of Organic Synthesis, Faculty of Engineering, Kyushu University.

1) Previous paper: S. Nagahama, H. Kobayashi and S. Akiyoshi, This Bulletin, **32**, 366 (1959).

2) For references to previous studies, see S. Akiyoshi and S. Nagahama, This Bulletin, **30**, 886 (1957).

3) Y. Hirose and T. Nakatsuka, *J. Jap. Wood Res. Soc.*, **4**, 26 (1958).

4) H. Erdtman and B. R. Thomas, *Acta Chem. Scand.*, **12**, 267 (1958).

5) H. Erdtman and Z. Pelchowicz, *Chem. Ber.*, **89**, 341 (1956); C. Enzell, *Acta Chem. Scand.*, **14**, 81 (1960); C. Pilo and J. Runeberg, ibid., **14**, 353 (1960); J. Runeberg, ibid., **14**, 797 (1960).

6) H. Erdtman and T. Norin, ibid., **13**, 1124 (1959).

7) S. Akiyoshi, H. Kobayashi and S. Nagahama, presented at the 2nd Symposium on Perfumary of Terpene and Essential Oil Chemistry, Hiroshima, October, 1958.

8) H. Kobayashi, S. Nagahama and S. Akiyoshi, This Bulletin, **32**, 203 (1959).

9) H. Erdtman and T. Norin, *Chem. & Ind.*, **1960**, 622.

10) K. Sisido and H. Nozaki, *J. Org. Chem.*, **25**, 875 (1960).

11) K. Sisido, H. Nozaki and Y. Imagawa, presented at the 4th Symposium on Natural Organic Compounds, Kyoto, October, 1960.

12) S. Forsén and T. Norin, *Acta Chem. Scand.*, in press. We thank Dr. Norin for the kind presentation of his manuscript of this paper.

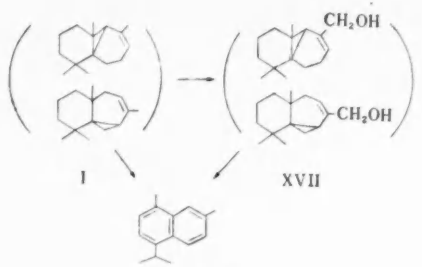

Fig. 4

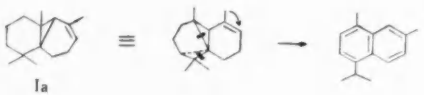

Fig. 5

to indicate the presence of the structure CH_3-C=C- in thujopsene.

C-

The keto acid II is, when treated with mineral acid, easily isomerized to a ketolactone (carbonyl absorptions 1774 and 1724 cm^{-1}) accompanied with a cleavage of a ring in the keto acid II. It possibly indicates the presence of a small ring in the keto acid II.

The C_{14}-dicarboxylic acid (III) gives two different monomethyl esters, $C_{15}H_{24}O_4$, one (IV) of which is obtained by acid catalyzed esterification with methanol and the other (V) by hydrolysis of dimethyl ester (VI) with methanolic potassium hydroxide. The former (IV) is also obtained from the methyl ester of II, when treated with hypobromite in aqueous dioxane, and it seems therefore that one of the two carboxyl groups in III is much more hindered than the other and that the former results from CH_3-CO- group in II.

The C_{14}-dicarboxylic acid (III) is dehydrated to an anhydride, $C_{14}H_{20}O_3$ (VII) (carbonyl adsorptions 1799 and 1752 cm^{-1}), which is easily pyrolyzed at about 300°C to a cycloketone, $C_{13}H_{20}O$ (VIII), accompanying decarboxylation[13].

Calcium and barium salt of dicarboxylic acid III also give cycloketone VIII by pyrolysis but they do so in poor yield.

Cycloketone VIII is condensed with ethyl formate in the presence of sodium metal to an enol, $C_{14}H_{20}O_2$ (IX), and is oxidized to a yellow 1,2-diketone, $C_{13}H_{18}O_2$ (X), with selenium dioxide in dioxane. Each of these two characteristic reactions results in the quantitative formation of the corresponding product and exclusively of only a single corresponding species. It seems therefore that the carbonyl group in VIII connects to a methylene group at one side and to a more substituted carbon atom at the other side. This presumption becomes more certain by the fact that 1,2-diketone (X) is converted into a dicarboxylic acid, $C_{13}H_{20}O_4$ (XI), without loss of the carbon atom when treated with alkaline hydrogen peroxide.

The C_{13}-dicarboxylic acid (XI) gives the corresponding anhydride, $C_{13}H_{18}O_3$ (XII), by heating. All attempts to get C_{12}-cycloketone from XI have failed.

XII shows infrared absorptions of the carbonyl group at 1799 and 1754 cm^{-1}. Therefore XII is considered to be of glutaric anhydride type, and the cycloketone to be of structure VIII, and further the ring containing an unsaturated bond in thujopsene is six-membered.

C_{13}-dicarboxylic acid (X), like acid III, also easily gives two different monomethyl esters, $C_{14}H_{20}O_4$, one (XIII) by esterification and the other (XIV) through hydrolysis of dimethyl ester.

Cycloketone VIII gives an alcohol, $C_{13}H_{22}O$ (XV), when reduced with lithium aluminum hydride. It is of interest that the reduction with lithium aluminum hydride proceeds stereospecifically and the epimer of XV does not occur[14].

Alcohol XV is dehydrogenated by selenium to 1-methylnaphthalene with loss of two carbon atoms. If the two carbon atoms eliminated on dehydrogenation are regarded as that of one methyl of the geminal dimethyl group and that of the angular methyl group, the skeleton of alcohol XV is considered as formula XV. The position of the hydroxyl group is determined as follows. By means of methyl magnesium iodide, a methyl group is introduced on the carbon atom of the carbonyl group in VIII, which leads to a corresponding alcohol, $C_{14}H_{24}O$ (XVI). Selenium dehydrogenation of alcohol XVI gives 1,6-dimethylnaphthalene. The methyl group introduced is on 6-position unless a migration of the methyl group occurs on dehydrogenation, and thus the groups in question are considered to be on the position indicated.

The enlarging of the five-membered ring in alcohol XV to the six-membered ring by aromatization, when considered together with the acid-catalyzed cleavage of a ring in the keto acid II, seems to indicate the presence of the

13) This ketone was first reported by T. Ozeki, S. Seto and T. Nozoe at the 10th Annual Meeting of the Chemical Society of Japan, Tokyo, 1957, and called "pyroketone" by them. On the preparation of this ketone by another route, see previous paper, Ref. 1.

14) The epimer of alcohol XV was obtained from lead tetraacetate oxidation product of thujopsene, see Ref. 1.

cyclopropane ring fused to the five-membered ring in XV. In addition, the infrared and ultraviolet spectral data of keto acid II, its methyl ester and cycloketone VIII are corroborative of the conjugation of the ketonic group with the cyclopropane ring[15].

Thus Ia or Ib is proposed for the structure of thujopsence. The fact that the dehydrogenation of thujopsene and its alcoholic derivative, $C_{15}H_{24}O$ (XVII), afford 1,7-dimethyl-4-isopropylnaphthalene is unfavorable for structure Ib which is less amenable to the rearrangement in regard to the naphthalene derivatives.

Experimental

Ester of Ketocarboxylic Acid II.—Methylation with diazomethane gave a methyl ester which was purified by distillation under reduced pressure, b. p. 151~158°C/7 mmHg, m. p. 42~43°C. Infrared max. (Nujol) 1700 and 1735 cm^{-1}; ultraviolet max. 222 $m\mu$ (ε 3160) and 284 $m\mu$ (ε 40). $[\alpha]_D^{26}$ −94.0° (c 1.54).

Found: C, 71.96; H, 9.84. Calcd. for $C_{16}H_{26}O_3$: C, 72.14; H, 9.84%.

Esters of Dicarboxylic Acid III.—Dimethyl ester VI was prepared through methylation with diazomethane in ether. The solution was evaporated to dryness, and the residue was purified by recrystallization from methanol, m. p. 72~73°C. Infrared max. (carbon tetrachloride) 1737 cm^{-1}.

Monomethyl ester IV was prepared from dicarboxylic acid III by esterification with methanol. The details were presented in the previous paper. Melting point 59~60°C. Infrared max. (Nujol) 1700 and 1736 cm^{-1}. This monomethyl ester was also obtained by treating the methyl ester of the ketocarboxylic acid II (2.50 g.) with excess of sodium hypobromite solution (aqueous dioxane 1 : 1) for 2.5 hr. at room temperature. The reaction mixture was diluted with water, acidified and extracted with ether. The ethereal extract was washed twice with water, extracted with aqueous sodium bicarbonate (7%) and then with aqueous sodium hydroxide (5%). When the sodium bicarbonate extract acidified, dicarboxylic acid III was mainly obtained, m. p. 209~210°C, mixed melting point with dicarboxylic acid III undepressed. From the sodium hydroxide extract the monomethyl ester (1.30 g.) was obtained, m. p. 58~59°C and mixed melting point with that obtained by esterification of III undepressed.

Monomethyl Ester V.—The dimethyl ester prepared by methylation with diazomethane was refluxed in methanolic potassium hydroxide (5%) for 6 hr. The reaction mixture was diluted with water, washed with ether, acidified, and extracted with ether. The last ethereal extract was washed with water, and extracted with aqueous sodium bicarbonate (7%) and then with aqueous sodium hydroxide (5%). The sodium bicarbonate extract was acidified and extracted with ether. The extract was washed with water, evaporated to dryness, the residue being recrystallized from aqueous methanol, m. p. 208~209°C. Mixed melting point with dicarboxylic acid III (m.p. 209~210°C) was undepressed. The sodium hydroxide extract was acidified and then treated as above. The product obtained was a monomethyl ester of m. p. 114.5~115.5°C. Infrared max. (chloroform) 1693 and 1720 cm^{-1}.

Found: C, 67.02; H, 9.02. Calcd. for $C_{15}H_{24}O_4$: C, 67.13; H, 9.02%.

This monomethyl ester was reconverted to dimethyl ester VI by methylation with diazomethane in ether.

Cycloketone VIII.—The acid anhydride VII (5.0 g.) was pyrolyzed at 280~320°C for 40 min. under air-cooling reflux; distillation of the product gave 3.4 g. of a distillate, which was refluxed in methanolic potassium hydroxide (5%) for an hour. The reaction mixture was diluted with water, extracted with ether, and the ethereal extract was washed with water and then the solvent was removed to dryness. The residue was steam-distilled and ketone VIII separated as crystalline precipitates was dissolved in ether and dried over sodium sulfate. After the solvent was removed to dryness, the residue was recrystallized from petroleum ether, m.p. 117~118°C, and was further purified by sublimation under reduced pressure, m.p. 118~119.5°C, yield 1.7 g.. Infrared max. (Nujol) 1727 cm^{-1}. Ultraviolet max. (ethanol) 278 $m\mu$ (ε 55.5). $[\alpha]_D^{26}$ +62.2° (c 0.602).

This ketone was also obtained by pyrolysis of calcium salt and of barium salt of III.

Hydroxymethylation of VIII, Enol IX.—The cycloketone VIII (600 mg.) and ethyl formate (700 mg.) were allowed to react in cold benzene solution (8 ml.) in the presence of sodium dust (200 mg.) for two days, when methanol was added to decompose the residual sodium metal. Water was added and the aqueous layer was acidified. The crude enol was collected (250 mg., m. p. 97~98°C) and decolorized with active charcoal. Recrystallization from aqueous ethanol gave white needles of m.p. 105~106°C, which gave purple color in the ferric chloride test. Infrared max. (chloroform) 1668 cm^{-1}, (Nujol) 1681 and 2680 cm^{-1}.

Found: C, 75.63; H, 9.22. Calcd. for $C_{14}H_{20}O_2$: C, 76.32; H, 9.15%.

From the benzene layer, the starting material (330 mg.) was recovered.

Diketone X.—Cycloketone VIII (130mg.), selenium dioxide (130 mg.) and dioxane (2.5 ml.) were heated in a sealed tube for 6 hr. at 200°C. Selenium was filtered off and washed with petroleum ether. The filtrate and washings were combined and water (30 ml.) was added to it; the yellow diketone was dissolved in ethereal layer. The aqueous layer was extracted with petroleum ether until the extract was no longer colored yellow. The combined extract was washed with water and dried over sodium sulfate. After the solvent was removed from the dried solution the residue solidified

15) E. N. Trachtenberg and G. Odian, *J. Am. Chem. Soc.*, **80**, 4018 (1958); R. J. Mohrbacher and N. H. Cromwell, ibid., **79**, 401 (1957).

immediately. Yield of crude product 130 mg., m.p. 170~171°C. Recrystallization from petroleum ether raised the melting point to 180~181°C. Infrared max. (Nujol) 1736 cm^{-1}.

Found: C, 75.78; H, 8.87. Calcd. for $C_{13}H_{19}O_2$: C, 75.69; H, 8.80%.

Dicarboxylic Acid XI[16].—To the mixture of diketone X (50 mg.), ethanol (6 ml.) and hydrogen peroxide (30%, 2 ml.) was dropwise added aqueous sodium hydroxide (10%, 2 ml.), and after being allowed to stand for half an hour, the reaction mixture was warmed at 80°C in a water bath for a few minutes and, after being cooled, was acidified and the crystalline precipitatates wese recrystallized from aqueous ethanol, m.p. 210~211°C. The dicarboxylic acid XI was dehydrated to the acid anhydride XII with acetic anhydride, and recrystallized from benzene-petroleum ether, m.p. 211~212°C.

No ketone formation was observed during the pyrolysis of the acid anhydride XII, which was also true in the cases of calcium- and barium dicarboxylate XI.

Alcohol XV.—An ethereal solution of lithium aluminum hydride (30 mg.) was added with swirling into an ethereal solution of cycloketone VIII (500 mg.). After being allowed to stand overnight, a small amount of water was added to decompose the residual lithium aluminum hydride. The resultant mixture was extracted with an additional amount of ether. The ethereal extract was washed with dilute sulfuric acid the then several times with saturated salt solution, and was dried over sodium sulfate. The solvent was evaporated to dryness and the residue was crystallized immediately, yield 450 mg., and recrystallized from petroleum ether, m.p. 132~133°C. Infrared max. (Nujol) 3280 cm^{-1}. $[\alpha]_D^{26}$ +19.2° (*c* 0.802).

Found: C, 80.30; H, 11.68. Calcd. for $C_{13}H_{22}O$: C, 80.35; H, 11.41%.

Alcohol XV (2.0 g.) was oxidized to cycloketone VIII by treatment with sodium bichromate (1.5 g.), water (2 ml.) and acetic acid (16 ml.) for 30 hr. at room temperature. The reaction mixture was diluted with water and was extracted with ether. The ethereal extract was washed several times with aqueous sodium bicarbonate (7%), with water and dried over sodium sulfate. After the solvent was removed to dryness the residue was crystallized immediately. Repeated recrystallization from petroleum ether gave m.p. 117~118°C. This substance was identified as being the original cycloketone VIII by mixed melting point test and infrared spectrum comparison.

Dehydrogenation of Alcohol XV.—The alcohol XV (2.0 g.) and selenium (3.0 g.) were heated under reflux at 400°C for 165 hr. The oily product was distilled and the main fraction (b.p. 230~240°C) was eluted from alumina (50×70 mm. column) with petroleum ether, yield 0.30 g., n_D^{17} 1.5803. The picrate of the above hydrocarbon compound was orange needles and recrystallizations from ethanol afforded the material of m.p. 137~138°C. The pure hydrocarbon compound was regenerated from picrate by elution from alumina with petroleum ether. n_D^{17} 1.6125.

Found: C, 92.86; H, 7.33. Calcd. for $C_{11}H_{10}$: C, 92.91; H, 7.09%.

Picrate of the purified material showed m.p. 138~139°C, and mixed melting point with the picrate of 1-methylnaphthalene[17] (m.p. 139~140°C) was undepressed.

Found: C, 54.89; H, 3.63; N, 11.39. Calcd. for $C_{17}H_{13}O_7N_3$: C, 54.99; H. 3.53; N, 11.32%.

Methylcarbinol XVI.—The ethereal solution of cycloketone (4.3 g.) was dropwise added to ethereal methyl magnesium iodide (from methyl iodide (3.6 g.), magnesium (0.6 g.) and ethyl ether (13 ml.)). The Grignard complex was decomposed by treatment with aqueous ammonium chloride. The methylcarbinol was extracted with an additional ether from the above reaction mixture, yield 4.2 g., and was purified by recrystallization from petroleum ether and sublimation under reduced pressure, m.p. 62~63°C. $[\alpha]_D^{26}$ +14.3° (*c* 1.87). Infrared max. 3245 cm^{-1}.

Found: C, 80.92; H, 11.76. Calcd. for $C_{14}H_{24}O$: C, 80.71; H, 11.61%.

Dehydrogenation of Methyl Carbinol XVI.—Methyl carbinol XVI (2.0 g.) and selenium (3.0 g.) were heated at 400°C for 104 hr. The same treatment as that of alcohol XV yielded an oily product (0.3 g.), the main fraction distilling at 240~250°C. The infrared spectrum of the hydrocarbon compound coincided with that of 1,6-dimethylnaphthalene and its picrate recrystallized from ethanol was of m.p. 111~112°C. The pure hydrocarbon compound was regenerated from picrate by means of elution from alumina with petroleum ether. n_D^{12} 1.6047.

Found: C, 92.13; H, 8.02. Calcd. for $C_{12}H_{12}$: C, 92.26; H, 7.74%.

Esters of the Dicarboxylic Acid XI.—The dimethyl ester was prepared by methylation with diazomethane by a method similar to the case of the dicarboxylic acid III. M. p. 70~72°C.

Monomethyl Ester XIII.—Dicarboxylic acid anhydride XII (490 mg.) was refluxed in methanol (2 ml.) containing two drops of concentrated sulfuric acid for half an hour. The reaction mixture was diluted with water and extracted with ether. The ethereal extract was washed with water and extracted with aqueous sodium bicarbonate (7%). The aqueous extract was washed with ether, acidified and extracted again with ether. The last ethereal extract was evaporated to dryness and the solid residue was recrystallized from aqueous methanol to give a compound, m.p. 58~62°C, which decomposed at about 90°C and again solidified and melted at 208~209°C. The decomposed product was identical with the dicarboxylic acid anhydride XII (mixed melting point test and infrared spectrum comparison).

The monomethyl ester was converted to the dimethyl ester with diazomethane, and hydrolyzed

16) The same dicarboxylic acid had been obtained in the series of lead tetraacetate oxidation of thujopsene and the chemical data of acid XI and its anhydride XII had been presented in Ref. 1.

17) An authentic sample was synthesized according to the direction of O. Grummitt et al., *J. Am. Chem. Soc.*, 65, 295 (1943).

to the original dicarboxylic acid with aqueous potassium hydroxide.

Monomethyl Ester XIV.—Dimethyl ester (1.0 g.) prepared by methylation with diazomethane was refluxed in methanolic potassium hydroxide (10%, 25 ml.) for 5 hr. The reaction mixture was diluted with water, and the neutral oil which separated, on solidification, was filtered off. The aqueous portion was acidified and the crystalline precipitates collected, yield 300 mg., were recrystallized from petroleum ether, m.p. 145~145.5°C, which was reconverted to the starting material by the methylation.

Dehydrogenation of Thujopsene.—Thujopsene (5.0 g.) and selenium (10.0 g.) were heated at 330°C for 190 hr. The oily product obtained on distillation (b.p. above 120°/5 mmHg) was eluted from alumina (50×50 mm. column) by petroleum ether, yield 0.54 g., n_D^{18} 1.5702; the product when chilled on dry ice gradually solidified. Repeated recrystallizations from methanol afforded colorless plates of m.p. 60~61°C. The infrared spectrum of the hydrocarbon compound agreed with that of 1,7-dimethyl-4-isopropylnaphthalene.

Found: C, 90.72; H, 9.41. Calcd. for $C_{15}H_{18}$: C, 90.85; H, 9.15%.

The picrate was recrystallized from ethanol and had m.p. 88~89°C.

Found: C, 58.96; H, 4.96; N, 9.85. Calcd. for $C_{21}H_{21}O_7N_3$: C, 59.01; H, 4.95; N, 9.83%.

Aldehyde[18].—Thujopsene (9.5 g.) was added to the ethanol solution of selenium dioxide (5.2 g. of selenium dioxide in 60 ml. of absolute ethanol). The mixture was gently refluxed for 20 hr. at boiling point. The reaction mixture, after the selenium (2.2 g.) was filtered off, was concentrated to about 20 ml. under reduced pressure and a large amount of water was added to the remainder, the organic portion of which was extracted by benzene. The benzene extract was washed twice with saturated salt solution, with saturated aqueous lead acetate and again with salt solution three times, and dried over sodium sulfate. After the solvent was removed the remainder was fractionated. The aldehyde was obtained from the fraction of b.p. 133~134.5°C/3.5 mmHg, yield of crude product 7.1 g.. Repetition of recrystsllization raised the melting point to 74~75°C. Infrared max. (Nujol) 1683 cm^{-1}.

Alcohol XVII.—The warm solution of aldehyde (5.54 g. of aldehyde in 26 ml. of methanol) was added to the solution of sodium borohydride (0.344 g. of the hydride in 3 ml. of methanol). After being heated for ten minutes, the mixture was left to cool at room temperature for two hours. Aqueous acetic acid was added to the reaction mixture to decompose the residual hydride. When the resulting mixture was diluted with water, the product was immediately solidified. The crystalline precipitates were collected and washed with water thoroughly. White needles of m. p. 102.5~103.5°C were obtained by recrystallization from petroleum ether. $[\alpha]_D^{20}-109°$ (c 0.90). Infrared max. (Nujol) 3320 cm^{-1}.

Found: C, 81.84; H, 11.01. Calcd. for $C_{15}H_{24}O$: C, 81.76; H, 10.98%.

Dehydrogenation of Alcohol XVII.—Alcohol XVII (5.0 g.) and selenium (10.0 g.) were heated at 330°C for 30 hr. The oily product obtained (b.p. above 120°C/4.5 mmHg) was eluted from alumina (20×100 mm. column) with petroleum ether, yield 0.20 g., n_D^{18} 1.5642. Though the picrate was prepared, its melting point could not be raised to that reported by Sörm[19]. The infrared spectrum of the hydrocarbon compound which was regenerated from the crude picrate coincided to a fair extent with that of 1,7-dimethyl-4-isopropylnaphthalene. The regenerated hydrocarbon compound was semi-solid, and rigid determination of its melting point was not conducted owing to the lack of a sample.

Department of Organic Synthesis
Faculty of Engineering
Kyushu University
Hakozaki, Fukuoka

18) This aldehyde is that reported by Erdtman and Norin, Ref. 6.

19) J. Priva, V. Herout, B. Schneider and F. Sörm, *Collection Czechoslov. Chem. Communs.*, **18**, 500 (1953).

Mercury Photosensitized Decomposition of Carbon Dioxide by 1849 Å ($Hg^*6^1P_1$)

By Yuji MORI

(Received January 24, 1961)

Few studies[1,2] have been made of reactions induced by the 1849 Å mercury resonance line, because of the difficulty of eliminating the effect of the other resonance line of mercury at 2537 Å.

In the case of carbon dioxide most of the above difficulties may be reduced. The possibility of direct photolysis by 2537 Å is eliminated since carbon dioxide is transparent above 1850 Å. The excitation energy of 6^3P_1 of mercury, 112.2 kcal., is insufficient to bring about the reaction

$$CO_2 + Hg^*(6^3P_1) \rightarrow CO + O + Hg(^1S_0)$$

and the reaction

$$CO_2 + Hg^*(^3P_1) \rightarrow CO + HgO$$

is slow and has no important effect[3] on the photosensitized decomposition by 6^1P_1 of mercury. The excitation energy of 6^1P_1 of mercury, 153.9 kcal., is sufficient to bring about the decomposition of carbon dioxide.

Therefore, it is possible to investigate the photosensitized decomposition and the direct photolysis of carbon dioxide induced by the resonance line at 1849 Å without any important interference caused by the resonance line at 2537 Å.

Experimental

Photosensitized Decomposition.—Carbon dioxide obtained from sodium bicarbonate was dried by passing it over calsium chloride and magnesium perchlorate. Then the gas was stored after purification by bulb to bulb distillation, using dry ice and liquid nitrogen. Before each run, gases noncondensable in ilquid nitrogen were remonved by pumping in liquid nitrogen.

The reaction was carried out in a cylindrical fused quartz cell (5 cm. in diameter 10 cm. long) illuminated by the radiation from a low pressure mercury lamp operated at a constant current 90 ma. from a 2000 V. leakage transformer. The gas saturated with mercury vapor by passing it over a mercury surface in a heated U tube, was introduced into the reaction cell. To keep the gas saturated with mercury vapor throughout a run, liquid mercury was intoduced into the reaction cell. When no liquid mercury was introduced in the cell, the reduction of the rate of the reaction was observed by the depletion of mercury due to the formation of the oxide of mercury. The temperature of the reaction cell was kept at room temperature.

The gaseous products, noncondensable in liquid nitrogen, were analysed in a conventional analysis system. The amount of noncondensable gas was measured by compressing it into a constant volume burette using a small mercury diffusion pump backed by a Töepler pump. The volume of carbon monoxide in the noncondensable products was determined by means of copper oxide heated at around 300°C.

Direct Photolysis.—In the investigation of the direct photolysis, the carbon dioxide used was prepared in a system completely free from mercury vapor in order to eliminate the mercury photosensitization. The pressure of carbon dioxide in the reaction cell was measured by means of a Bourdon gauge. After the photolysis, the gaseous products noncondensable in liquid nitrogen, were analysed by connecting the reaction cell to an analysis system by means of a ground joint.

Since the absorption coefficient of carbon dioxide at 1849 Å is very small[4], the investigation was carried out in a higher pressure region than in the case of photosensitization. The reaction was carried out at room temperature.

Results

Photosensitization.—Carbon monoxide was the only product which was noncondensable in liquid nitrogen, and no oxygen was detected. This means that the rate of formation of oxygen is at most a few percent of that of carbon monoxide. A colored substance, assumed to be an oxide of mercury, was found on the surface of the front window of the reaction cell. This was soluble in dilute sulfuric acid and was removed by flaming in vacuum.

The average rate of production of carbon monoxide, (amount of carbon monoxide produced)/(irrandiation time), depends on the time of irradiation and the pressure of carbon

1) C. C. McDonald, A. Kahn and H. E. Gunning, *J. Chem. Phys.*, **22**, 908 (1954).

2) J. D. McGilvery and C. A. Winkler, *Can. J. Chem.*, **30**, 194 (1952).

3) In fact, the formation of an oxide of mercury and carbon monoxide was observed in the experiment using a filter which cuts off the light below 2300 Å. But the rate of this reaction was very slow and showed that its effect would be negligible.

4) E. C. Y. Inn, K. Watanabe and M. Zelikoff, *J. Chem. Phys.*, **21**, 1648 (1953).

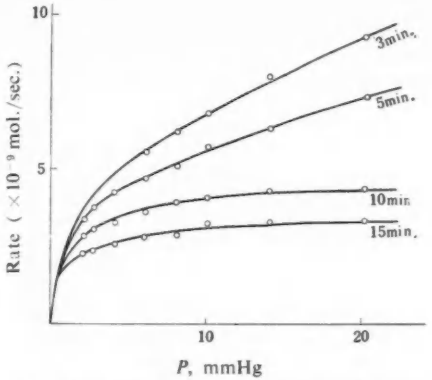

Fig. 1. The average rate of production of carbon monoxide in photosensitized decomposition of carbon dioxide.

TABLE I. THE AVERAGE RATE OF PRODUCTION OF CARBON MONOXIDE IN PHOTOSENSITIZED DECOMPOSITION OF CARBON DIOXIDE

Pressure	Rate ($\times 10^{-9}$ mol./sec.)				$r_0(t=0)$
mmHg	3 min.	5 min.	10 min.	15 min.	
2.0		3.39	2.78	2.23	4.06
2.6		3.79	3.00	2.30	5.27
4.0		4.22	3.23	2.59	5.56
6.0	5.56	4.66	3.58	2.80	7.41
8.0	6.18	5.10	3.89	2.86	8.44
10.0	6.78	5.70	4.00	3.21	8.83
14.0	7.97	6.26	4.28	3.25	11.52
20.0	9.30	6.98	4.30	3.30	14.11
40.0	13.62	11.56	8.57		17.64

dioxide as shown in Table I and in the plots in Fig. 1.

The gradual decrease of transparency of the front window of the reaction cell by the formation of the oxide of mercury, decreases the rate of production of carbon monoxide (i. e., the rate of decomposition of carbon dioxide) with the increase of irradiation time t. Therefore, the initial rate r_0 was obtained by extrapolation to $t=0$ assuming the formula

$$r = r_0 + at + bt^2$$

where the constants a and b depend on the pressure of carbon dioxide.

The initial rates for various pressures are given in Table I (last column) and the plots in Fig. 2.

Direct Photolysis. — The products, non-condensable in liquid nitrogen, were oxygen and carbon monoxide in a ratio around 1 : 5, which is far from the stoichiometric ratio of 1 : 2. No solid deposit was found on the front window of the reaction cell. The results are shown in Table II and in Fig. 3. It will be

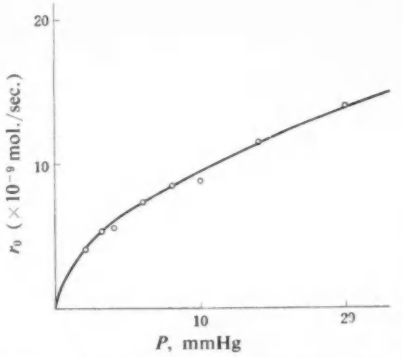

Fig. 2. The initial rate of carbon monoxide in photosensitisation.

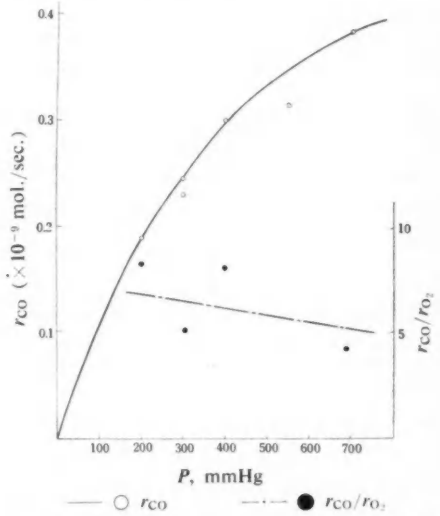

Fig. 3. The results of direct photolysis of carbon dioxide by 1849 Å.

TABLE II. THE RESULTS OF DIRECT PHOTOLYSIS OF CARBON DIOXIDE BY 1849 Å

Pressure	Rate ($\times 10^{-9}$mol./sec.)		
mmHg	r_{CO}	r_{O_2}	r_{CO}/r_{O_2}
200	0.189	0.027	7.0
300	0.229	0.044	5.2
	0.245	0.013	18.8*
400	0.299	0.042	7.1
550	0.312	0.009	34.6*
700	0.383	0.090	4.3

* The reaction cell was flamed and pumped before introduction of carbon dioxide.

seen from the data in Table II that the rate of oxygen formation was markedly reduced when the reaction cell was flamed in pumping before a run.

Discussion

In the case of direct photolysis, the deficiency of oxygen produced is greatly affected by the flaming in pumping. Therefore this deficiency of oxygen could be explained by assuming the wall reaction

$$O + O + \text{Wall} \rightarrow O_2\ (\text{Wall})$$

In the investigation of photodecomposition of carbon dioxide by the resonance radiation from the xenon lamp, Wijnen[5] and Tanaka[6] observed that oxygen and carbon monoxide were obtained in the ratio 1 : 9 at room temperature and 1 : 3 at 300°C. This increase of oxygen production at a higher temperature can be explained by the decrease of oxygen adsorbed (or absorbed) on the wall of the reaction cell.

Some of the deficiency of oxygen may be the result of the formation of ozone by the reaction

$$O_2 + O + M \rightarrow O_3 + M$$

Mahan[7] observed that ozone was formed in his experiment of the photodecomposition of carbon dioxide by the xenon lamp. Since ozone absorbs the resonance line at 2537 Å and is then decomposed, the deficiency of oxygen can not be explained entirely by the formation of ozone.

In the photosensitized decomposition, no oxygen was detected and the oxide of mercury was deposited on the window of the cell. Therefore, the possible reactions which will form the oxide of mercury may be as follows:

a) $CO_2 + Hg^*(6^1P_1) \rightarrow CO + HgO$

or

b)
$$\begin{aligned} CO_2 + Hg^*(6^1P_1) &\rightarrow CO_2^* + Hg(^1S_0) \\ CO_2^* &\rightarrow CO_2 + h\nu \\ CO_2^* &\rightarrow CO + O \\ O + Hg + M &\rightarrow HgO + M \\ O + O + \text{Wall} &\rightarrow O_2\ (\text{Wall}) \end{aligned}$$

Callear, Patrick and Robb[8] suggested that the oxide of mercury was formed in the mercury photosensitized reaction of oxygen by the following

$$O_3 + Hg^* \rightarrow O_2 + HgO$$

In the present investigation, however, it is unlikely that the oxide of mercury was formed by the above reaction, since the concentration of oxygen in the reaction cell was very low.

The approximate value of the quenching cross section (σ^2) of carbon dioxide for excited mercury atoms $Hg^*(6^1P_1)$ may be obtained by assuming that the rate of production of the carbon monoxide is equal to the rate of decomposition and to the rate of the quenching reaction of excited mercury atoms by carbon dioxide. From this view point, the mechanism is assumed to be the following:

$$\begin{aligned} Hg + h\nu &\rightarrow Hg^*(6^1P_1) && I_{abs} \\ Hg^*(6^1P_1) &\rightarrow Hg + h\nu && k_1 \\ Hg^*(6^1P_1) + CO_2 &\rightarrow CO + HgO \\ \text{or} &\rightarrow Hg + CO + O && k_2 \end{aligned}$$

Thus the relation between the initial rate of production of carbon monoxide and the pressure of carbon dioxide will be written as

$$1/r_0 = 1/I_{abs} + k_1/I_{abs}k_2P \qquad (1)$$

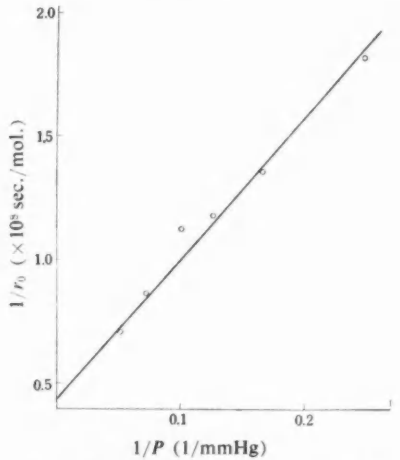

Fig. 4. The plots of $1/r_0$ against $1/P$.

where r_0 is the initial rate of production of carbon monoxide and P is pressure of carbon dioxide. The plots of $1/r_0$ against $1/P$ is linear as shown in Fig. 4. Therefore, utilizing Eq. 1 and from the result shown in Fig. 4, it was found that $\sigma^2 = 320$ or 64 Å^2 according to whether the life time of excited mercury atom, $Hg^*(6^1P_1)$, is 0.3×10^{-9} or 1.6×10^{-9} sec.[9]

It will be difficult to determine the correct value of the quenching cross section even if the exact life time of the excited mercury atom is given. The value of the apparent quenching cross section calculated by Eq. 1 will be smaller than the correct one when other quenching reactions which do not form carbon monoxide are not negligible. Another

5) M. H. J. Wijnen, ibid., **24**, 851 (1956).
6) Unpublished data.
7) B. H. Mahan, *J. Chem. Phys.*, **33**, 959 (1960).
8) A. B. Callear, C. R. Patrick and J. C. Robb, *Trans. Faraday Soc.*, **55**, 280 (1959).
9) A. C. G. Mitchel and M. W. Zemansky, "Resonance Radiation and Excited Atoms", The McMillan Co., New York (1934).

difficulty will be in the uncertainty in the effective life time of excited mercury atom due to reabsorption of the resonance radiation of 1849 Å. The resonance radiation emitted by an excited mercury atom will be absorbed by another mercury atom in the ground state, with some probability. This leads to an increase of the effective life time of the excited mercury atom and to an increase in the apparent quenching cross section.

However, it is possible to think that the quenching cross section of carbon dioxide for $Hg^*(6^1P_1)$ is larger than 2.48 $Å^2$ for $Hg^*(6^3P_1)$[10].

This is supported by the consideration that the attractive interaction between the excited mercury atom $Hg^*(6^1P_1)$ and carbon dioxide is stronger than that between $Hg^*(^3P_1)$ and carbon dioxide. The lower excited singlet states of carbon dioxide have higher energies than $Hg^*(6^1P_1)$[11]. The lowering of the energies of the excited states of mercury atom due to the induced dipole-dipole interaction at large intermolecular distance is written

$$\Delta E_k = \sum_j W(\mu_k \cdot \mu_j)/E_k - E_j$$

where E_k is the energy of the excited state k of the mercury atom, E_j is the energy of the excited state j of carbon dioxide and $W(\mu_k \cdot \mu_j)$ is the interaction energy between transition moment of the mercury atom μ_k and that of carbon dioxide μ_j. Therefore, this induced dipole-dipole interaction has a much stronger effect for $Hg^*(6^1P_1)$ than for $Hg^*(6^3P_1)$ because of their energies and transition moments. In a similar consideration the charge transfer interaction is more effective in $Hg^*(6^1P_1)$ since the energy difference between $Hg^*(6^1P_1)$ and the charge transfer state is smaller than in the case of $Hg^*(6^3P_1)$.

10) M. W. Zemansky, *Phys. Rev.*, **36**, 919 (1930).
11) R. S. Mulliken, *Can. J. Chem.*, **36**, 10 (1958).

Summary

The photosensitized decomposition of carbon dioxide by $Hg^*(6^1P_1)$ and the direct photolysis by 1849 Å was investigated by the static method.

The product in photosensitization was carbon monoxide and no oxygen was detected. The deficiency of oxygen in the product may be due to the formation of an oxide of mercury which was deposited on the front window of the reaction cell.

In photolysis of carbon dioxide, carbon monoxide and oxygen were produced in the ratio around 5 : 1. The deficiency of oxygen may be due to the wall effect and partly due to the formation of ozone.

The apparent quenching cross section was obtained by assuming a simple mechanism. The large value of the apparent quanching cross section of $Hg^*(6^1P_1)$ is discussed from the point of view of intermolecular interaction between the excited mercury atom and carbon dioxide in the ground state.

The author is greatly indebted to Professor Ikuzo Tanaka for his continuous encouragement and discussions.

Laboratory of Physical Chemistry
Tokyo Institute of Technology
Meguro-ku, Tokyo

Kinetic Studies on Solvolysis. VI. Kinetic Evidence of the Distinct Rôle of the Hydrogen Atom of Hydroxylic Solvent Molecules as an Attacking Center at the First Ionization Stage

By Kunio Okamoto and Haruo Shingu

(Received October 22, 1960)

Acceleration by hydroxylic groups has been well known for solvolytic reactions of several secondary and tertiary halides[1], and it was previously pointed out[1a,2] that this kind of acceleration would be a specific driving force by hydrogen-bonding to the leaving halide ion and that it was superimposed on the acceleration by general solvent effect which was assumed to be proportional to the reciprocals of dielectric constants of the solvents[2]. However, previous investigations[1,2] have not given any evidence of the distinct rôle of the hydrogen atom as a reactive center in the

1) a) For the review see A. Streitwieser, Jr., *Chem. Revs.*, **56**, 622 (1956). b) Y. Pocker, *J. Chem. Soc.*, **1959**, 1179.
2) Part IV. H. Shingu and K. Okamoto, *J. Chem. Soc. Japan, Pure Chem. Sec.* (*Nippon Kagaku Zasshi*), **78**, 558 (1957).

hydroxyl group. In the present investigation linear catalysis by ortho- and para-substituted phenols, mono- and di-hydric alcohols and several polar molecules in acetolysis of *tert*-butyl bromide has been examined in order to see if the intramolecularly fixed, or chelated, hydrogen atom of the hydroxyl group would lose its accelerating function as a hydrogen-bonding center, and also to ascertain if there was co-operating acceleration by two adjacent hydroxylic groups in a molecule. Furthermore, the solvolysis rates of *tert*-butyl bromide in phenol-carbon tetrachloride mixtures have been quantitatively discussed from the point of view that the hydrogen atoms of the various species of "associated" phenol molecules would be operative as the key atoms at the first ionization stage of the solvolysis in these phenolic solvents.

When *tert*-butyl bromide was subjected to acetolysis in acetic acid-carbon tetrachloride mixture (1 : 3 by vol.) in the presence of sodium acetate, it was found that several phenols, glycols, and some other polar molecules showed linear catalysis, as has previously been known in the case of the unimolecular reaction in nitromethane[1b]. In Table I the catalytic constants of these hydroxylic molecules are compared. The catalytic constants of the ortho-substituted phenols in which the hydroxyl groups are intramolecularly fixed by a hydrogen bridge are smaller than those of corresponding para-derivatives, as evidenced by the data for nitro-, chloro-, hydroxy- and methyl derivatives of phenols. Among them the effect of the *o*-nitro group is particularly striking in that the catalytic constant of *o*-nitrophenol is the smallest and comparable to that of nitrobenzene, while that of *p*-nitrophenol is the largest one. These observations may lead to the conclusion that the hydrogen atom in the free, or non-chelated, hydroxyl group is the center of reaction in the first ionization stage of the S_N1-type solvolysis.

Table I. Catalytic constants of phenols, alcohols and several polar and non-polar compounds in acetolysis of *tert*-butyl bromide in acetic acid-carbon tetrachloride mixture (1 : 3 by vol. at 25.0°C) at 70.0°C

Accelerating substance	$10^5 \times$Catalytic constants* $sec^{-1}M^{-1}$
Phenol	2.53
p-Cresol	4.44
o-Cresol	2.90
p-Chlorophenol	5.34
o-Chlorophenol	2.52
p-Nitrophenol	11.75
o-Nitrophenol	0.925
Hydroquinone	10.8
Catechol	8.34
Carbon tetrachloride	−0.100
Dioxane	−0.745
Acetone	1.38
Acetic acid	1.15
Water	5.41
Methanol	2.63
Ethanol	1.41
Ethylene glycol	7.69
Cyclohexanol	0.90
cis-1,2-Cyclohexanediol	3.04
trans-1,2-Cyclohexanediol	3.09
Benzene	0.440
Toluene	0.370
Chlorobenzene	0.810
Nitrobenzene	0.955

* Initial concentration of sodium acetate, 0.0500 N; standard rate constant k_1°, 6.72×10^{-6} (sec^{-1}).

For this acetolysis the catalytic order of the substituted phenols is qualitatively, but not quantitatively, the same as the acidity order, while for the solvolysis in nitromethane[1b] this correlation was found to be quantitatively applicable. This inconsistency would probably be due to the complexity resulting from the hydrogen-bonding interaction between these phenols and acetic acid.

In this connection it is noteworthy that even non-hydroxylic polar molecules, e. g., toluene, chlorobenzene, nitrobenzene, and acetone, and also benzene could give small but definitely positive catalytic constants which were comparable to that of acetic acid per se. This may be explained on the basis that these molecules would modify the self-hydrogen-bonding interaction of the acetic acid molecules to the extent that a certain increase of their free hydrogen atoms and, therefore, relative enhancement of ionizing power of acetic acid would result.

The negative catalytic constant for dioxane can be explained on a basis similar to the above consideration by supression of the catalytic action of acetic acid due to the hydrogen-bonding, or hydrogen-accepting, nature of dioxane.

A further evidence of the necessity of free hydroxyl groups is revealed by the following fact: that in intramolecularly hydrogen-bonded methyl salicylate solvent, *tert*-butyl bromide did not show any hydrogen bromide evolution for 4.0 hr. at 70°C, while in phenolic solvent this bromide was easily solvolysed even at room temperature.

For dihydroxylic compounds, like 1,2-cyclohexanediols, ethylene glycol, catechol and water, the catalytic constants are greater than

TABLE II. VALUES* OF S_n's AND k's IN EQUATION 1 : $k=\sum_1^n S_n k_n$

Phenol concn. M	Phenolysis rate const. k, sec^{-1}	S_1	S_2	S_3	S_4	S_5	S_6	S_7	S_8	S_9	S_{10}	$S_{>10}$**
3.4	1.0×10^{-4}	31	22	15	10	7.1	5.1	3.7	2.5	1.7	1.2	3.4
3.0	6.6×10^{-5}	30	21	14	9.9	6.6	4.5	3.0	2.1	1.5	0.9	2.4
2.5	4.1×10^{-5}	28	19	13	8.2	5.5	3.8	2.3	1.6	1.1	0.8	1.7
2.25	3.3×10^{-5}	27	18	12	7.7	5.0	3.2	1.9	1.3	0.9	0.6	1.3
2.0	2.7×10^{-5}	27	17	11	7.4	4.4	2.6	1.7	1.0	0.7	0.4	1.0
1.75	2.2×10^{-5}	26	17	10	6.5	3.9	2.3	1.2	0.8	0.5	0.2	0.6
1.5	1.6×10^{-5}	26	17	9.0	5.6	3.0	1.8	1.1	0.6	0.3	0.2	0.4
1.25	1.1×10^{-5}	24	14	7.9	4.6	2.5	1.3	0.7	0.3	0.3	0.1	0.1
1.0	7.0×10^{-6}	23	12	6.3	3.3	1.6	0.8	0.4	0.3	0.1	0.1	0.1
0.75	4.2×10^{-6}	21	9.7	4.5	2.2	1.1	0.5	0.2	0.1	—	—	—
0.50	2.2×10^{-6}	18	7.0	2.8	1.2	0.5	0.2	0.1	—	—	—	—

* Calculated from interpolated values of α_n's using Eq. 2.
** For phenol polymer species with more than eleven phenol molecules. The average number of n was assumed to be thirteen.

twice those of monohydroxylic compounds, like cyclohexanol, ethanol, phenol and methanol, respectively (cf. Table I). Although some electronic effect, especially in the dihydroxylic phenols, might be responsible for these results, the marked acceleration would be mostly attributed to the sterically co-operating attack of two adjacent hydroxyl groups in these molecules.

On the basis of the foregoing discussion, it appears to be reasonable to reconsider the solvent effect of hydroxylic compounds from the point of view that the ionization is controlled by the co-operating attack of hydroxyl groups of the various species of associated hydroxylic molecules. For a discussion of this problem the data for the association degree of those compounds are required. Fortunately the calculated results for the distribution of various associated phenol species in carbon tetrachloride at 20.0°C are available[3]. Therefore, the solvolysis rates of *tert*-butyl bromide in various phenol-carbon tetrachloride mixtures were measured in the presence of sodium phenolate at 20.0°C and after suitable correction for the initial concentrations of sodium phenolate (see Experimental) the data were tested by the following equations which were derived in order to correlate the observed solvolysis rates with the concentrations of the various species of associated phenol molecules.

Provided that reacting phenols are short-lived polyhydroxylic polymers with various degrees of association, the total rate of the solvolysis may be expressed in the Eq. 1,

$$\text{rate}=(\sum_1^n k_n[S_n])[RX]=k[RX] \qquad (1)$$

where S_n represents the time-average concentration of a phenol polymer species n, and k_n represents the rate constant for the phenol polymer species n. Furthermore, the S_n in the Eq. 1 is expressed by Eq. 2,

$$S_n=(\text{Phenol conc.})\times\alpha_n/n\times100 \qquad (2)$$

where α_n represents the percentage of the number of the phenol molecules forming polymer species n to the total number of the phenol molecules. Thus, using the values of α_n's given by Kempter and Mecke[3] and of the observed rate constants for the corresponding phenol-carbon tetrachloride mixtures, we can estimate the approximate values for k_n's. In Table II the values for the coefficients of k_n's, i.e., the values of S_n's in Eq. 1, are shown along with the corresponding eleven interpolated values of observed total rate constants.

In examining the relation between the observed total rate constants and the S_n's in eleven simultaneous equations obtained from the values in Table II, it is obvious that an increasing series of values for k_n's is required for good agreement between the observed total rate constants and those calculated from the right side of Eq. 1, and one of such series for the k_n's is shown in the following: $k_1, k_2=0.05\times10^{-4}$, $k_3, k_4=0.1\times10^{-4}$, $k_5, k_6=0.3\times10^{-4}$, $k_7, k_8=1\times10^{-4}$, $k_9, k_{10}=6\times10^{-4}$, $k_{>10}=18\times10^{-4}$ (sec^{-1}). Using these k_n's the calculated values for the total rate constants are compared with the observed ones in Fig. 1.

Thus, on the basis of Mecke's polymer distribution values[3] for phenol polymer species in carbon tetrachloride, we may conclude that

3) H. Kempter and R. Mecke, *Z. physik. Chem. Abt. B*, **46**, 229 (1946).

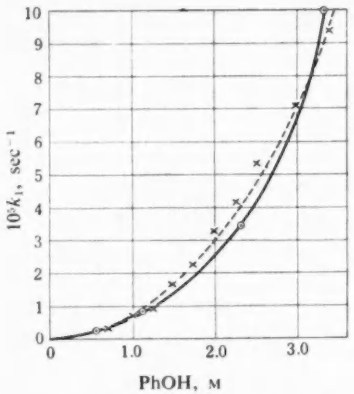

Fig. 1. Phenolysis rate of *tert*-butyl bromide in phenol-carbon tetrachloride mixtures at 20.0°C.
• Observed × Calcd. from Eq. 1

the phenol polymer species with higher association degree should show more effective acceleration presumably because of their cooperative action as a kind of polyhydroxylic molecule. This would be a more detailed expression of the "polymolecular"[4] acceleration in solvolysis.

Experimental[5]

Materials.—*tert*-Butyl bromide[6], *cis*-[7] and *trans*-[8] cyclohexanediol were prepared by published procedures. Sodium phenolate was previously prepared[9]. Sodium acetate[9], dioxane[9], phenol[9] and acetic acid[10] were purified by a previously reported method. All the reagents employed were of reagent grade quality, and purified by fractional distillation or by recrystallization. *o*-Cresol, m. p. 30.0~31.0 °C; *p*-cresol, m. p. 33.0~34.0°C; *p*-nitrophenol, m. p. 113.0~114.0°C; *o*-nitrophenol, m. p. 44.0~45.0°C; *p*-chlorophenol, m. p. 41.0~42.0°C; catechol, m. p. 104.0~105.0°C; hydroquinone, m.p. 172.0°C; *cis*-1,2-cyclohexanediol, m. p. 97.5~98.0 °C; *trans*-1,2-cyclohexanediol, m. p. 103.5~104.0 °C; *tert*-butyl bromide, b. p. 73.0°C; methanol, b. p. 64.0~65.0°C; ethanol, b. p. 78.0°C; phenol, b. p. 180.0~181.0°C; cyclohexanol, b. p. 161.0°C; ethylene glycol, b. p. 197.0~198.0°C; *o*-chlorophenol, b. p. 175.0~176.0°C; benzene, b. p. 80.0°C; toluene, b. p. 110.0°C; acetone, b. p. 56.0°C; dioxane, b. p. 101.0°C; carbon tetrachloride, b. p. 76.0°C; chlorobenzene, b. p. 132.0°C; nitrobenzene, b. p. 210.0~211.0°C; acetic acid, b. p. 117.0°C.

The solvent for the kinetic determinations of the acetolysis rates consisted of one volume of acetic acid and three volumes of carbon tetrachloride at 25.0°C. The solvents for the phenolysis were prepared at 25.0°C.

Rate Measurements.—A) *Acetolyses in Carbon Tetrachloride-Acetic Acid (3 : 1 by vol.).*—A sealed-ampoule technique was used. The reaction mixtures were prepared by mixing the weighed amounts of *tert*-butyl bromide and aliquots of solutions of known concentrations of sodium acetate and of hydroxylic compounds in carbon tetrachloride-acetic acid mixutre at 25.0°C. Each ampoule contained 1.000 cc. of aliquot of the reaction mixture. The thermostat was controlled to ±0.01° at 70.0°C. After reaction for appropriate lengths of time, the ampoules were cooled. Each sample was run into a flask and after being rinsed with about 5 cc. of acetic acid the unchanged sodium acetate was titrated with 0.050 N perchloric acid solution in acetic acid with crystal violet indicator. Rate constants were calculated graphically assuming that the reaction was of the first order. Decrease of sodium acetate associated with solvolysis of *tert*-butyl bromide in each run obeyed good first-order kinetics, this being illustrated graphically in Fig. 2 for several runs.

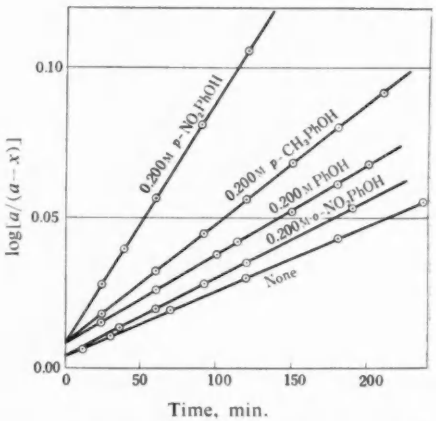

Fig. 2. Rates of acetolyses of *tert*-butyl bromide in acetic acid-carbon tetrachloride (1 : 3 by vol., at 25.0°C) in the presence of phenols at 70.0±0.01°C, 0.100 M *t*-BuBr, 0.0500 N NaOAc.

B) *Solvolyses in Phenol-Carbon Tetrachloride Mixtures.*—A weighed amount of *tert*-butyl bromide and an aliquot of the solution of a known concentration of sodium phenolate in an appropriate mixture of phenol and carbon tetrachloride were mixed in a measuring flask placed in a thermostat kept at 20.0±0.01°C. At appropriate time intervals, aliquot portions (1.000 cc.) were pipetted into 2 cc. of cold acetic acid at 15°C and the solutions were titrated according to the method described in section A. Rate constants were calculated from the first

4) L. P. Hammett, "Physical Organic Chemistry", McGraw-Hill Book Co., Inc., New York (1940), p. 169.
5) Melting points are not corrected.
6) K. A. Cooper and E. D. Hughes, *J. Chem. Soc.*, **1937**, 1185.
7) S. Winstein, H. V. Hess and R. E. Buckles, *J. Am. Chem. Soc.*, **64**, 2796 (1942).
8) A. Roebuck and H. Adkins, "Organic Syntheses", Coll. Vol. 3 (1955), p. 217.
9) H. Shingu and K. Okamoto, *J. Chem. Soc. Japan, Pure Chem. Sec. (Nippon Kagaku Zasshi)*, **81**, 111 (1960).
10) H. Shingu, K. Okamoto and E. Ajisaka, ibid., **78**, 554 (1957).

TABLE III. SUMMARY OF RATE CONSTANTS FOR ACETOLYSIS OF *tert*-BUTYL BROMIDE IN ACETIC ACID-CARBON TETRACHLORIDE MIXTURE (1 : 3 BY VOL. AT 25.0°C) AT 70.0°C

Exp. No.	Accelerating substance	Concn. M	$10^6 \times k_1$* sec^{-1}	Exp. No.	Accelerating substance	Concn. M	$10^6 \times k_1$* sec^{-1}
40	None		6.72	27	Methanol	0.200	11.5
29	None		6.72	53	Ethanol	0.100	8.23
14	None		6.72	24	Ethanol	0.200	9.32
58	None		6.72	55	Ethylene glycol	0.100	14.4
39	Phenol	0.100	9.23	54	Ethylene glycol	0.200	22.3
13	Phenol	0.200	11.8	60	Cyclohexanol	0.100	7.60
19	*p*-Cresol	0.100	11.2	59	Cyclohexanol	0.200	8.52
12	*p*-Cresol	0.200	15.5	66	*cis*-1, 2-Cyclohexanediol	0.100	9.98
52	*o*-Cresol	0.100	9.67	65	*cis*-1, 2-Cyclohexanediol	0.200	12.4
51	*o*-Cresol	0.200	12.5	64	*trans*-1, 2-Cyclohexanediol	0.100	9.98
43	*p*-Chlorophenol	0.100	12.4	63	*trans*-1, 2-Cyclohexanediol	0.200	12.5
16	*p*-Chlorophenol	0.200	16.7	38	Nitrobenzene	0.100	7.68
47	*o*-Chlorophenol	0.100	9.25	15	Nitrobenzene	0.200	8.62
22	*o*-Chlorophenol	0.200	11.7	20	Chlorobenzene	0.200	8.34
18	*p*-Nitrophenol	0.100	18.5	42	Toluene	0.100	7.08
11	*p*-Nitrophenol	0.200	30.1	21	Toluene	0.200	7.47
56	Hydroquinone	0.050	12.1	28	Acetone	0.200	9.48
62	Catechol	0.100	14.0	23	Benzene	0.200	7.60
61	Catechol	0.200	25.5	32	Dioxane	0.200	6.23
49	Water	0.100	12.1	31	Carbon tetrachloride	0.200	6.52
26	Water	0.200	17.6	17	Acetic acid	0.200	7.87
50	Methanol	0.100	9.58				

* Initial concentrations; *tert*-butyl bromide 0.100 M, sodium acetate 0.0500 N.

TABLE IV. SUMMARY OF RATE CONSTANTS FOR PHENOLYSIS OF *tert*-BUTYL BROMIDE IN PHENOL-CARBON TETRACHLORIDE MIXTURES AT 20.0°C

Exp. No.	Phenol concn. vol. %*	Phenol concn. M	Concn. of sodium phenolate, N	k_1 sec^{-1}	k_1 N=∞
8	50.0	5.68	0.0456	2.35×10^{-4}	
9	50.0	5.68	0.0225	2.12×10^{-4}	
					2.70×10^{-4}
14	40.0	4.45	0.0754	1.45×10^{-4}	
12	40.0	4.45	0.0505	1.26×10^{-4}	
13	40.0	4.45	0.0251	1.15×10^{-4}	
					1.64×10^{-4}
5	30.0	3.37	0.0995	8.37×10^{-5}	
6	30.0	3.37	0.0496	7.40×10^{-5}	
7	30.0	3.37	0.0245	6.75×10^{-5}	
					1.00×10^{-4}
17	20.0	2.33	0.0525	3.05×10^{-5}	
18	20.0	2.33	0.0257	2.80×10^{-5}	
					3.39×10^{-5}
16	10.0	1.11	0.0313	7.34×10^{-6}	
19	10.0	1.11	0.0157	6.71×10^{-6}	
					8.33×10^{-6}
20	5.00	0.559	0.0147	1.45×10^{-6}	
21	5.00	0.559	0.0104	1.21×10^{-6}	
					2.70×10^{-6}

* at 25.0°C

** Initial concentration of *tert*-butyl bromide, 0.100 M.

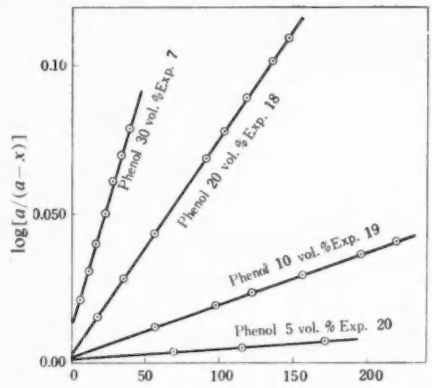

Fig. 3. Rates of phenolyses of *tert*-butyl bromide in phenol-carbon tetrachloride mixtures at 20.0°C, 0.100 M *t*-BuBr, 0.147 ~0.0245 N NaOPh.

order rate equation by a graphical method, and satisfactory first order behavior was observed for each run, this being shown graphically in Fig. 3.

Results

The rate constants of acetolyses used for the calculation of catalytic constants of phenols, alcohols, and several polar and non-polar compounds are summarized in Table III. The catalytic constants were calculated by Eq. 3.

$$k_1(\text{obs.}) = k_1^{\circ} + k_2(\text{Conc. of the accelerating substance}) \quad (3)$$

where k_1° represents the standard rate constant and k_2 represents the catalytic constant.

The first order rate constants for the solvolyses of *tert*-butyl bromide in phenol-cardon tetrachloride mixtures depended on the initial concentrations of sodium phenolate and at high concentrations they increased reaching the maximum values which were previously concluded to be the rates of the first ionization step of *tert*-butyl bromide[9]. According to the total rate expression[9] for the phenolysis of this compound, these maximum values for the rate of ionization were estimated from the plots of the reciprocals of observed rate constants vs. those of the initial concentrations of sodium phenolate. In Table IV, the observed rate constants are summarized along with the estimated maximum values for the rate of ionization (k_1, N = ∞).

Summary

The catalytic constants of phenols, alcohols, and several polar and non-polar molecules in acetolysis of *tert*-butyl bromide were measured in acetic acid-carbon tetrachloride (1 : 3 by vol., at 25.0°C) in the presence of sodium acetate at 70.0°C. Ortho substituted (NO_2, Cl, CH_3, OH) phenols gave smaller constants than those of corresponding para derivatives, and among them *o*-nitrophenol gave the smallest one which was comparable to that of nitrobenzene. Dihydroxylic compounds, like 1,2-cyclohexanediols, ethylene glycol, catechol and water, gave constants greater than twice those of the corresponding monohydroxylic compounds, like cyclohexanol, ethanol, phenol and methanol, respectively. It was concluded that, in view of the lack of catalytic action of intramolecularly hydrogen-bridged hydroxylic compounds, the hydrogen atom of those hydroxylic molecules was distinctly the center of attack in the first ionization stage of the solvolysis and that two adjacent hydroxyl groups in dihydric compounds sterically co-operated in this stage. On these bases, similar accelerating action of various species of associated phenol molecules was suggested and illustrated by the analysis of the data of solvolysis rates of *tert*-butyl bromide in phenol-carbon tetrachloride mixtures at 20.0°C. It was shown that phenol polymer species with higher association degree exhibited more effective acceleration.

The authors are indebted to Mr. Ken-ichi Takeuchi who measured part of the phenolysis rates.

Department of Fuel Chemistry
Faculty of Engineering
Kyoto University
Sakyo-ku, Kyoto

Kinetic Studies on Solvolysis. VII. On the Kinetic Resolution at the First Stage of the S_N1-type Solvolysis of α-Phenethyl Chloride in Optically Active Carboxylic Acid Solvents

By Kunio Okamoto, Ken-ichi Takeuchi and Haruo Shingu

(Received November 21, 1960)

In the previous paper[1] we have demonstrated that the acetolysis of *tert*-butyl bromide proceeds with some linear rate acceleration in the presence of *p*-nitrophenol and some other *p*-substituted phenols, while the presence of *o*-substituted phenols in which the hydroxyl groups are fixed by intramolecular hydrogen-bridge does not cause any catalytic acceleration. From this it was concluded that the free hydroxyl group was distinctly the center of the reaction in those hydroxylic molecules including alcohols, phenols, carboxylic acids and water. It is, therefore, clear that they play a rôle not only as a general solvent but also as a kind of reactant molecule in the first ionization stage of the S_N1-type solvolysis.

Thus it may be anticipated that, when the S_N1-type solvolysis of a racemic halide is carried out in an optically active solvent, there would be observed a kinetic resolution in the first stage of the solvolysis with the result that the unchanged asymmetric halide may have some optical activity. This possibility of asymmetric solvolysis of S_N1-type was examined in the case of the solvolysis of (±)-α-phenethyl chloride in (+)-α-methyl hydrogen camphorate and in (−)-pinonic acid. This paper presents evidence in support of the existence of such kinetic resolution in those optically active solvents.

S_N2-type Kinetic Resolution of (±)-α-Phenethyl Chloride in Dioxane.—The rate studies on the S_N1-type solvolysis in these optically active solvents in the presence of 0.1 M of triethylamine showed that both of the reactions were of the first order in α-phenethyl chloride and of zero order in the added base, this being illustrated in Figs. 1 and 2. Although these results indicate that the reactions proceed predominantly by S_N1 mechanism, they do not exclude a slight, presumably less than 1%, concurrency of S_N2 mechanism[2].

As a control experiment, thererfore, the extent and direction of the S_N2-type kinetic resolution of α-phenethyl chloride was examined under the reaction conditions comparable to those of the S_N1-type resolution. For this purpose the S_N2-reaction of α-phenethyl chloride and triethylammonium salt of the optically active carboxylic acid was carried out in dioxane, which is a favorable solvent for the

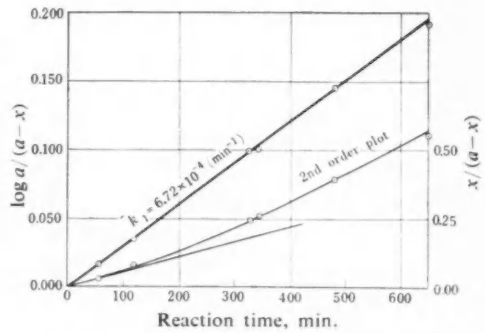

Fig. 1. Solvolysis rate of (±)-α-phenethyl chloride in (−)-pinonic acid, $[\alpha]_D^{19}$ −51.5°, in the presence of 0.116 M of triethylamine at 80.0±0.1°C. The initial concentration of the chloride, 0.116 M.

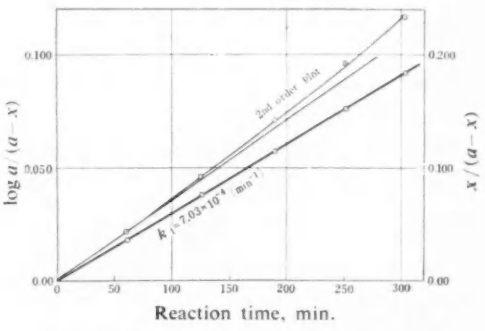

Fig. 2. Solvolysis rate of (±)-α-phenethyl chloride in α-methyl hydrogen camphorate, $[\alpha]_D^{15}$ 58.0°, in the presence of 0.123 M of triethylamine at 98.0±0.1°C. The initial concentration of the chloride, 0.123 M.

1) K. Okamoto and H. Shingu, This Bulletin, **34**, 1131 (1961).

2) H. Shingu and K. Okamoto, *J. Chem. Soc. Japan, Pure Chem. Sec.* (*Nippon Kagaku Zasshi*), **78**, 547 (1957).

Table I. Summary of optical purities of the recovered α-phenethyl chloride and of α-phenethyl alcohol in the S_N1-type solvolysis of (±)-α-phenethyl chloride

Solvent	Nucleophile	Temp. °C	Time[a] hr.	Optical purity, % α-Phenethyl chloride (recovered)	α-Phenethyl alcohol[b]
(+)-α-Methyl hydrogen camphorate $[\alpha]_D^{15}$ 58.0°	Triethyl-ammonium (+)-α-methyl camphorate	98~100	7.5	L[c] 0.54±0.13	L 2.24±0.28
		98		L 0.58±0.09	L 2.95±0.74
		100		(L 2.82±0.01[d])	(D[c] 10.6 ±0.09)
(−)-Pinonic acid $[\alpha]_D^{18}$ −10.9°	Triethyl-ammonium	70	15	D 0.27±0.08	D 0.57±0.07
$[\alpha]_D^{20}$ −51.5°		70~80	15.5	D 0.20±0.05	D 1.04±0.25
$[\alpha]_D^{18}$ −76.1°		70	15	D 0.13±0.02	L 1.56±0.39
Acetonitrile	Anilinium (+)-α-methyl camphorate[e]	85	4.85	0.00±0.02	—
	Anilinium (−)-pinonate[f]	85	4.35	0.00±0.03	L 3.22±1.38
Dioxane[g]	Triethyl-ammonium (+)-α-methyl camphorate[e]	100	9[h]	L 0.08±0.01	(L)[i]
	Triethyl-ammonium (−)-pinonate[f]	70	16[h]	L 0.15±0.01	(L)[i]

a) Approximately the half life time for each reaction.
b) The alcohol obtained from α-phenethyl ester.
c) Configuration.
d) The run with L-(+)-α-phenethyl chloride; $[\alpha]_D^{16}$ 30.4°, optical purity 28.7%.
e) The acid, $[\alpha]_D^{15}$ 58.0°, chloroform.
f) The acid, $[\alpha]_D^{20}$ −75.0°, chloroform.
g) The reaction under S_N2 mechanism.
h) The reaction time for the stage of 5% conversion of the chloride.
i) Deduced from the principle that the inversion of configuration occurs in the S_N2-type reaction.

S_N2 mechanism. In the reaction with triethylammonium (−)-pinonate (the acid $[\alpha]_D^{20}$ −75°), about 5% of (±)-α-phenethyl chloride was consumed in 16 hr. at 70°C and the unchanged chloride of 0.15% optical purity (L configuration) was obtained (cf. Table I). A similar reaction was carried out with triethylammonium (+)-α-methyl camphorate (the acid $[\alpha]_D^{15}$ +58°) and the unchanged α-phenethyl chloride showed 0.08% of optical purity (L configuration) after 9 hr. at 100°C at the stage of about 5% conversion. These values would indicate the extent of the kinetic resolution caused by the supposedly co-existing S_N2 mechanism in the S_N1-type reactions in these optically active carboxylic acid solvents.

Possibility of the Induced Resolution Caused by Kinetic Resolution at the Second Stage of S_N1-type Solvolysis. — The slight resolution observed in the S_N2 condition would indicate another mechanism for interpretation of the results of the S_N1-type resolution. Since the intermediate in the S_N1-type solvolysis is converted to the product by a process quite similar to the S_N2 mechanism, the starting chloride which is in equilibrium with the intermediate may also become optically active, even if the intermediate was kinetically resolved by an optically active nucleophile at the second stage of solvolysis, instead of being resolved at the first ionizing stage.

In order to examine this possibility, another control experiment was carried out under conditions that should cause kinetic resolution only at the second stage, i.e., the product forming stage. For this purpose acetonitrile, which does not react with the intermediate, was used as a solvent for the solvolysis of α-phenethyl chloride. As is expected from the S_N1 mechanism, the solvolysis rates optically active nucleophiles (anilinium (−)-pinonate and (+)-α-methyl camphorate) were found to obey good first order kinetics at 85°C, this being shown in Figs. 3 and 4. Half way through the reactions the recovered α-phenethyl chloride did not give any optical activity for either

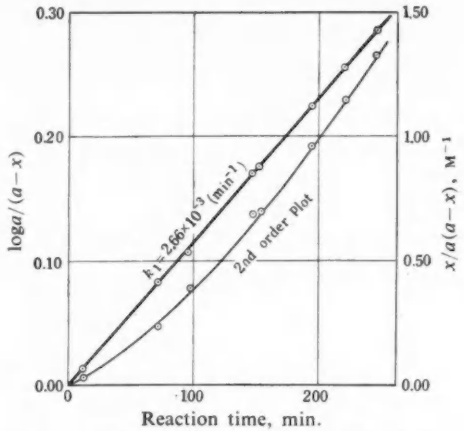

Fig. 3. Solvolysis rate of (±)-α-phenethyl chloride in acetonitrile in the presence of 0.675 N anilinium (−)-pinonate at 85.0±0.1°C. The initial concentration of the chloride, 0.675 M.

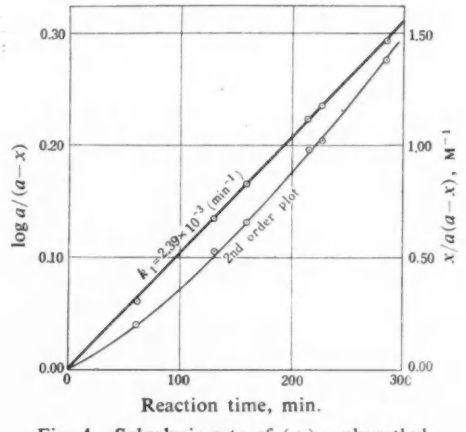

Fig. 4. Solvolysis rate of (±)-α-phenethyl chloride in acetonitrile in the presence of 0.682 N anilinium (+)-α-methyl camphorate at 85.0±0.1°C. The initial concentration of the chloride, 0.682 M.

of the nucleophiles within the experimental error, while the small amount of α-phenethyl alcohol obtained after hydrolysis of α-phenethyl pinonate showed about 5% of optical purity (D-configuration) (cf. Table I). This eliminates the possibility that the kinetic resolution at the second stage of the S_N1-type solvolysis can induce any preceptible resolution at the first ionization stage.

Kinetic Resolution at the Ionization Stage of the S_N1-type Solvolysis.—With these considerations in mind, we first carried out the S_N1-type solvolysis in (+)-α-methyl hydrogen camphorate in the presence of triethylamine at 98~100°C for 7.5 hr. until about 50% of α-phenethyl chloride was consumed, and the unchanged chloride had 0.54±0.13% of optical purity (L-configuration) (cf. Table I). In a similar experiment at 98°C for 9.5 hr., α-phenethyl chloride of 0.58±0.09% of optical purity (L-configuration) was recovered. Although the direction of the rotation of the recovered chlorides was the same as in the above mentioned reaction of the S_N2 mechanism in dioxane, the degree of optical purity, i.e., the extent of the kinetic resolution, is obviously greater than the one expected in the S_N2-type reaction under the corresponding reaction conditions, even after the correction of optical purity for the difference of the reaction percentage in both of the mechanisms. Hence it is evident that the optical rotation in the recovered chloride was predominantly caused by the kinetic resolution at the first ionization stage of the S_N1-type solvolysis in (+)-α-methyl hydrogen camphorate.

In a similar manner analogous experiments on the S_N1-type solvolysis of α-phenethyl chloride in the other optically active solvent was carried out in the presence of triethylamine in (−)-pinonic acids of various optical rotations for 15 hr. at about 70°C. In pinonic acid of optical rotations, $[\alpha]_D^{18}$ −10.9°, $[\alpha]_D^{20}$ −51.5° and $[\alpha]_D^{18}$ −76.1°, the unreacted chlorides showed 0.27±0.08, 0.20±0.05 and 0.13±0.02% of optical purity (D-configuration), respectively.

As above mentioned, in the resolution of the S_N2 mechanism with triethylammonium (−)-pinonate in dioxane the direction of rotation of the unreacted chloride was that of L-configuration, and this is just opposite to the one (D-configuration) observed in the reactions carried out in (−)-pinonic acid. This result clearly indicates that the kinetic resolution occurred at the first ionization stage of the S_N1-type solvolysis in this optically active solvent.

Finally, the kinetic resolution at the ionization stage of these S_N1-type solvolyses may be considered as a further evidence for the solvent molecule playing a rôle as a kind of reactant in this stage[1].

Configuration of the Optically Active α-Phenethyl Alcohol Derived from α-Phenethyl Esters of Optically Active Carboxylic Acids.—In the reactions in (+)-α-methyl hydrogen camphorate the isolated β-(α-phenethyl) α-methyl camphorate was hydrolysed with alcoholic sodium hydroxide or reduced with lithium aluminum hydride, and the optical purity of the recovered α-phenethyl alcohol

Table II. Relationship between configurations of recovered α-phenethyl chloride and α-phenethyl alcohol derived from α-phenethyl ester obtained in the S_N1-type solvolysis of (±)-α-phenethyl chloride in optically active carboxylic acids

Configuration of recovered α-phenethyl chloride	Resolution controlling stage for α-phenethyl alcohol	Configuration for α-phenethyl alcohol derived from α-phenethyl esters	Optically active carboxylic acids as a solvolytic solvent
L	first	L	(+)-α-Methyl hydrogen camphorate
	second*	L	——
D	first	D	(−)-Pinonic acid, $[\alpha]_D$ −10.9° and −51.5°
	second*	L	(−)-Pinonic acid, $[\alpha]_D$ −76.1°

* It is assumed that the resolution at the second stage gives the alcohol with L-configuration by the S_N2 mechanism (see text).

amounted to 2.24±0.28 and 2.95±0.74% (L-configuration) for each run (cf. Table I), while α-phenethyl alcohols derived from α-phenethyl (−)-pinonate by alkaline hydrolyses showed optical purities of 0.57±0.07 (D-configuration), 1.04±0.25 (D-configuration) and 1.56± 0.39% (L-configuration) for the reactions in (−)-pinonic acid with optical rotations, $[\alpha]_D^{18}$ −10.9°, $[\alpha]_D^{20}$ −51.5° and $[\alpha]_D^{18}$ −76.1°, respectively (cf. Table I).

In these reactions the directions of rotation for the α-phenethyl alcohols derived from the ester of the optically active carboxylic acids doubtless controlled, generally, by two factors, namely, the kinetic resolution caused by the attack of the optically active nucleophile at the second stage of the solvolysis and the resolution in the intermediate determined by the electrophilic attack by optically active solvent molecules at the first ionization stage.

The resolution at the first ionization stage has already been discussed in the previous section. For the discussion of the results of the resolution at the second stage the knowledge about the steric behavior of α-phenethyl chloride at this stage is required, since it is uncertain whether the configuration of the chloride would invert at the second stage of the S_N1-type reaction in these optically active carboxylic acids. Thus, the solvolysis of originally optically active chloride, L-(+)-α-phenethyl chloride, was carried out in (+)-α-methyl hydrogen camphorate in the presence of triethylamine at 100°C. Half way through the reaction α-phenethyl alcohol of 37% inversion, 63% racemization of configuration was obtained after reductive hydrolysis of β-(α-phenethyl) α-methyl camphorate (cf. Table I)[3]. This indicates that at the second stage of this solvolysis the chloride reacted predominantly with inversion of the configuration. This is consistent with the results previously known in the reaction of this chloride in the other hydroxylic solvents[1].

Considering this inversion of configuration of α-phenethyl chloride at the second stage of the S_N1-type solvolysis, we may expect that the direction of the second stage resolution would be the same as that of the resolution by the S_N2-type mechanism. This is verified by the fact that the S_N1-type resolution of (±)-α-phenethyl chloride with anilinium (−)-pinonate in acetonitrile, used as a solvent in which the resolution occurs only at the second stage, gives alcohol with L-configuration which is the same type obtainable in the S_N2-type resolution, e. g., in dioxane (cf. Table I).

Assuming that the direction of second stage resolution in the S_N1-type solvolysis in the optically active carboxylic acids would be the same as in acetonitrile, we can determine the resolution controlling stage, first or second, for the α-phenethyl alcohol derived from the esters by comparing the direction of resolution for the recovered chloride with those of the alcohol obtained, this being indicated in Table II.

In Table II it is shown that in (−)-pinonic acids, $[\alpha]_D$ −10.9° and −51.5°, the configuration of the resolved α-phenethyl alcohol (cf. Table I) is predominantly determined at the first ionization stage, while in almost optically pure (−)-pinonic acid with $[\alpha]_D$ −76.1° it is determined at the second stage of the reaction. In α-methyl hydrogen camphorate it seems likely that the configuration of α-phenethyl alcohol (cf. Table I) is predominantly controlled at the first ionization stage, since the

3) The recovered α-phenethyl chloride was mostly racemic and retained only 10% of the original optical purity, as is expected from the reversibility of the ionization process at the first stage of the S_N1-type solvolysis.

4) E. D. Hughes, C. K. Ingold and A. D. Scott, *J. Chem. Soc.*, **1937**, 1201.

resolution percentage of α-phenethyl chloride at the S_N2 condition, i.e., in dioxane, is considerably less than that observed at the S_N1-type reaction in this optically active solvent.

Experimental[5]

Specific Rotations in Chloroform for Optically Pure α-Phenethyl Alcohol and α-Phenethyl Chloride.—Because of the lack of previously reported data, specific rotations in chloroform for α-phenethyl alcohol of the rotations α_D, neat, −37.0° (at 15.0°C), +19.4° (at 24.4°C) and −40.1° (at 25.4°C), *l* 1 dm. for all, were measured, and the following results were obtained: $[\alpha]_D$ −47.5° (at 15.0°C, *c* 16.0), +24.8° (at 24.4°C, *c* 6.70) and −50.7° (at 25.4°C, *c* 6.70), respectively. From these values and the reported value[6] for neat rotation of optically pure α-phenethyl alcohol (α_D^{25} 43.7°, *l* 1 dm.), a specific rotation in chloroform for the optically pure alcohol was estimated to be 55.9° (at 15∼25°C, *c* 6.70∼16.0). In a similar manner, a specific rotation in chloroform for optically pure α-phenethyl chloride was estimated to be 105∼107° (at 17∼25°C, *c* 6.8∼6.9) from the following data: reported value[7] for neat rotation of optically pure chloride, α_D^{25} 126∼129°, *l* 1 dm.; observed specific rotations in chloroform for α-phenethyl chloride of neat rotations α_D −34.8° (at 17.0°C, *l* 1 dm.) and +17.8° (at 25.7°C, *l* 1 dm.): −28.9° (at 17.0°C, *c* 6.83) and −14.9° (at 25.7°C, *c* 6.90), respectively.

Reaction of (±)-α-Phenethyl Chloride and Triethylammonium (−)-Pinonate in (−)-Pinonic Acid.—(−)-Pinonic acid was prepared by potassium permanganate oxidation of α-pinene according to the previously reported method[8]. A mixture of pinonic acid (35.0 g., b. p. 152∼156°C/4 mmHg, $[\alpha]_D^{18}$ −10.9°, *c* 10.9, chloroform), triethylamine (7.0 g., b. p. 88∼89°C) and (±)-α-phenethyl chloride (10.45 g., b. p. 92.0°C/36 mmHg) was kept at 70°C for 15 hr. After addition of ether (50 cc.) the ethereal solution containing crystals of triethylammonium hydrochloride was washed successively with two 50 cc. portions of 10% aqueous sodium hydroxide and two 50 cc. portions of water, dried, and concentrated. The residue was fractionally distilled in vacuo, giving α-phenethyl chloride (6.9 g., b. p. 77.0∼78.0°C/18 mmHg., n_D^{20} 1.5265, α_D^{18} −0.180±0.005°, $[\alpha]_D^{18}$ −0.287°, *l* 2 dm., *c* 31.4, chloroform, Found: C, 68.18; H, 6.27. Calcd. for C_8H_9Cl: C, 68.33; H, 6.45%). The residual mass was refluxed with a mixture of 20% aqueous sodium hydroxide (15 cc.) and ethanol (10 cc.) for 4 hr. and distilled with steam. The distillate (about 100 cc.) was extracted with two 50 cc. portions of ether. Concentration of the combined ether solutions afforded an oily material which was distilled in vacuo to give α-phenethyl alcohol (2.2 g., b. p. 80.0∼81.0°C/7 mmHg, n_D^{20} 1.5245, α_D^{17} −0.040 ±0.005°, $[\alpha]_D^{17}$ −0.320°, *l* 2 dm., *c* 6.23, chloroform, Found: C, 78.62; H, 8.26. Calcd. for $C_8H_{10}O$: C, 78.65; H, 8.25%).

The second run carried out under similar conditions, 70∼80°C, 15.5 hr., with pinonic acid (20.0 g., b. p. 152.0°C/7 mmHg, m. p. 70∼80°C, $[\alpha]_D^{20}$ −51.5°, chloroform), triethylamine (5.0 g.) and (±)-α-phenethyl chloride (7.0 g.) afforded α-phenethyl chloride (3.3 g., b. p. 58.0°C/7.5 mmHg, α_D^{15} −0.100±0.025°, $[\alpha]_D^{15}$ −0.21°, *l* 2 dm., *c* 23.8, chloroform) and α-phenethyl alcohol (2.2 g., b. p. 80∼82.0°C/9 mmHg, α_D^{18} −0.105±0.025°, $[\alpha]_D^{18}$ −0.58°, *l* 2 dm., *c* 9.1, chloroform, Found: C, 78.58; H, 8.06%).

Starting from pinonic acid (25.0 g., m. p. 65.0∼75.0°C, $[\alpha]_D^{18}$ −76.1°, *c* 9.63, chloroform), triethylamine (5.0 g.) and α-phenethyl chloride (6.75 g.), the third run afforded at 70°C for 15 hr. α-phenethyl chloride (4.0 g., b. p. 58.0∼59.0°C/9 mmHg, n_D^{20} 1.5230, α_D^{18} −0.040±0.005°, $[\alpha]_D^{18}$ −0.141°, *l* 2 dm., *c* 14.2, chloroform, Found: C, 68.38; H, 6.59%) and α-phenethyl alcohol (0.50 g., b. p. 68.0∼69.0°C/3 mmHg, n_D^{20} 1.5210, α_D^{18} 0.020±0.005°, $[\alpha]_D^{18}$ 0.872°, *l* 2 dm., *c* 1.15, Found: C, 78.35; H, 8.44%).

Reaction of (±)-α-Phenethyl Chloride and Triethylammonium (+)-α-Methyl Camphorate in (+)-α-Methyl Hydrogen Camphorate.—α-Methyl hydrogen camphorate was obtained by esterification of camphoric acid according to the previously reported method[9]. To a mixture of α-methyl hydrogen camphorate (52.5 g., m. p. 56.0∼57.0°C, $[\alpha]_D^{15}$ 58.0°, chloroform) and triethylamine (10.0 g.), (±)-α-phenethyl chloride (14.0 g.) was added. After being kept at 98∼100°C for 7.5 hr., the reaction mixture was taken into ether (100 cc.), and washed successively with water (100 cc.), three 50 cc. portions of 10% aqueous sodium hydroxide, and two 50 cc. portions of water. The ethereal solution was dried with anhydrous sodium sulfate and concentrated. The oily material was fractionally distilled in vacuo, giving a fore-run (1.0 g.), containing styrene and a small amount of α-phenethyl chloride, α-phenethyl chloride (5.6 g., b. p. 53.0∼55.0°C/8.5 mmHg, n_D^{20} 1.5274, α_D^{13} 0.020±0.005°, $[\alpha]_D^{13}$ 0.57°, *l* 2 dm., *c* 1.71, chloroform, Found: C, 68.14; H, 6.58%) and β-(α-phenethyl) α-methyl camphorate (10.4 g., b. p. 165∼168°C/2 mmHg, n_D^{20} 1.5052).

Found: C, 71.41; H, 8.11. Calcd. for $C_{19}H_{26}O_4$: C, 71.67; H, 8.23%.

β-(α-Phenethyl) α-methyl camphorate was reduced with lithium aluminum hydride. A mixture of lithium aluminum hydride (5.0 g.) and dry ether (250 cc.) was stirred for 1 hr. under a nitrogen atmosphere and treated with β-(α-phenethyl) α-methyl camphorate (10.0 g.) dissolved in ether (50 cc.) over a period of 5 min. After being stirred for 5 hr. and being kept overnight at 15°C, the mixture was treated with water (10 cc.) which was added over a period of half an hour. The precipitated material was filtered and washed with ether (100 cc.), and the combined ether solution was concentrated. The residue was distilled under reduced pressure to give α-phenethyl alcohol (2.6 g., b. p. 70.0∼71.0°C/7 mmHg, n_D^{20} 1.5260, α_D^{17}

5) Microanalyses by Microanalytical Center, Kyoto University. Melting points are not corrected. For the measurement of optical rotations "Zeiss Winckel, Kreispolarimeter, 0.01°" was used.

6) E. Downer and J. Kenyon, *J. Chem. Soc.*, **1939**, 1156.

7) R. L. Burwell, Jr., A. D. Shields and H. Hart, *J. Am. Chem. Soc.*, **76**, 908 (1954).

8) G. Dupont and G. Brus, *Ann. Chim.*, **19**, 186 (1923).

9) J. Walker, *J. Chem. Soc.*, **61**, 1088 (1892).

0.400±0.005°, $[\alpha]_D^{17}$ 1.25°, *l* 2 dm., *c* 16.0, chloroform. Found: C, 78.75; H, 8.36%).

The second run carried out at 98°C for 9.5 hr. with α-methyl hydrogen camphorate (23.0 g.), triethylamine (5.0 g.), and (±)-α-phenethyl chloride (7.0 g.), afforded α-phenethyl chloride (1.9 g., b. p. 49.0~51.0°C/6 mmHg, α_D^{15} 0.13±0.02°, $[\alpha]_D^{15}$ 0.62°, *l* 2 dm., *c* 10.5, chloroform) and after alkaline hydrolysis of the ester α-phenethyl alcohol (0.15 g., b. p. 80.0°C/9 mmHg, α_D^{15} 0.04±0.01°, $[\alpha]_D^{15}$ 1.65°, *l* 2 dm., *c* 1.21, chloroform) was obtained.

Reaction of (+)-α-Phenethyl Chloride and Triethylammonium α-Methyl Camphorate in (+)-α-Methyl Hydrogen Camphorate.—(±)-α-Phenethyl alcohol was resolved according to the published method[6] and the first crop of brucine salt of α-phenethyl hydrogen phthalate gave (−)-α-phenethyl alcohol, $[\alpha]_D^{15}$ −47.5°, *c* 16.0, chloroform, From the first mother liquors (+)-α-phenethyl alcohol ($[\alpha]_D^{13}$ 37.0°, *c* 15.4, chloroform) was obtained. From this (+)-alcohol (+)-α-phenethyl chloride ($[\alpha]_D^{15}$ 30.4°, *c* 7.15, chloroform) was prepared by chlorination with thionyl chloride according to the previously reported method[9]. The reaction was carried out with (+)-α-methyl hydrogen camphorate (50.0 g.), triethylamine (4.5 g.) and (+)-α-phenenethyl chloride (5.6 g., $[\alpha]_D^{15}$ 30.4°) at 100°C for 8 hr. After treatment similar to the previous experiment with (±)-α-phenethyl chloride, α-phenethyl chloride (2.4 g., b. p. 51.0~52.0°C/6 mmHg, n_D^{20} 1.5268, α_D^{15} 0.450±0.01°, $[\alpha]_D^{15}$ 2.98°, *l* 2 dm., *c* 7.55, chloroform, Found: C, 68.40; H, 6.37%) was recovered.

After reduction with lithium aluminum hydride, β-(α-phenethyl) α-methyl camphorate (4.6 g., b. p. 173°C/2 mmHg, n_D^{19} 1.5034, Found: C, 71.88; H, 8.31%.) afforded α-phenethyl alcohol (0.9 g., b. p. 63.0~67.0°C/3 mmHg, n_D^{19} 1.5169, α_D^{15} −0.580±0.005°, $[\alpha]_D^{15}$ −5.93°, *l* 2 dm., *c* 4.90, chloroform, Found: C, 78.48; H, 8.43%).

Reaction of (±)-α-Phenethyl Chloride and Triethylammonium (+)-α-Methyl Camphorate in Dioxane. — Triethylammonium (+)-α-methyl camphorate was prepared by mixing the equivalent amounts of triethylamine and (+)-α-methyl hydrogen camphorate in dioxane. A mixture of triethylamine (5.0 g.), (+)-α-methyl hydrogen camphorate (10.6 g.), dry dioxane (24.5 g.) and (±)-α-phenethyl chloride (7.0 g.) was kept at 100°C for 9 hr. The reaction percentage of the chloride was estimated to be about 5% from the aliquot titration of unchanged triethylammonium α-methyl camphorate with acetic acid solution of perchloric acid. After addition of ether (100 cc.) the mixture was washed with four 100 cc. portions of water, dried with anhydrous sodium sulfate, and concentrated. The residue was fractionally distilled under reduced pressure to give α-phenethyl chloride (5.8 g., b. p. 89.0°C/38 mmHg, n_D^{20} 1.5264, α_D^{20} 0.055±0.005°, $[\alpha]_D^{20}$ 0.086°, *l* 2 dm., *c* 31.8, chloroform, Found: C, 68.58; H, 6.52%).

Reaction of (±)-α-Phenethyl Chloride and Triethylammonium (−)-Pinonate in Dioxane. — A mixture of triethylamine (5.0 g.), (−)-pinonic acid (9.2 g., $[\alpha]_D^{19}$ −75.0°, chloroform), dry dioxane (25 cc.) and (±)-α-phenethyl chloride (7.0 g.) was kept at 70°C for 16 hr. The reaction percentage of the chloride was estimated to be about 5% from the titration of unchanged triethylammonium pinonate. After addition of ether (100 cc.) the mixture was treated in a manner similar to the reaction with triethyl ammonium α-methyl camphorate. The recovered α-phenethyl chloride gave the following constants; b. p. 89.0°C/37 mmHg, n_D^{19} 1.5272, α_D^{20} 0.09±0.005°, $[\alpha]_D^{20}$ 0.16°, *l* 2 dm., *c* 28.0, chloroform, Found: C, 68.58; H, 6.52%.

Reaction of (±)-α-Phenethyl Chloride and Anilinium (+)-α-Methyl Camphorate in Acetonitrile. — Anilinium α-methyl camphorate solution (0.750 N) was prepared from equivalent amounts of aniline and (+)-α-methyl hydrogen camphorate ($[\alpha]_D^{15}$ 58.0°) in acetonitrile. (±)-α-Phenethyl chloride (4.92 g.) was dissolved in the anilinium salt solution and diluted to a volume of 50 cc. with the solution. The mixture was kept in a sealed tube for 291 min. (half life time of the reaction) at 85.0°C. Ether (100 cc.) was added to the cooled reaction mixture, and the mixture washed with water (50 cc.). After evaporation of ether the residual oily mass gave α-phenethyl chloride (2.3 g., b. p. 55.0~56.0°C/6 mmHg, n_D^{19} 1.5251, α_D^{21} 0.00±0.02°, *l* 1 dm., neat). In the distillation residue no ester was found.

Reaction (±)-α-Phenethyl Chloride and Anilinium (−)-Pinonate in Acetonitrile.—In a manner similar to the reaction with anilinium (+)-α-methyl camphorate (±)-α-phenethyl chloride (5.81 g.) was kept with 0.750 N anilinium (−)-pinonate (the acid $[\alpha]_D^{20}$ −75.0) solution for 261 min. (half life time of the reaction) at 85.0°C. The recovered chloride (2.22 g.) gave the following constants; b. p. 53.0°C/2 mmHg, n_D^{20} 1.5239, α_D^{21} 0.00±0.03°, *l* 1 dm., neat, Found: C, 68.63; H, 6.60%. The higher boiling fraction (5.24 g., 137~140°C/0.8 mmHg) was hydrolysed with 20% aqueous sodium hydroxide (15 cc.) and ethanol (10 cc.) for 4 hr., and distilled with steam. The recovered α-phenethyl alcohol (0.05 g.) gave slight optical activity (α_D^{20} 0.07±0.03°, $[\alpha]_D^{20}$ 1.8°, *l* 1 dm. *c* about 4, chloroform).

Kinetic Measurement.—The reactions in (+)-α-methyl hydrogen camphorate ($[\alpha]_D^{15}$ 58°) and (−)-pinonic acid ($[\alpha]_D^{19}$ −51.5°) were carried out in a 15 cc. measuring flask placed in a thermostat. To a weighed amount of α-phenethyl chloride in the flask the optically active carboxylic acid solution of triethylamine was added to the volume of 15 cc. at the reaction temperature. After various periods of time, aliquot portions (1.000 cc.) were pipetted into 5 cc. of cold acetic acid and the solutions were titrated with 0.0672 N perchloric acid in acetic acid with crystal violet indicator. The rates in acetonitlile were measured by a sealed-ampoule technique. Each sample (1.000 cc.) was titrated with 0.245 N perchloric acid in acetic acid. The rate constants were calculated from the first order rate equation by a graphical method.

Summary

1) In S_N2 displacement reactions of (±)-α-phenethyl chloride with triethylammonium (+)-α-methyl camphorate and with triethylammonium (−)-pinonate in dioxane, α-phenethyl chloride of 0.08% of optical purity (L-

configuration) and of 0.15% of optical purity (L-configuration) were recovered at the stage of about 5% conversion, respectively.

2) In S_N1-type solvolysis of (±)-α-phenethyl chloride with anilinium (+)-α-methyl camphorate and (−)-pinonate in acetonitrile, the recovered α-phenethyl chlorides showed no perceptible optical activity on the half way for each of the reactions. From this, the possibility of the induced resolution caused at the first stage by kinetic resolution at the second stage of the S_N1-type solvolysis was eliminated.

3) In S_N1-type solvolysis of (±)-α-phenethyl chloride in (+)-α-methyl hydrogen camphorate and in (−)-pinonate, about half of the chloride was converted to the ester at the similar reaction conditions (temperature and time) to the S_N2 displacement reactions carried out in dioxane. The recovered chloride in the reaction in hydrogen camphorate showed optical purity of 0.54~0.58% (L-configuration). In pinonic acids with various optical activities the recovered chlorides possessed optical purity of 0.13~0.27% (D-configuration).

4) In comparing the configurations and optical purities in S_N1- and S_N2-conditions, it is concluded that optically active solvent molecules, like (+)-α-methyl hydrogen camphorate and (−)-pinonic acid, can cause kinetic resolution in the first ionization stage of the S_N1-type solvolysis and therefore they obviously play a rôle as a kind of reactant molecule which controls the steric course of the solvation reaction in the first stage of this solvolysis.

5) In the S_N1-type solvolysis of optically active α-phenethyl chloride in presence of triethylamine in (+)-α-methyl hydrogen camphorate, optically active β-(α-phenethyl)-α-methyl camphorate gave optically active α-phenethyl alcohol of 37% inversion, 63% racemization of configuration. From this it was concluded that S_N2-like spatial orientation predominates at the second stage of this solvolysis.

6) For each of the resolution results of α-phenethyl chloride under S_N1- and S_N2-conditions, the relationship between the configuration of the resolved alcohol and the resolution-controlling stage was predicted on the basis of the observed inversion at the second stage of the solvolysis. The configurations observed for the α-phenethyl alcohols were found to be consistent with the predictions.

The authors wish to thank Mr. Ryôichi Kanô for his assistance in preparation of (−)-pinonic acid.

Department of Fuel Chemistry
Faculty of Engineering
Kyoto University
Sakyo-ku, Kyoto

Study on Metal Complexes of Analytical Importance. I. Vanadium Complexes of 8-Quinolinol and 2-Methyl-8-quinolinol[1]

By Hiroji NAKAMURA, Yoichi SHIMURA and Ryutaro TSUCHIDA

(Received November 24, 1960)

8-Quinolinol (A) is a popular analytical reagent, being used in the analysis of vanadium.

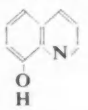

A

8-Quinolinol
(symbol : oxinH)

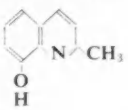

B

2-Methyl-8-quinolinol
(symbol : CH_3-oxinH)

The reaction of vanadate with 8-quinolinol in aqueous solution at pH 4~5 produces a bluish-black complex. This complex dissolves in lower aliphatic alcohols to give red solutions, while in chloroform it gives a violet one[2]. From boiling alcohol solutions saturated with this complex is deposited a brownish black complex on cooling, which dissolves in chloroform to show red color instead of violet.

Bielig and Bayer[2] reported that these two complexes were geometrical isomers which had a molecular formula $[VO(OH)(oxin)_2]$, and they named the bluish-black complex "violet form" and the brownish black complex "red form" by the colors of the chloroform solutions of these complexes.

1) A part of this study was presented at the Symposium on Coordination Compounds of the Chemical Society of Japan, Sendai, September, 1960.

2) H.-J. Bielig and E. Bayer, *Ann.*, **584**, 96 (1953).

Based on rather weak experimental evidences, they reported that the violet form had the cis structure and that the red form had the trans structure which are shown in Fig. 1.

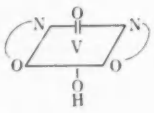

cis structure
Fig. 1 (a)

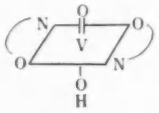

trans structure
Fig. 1 (b)

Contrary to their conclusion, Blair and Pantony[3] assumed that the red form had the molecular formula $[VO(O\text{-}R)(oxin)_2]$ (R is an alkyl group), namely that the complex was an alkyl ester of $[VO(OH)(oxin)_2]$. As for the violet form, Blair and Pantony explained that it had the trans structure, but no experimental evidence was given.

In order to decide the configurations of the complexes, we have prepared new complexes of 2-methyl-8-quinolinol, and from experimental data of these complexes have discussed the problem.

Results and Discussion

Complexes of 2-Methyl-8-quinolinol with Vanadium(V).—As will be seen in the experimental part, 2-methyl-8-quinolinol produces with vanadate a yellow complex, not a black one. In the case of 8-quinolinol a bluish-black complex (violet form) is separated under the same conditions. In this respect, the yellow complex resembles neither the violet nor the red form.

Recrystallization of the yellow complex from 98% methanol also produces a yellow complex. The complex thus obtained is yellow in crystalline state, but shows red color in absolute methanol giving an absorption band at $60.6 \times 10^{13}\,sec^{-1}$ (Fig. 2a). The solution in 98% methanol gives a weaker band at the same frequency (Fig. 2b). The higher the water content of the solvent is, the weaker is the absorption band (Fig. 2b-f). Thus, the color in 90% methanol solution is almost yellow.

Elementary analysis of the yellow complex shows that it has the formula of $VO(OH)(CH_3\text{-}oxin)_2 \cdot 2H_2O$, and over phosphorus pentoxide in vacuo the complex gradually changes black with decrease of its weight. In three weeks the color changes completely to black, and the decrease of weight corresponds to two molecules of water. The black complex thus obtained has the empirical formula $VO(OH)(CH_3\text{-}$

3) A. J. Blair and D. A. Pantony, *J. Inorg. Nucl. Chem.*, 5, 316 (1958).

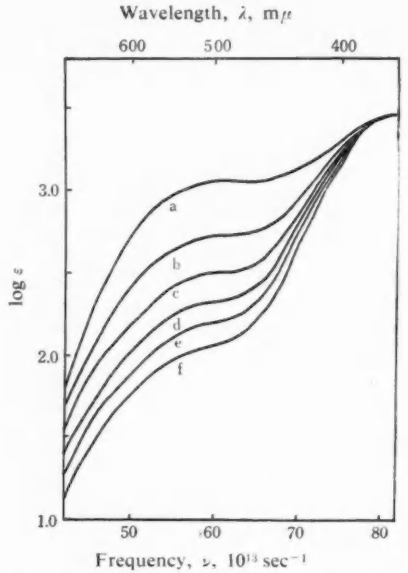

Fig. 2. Absorption spectra of $[VO(OH)(CH_3\text{-}oxin)_2(OH_2)_2]$ in absolute methanol and in diluted methanol.
a, absolute; b, 98%; c, 96% d, 94%; e, 92%; f, 90%.

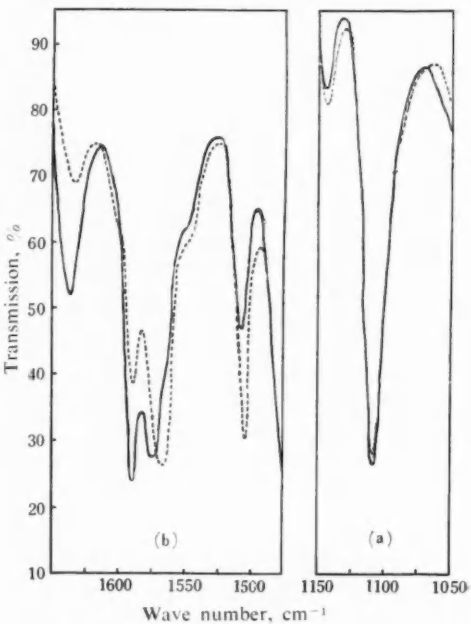

Fig. 3. Infrared absorption spectra of $[VO(OH)(CH_3\text{-oxin})_2(OH_2)_2]$ (——) and $[VO(OH)(CH_3\text{-oxin})_2]$ (----).
(a): C–O stretching band
(b): C=N or C=C stretching bands

oxin)$_2$. Accordingly it is clear that the difference between the yellow and the black colors is due to the water molecules. Judging from the marked change of the color, the water molecules are not merely of crystallization character but are coordinated. The black complex cannot have the cis structure owing to the steric hindrance between the methyl groups of the ligands. It is considered to have the trans structure (Fig. 1).

Since the maximum coordination number of the quinquevalent vanadium is six, the yellow complex [VO(OH)(CH$_3$-oxin)$_2$(OH$_2$)$_2$] must have an octahedral configuration. Consequently the two 2-methyl-8-quinolinol ions are coordinated as unidentate ligands. The difference between 8-quinolinol and 2-methyl-8-quinolinol is only that the latter has a methyl group at the carbon atom adjacent to the nitrogen atom. Therefore, it seems that the nitrogen atoms are not bound to the vanadium ion. Infrared absorption spectra of these two complexes show that this consideration is correct.

Both the yellow and the black complexes exhibit a strong band of C–O stretching[4] at the same wave number 1108 cm^{-1} (Fig. 3). This shows that in each complex, oxygen atoms are bound to the vanadium ion. If the bond V–O were broken in the yellow complex, the position of the C–O stretching band of the complex would differ from that of the black. Moreover, these complexes show four bands over the region between 1640 and 1500 cm^{-1} which are considered to be C=N or C=C stretching vibrations[5] in the ligands. Considerable differences are recognized between the corresponding bands of the two complexes not only in their positions, but also in intensities (Fig. 3). These differences suggest that in the yellow complex the nitrogen atoms are not bound to the central vanadium ion.

Now we have been led to the conclusion that the yellow complex [VO(OH)(CH$_3$-oxin)$_2$(OH$_2$)$_2$] has an octahedral structure and that the 8-quinolinol ions are not bidentate but unidentate ligands which are bound to the central vanadium ion by their oxygen atoms.

Structure of the Red Form.—As was described in the preceding section, the black complex [VO(OH)(CH$_3$-oxin)$_2$] has the trans structure. Therefore, the comparison of the absorption spectrum of [VO(OH)(CH$_3$-oxin)$_2$] with those of the red and the violet forms may give us some suggestions about the structures of these complexes.

The absorption spectra of these three complexes in chloroform are shown in Fig. 4. [VO(OH)(CH$_3$-oxin)$_2$] shows two bands at 60.6×10^{13} and 80.6×10^{13} sec^{-1}. The positions

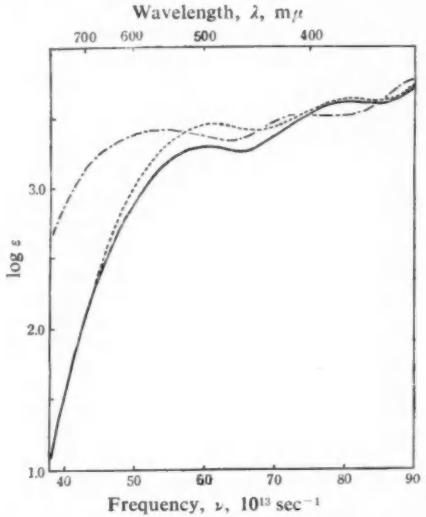

Fig. 4. Absorption spectra of 8-quinolinol-vanadium complexes and 2-methyl-8-quinolinol-vanadium complex in chloroform.
—·— violet form
---- red form
—— [VO(OH)(CH$_3$-oxin)$_2$] (trans)

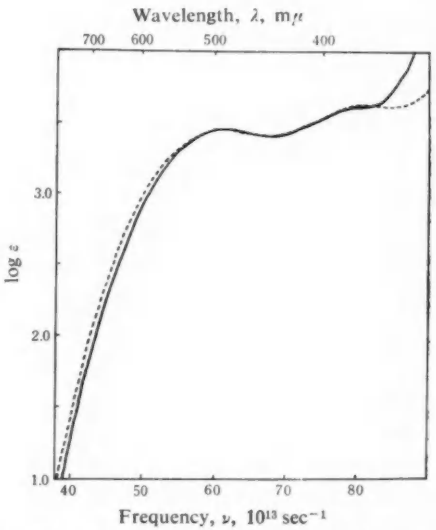

Fig. 5. Absorption spectra of [VO(OH)(oxin)$_2$] (red form) (——) and [VO(O-CH$_3$)(oxin)$_2$] (----) in benzene. The enhancement of the curve (——) at the shorter wavelength region is owing to the absorption of 8-quinolinol which is added in excess.

4) R. G. Charles, H. Freiser, R. Friedel, L. E. Hillard and W. D. Johnstone, *Spectrochim. Acta*, **8**, 1 (1956).
5) L. J. Bellamy, "The Infrared Spectra of Complex Molecules", 2nd ed. (1958), pp. 270-286.

of the bands coincide with those of the red form. Accordingly it seems that the red form has the trans and the violet form has the cis structure. In this respect, these results support Bielig's opinion. But as will be seen in the experimental part, Blair's opinion that the red form has a formula $[VO(O\text{-}R)(oxin)_2]$ is also correct. 8-Quinolinol complexes which are recrystallized from boiling methanol and isopropyl alcohol respectively have the empirical formulae corresponding to $[VO(O\text{-}CH_3)(oxin)_2]$ and $[VO(O\text{-}C_3H_7)(oxin)_2]$. To obtain a red 8-quinolinol complex without using alcohols, we examined many solvents. No solvent, however, was effective. Next, the reaction between vanadium(V) quinaldinate and 8-quinolinol in benzene was tried. Instantly the color changed to red and the absorption spectrum of the solution was quite like that of the red form which was obtained from boiling methanol solution (Fig. 5).

Now we can conclude that the violet form has the cis structure, while the red form has the trans structure, and further that the esterification of the red form does not induce any striking change of color.

Yellow 8-Quinolinol Complex.—Both the violet and the red forms are almost black in the crystalline state, as was described in the preceding section. But a yellow 8-quinolinol complex can also be obtained, which is prepared as a sodium salt at higher pH[2]. Bielig and Bayer gave the formula $Na[VO(O)(oxin)_2]\cdot H_2O$ to the yellow complex salt. They carried out the chemical analysis of the yellow complex after drying it over phosphorus pentoxide at 100°C in a high vacuum. The sodium salt which was dried in air has an empirical formula $NaVO(O)(oxin)_2\cdot 4H_2O$. The yellow color of this salt may be understandable on the assumption that it has the formula $Na[VO(O)(oxin)_2(OH_2)_2]\cdot 2H_2O$ corresponding to the yellow 2-methyl-8-quinolinol complex $[VO(OH)(CH_3\text{-}oxin)_2(OH_2)_2]$.

Experimental

Preparation of 2-Methyl-8-quinolinol Complexes of Vanadium.—The yellow complex was prepared as follows: 3.2 g. of 2-methyl-8-quinolinol was dissolved in 60 ml. of 1 N acetic acid and was diluted to 250 ml. To the solution was added drop by drop 2.0 g. of sodium metavanadate tetrahydrate ($NaVO_3\cdot 4H_2O$) dissolved in 100 ml. of 0.2 N sodium hydroxide. A muddy yellow precipitate appeared. The pH of the mixture was adjusted to 5.0 by the use of 1 N acetic acid and it was digested for two hours at 70°C. The crude complex thus obtained was recrystallized three times from 98% methanol by evaporating the solvent at 40°C in vacuo. The yellow complex obtained as pure crystals was dried over calcium chloride. For analyzing the coordinated water of this complex, heating is not suitable, since the complex decomposes at a high temperature. Therefore, drying over phosphorus pentoxide was adopted for the analysis of the coordinated water.

Found: H_2O, 8.10; C, 54.96; H, 4.85; N, 6.40; V, 11.51. Calcd. for $C_{20}H_{17}O_5N_2V\cdot 2H_2O = [VO(OH)(CH_3\text{-}oxin)(OH_2)_2]$: H_2O, 8.26; C, 55.04; H, 4.85; N, 6.42; V, 11.68%.

The complex is soluble in lower aliphatic alcohols, cyclohexanone, pyridine and diluted solution of alkali, and insoluble in ethyl ether, 2-butanone, cyclohexane, benzene, chloroform, carbon tetrachloride and water.

The black complex was prepared by expeling the water molecules of the yellow complex over phosphorus pentoxide in vacuo.

Found: C, 60.04; H, 4.18; N, 7.10; V, 12.65. Calcd. for $C_{20}H_{17}O_4N_2V = [VO(OH)(CH_3\text{-}oxin)_2]$: C, 60.00; H, 4.28; N, 7.00; V, 12.73%.

The black complex is soluble in chloroform, benzene and whatever the yellow complex is soluble in, sparingly soluble in ethyl ether, insoluble in cyclohexane, carbon tetrachloride and in water, and soluble with decomposition in dioxane, acetone and 2-butanone.

Violet Form of 8-Quinolinol-Vanadium Complex.—This complex was prepared by the method of Bielig and Bayer[2] and also of Blair and Pantony[3].

Red Forms of 8-Quinolinol-Vanadium Complex.—The methyl ester was prepared as follows: 1.0 g. of violet form was refluxed for 90 min. with 400 ml. of methanol. After filtration, the solution was concentrated to about 40 ml. The brownish black crystals then separated were filtered and dried in air.

Found: C, 59.16; H, 4.20; N, 7.35; V, 13.01. Calcd. for $C_{19}H_{15}O_4N_2V = [VO(O\text{-}CH_3)(oxin)_2]$: C, 59.09; H, 3.91; N, 7.25; V, 13.19%.

The isopropyl ester was prepared in almost the same way as was the methyl ester.

Found: C, 61.61; H, 4.66; N, 6.81; V, 12.08. Calcd. for $C_{21}H_{19}O_4N_2V = [VO(O\text{-}C_3H_7)(oxin)_2]$: C, 60.80; H, 4.62; N, 6.80; V, 12.30%.

Yellow 8-Quinolinol Complex of Vanadium.—This complex was prepared by the method of Bielig and Bayer[2] and was analyzed after being dried in air.

Found: C, 45.52; H, 4.25; N, 5.91; V, 10.60. Calcd. for $C_{18}H_{20}O_5N_2NaV = Na[VO(O)(oxin)_2(OH_2)_2]\cdot 2H_2O$: C, 45.87; H, 4.27; N, 5.94; V, 10.81%.

Preparation of Sodium Salt of 2-Methyl-8-quinolinol-Vanadium Complex.—The same method as that used in the preparation of $Na[VO(O)(oxin)_2(OH_2)_2]\cdot 2H_2O$ was not effective for the preparation of this complex. So the desired complex was prepared as follows: 2.1 g. of $[VO(OH)(CH_3\text{-}oxin)_2(OH_2)_2]$ was dissolved in 200 ml. of 0.2 N sodium hydroxide. After being filtered, the solution was concentrated at 50°C in vacuo to 20 ml. The complex salt thus obtained was recrystallized twice from 98% methanol.

Found: C, 48.59; H, 4.65; N, 5.42; V, 10.05. Calcd. for $C_{20}H_{24}O_9N_2NaV = Na[VO(O)(CH_3\text{-}oxin)_2(OH_2)_2]\cdot 2H_2O$: C, 48.59; H, 4.89; N, 5.67; V, 10.30%.

Absorption Spectrum of the Red Form which is Not Esterified.—For the first time, vanadium quinaldinate was prepared as follows: 0.97 g. of $NaVO_3 \cdot 4H_2O$ was dissolved in 50 ml. of 2 N sodium hydroxide. To this solution was added 1.73 g. of quinaldinic acid dissolved in 50 ml. of 2 N sodium hydroxide. This mixture was acidified with 10 ml. of 2 N acetic acid. The white precipitate which appeared was separated by filtration after it had been digested for two hours at 60°C.

The benzene solution of this complex was colorless. To the solution was added a benzene solution of 8-quinolinol (almost colorless). The solution instantly became red, which was quite similar to the color of the solution of the red form prepared from the violet form by the use of methanol (Fig. 5). The same behavior was recognized in dioxane too.

Measurements.—Visible and ultraviolet absorption spectra were determined with a Beckman DU and a Hitachi EPU-2A spectrophotometers using the cells which have 1 and 10 cm. light paths.

Infrared absorption measurements were made by the pressed disk technique in a Hitachi EPI-2 infrared spectrophotometer, the disks being 200 mg. of dried potassium bromide containing 1.5 mg. of complexes.

Summary

New complexes, $[VO(OH)(CH_3\text{-oxin})_2]$, $[VO(OH)(CH_3\text{-oxin})_2(OH_2)_2]$ and $Na[VO(O)(CH_3\text{-oxin})_2(OH_2)_2] \cdot 2H_2O$ have been prepared and discussed in relation to the structures.

From experimental evidences of these complexes and of 8-quinolinol-vanadium complexes, we have concluded that the violet form of 8-quinolinol-vanadium complex has a cis configuration and that the red form has a trans one.

Department of Chemistry
Faculty of Science
Osaka University
Kita-ku, Osaka

Studies on the Thiocarbamoylthiocarbonates. II. Synthesis and Thermal Decomposition of Aryl Thiocarbamoyltrithiocarbonates

By Aritsune KAJI

(Received November 24, 1960)

The syntheses and characteristics of *N*, *N*-disubstituted *O*-aryl *S*-thiocarbamoyldithiocarbonates have been reported previously[1]. Aryl esters of *N*, *N*-disubstituted thiocarbamoyltrithiocarbonic acid were also synthesized by the reaction of aryl chlorodithioformates with sodium or ammonium salts of *N*, *N*-disubstituted dithiocarbamic acid as shown in Eq. 1.

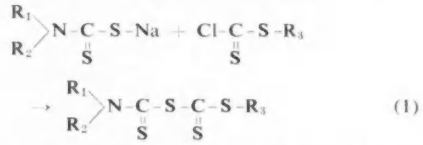

(1)

In this way, various compounds were obtained in good yields as shown in Tables I—IV.

N-Monosubstituted aryl thiocarbamoyltrithiocarbonates could not be obtained, however, by this method, owing to their probable decomposition during the reaction.

As has been described in the previous paper[1], aryl ester of *N*, *N*-disubstituted *S*-thiocarbamoyldithiocarbonic acid, when kept at a temperature higher than its melting point, decomposes into *N*, *N*-disubstituted *O*-aryl thionocarbamate liberating carbon disulfide (Eq. 2).

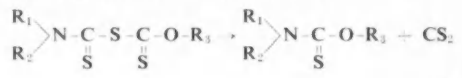

(2)

It is easily seen that two ways are possible to eliminate carbon disulfide, which can be shown in Eqs. 3 and 4.

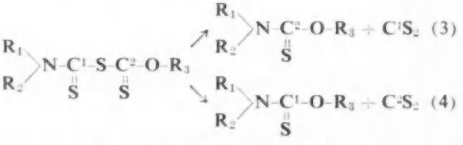

In order to decide the preferable course of the elimination reaction, the thermal decomposition of the compounds labeled with radioactive sulfur was studied. By the thermal decomposition of *O*-(4-tolyl) *S*-(*N*, *N*-dimethylthiocarbamoyl)dithiocarbonate (I), in which

1) A. Kaji, This Bulletin, 34, 254 (1961).

TABLE I. ARYL *N,N*-DIALKYLTHIOCARBAMOYLTRITHIOCARBONATES

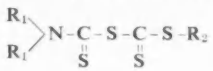

R_1	R_2	Appearance	M. p., °C	Yield %	Formula	Anal. C, % Found (calcd.)	Anal. H, % Found (calcd.)
Methyl	Phenyl	Orange prisms	134 ~134.5	87	$C_{10}H_{11}NS_4$	44.50 (43.96)	4.06 (4.03)
Methyl	2-Tolyl	Orange prisms	80 ~ 81	75	$C_{11}H_{13}NS_4$	46.60 (45.99)	4.35 (4.53)
Methyl	4-Tolyl	Orange needles	107 ~108	87	$C_{11}H_{13}NS_4$	46.47 (45.99)	4.99 (4.53)
Methyl	2-Chlorophenyl	Orange pillars	93 ~ 94	65	$C_{10}H_{10}ClNS_4$	39.45 (39.02)	3.35 (3.25)
Methyl	4-Chlorophenyl	Orange prisms	104 ~105	81	$C_{10}H_{10}ClNS_4$	39.45 (39.02)	3.21 (3.25)
Methyl	2,4,5-Trichlorophenyl	Orange prisms	112 ~112.5	94	$C_{10}H_8Cl_3NS_4$	32.08 (31.87)	2.18 (2.12)
Methyl	1-Naphthyl	Orange prisms	97 ~ 98	58	$C_{14}H_{13}NS_4$	52.30 (52.01)	4.05 (4.02)
Ethyl	Phenyl	Orange needles	68.5~ 69.5	75	$C_{11}H_{15}NS_4$	47.95 (47.84)	5.05 (4.98)
Ethyl	4-Chlorophenyl	Orange needles	72 ~ 73	64	$C_{12}H_{14}ClNS_4$	42.50 (42.92)	4.21 (4.17)
Ethyl	2,4,5-Trichlorophenyl	Orange needles	129 ~130	70	$C_{12}H_{12}Cl_3NS_4$	35.85 (35.60)	2.94 (2.97)
Ethyl	Pentachlorophenyl	Orange prisms	121 ~122	68	$C_{12}H_{10}Cl_5NS_4$	30.93 (30.80)	2.46 (2.14)
Ethyl	4-Tolyl	Orange needles	66 ~ 67	60	$C_{13}H_{17}NS_4$	49.42 (49.52)	5.64 (5.40)

TABLE II. ARYL PIPERIDINOTHIOCARBONYLTRITHIOCARBONATES

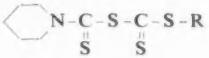

R	Appearance	M. p., °C	Yield, %	Formular	Anal. C, % Found (calcd.)	Anal. H, % Found (calcd.)
Phenyl	Orange prisms	76.5~ 77	60	$C_{13}H_{15}NS_4$	49.75 (49.84)	5.13 (4.79)
4-Tolyl	Orange prisms	108 ~110	71.5	$C_{14}H_{17}NS_4$	51.62 (51.68)	5.12 (5.20)
4-Chlorophenyl	Orange prisms	135 ~136	86	$C_{13}H_{14}ClNS_4$	45.37 (44.92)	4.10 (4.03)

TABLE III. ARYL MORPHOLINOTHIOCARBONYLTRITHIOCARBONATES

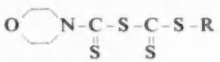

R	Appearance	M. p., °C	Yield, %	Formular	Anal. C, % Found (calcd.)	Anal. H, % Found (calcd.)
2-Tolyl	Yellow prisms	104 ~105	63	$C_{13}H_{15}NOS_4$	47.30 (47.42)	4.48 (4.56)
4-Tolyl	Orange prisms	122 ~123	67.5	$C_{13}H_{15}NOS_4$	47.57 (47.42)	4.84 (4.56)
2-Chlorophenyl	Orange prisms	114.5~115.5	67	$C_{12}H_{12}ClNOS_4$	41.45 (41.20)	3.77 (3.43)
2,4,5-Trichlorophenyl	Orange prisms	142 ~143	86	$C_{12}H_{10}Cl_3NOS_4$	34.85 (34.41)	2.49 (2.39)

TABLE IV. ARYL ARYLTHIOCARBAMOYLTRITHIOCARBONATES

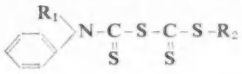

R_1	R_2	Appearance	M. p., °C	Yield %	Formula	Anal. C, % Found (calcd.)	Anal. H, % Found (calcd.)
Methyl	4-Tolyl	Orange prisms	98 ~ 99	86	$C_{15}H_{13}NS_4$	54.88 (55.01)	4.50 (4.30)
Methyl	4-Chlorophenyl	Orange prisms	87 ~ 88	74	$C_{15}H_{12}ClNS_4$	48.90 (48.71)	2.87 (3.25)
Phenyl	4-Tolyl	Orange plates	101 ~102	65	$C_{21}H_{17}NS_4$	60.70 (61.31)	4.22 (4.14)
Phenyl	4-Chlorophenyl	Orange prisms	125.5~126.5	54	$C_{20}H_{14}ClNS_4$	55.95 (55.62)	3.30 (3.24)

TABLE V. ARYL *N,N*-DISUBSTITUTED-DITHIOCARBAMATES

R_1	R_2	Appearance	M. p., °C	Yield %	Formula	Anal. C, % Found (calcd.)	Anal. H, % Found (calcd.)
Methyl	4-Tolyl	Colorless prisms	112~113	77.5	$C_{10}H_{13}NS_2$	56.71 (56.87)	6.21 (6.16)
Methyl	4-Chlorophenyl	Colorless needles	101~103	82	$C_9H_{10}ClNS_2$	47.15 (46.65)	4.13 (4.32)
Phenyl	4-Tolyl	Colorless needles	132~133	76	$C_{15}H_{15}NS_2$	66.25 (65.93)	5.38 (5.49)
Phenyl	4-Chlorophenyl	Colorless lozenges	147~149	80.5	$C_{14}H_{12}ClNS_2$	57.56 (57.24)	4.12 (4.07)

two S atoms in the thiocarbamoylthio group were labeled with $^{35}_{16}S$, radio-active *O*-(4-tolyl) *N,N*-dimethylthionocarbamate (II) was produced. The relative activity of II against I was found to be 0.2625, while the theoretical value, based on Eq. 5 should be zero, and based on Eq. 6, it should be 0.5000.

But this result may be explained if one postulates that the two courses of decomposition (Eqs. 5 and 6) occur simultaneously at the rate of 47.5 : 52.5.

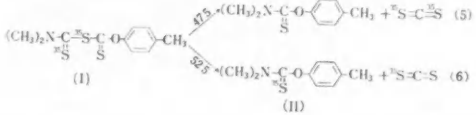

N,N-Disubstituted aryl thiocarbamoyltrithiocarbonates were found to decompose, when kept at temperatures higher than their melting points, into *N,N*-disubstituted aryl dithiocarbamates liberating carbon disulfide. The crystalline decomposition products of some trithiocarbonates are listed in Table V.

By the thermal decomposition of *S*-(4-tolyl) *S*-(*N,N*-dimethylthiocarbamoyl) trithiocarbonate (III) in which the two S atoms were labeled with $^{35}_{16}S$ similarly as in the case of I, radio-active 4-tolyl *N,N*-dimethyldithiocarbamate (IV) was given. But the relative activity of IV against III was found to be 0.3305. Thus the proportion of the two courses was concluded to be 33.9 : 66.1 (Eqs. 7 and 8) in this case.

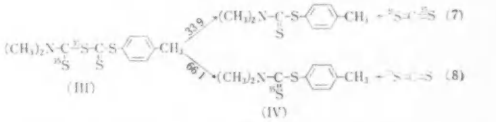

These facts show that the two courses of decomposition can occur simultaneously, but the rate of their occurrence is strongly influenced by substituting O atom with S atom.

To discover what influences would appear when another one of the S atoms was substituted with an O atom, the thermal decomposition of the compounds containing $>C^2=O$ in place of $>C^2=S$ (cf. Eqs. 3 and 4) was studied. This could produce carbon disulfide if the reaction occurred as Eq. 3, or carbon oxysulfide if the reaction followed Eq. 4. By the thermal decomposition of V and VI, both carbon disulfide

and carbon oxysulfide were evolved as decomposition fragments in each case (cf. Eqs. 9—12). Also, the volume rates of CS_2 : COS were found to be 99.5 : 0.5 and 89 : 11 respectively, by gas-chromatographic analyses of the above fragments.

These results show that the proportions of the two courses in each case should be 99.5 : 0.5 (Eqs. 9 and 10), and 89 : 11 (Eqs. 11 and 12).

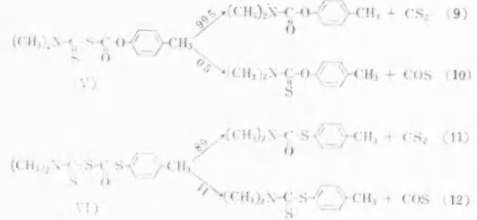

These results show that the proportion of the occurrence of reaction 13 against reaction 14 increases according to the variation of X and Y to S or O atom as follows.

X Y O>X S, Y O>X O, Y S>X Y S

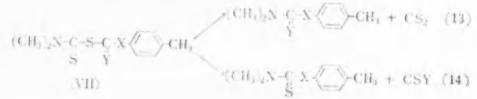

Summarizing the decomposition reactions mentioned above, it may be concluded that there are two reaction mechanisms on the thermal decomposition reaction of *N*, *N*-disubstituted aryl thiocarbamoylthiocarbonates, which can be written as follows.

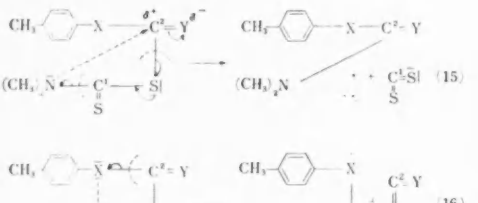

(X, Y : O and/or S)

Reaction 15 occurs by co-ordination of $(C^2)^+$ to $\overline{N}$, and reaction 16, by co-ordination of $(C^1)^+$ to $\overline{X}$. The electron density on C^2 and electro-negativity of –X–, which vary according to the variation of X and Y to S or O atom, may have some influence on the reaction courses.

By comparison of the electron densities on C^1 in $>N-C^1=S$ and C^2 in $-X-C^2=Y$, when both X and Y are O atoms, the electron density on C^2 is far smaller than that on C^1, owing to the greater polarization of $>C=O$ than that of $>C=S$ and greater electro-negativity of –O– than that of –S–. Thus reaction 15 may occur almost exclusively in this case. When X is an S atom, however, the electron density on C^2 increases, for the electro-negativity of –X– becomes smaller owing to replacement of O atom by S atom. This will make not only the co-ordination of $(C^2)^+$ to $\overline{N}$ unfavorable, but also the co-ordination of $(C^1)^+$ to $\overline{X}$ favorable. Thus reaction 16 may occur to some extent in this case. When Y is an S atom, the difference of the electron densities on C^1 and on C^2, due to the respective polarity of $>C=Y$ and $>C=S$, will disappear. Thus the two sorts of co-ordination become concurrent. When X is also an S atom, reaction 16 occurs most easily for the reasons mentioned above.

These situations may explain the relationships between the mechanisms of thermal decomposition of the compounds VII and their structures.

Experimental

Starting Materials.—Sodium or ammonium salts of *N*, *N*-disubstituted-dithiocarbamic acid were synthesized by the known methods[1]. Aryl esters of chlorodithioformic acid were synthesized similarly to aryl chlorothionoformates which were previously reported[1], by the reaction of thiophosgen, thicphenol and sodium hydroxide.

4-Tolyl *N*, *N*-Dimethylthiocarbamoyltrithiocarbonate.—To a solution of 14.3 g. (0.1 mol.) of sodium dimethyldithiocarbamate in 100 cc. of water, was added gradually 20.3 g. (0.1 mol.) of 4-tolyl chlorodithioformate, keeping the temperature at 10~15°C during the reaction period of 2 hr. The reaction mixture produced 25 g. (yield, 87%) of orange crystals with m. p. 105~106°C. Recrystallization from acetone-ethanol gave orange needles of m. p. 107~108°C.

4-Tolyl *N*-Methyl-*N*-phenylthiocarbamoyltrithiocarbonate.—To a suspension of 20 g. (0.1 mol.) of ammonium *N*-methyl-*N*-phenyldithiocarbamate in 100 cc. of acetone, was added gradually 20.3 g. (0.1 mol.) of 4-tolyl chlorodithioformate, keeping the temperature at 5~10°C during the reaction period of 1 hr. The reaction mixture poured into 200 cc. of cold water produced 30 g. (yield, 86%) of orange crystals with m. p. 96~99°C. Recrystallization from acetone-ethanol gave orange prisms with m. p. 98~99°C.

The other esters shown in Tables I—IV were synthesized similarly to the synthesis of the above examples.

***S*-(4-Tolyl) *S*-(*N*, *N*-Dimethylthiocarbamoyl)dithiocarbonate (VI).**—This could also be synthesized in a similar way, by reacting 27.1 g. (0.1 mol.) of *S*-(4-tolyl) chlorothiolformate with 14.3 g. (0.1 mol.) of sodium dimethyldithiocarbamete in 150 cc. of acetone. Yield : 27.8%; Yellow needles of m. p. 69~70°C.

Found: C, 48.66; H, 4.72; N, 5.33. Calcd. for $C_{11}H_{13}NOS_2$: C, 48.71; H, 4.80; N, 5.17%.

Thermal Decomposition of V and VI. — In a sealed flask (1000 cc. in volume) which was filled with nitrogen gas at 10 mmHg., 2 g. of V or VI was fused at 160°C for 1 hr. After the subsidence of evolution of gas, nitrogen gas was led into the flask until the pressure became 760 mmHg. Further, the ratio of carbon oxysulfied and carbon disulfide, in the gas obtained, was measured by gas-chromatography (column: tricresyl phosphate, at 42.5°C; carrier: H_2).

Thermal Decomposition of Radio-active 4-Tolyl *N*, *N*-Dimethylthiocarbamoyltrithiocarbonate (III). —In an oil bath, 0.575 g. of III (specific activity: 47.84 mc./mol.), synthesized by the reaction between 4-tolyl chlorodithioformate and radio-active sodium *N*, *N*-dimethyldithiocarbamate in which the two S atoms were labeled with $^{35}_{16}S$, was fused at 160°C for 1 hr. in nitrogen atmosphere of 10 mmHg. After the subsidence of evolution of radio-active carbon disulfide, the decomposition product was twice recrystallized from 2.4 cc. of ethanol and produced 0.327 g. (yield, 77.5%) of radio-active 4-tolyl *N*, *N*-dimethyldithiocarbamate (VI), of which the specific activity was 15.81 mc./mol. with m. p. 112~113°C. The relative specific activity of VI against III was 0.3305 (=15.81/47.84).

By the thermal decomposition of radio-active *O*-(4-tolyl) *S*-(*N*, *N*-dimethylthiocarbamoyl)dithiocarbonate (I) (specific activity: 23.85 mc./mol.), radio-active *O*-(4-tolyl) *N*, *N*-dimethylthionocarbamate (II) (specific activity: 6.26 mc./mol.) was produced in a similar way. Thus the relative activity of II against I was 0.2625.

The author wishes to express his sincere thanks to Professor Dr. Ryozo Goto, Kyoto University, for his guidance and encouragement throughout this work. The author also thanks Professor Dr. Hiroshi Watanabe, Konan University, for his helpful advice. He is also grateful to Dr. N. Oda, Mr. M. Kubo, Mr. K. Norishima, Mr. G. Tsuchihashi, Mr. S. Ono and Mr. A. Nomura for gas-chromatographic and elemental analyses, to Dr. K. Taniguchi for his guidance, and to Mr. K. Miyazaki, Mr. K. Hashimoto and Mr. Y. Aoki for their assistance with the experimental work.

Takaoka Factory, Nippon Soda Co., Ltd.
Mukaino-honmachi, Takaoka, Toyama

Benzylideneaniline. III. Anils of Substituted Benzaldehydes

By Nozomu Ebara

(Received January 21, 1961)

In the first paper of this series[1] a non-planar structure was proposed for benzylideneaniline, where the benzene ring of aniline part is almost perpendicular to the rest of the molecule (Fig. 1). In such a case the ultraviolet absorption spectrum of this molecule would be closely allied to those of benzaldehyde type I and aniline type II molecular halves, and it was assumed that the absorption maxima at 263 mμ (A) and at 315 mμ (B) is due to I and II respectively. The effects of substituents upon these bands were examined and it was found that the substituents on II had little to do with band A, whereas marked shifts were experienced by band B.

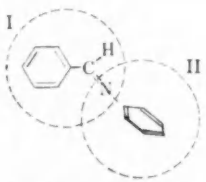

Fig. 1. Assumed structure of benzylideneaniline.

In the present paper, derivatives of benzylideneaniline of which the substituents are on aldehyde ring I, together with anils bearing aliphatic halves, were synthesized and their spectral features as well as other properties were examined.

Ultraviolet Absorption Spectra. —Ultraviolet absorption spectra of anils were measured in *n*-heptane, ethyl alcohol and 50% mixture of hydrochloric acid and ethyl alcohol. The spectra in *n*-heptane are illustrated in Fig. 2 and pertinent data are listed in Table I.

Bands A.—Bands A shift markedly as substituents vary, in contrast to the case where the substituents are on II. Moreover, they shift furthermore towards longer wavelengths when alcohol is used as solvent. In acidic

1) N. Ebara, This Bulletin, 33, 534 (1960).

Table I. Wavelengths of UV absorption maxima

(in Å)

R	Solvent			Crystal state	in	in	in
	C_7H_{16}	C_2H_5OH	HCl+ C_2H_5OH		C_2H_5OH (above 3000 Å)	C_2H_5OH	C_7H_{16}
p-OH	2750 3150	(2950) 3140			—	2815	
p-OCH_3	2790 3150	(2790) 3030		2800 3250	—	2765	2680
o-OH	2680 3010 3180 3415	2700 2990 3160 3360	2570 3240	3100～3500	3280	2540 3244	2540 2590 3170
o-OCH_3	2650 3220	2660 3280			3200?	2528 3210	
p-NO_2	2860 3130 3420	2910 3180	2340 (3500)		—		
p-NMe_2	3000 3100 3200 3270	3430	2430 2815 (3500)		—	3420	3390
p-Cl	2680 3180	2685 3150	2590 2900 (3480)		—		
m-NO_2	2550 3220	2580 3180	2340 (3480)		—		
m,*m*'-$(NO_2)_2$	2550 3160	2590 3200	2640 3180 (3670)				

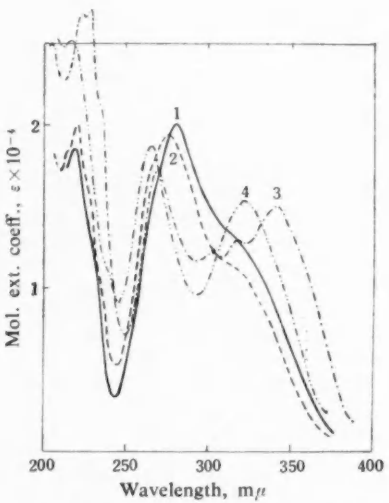

Fig. 2(A). Spectra of anils in *n*-heptane.

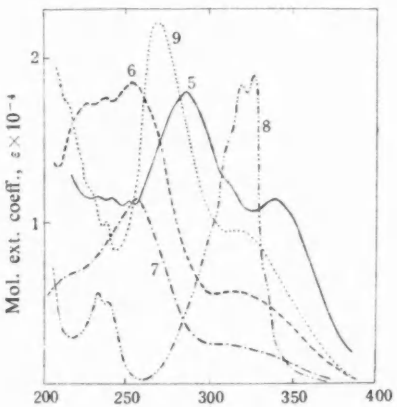

Fig. 2(B). Spectra of anils in *n*-heptane:

R= 1) *p*-OH; 2) *p*-OCH_3; 3) *o*-OH; 4) *o*-OCH_3; 5) *p*-NO_2; 6) *m*-NO_2; 7) *m*,*m*'-diNO_2; 8) *p*-$N(CH_3)_2$; 9) *p*-Cl;
(Intensities of 3 and 7 are in arbitrary unit and that of 8 in half scale).

medium, the blue shift is again observed with these bands as in the former case[1], but their maxima are by no means at the same position, but vary in a manner similar to those of corresponding anils and aldehydes. These facts are in good accordance with the above proposal that band A is largely of the nature of CT band of I.

Bands B.—Unfortunately the behavior of bands B is not quite obvious as anils bearing the electron-donating groups at the ortho position of I exhibit the expected maxima of enhanced intensities at the longer wavelength region (presumably the second CT bands[2] from I) and the positions of bands B become obscure. But in cases where they are observable, they are in general almost at the same position. It is perplexing, however, that substitution at the para position of I by NO_2 group also gives rise to a new band at the longer wavelength region, of which the explanation is not yet deduced.

There remains another discrepancy as to the intensities of bands B, which are too much enhanced to be largely of the nature of A_1-B_2 transition of II.

Comparison with the Anils Bearing Aliphatic Halves.—Benzylidene-*n*-butylamine, anisylideneisopropylamine, *p*-dimethylaminobenzylideneisopropylamine, salicylideneisopropylamine and *n*-butylideneaniline were synthesized and their spectra were measured (Fig. 3).

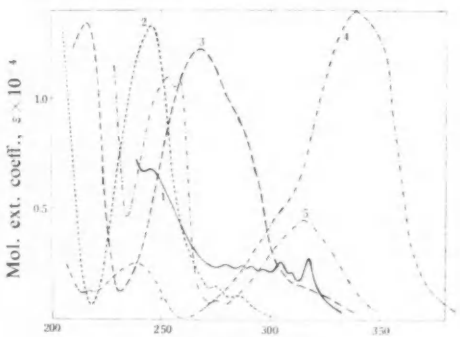

Fig. 3. Spectra of aliphatic anils in *n*-heptane:
1) ;
2) $CH_3CH_2CH_2CH_2N{=}CH-C_6H_5$;
3) $(CH_3)_2CHN{=}CH-C_6H_4-OCH_3$;
4) $(CH_3)_2CHN{=}CH-C_6H_4-N(CH_3)_2$;
5) 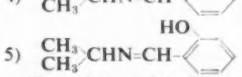
(Intensity of 4 is in half scale).

Anils of aliphatic amines and aromatic aldehydes exhibit intense bands in the proximity of those of aldehydes, which may therefore be correlated to bands A of aromatic anils. Bands B vanish completely in these anils.

n-Butylideneaniline shows an intense band at 2470 Å and a weak one with a structure between 2820 and 3200 Å, which should correspond to those of aniline. The position of the latter band coincides almost exactly with band B of benzylideneaniline, although their intensities differ considerably. It is not certain whether *n*-butylideneaniline assumes benzaldehyde type or aniline type structure (presumably, the former), but apart from this, it may be concluded that $A_{1g}-B_{2u}$ transition of benzene at 2600 Å rises to this position in the presence of the perturbation of R-CH=N- and that this band shifts no more towards longer wavelengths when R turns from aliphatic to aromatic groups.

Therefore, no substantial difference seems to exist between the spectra of aliphatic and aromatic anils.

Spectra of *N*-Methylated and Protonated Anils.—Similar spectra are observed with *N*-methylated anils and with *N*-protonated anils. Bands B vanish completely, whereas bands A shift towards shorter wavelengths: the explanation of the latter phenomenon was given tentatively in terms of hybridization change in the previous paper[1].

No anils giving rise to second CT bands of I miss these bands when they are methylated or protonated.

***p*-Hydroxybenzylidene- and Anisylideneaniline.**—Striking are the features of the spectra of

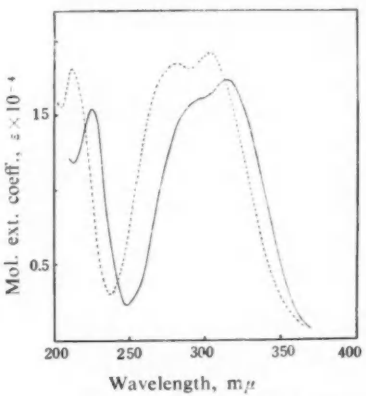

Fig. 4. Spectra of 1) 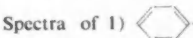 and 2) 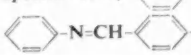 in C_2H_5OH.

2) J. Tanaka and S. Nagakura, *J. Chem. Soc. Japan, Pure Chem. Sec.* (*Nippon Kagaku Zasshi*), **78**, 1200 (1957).

p-hydroxybenzylidene- and anisylideneaniline, where the spectra are very greatly different in alcohol as compared with those in *n*-heptane, the latter exhibiting the ordinary shape of anils (Fig. 4). In contrast to this, the spectra of anils bearing these substituents on II are free from any remarkable solvent effect. It seems plausible to assume that the bands A at 2750 Å and at 2790 Å of these compounds in *n*-heptane, presumably the CT band of I, shift to 3140 and 3030 Å in alcohol, respectively, owing to the pronounced stabilization of the solvated excited states where there are large resonance polarizations due to strongly electron-donating substituents at the para positions. These molecules decompose very quickly in alcohol, as will be described in a following section, and the bands near 2800~2900 Å may be attributed to the inevitably present decomposition products.

Salicylidene- and *o*-Methoxybenzylideneaniline. Another peculiar feature is that of salicylideneaniline, where three bands are observed above 3010 Å, which are too conspicuous to be the vibrational structure. It had been reported that strong hydrogen bonding exists between hydroxyl hydrogen and azomethine nitrogen atoms[3], and that this would be responsible for the unusual spectrum of this molecule[4]. But it is highly improbable that a hydrogen bonding would cause such a large variation in the spectrum as the appearance of new bands.

In phenylazonaphthol a tautomerism is known to exist between azo and hydrazone forms[5], whereas *o*-hydroxyazobenzene does not exhibit this tautomerism[6]. To see whether this is the case or not with salicylideneaniline, and to examine whether or not some of these bands correspond to the tautomeric enamine form, the temperature dependence of the ultraviolet absorption spectrum was examined. The

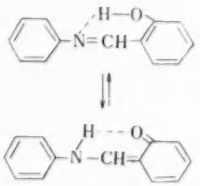

spectrum was measured at several temperatures between −60 and 47°C, but no remarkable change was observed except for the ordinary sharpening and broadening of the peaks accompanying the temperature change. The infrared spectrum was also examined in carbon tetrachloride solution and in solid state, but there was observed no band attributable to C=O stretching vibrational mode. Moreover the spectra in the solution and in the solid state resemble each other very closely, indicating that the molecular structure is not so greatly different in these two states, and that there seemes to exist no tautomeric equilibrium between the above two structures. The shift of C=N stretching vibration from that of unsubstituted benzylideneaniline is considerably great as compared with other anils where the shifts are at most within a few cm^{-1} (Table II). OH stretching vibration is hidden under the lower frequency side of CH stretching vibration. Deuterated salicylideneaniline was synthesized. This gives rise to a very broad band between 2020~2180 cm^{-1}, doubtless attributable to OD stretching vibration, from which the position of the original OH band is calculated to lie between 2800~3000 cm^{-1}, showing an unusual shift towards lower frequencies.

TABLE II. WAVE NUMBERS OF C=N STRETCHING VIBRATIONS

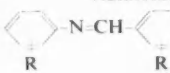

in CCl_4

R	R'	Wave number, cm^{-1}
H	H	1629
p-OCH_3	H	1626
o-Cl	H	1630
m-Cl	H	1631
p-Cl	H	1628
m-NO_2	H	1631
H	*p*-OCH_3	1624
H	*o*-OCH_3	1620
H	*m*-NO_2	1629
H	*p*-NO_2	1629
H	*o*-OH	1616

Presumably a large resonance coupling would exist between azomethine and enamine forms, the former still being predominant. The molecule may safely be referred to as existing almost exclusively in azomethine form rather than in enamine form in the solution as well as in the solid state, and the new ultraviolet absorption bands might not be ascribed to the tautomerism.

Ionization equilibrium might exist in this molecule between phenolic and phenolate structures, and some of the bands might be attributed to anion form. But this seems also not to be the case, as the change of solvent, as well as of temperature, proves no evidence of the noticeable variation in the ionization constant. Moreover, in alkaline solution, the

3) e. g., L. Kahovec and K. W. Kohlrausch, *Zeitschr. phys. Chem.*, (B) **38**, 119 (1938).
4) A. von Kiss and G. Auer, ibid., (A) **189**, 344 (1941).
5) e. g., A. Burawoy and I. Markowitsch, *Ann.*, **503**, 180 (1933).
6) e. g., D. Hadži. *J. Chem. Soc.*, **1956**, 2143.

bands above 3010 Å disappear and a new band comes out at 3800 Å, which is raised too much to be led back to any of the bands of salicylideneaniline.

It turns out that an intense band exists at 3220 Å in the spectrum of *o*-methoxybenzylideneaniline. This is all but congruent with that at 3210 Å of *o*-methoxybenzaldehyde and is presumably the second CT band of I. Salicylaldehyde, salicylaldoxime[7], salicylaldimine[7] and bis-salicylidene-ethylenediamine[8] as well as *N*-methyl-salicylideneanilinium ion exhibit similar bands. All of these bands may demand their replica in the spectrum of salicylideneaniline: the band at 3415 Å is the most adequate for this, though it is conflicting that this band experiences the blue shift when alcohol is used as solvent.

One of the other two bands at 3010 and 3180 Å, preferably the latter, may be assigned as band B, which comes from I of the molecule.

Hydrolyzation Reaction of *p*-Hydroxybenzylidene-, Anisylidene- and *o*-Methoxybenzylideneaniline.—These three compounds decompose very quickly in alcoholic solutions. The reaction rates were found to depend upon the water content of alcohol, and would conceivably be hydrolyzation reactions. The rates of these reactions were measured at several temperatures by tracking their spectral changes, and it was found that the reactions are first-order as to the concentrations of anils in the presence of excess water. The results are shown in Table III and in Figs. 5, 6 and 7.

Table III. Hydrolyzation reaction rates in $C_2H_5OH(2)+H_2O(1)$

Temp., °C	$k\times10^2$	E, kcal./mol.	A
o-Methoxybenzylideneaniline			
31.6	9.90	7.72	1.6×10^4
26.0	7.92		
20.6	6.40		
12.0	4.40		
p-Hydroxybenzylideneaniline			
45.6	5.87	6.56	2.5×10^3
40.1	4.95		
25.85	2.97		
13.95	1.89		
Anisylideneaniline			
45.5	5.16	6.11	1.0×10^3
39.7	4.28		
24.5	2.62		
13.85	1.77		

It is probable that owing to the strongly electron-donating properties of the substituents, the addition of proton at the nitrogen atom, or conceivably the heterolytic fission of OH bond of hydrogen-bonded water at the nitrogen atom, accompanied by the addition of OH^- to the azomethine carbon atom, would proceed easily.

The activation energies are almost equal in these three cases, whereas the frequency factor is the largest in *o*-methoxybenzylideneaniline. One tentative explanation is that owing to the closely standing hydrogen-bonded *o*-methoxyl group, the chance of the reaction in which water participates is greater in this case.

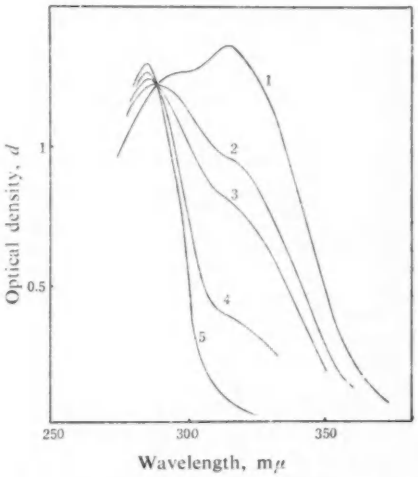

Fig. 5. Time-dependence of the spectrum of

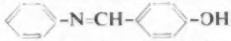

1) Immediately after dissolution;
2) After 7 min.; 3) After 10 min.;
4) After 24 min.; 5) After 4 hr.

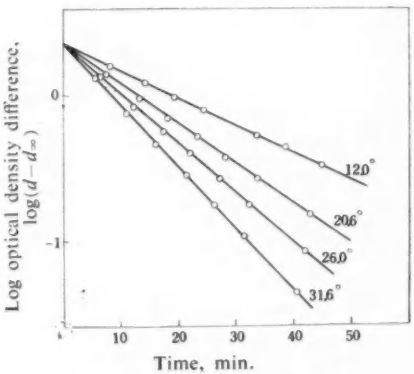

Fig. 6. Hydrolyzation reaction of

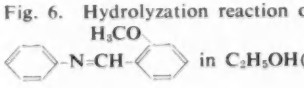

in $C_2H_5OH(2)+H_2O(1)$.

7) K. Sone, *J. Am. Chem. Soc.*, **75**, 5207 (1953).
8) L. N. Ferguson and I. Kelly, ibid., **73**, 3707 (1951).

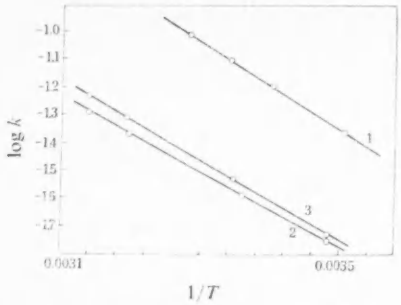

Fig. 7. Temperature dependences of

1) 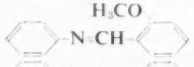

2) 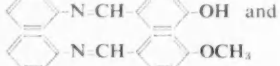

3) 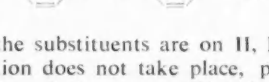

When the substituents are on II, hydrolyzation reaction does not take place, presumably because the substituents would only affect the C=N bond through the participation in the migration aptitude of nitrogen non-bonding electrons.

Spectra in the Solid States.—The spectra of benzylideneaniline, anisylideneaniline, salicylideneaniline, salicylidene-*p*-chloraniline and salicylidene-*p*-bromoaniline were measured in the solid states by means of either the potassium chloride disk method or the film method (Fig. 8). In the former three cases the spectra are very similar to those in *n*-heptane solutions, indicating that the molecular shapes are not greatly different in these two states, provided that the ignorance of the effect due to the orientation of the crystal axis may be permitted in the latter method. In the latter two cases, single peaks are always observed above 3000 Å instead of three, though their spectra in the solution are very similar to that of salicylideneaniline. It is not certain whether this is due to the variation in molecular shapes or due to the difference in crystal structures, or in turn due to the preferred orientation of crystal axis against the plates, which tends to favor the absorption band whose transition moment is perpendicular to it.

Trial Interpretation of UV Spectrum on the Basis of Planar Model.—Because of some discrepancies arising in the above consideration, the interpretation of the ultraviolet spectrum of benzylideneaniline is intended tentatively to be regarded on the basis of the planar model.

The symmetry C_{2v} may be assigned to the molecule, so far as the π electrons are concerned. In this approximation, the allowed

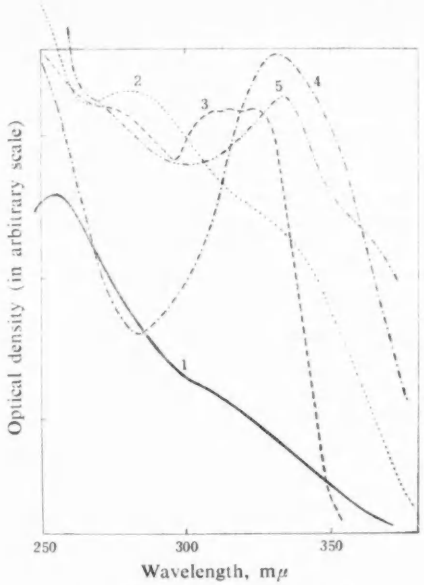

Fig. 8. Spectra in solid states,

1) 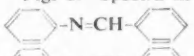

2) 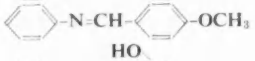

3) 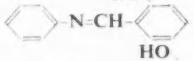

4) 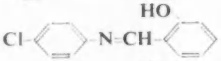

5) 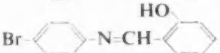

electronic transitions are A_1-A_1 and A_1-B_2 (A_1-B_1 may be excluded, because the π electronic levels are always constructed with atomic 2p orbitals).

Following the method of Nagakura and Tanaka[9], the perturbation diagram of this molecule is drawn, where the ionization potential and electron affinity of C=N group are assumed to lie between those of C=O and C=C, largely approaching the former (Fig. 9). Although the coefficients of atomic orbitals at N and C atoms in the MO of C=N group differ from each other, the resulting molecular energy level diagram might not be so far from those of stilbene and azobenzene at least in the lower region, and the lower excitations should be $\pi-\pi^*$ (or A_1-A_1) and $\pi-\phi^*$ (or A_1-B_2)[10]. The former should involve the charge transfer from two benzene rings to the

9) S. Nagakura and J. Tanaka, *J. Chem. Phys.*, **22**, 236 (1954).

10) The energy diagram is drawn by taking account of Jaffé's calculations (see Ref. 11).

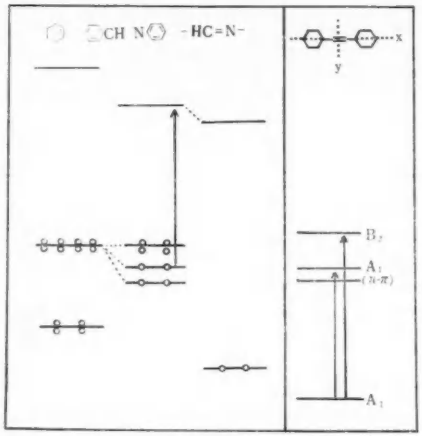

Fig. 9. Energy level diagrams of planar benzylideneaniline molecule.

central C=N part, although the mixing with other configurations would in part reduce it. The latter has much in common with benzene $A_{1g}-B_{2u}$ transition except that it becomes allowed by the perturbation. The intensity of the former should be reduced by the unsymmetrically situated central N atom and that of the latter would be much lower.

Two bands, A and B, arising in the spectrum of benzylideneaniline must be interpreted from the above standpoint. Jaffé[11] had assumed that they are $\pi-\phi^*$ and $\pi-\pi^*$, respectively.

In the present experiment, however, it was found that band A has the character of CT band, whereas band B does not, and that the nitrogen non-bonding electrons are responsible for the appearance of band B. Moreover this band is too intense to be A_1-B_2 transition. These findings go behind with Jaffé's interpretation.

An alternative interpretation in which band A is assigned as $\pi-\pi^*$ does not hold, as the energy of this transition might not be so great.

Thus, the planar model presents more discrepancies with regard to the ultraviolet spectrum of the molecule.

Conclusion

The results obtained here can be explained adequately by the non-planar model proposed in the previous paper. In particular, the coincidence in the ultraviolet spectrum seems to be excellent. But the explanation is not unique and leaves many discrepancies. It remains in doubt whether or not the failure of explaining the spectrum of this molecule with the hitherto believed planar model might be ascribed to the misestimation or ignorance of some quantities which will arise in the calculation of molecular energies.

The molecule seems to assume the same conformation in the solid state as in the solution. The X-ray crystal analysis is now in progress. This will provide indisputable information with regard to the precise conformation of benzylideneaniline molecule.

Experimental

Materials.—Benzylidene-, *p*-hydroxybenzylidene-, *p*-chlorobenzylidene-, *p*-nitrobenzylidene, *m*-nitrobenzylidene-, anisylidene-, *p*-dimethylaminobenzylidene- and salicylideneaniline were prepared by the direct condensation of aniline with corresponding aldehydes, without any dehydrating agent and were recrystallized from ethyl or isopropyl alcohol. M. p. 63, 193~194, 61~62, 90~90.5, 64.5~65, 51.5~52, 67~68 and 50~50.5°C, respectively.

o-Methoxybenzaldehyde was prepared from salicylaldehyde by methylating it with dimethyl sulfate. The distilled and crystallized aldehyde was readily submitted to condensation reaction with aniline, affording *o*-methoxybenzylideneaniline. The product was dehydrated and distilled and then recrystallized from isopropyl alcohol. M. p. 39~40°C.

Salicylidene-*p*-chloraniline and -*p*-bromaniline were synthesized by the condensation of salicylaldehyde with corresponding anilines and recrystallized from ethyl alcohol. M. p. 100 and 107°C, respectively.

n-Butylideneaniline, benzylidene-*n*-butylamine and anisylidene-, salicylidene- and *p*-dimethylaminobenzylideneisopropylamine were prepared by the following procedure. Equimolecular amounts of corresponding amines and aldehydes were put into a round-bottomed flask equipped with a good condenser. Vigorous reaction took place and water was separated out. The mixture was heated on a water bath for about one hour, then shaken with ether, dried over calcium chloride and distilled under reduced pressure. B. p. 118°C/13 mmHg, 111°C/17 mmHg, 119~120°C/14 mmHg., 155°C/25 mmHg, respectively.

Deuterated Salicylideneaniline. — Deuterated ethyl alcohol was prepared from sodium ethoxide and deuterium oxide, and this alcohol was again used for the preparation of sodium ethoxide. The procedure was repeated so as to reduce the hydrogen content of the resulting alcohol. Salicylideneaniline was dissolved in this alcohol and the solvent was evaporated at room temperature under reduced pressure. The moisture was carefully excluded throughout the whole process.

***N*-Methylated Anils.**—Excess amounts of methyl iodide were added in the solutions of anils and they were kept standing for several hours. The absorption spectra were measured at times in order to check the degree of completion of the reaction. The intense absorbancy due to methyl iodide was compensated for, but the spectra below 3000 Å could not be measured. Another method is

11) H. H. Jaffé, Si-Jung Yeh and R. W. Gardner, *J. Molecular Spectroscopy*, 2, 120 (1958).

employed as well, in which anils were dissolved in pure methyl iodide, kept standing for a night, desiccated to dryness, dissolved in alcohol and subjected to the measurements of absorption spectra.

Measurements.—Ultraviolet spectra were measured by means of a Cary 14-type self-recording spectrophotometer using 1 cm. quartz cell. To follow the reaction rate, the spectra were measured by the use of Hitachi EPU 2-type spectrophotometer.

Hydrolyzation Reactions.—The anils were dissolved in alcohol containing one-third the amount of water, and immersed in a thermostat. The absorbances of the solutions were measured at times in the vanishing band region. The final absorbances were also measured from which a rate equation could be derived. The plotted points fell on straight lines in very good coincidence.

Infrared spectra were measured by means of Nihon-bunko self-recording spectrophotometer model 301, using sodium chloride prism and sodium chloride cells of 0.1 mm. in thickness. Solid samples were prepared by allowing the melt to cool between sodium chloride plates pressed together.

Solid samples for the ultraviolet measurements were prepared either by allowing the melt to cool between quartz plates or by pressing the mixtures of finely powdered materials with specially prepared potassium chloride crystals[12].

The author wishes to express his sincere thanks to Professor Saburo Nagakura of the University of Tokyo for his kind guidance throughout this study.

Department of Chemistry
College of General Education
The University of Tokyo
Meguro-ku, Tokyo

12) J. L. Hales and W. Kynaston, *Analyst*, **79**, 702 (1954).

*Abnormal Acceleration of the Rate of Bulk Polymerization of Styrene**

By Norio NISHIMURA

(Received November 21, 1960)

It is well known that an acceleration in rate can be observed during polymerization reactions. In the early stage of this investigation, Trommsdorff et al.[1] ascribed this phenomenon to the increase in viscosity of the reaction system. It is now currently accepted that the increase in both rate and degree of polymerization is brought about by a decrease in termination constant due to the gel effect (or Trommsdorff effect). In a viscous solution, the termination constant is affected first. Propagation and transfer reactions involving small monomer and catalyst molecules are less affected by viscosity.

There have been some investigations on the effect of viscosity on the reaction rate and the individual rate constants[1-4].

Recently, Tobolsky et al.[5] have shown that the limiting fractional conversion at infinite time of a radical initiated vinyl polymerization could be predicted from a knowledge of the kinetic rate constants under certain conditions where the gel effect does not invalidate the theory.

Experimental

Reagents.—Commercial 2,2'-azobisisobutyronitrile was recrystallized twice from ether solution m. p. 103~103.5°C. Styrene monomer was washed with 10% sodium hydroxide and then with water. After drying over calcium chloride, the monomer was distilled and stored in the dark. Just before use, it was fractionated at 25 mmHg and the middle fraction was used. Benzene was washed in turn with concentrated sulfuric acid, dilute sodium hydroxide and water. Then it was dried over calcium chloride, then over metallic sodium wire and distilled. *n*-Butanol of reagent grade was used after distillation.

Procedure.—All polymerizations were carried out in glass dilatometers, the type of which was similar to that used before[6]. After being filled with the requisite amounts of catalyst and monomer, the tubes were connected to a vacuum line and sealed off. The tubes were then held in a thermostat at 60°C.

The volume contraction of the solution was

* Presented at the Local Meeting of the Chemical Society of Japan, Hiroshima, November, 1960.

1) E. Trommsdorff, H. Köhle and P. Lagally, *Makromol. Chem.*, **1**, 169 (1948).

2) S. W. Benson and A. M. North, *J. Am. Chem. Soc.*, **81**, 1339 (1959).

3) H. Miyama, *J. Chem. Soc. Japan, Pure Chem. Sec. (Nippon Kagaku Zasshi)*, **78**, 714 (1957).

4) M. F. Vaughan, *Trans. Faraday Soc.*, **48**, 576 (1952).

5) G. V. Tobolsky, C. E. Rogers and R. D. Brickman, *J. Am. Chem. Soc.*, **82**, 1277 (1960).

6) S. Hasegawa, N. Hirai, N. Nishimura and T. Kawano, This Bulletin, **31**, 696 (1958).

followed with a travelling microscope. At high conversion where dilatometric technique could not be applied because of high viscosity, the gravimetric method was used. In order to calculate the degree of conversion from the contraction of the solution, the densities of polystyrene in the monomer (solution polymer density) and styrene monomer at 60°C were taken as 1.0563 and 0.869[7], respectively. Hence, for bulk polymerization of styrene, 100% conversion corresponds to a 17.7% contraction in volume of the original monomer.

The induction period could not be observed in every experiment. At specified times, the contents of the tubes were properly dissolved in benzene and then poured dropwise into a much greater quantity of ice-methanol. The precipitate was filtered off and dried in vacuo.

The intrinsic viscosities of the benzene solutions of polystyrene were determined at 30±0.01°C using an Ostwald viscometer. The number average degree of polymerization was estimated from the following equation[8]

$$\bar{P}_n = 1770[\eta]^{1.40}$$

In order to obtain the distribution of the degrees of polymerization at high conversion, *n*-butanol was slowly added to the benzene solution of the polymer (about 1.5%). The addition of the *n*-butanol was stopped before precipitation of the polymer appeared. By slow evaporation of the relatively volatile benzene, the solution becomes richer in less volatile *n*-butanol, and the precipitation of polystyrene results. After temperature equilibrium was attained in a thermost at 30°C, the precipitate in a gel state was separated by decantation from the solution and the same procedure was repeated. The precipitate was then dissolved again in benzene and poured into ice-methanol followed by drying in vacuo. This method is almost the same as that adopted by Chitani et al.[9]

Theoretical

Notation

M — Number of moles of monomer,
P — Number of moles of polymer,
I — Number of moles of catalyst,
f — Catalyst efficiency,
k_p — Rate constant for propagation,
k_t — Rate constant for termination,
k_d — Rate constant for the first order decomposition of catalyst,
α — Total volume shrinkage for the complete conversion of monomer to polymer,
$\bar{P}_n$ — Cumulative value for number average degree of polymerization,
$\bar{\bar{P}}_n$ — Instantaneous value for number average degree of polymerization.

It is well known that the rate of radical polymerization initiated by a catalyst is expressed as

$$-\frac{d[M]}{dt} = K[I]^{1/2}[M] \tag{1}$$

where

$$K \equiv \frac{k_p}{k_t^{1/2}} k_d^{1/2} f^{1/2} \tag{2}$$

If the decomposition rate of the catalyst is of the first order with respect to its concentration, then the conversion x at time t may be expressed by

$$x = 1 - \exp\{A(e^{-(1/2)k_d t} - 1)\} \tag{3}$$

where

$$A \equiv \frac{2K}{k_d}[I]_0^{1/2} \tag{4}$$

The value of K can easily be obtained from the slope of the initial rate of polymerization against the square root of the catalyst concentration. From Eq. 3 it may be seen that the fractional conversion x reaches a limiting value x_∞ when $t \to \infty$.

$$x_\infty = 1 - \exp(-A) \tag{5}$$

Tobolsky[10] showed this relationship and compared it with experimental results. In the previous paper[6], which describes the polymerization of vinyl acetate in the benzoyl peroxide-iron(II)-benzoin redox system, the same concept of the limiting conversion was proposed by us. Later Tobolsky et al.[5] proposed a modified form of the kinetic expressions. The equations derived above have not been corrected for a net volume shrinkage of the system. If the volume shrinkage is taken into account, then the effective monomer and catalyst concentrations are

$$[M] = \frac{[M]_0}{(1-\alpha x)}(1-x) \tag{6}$$

$$[I] = \frac{[I]_0}{(1-\alpha x)} e^{-k_d t} \tag{7}$$

respectively. From Eqs. 1, 6 and 7, one obtains

$$\frac{(1-\alpha x)^{3/2}}{(1-x)} dx = K[I]_0^{1/2} e^{-(1/2)k_d t} \cdot dt \tag{8}$$

Integration of Eq. 8 leads to

$$\frac{2}{3}y^3 + 2a^2 y + a^3 \ln\frac{(y-a)}{(y+a)} = Ae^{-(1/2)k_d t} + C \tag{9}$$

where

$$\left.\begin{aligned} C &\equiv \frac{2}{3} + 2a^2 + a^3 \ln\frac{(1-a)}{(1+a)} - A \\ y &\equiv (1-\alpha x)^{1/2}; \quad a \equiv (1-\alpha)^{1/2} \end{aligned}\right\} \tag{10}$$

7) M. S. Matheson, E. E. Auer, E. B. Bevilacqua and E. T. Hart, *J. Am. Chem. Soc.*, **73**, 1700 (1951).
8) D. H. Johnson and A. V. Tobolsky, ibid., **74**, 938 (1952).
9) T. Chitani, G. Meshitsuka and Y. Matsui, *High Polym. Chem.* (*Kobunshi Kagaku*), **10**, 175 (1953).
10) A. V. Tobolsky, *J. Am. Chem. Soc.*, **80**, 5927 (1958).

Eqs. 8 and 9 are somewhat different from the similar expressions derived by Tobolsky et al.[5]

It is rather complex to calculate the limiting conversion x_∞ from Eq. 9. But if the corresponding value of y is expressed by y_∞, then from Eq. 9,

$$Z \equiv \frac{2}{3}(y^3 - y_\infty^3) + 2a^2(y - y_\infty) + a^3 \ln \frac{(y-a)(y_\infty + a)}{(y+a)(y_\infty - a)} = Ae^{-(1/2)k_d t} \quad (11)$$

or taking the logarithm,

$$\ln Z = \ln A - \frac{1}{2} k_d t \quad (12)$$

Therefore, if the values of K and k_d are accurately known, it is possible to draw an $x \sim t$ curve over the whole course of polymerization and compare it with the experimental curve. And if a deviation between them is seen, it might be explained as indicative of a change in circumstance such as gel formation. In a case where no such deviation occurs, one can obtain K and k_d directly by applying Eq. 12. In Eq. 12, if $\ln Z$ is plotted against time t, a straight line should be obtained and the slope and the intercept will give $(1/2)k_d$ and $\ln A$, respectively.

The number average degrees of polymerization of a polymer instantaneously formed and cumulatively formed are related to each other by Eq. 13.

$$\bar{\bar{P}}_n = \frac{\bar{P}_n}{1 - \dfrac{x}{P_n} \cdot \dfrac{dP_n}{dx}} \quad (13)$$

Applying Eq. 13, one can calculate $\bar{\bar{P}}_n$ from the $\bar{P}_n \sim x$ curve which can be obtained experimentally. Eq. 13 was derived by Schulz et al.[11] and Wall et al.[12], independently.

It is of great interest to note that according to Eq. 13, the value of the instantaneous degree of polymerization will become infinitely large when the value of $(x/\bar{P}_n) \cdot (d\bar{P}_n/dx)$ approaches unity. So, one can tentatively refer $\bar{\bar{P}}_n \to \infty$ as a measure of gel formation.

In a bulk polymerization of vinyl monomer, if chain transfers to monomer and initiator are both neglected, $\bar{P}_n$ may be expressed as

$$\bar{P}_n = \frac{[M]_0 - [M]}{f\{[I]_0 - [I]\}} \quad (14)$$

for combination termination.

In a case where volume shrinkage can be neglected,

$$\bar{P}_n = \frac{[M]_0}{f[I]_0} \cdot \frac{x}{1 - \exp(-k_d t)} \quad (15)$$

Taking the volume shrinkage into account, it follows that

$$\bar{P}_n = \frac{[M]_0}{f[I]_0} \cdot \frac{x}{1 - \alpha x - \exp(-k_d t)} \quad (16)$$

It was pointed out by Robertson[13] that the catalyst efficiency f started to decrease rapidly as bulk polymerization proceeded in the case of styrene and methyl methacrylate. In this case, remembering that $\bar{P}_n$ is a cumulative value for the number average degree of polymerization, the catalyst efficiency f in Eq. 14 must also be a cumulative one. Then, rearranging Eq. 14 and inserting $\bar{f}$ instead of f,

$$\bar{f} = \frac{[M]_0 - [M]}{P_n([I]_0 - [I])} \quad (17)$$

The true value of f at conversion x may be expressed by

$$f = \bar{f} + x \frac{df}{dx} \quad (18)$$

It is well known that an abnormal explosive reaction is followed by an increase in the degree of polymerization. Hence, the comparison of the experimental molecular weight distribution with the theoretical one will offer interesting information.

According to rigorous kinetics, the molecular distribution for combination termination is given by[14]

$$r[M_r] = \frac{1}{2} R_i \delta^2 r \left[\left(\frac{r}{[M]_0} + \frac{1}{R_i^{1/2}\delta} \right) \exp\left\{ -\frac{R_i^{1/2}\delta}{[M]_0}(r-1) \right\} - \left(\frac{r}{[M]} + \frac{1}{R_i^{1/2}\delta} \right) \exp\left\{ -\frac{R_i^{1/2}\delta}{[M]}(r-1) \right\} \right] \quad (19)$$

where M_r is the number of moles of a polymer having r monomer nuits, δ a quantity approximated to $k_t^{1/2}/k_p$ and R_i the rate of initiation.

Results and Discussion

The bulk polymerizations of styrene catalyzed by 2, 2'-azobisisobutyronitrile were carried out at 60°C, and the fractional conversion x was

11) G. V. Schulz and G. Harborth, *Makromol. Chem.*, **1**, 106 (1947).
12) F. T. Wall and L. F. Beste, *J. Am. Chem. Soc.*, 69, 1761 (1947).
13) E. R. Robertson, *Tsans. Faraday Soc.*, **52**, 426 (1956).
14) E. F. Herrington and A. Robertson, ibid., **40**, 236 (1944); G. M. Burnett, "Mechanism of Polymer Reactions", Interscience Publishers, New York (1954), p. 106.

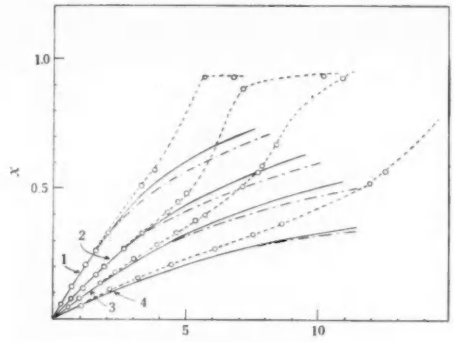

$t \times 10^{-4}$ sec.

Fig. 1. Fractional conversion x vs. t for the bulk polymerization of styrene at 60°C, using 2,2'-azobisisobutyronitrile as initiator.
--○-- experimental ——— calcd. by Eq. 9
——— by Eq. 3 $[I]_0 \times 10^2$ mol./l.: 1, 5.00; 2, 2.00; 3, 1.00; 4, 0.36

plotted against time t over the whole course of polymerization as shown in Fig. 1.

The initial rates of the reaction R_0 obtained from the figure were plotted against the square root of the initial concentrations of the catalyst, giving a straight line as expected from Eq. 1. This is shown in Fig. 2. From the slope, the value of K was found to be 0.86×10^{-4} $\text{mol}^{-(1/2)}\,l^{1/2}\,\text{sec}^{-1}$, which is in good agreement with the value obtained by Tobolsky et al.[8] The spontaneous decomposition of 2,2'-azobisisobutyronitrile has been widely studied and various values for the rate constant k_d have been reported. Using the ^{14}C labelled initiator, Bevington[15] proposed the value of $1.20 \times 10^{-5}\,\text{sec}^{-1}$ as the best. Using this value together with the above-mentioned value of K, one can calculate the whole course of the

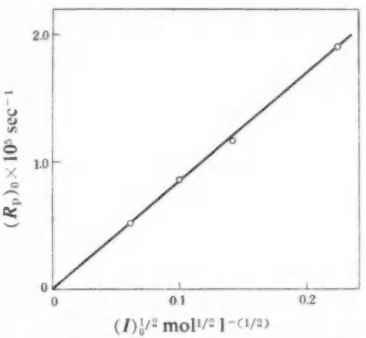

Fig. 2. Initial rate of conversion $(dx/dt)_0$ vs. $[I]_0^{1/2}$.

15) J. C. Bevington, *Trans. Faraday Soc.*, **51**, 1392 (1955).

Table I. Experimental values of x, $\bar{P}_n$ and $\bar{f}$

$[I]_0$ mol./l.	$t \times 10^{-4}$ sec.	x	$\bar{P}_n$	$\bar{f}$ (Eq. 15)	$\bar{f}$ (Eq. 16)
0.05	0.72	0.130	375	0.70	0.79
	1.80	0.297	353	0.72	0.82
	3.96	0.595	579	0.45	0.52
	5.76	0.937	1920	0.16	0.20
	6.84	0.934	1879	0.15	0.17
0.02	1.26	0.141	608	0.69	0.69
	2.70	0.274	608	0.68	0.68
	4.32	0.420	739	0.59	0.59
	7.20	0.891	2835	0.23	0.26
	10.26	0.941	3123	0.18	0.19
0.01	1.80	0.150	890	0.72	0.69
	3.24	0.249	948	0.68	0.65
	5.76	0.405	1010	0.67	0.65
	8.46	0.674	2023	0.44	0.44
	10.98	0.931	4671	0.23	0.24
0.0036	2.16	0.120	1684	0.72	0.66
	6.12	0.277	1921	0.64	0.58
	8.82	0.380	2246	0.60	0.55
	12.54	0.577	3598	0.48	0.45
	17.28	0.903	6853	0.35	0.35

Table II. Calculated values of x and $\bar{P}_n$ applying Eqs. 3 and 15*

$t \times 10^{-4}$ sec.	$[I]_0$ mol./l.	x	$\bar{P}_n$
0	0.05	0.000	382
1		0.170	359
2		0.304	340
3		0.411	324
4		0.495	310
5		0.564	298
7		0.667	280
10		0.765	261
∞		0.960	229
0	0.02	0.000	605
1		0.111	585
2		0.203	568
3		0.285	562
4		0.351	549
5		0.409	540
7		0.501	525
10		0.600	511
∞		0.869	517
0	0.01	0.000	852
1		0.080	843
2		0.149	833
3		0.210	828
4		0.263	822
5		0.309	816
7		0.388	814
10		0.475	810
∞		0.761	906
0	0.0036	0.000	1423
1		0.049	1435
2		0.093	1445
3		0.132	1447
4		0.167	1451
5		0.200	1468
7		0.255	1486
10		0.321	1520
∞		0.577	1910

* $K = 0.86 \times 10^{-4}\,\text{mol}^{-(1/2)}\,l^{1/2}\,\text{sec}^{-1}$, $k_d = 1.20 \times 10^{-5}\,\text{sec}^{-1}$ and $\bar{f} = 0.70$ was used.

polymerization by Eq. 3 or, exactly, by Eq. 9. Some experimental and calculated values of x at various times are listed in Table I and Table II, and predicted $x \sim t$ curves are also shown in Fig. 1, $\alpha = 0.177$ being used in Eq. 9.

As seen in the figure, these two calculated curves coincide with each other almost perfectly below 20% conversion, and above it, they separate gradually. At high convertion, the difference becomes fairly appreciable. Such a fact must be taken into account when polymerization, are followed by large valume shrinkage as seen in the bulk polymerization of vinyl acetate. Comparing the predicted and experimental values of x in each catalyst concentration, it seems that, at very low conversion, these values agree fairly well. In the second step, however, there appears a clear deviation between them which seems to appear at lower conversion in lower initial catalyst concentration. The accelerated polymerizations proceed almost linearly with respect to time. Then, there is a third step where the rate of the polymerization becomes explosive, and at the beginning of the step, production of gas bubbles was always seen. It made the dilatometric analysis impossible. Above 90% conversion, the viscous solution changed into hard plastic and the reaction ceased few percent less than perfect conversion. Since this anomalous rate acceleration cannot be considered as associated with change in k_d, it must be owing to change in K. The values of K at any fractional conversions can be calculated by Eq. 8, in which the slope dx/dt at x may be obtained from Fig. 1, the value of k_d being taken again as 1.20×10^{-5} sec^{-1} and as constant at any conversions. It must be noted that in deriving the values of K from Eq. 8, it was tacitly assumed that the steady state for radicals holds even at the explosive step.

Remembering that $K = k_p k_d^{1/2} f^{1/2} / k t^{1/2}$, the values of $f^{1/2} k_p / k t^{1/2}$ were plotted against x as shown in Fig. 3. The form of the curves in the figure is quite similar to one which was reported by other investigators[5,13].

From Fig. 3, it is obvious that the values of $f^{1/2} k_p / k_t^{1/2}$ are almost constant up to 20~30% conversion in every initial catalyst concentration. They increase gradually and then rapidly as x increases. It is clear that the increase in $f^{1/2} k_p / k_t^{1/2}$ occurs at lower fractional conversion the lower the initial catalyst concentration is. The reasonable explanation is as follows: As has been pointed out by some investigators, the termination constant k_t including two large growing polymer chains is first diffusion-controlled. The lower the catalyst concentration, the greater becomes the degree of polmerization and hence the viscosity of solution. If k_t is affected first, the increase

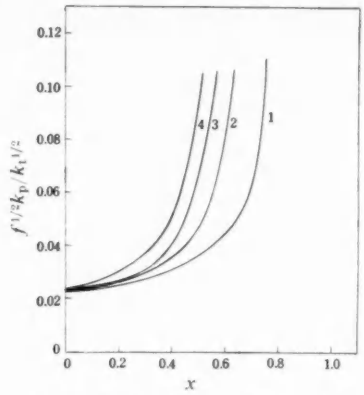

Fig. 3. $f^{1/2} k_p / k_t^{1/2}$ determined from the rate of polymerization data (Eq. 8) vs. x.
$[I]_0 \times 10^2$ mol./l.: 1, 5.00; 2, 2.00; 3, 1.00; 4, 0.36

in viscosity will result in the decrease in k_t.

The increase in $f^{1/2} k_p / k_t^{1/2}$ may also be reflected on the fact that the experimental conversions were higher than the predicted ones in each experiment with one exception. According to Eq. 5, as A and hence $f^{1/2} k_p / k_t^{1/2}$ increase, the value of x approaches unity.

The explosive polymerization is usually followed by an increase in the degree of polymerization. In the polymerization of styrene, the chain transfer to monomer is small and so, its contribution to the degree of polymerization may be neglected if catalyst concentration is properly chosen.

Since chain termination by combination is exclusive in the polymerization of styrene, the cumulative number average degree of polymerization $\bar{P}_n$ may be expressed approximately by Eq. 14. In Figs. 4 and 5, $\bar{P}_n$ is plotted against x.

Applying Eq. 14 ($f = 0.7$ was used), the theoretical plots of $\bar{P}_n$ vs. x are expressed by curves I and I' in each figure, the volume shrinkage being neglected for simplicity. As seen in the figure, the predicted value of $\bar{P}_n$ is not so much affected by the fractional conversion unless the catalyst concentration is extremely small or very large. The experimental plots of $\bar{P}_n$ vs. x which are denoted by curves II and II', show that the values of $\bar{P}_n$ in each run agree fairly well with the predicted value up to 20~30% conversion. With $[I]_0 = 0.0036$ mol./l., the deviation is the greatest. However the value of $\bar{P}_n$ increases gradually thereafter, then more rapidly toward the last.

According to Eq. 14, $\bar{P}_n$ is a function of

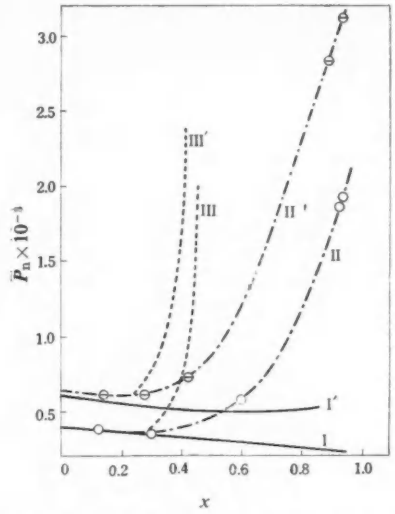

Fig. 4. Cumulative and instantaneous average degree of polymerization $\bar{P}_n$ and $\bar{\bar{P}}_n$ vs. x.
—— theoretical (Eq. 15) —·— experimental plots of $\bar{P}_n$; ---- experimental $\bar{\bar{P}}_n$ (Eq. 13)
I, II and III for $[I]_0=0.05$, I', II' and III' for $[I]_0=0.02$ mol./l., respectively

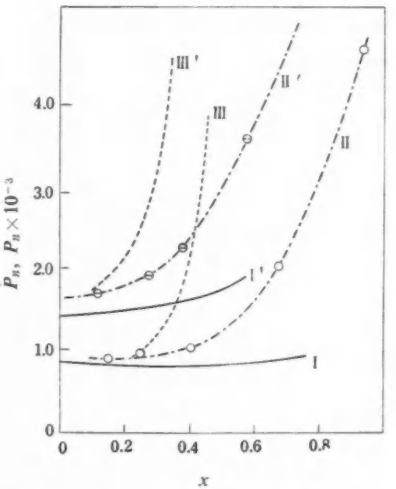

Fig. 5. Cumulative and instantaneous average degree of polymerization $\bar{P}_n$ and $\bar{\bar{P}}_n$ vs. x.
—— theoretical (Eq. 15) —·— experimental plots of $\bar{P}_n$; ---- experimental $\bar{\bar{P}}_n$ (Eq. 13)
I, II and III for $[I]_0=0.01$, I', II' and III' for $[I]_0=0.0036$ mol./l., respectively

monomer and catalyst concentrations and catalyst efficiency. Accordingly, the (cumulative) catalyst efficiency $\bar{f}$ can be obtained on inserting the experimental values of $\bar{P}_n$, $[M]$ and calculated values of $[I]$ into Eq. 17. In Table I are listed some values of $\bar{f}$ which were calculated by Eqs. 15 and 16, the volume shrinkage being taken into account in the latter equation. As may be seen in Fig. 6, the values of $\bar{f}$ are plotted against x. The average value of $\bar{f}$ at low conversion is about 0.7, which is very close to the value obtained by Tobolsky et al.[5] It is of interest to note that the catalyst efficiency $\bar{f}$ seems to depend only upon conversion and not upon the initial concentration of the catalyst. The instantaneous catalyst efficiency f which was calculated by Eq. 23 may also be seen in Fig. 6.

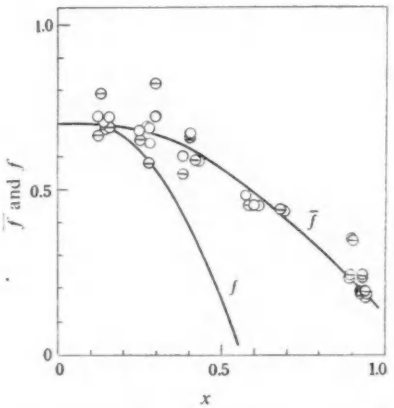

Fig. 6. Apparent dependence of cumulative and instantaneous catalyst efficiency $\bar{f}$ and f upon x.
○ calcd. by Eq. 15; ⊖ calcd. by Eq. 16

The shape of the curves is similar to but somewhat different from that obtained by Robertson[13]. This true value of catalyst efficiency at any x decreases rapidly with increasing conversion. There is a doubt as to whether or not the catalyst efficiency is much affected by change in environment such as an increase in viscosity. Since the dimensions of the catalyst and the monomer are very small compared with the dimension of the polymer, it is unlikely that those molecules suffer an effect of diffusion in such a low conversion step. Hence it is very doubtful whether the catalyst efficiency is diffusion controlled. In deriving Eq. 16, it was tacitly assumed that the chain transfer to polymer does not take place and hence each polymer produced is a long chain molecule which has two catalyst fragments at its ends. If this is not so and the chain transfer to already dead polymers might occur

considerably Eq. 16 would no more be applied. If the chain transfers to polymers occur in such a manner as to cross-link together the polymers previously formed, a rapid increase in the average degree of polymerization will result. The apparent decrease in f might be owing to this fact.

The instantaneous degree of polymerization $\bar{\bar{P}}_n$ at any conversion may be calculated by Eq. 15. In Figs. 4 and 5, $\bar{\bar{P}}_n$ is plotted against x as shown in curves III and III'. As seen in these figures, each value of $\bar{\bar{P}}_n$ increases steeply toward infinity as x increases. Above 40~50% conversion, the value of $\bar{\bar{P}}_n$ takes a negative value in each experiment.

This interesting phenomenon was first observed by Wall et al.[12] According to them, the formation of cross-linking of polymer molecules not only increases the average molecular weight, but simultaneously, diminishes the number of polymer molecules, thus accounting for the observed results. It is clear from the definition $\bar{\bar{P}}_n = -dM/dP$ that $\bar{\bar{P}}_n$ takes a negative sign when dP is negative.

On account of the fact that any polymers produced by chain reactions must have a certain dispersion of molecular sizes, the study of size distribution in polymers is of great importance in connection with the kinetic mechanisms of polymerizations. Among several experimental techniques for the fractionation of polymers, those based on solubility are most generally used. However, the fractions obtained in any experimental techniques are always heterogeneous with respect to molecular weight and, so far, the problem of the overlapping of the polymer species has never been overcome.

The fractionations of two samples were carried out in order to obtain the distribution of molecular sizes at high conversion, and the results are listed in Table III. As an approximation, the degrees of polymerization in each fraction were calculated from the data of viscosity measurements, using the relation $\bar{P}_n = 1770 [\eta]^{1.40}$ which was applied for the unfractionated polymers.

TABLE III. FRACTIONATION RESULTS OF POLYMERS

Fraction No.	Weight, g.	%	$\bar{DP}$
Unfractionated	6.000		6853
1	1.347	22.7	26980
2	0.575	9.7	11480
3	1.174	19.7	9820
4	0.369	6.2	5681
5	0.745	12.5	4142
6	1.277	21.5	2258
7	0.455	7.7	818
Unfractionated	5.523		3123
1	0.465	8.4	14090
2	0.788	14·3	8048
3	0.392	7.1	4508
4	1.279	23.2	2501
5	1.112	20.1	1183
6	1.140	20.7	652
7	0.344	6.2	242

The integral weight distribution curves were obtained by plotting the weight of each fraction as a function of the degree of polymerization, adding the weight of each fraction to the weight of the preceding fraction. The smooth lines drawn in Fig. 7 are the integral and

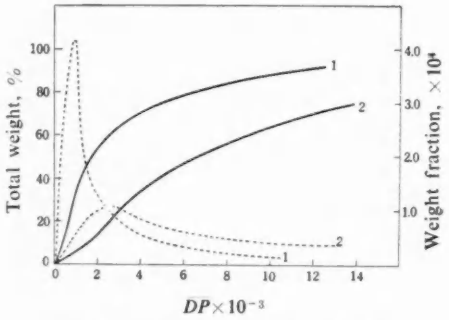

Fig. 7. Molecular weight distribution.
—— integral, ---- differental weight distributions
1: $[I]_0 = 0.02$ mol./l., $x = 0.941$, $\bar{P}_n = 3123$
2: $[I]_0 = 0.0036$ mol./l., $x = 0.903$, $\bar{P}_n = 6853$

differential weight distribution curves. The latter lines were obtained by taking the slope of the integral weight distribution curves as a function of the degree of polymerization.

It was pointed out by Guzmán[16] that this classical method of approaching the problem about molecular weight distribution is rather imperfect because there is an inevitable source of error such as the overlapping of polymer species. He compared the results obtained by the classical procedure with those obtained statistically, based on the same experimental data, and showed that there was a considerable difference between them. In spite of being more logical and reasonable, the statistical approach involves a great labor of mathematical computation and is not easy to handle.

Instead, the size distribution curves of the polymer at conversion $x = 4\%$ were drawn as shown in Fig. 8 in accordance with Eq. 21 which was derived from the kinetic mechanism of the initial polmerization step alone.

16) G. M. Guzmán, *J. Polymer Sci.*, **19**, 519 (1956).

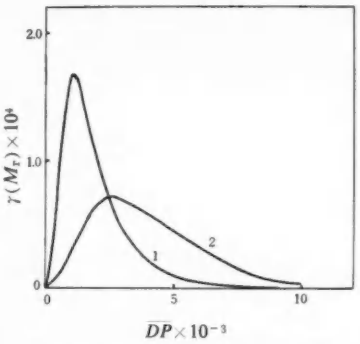

Fig. 8. Theoretical differential weight distributions (Eq. 19) at $x=0.04$.
1: $[I]_0=0.02$; 2: $[I]_0=0.0036$ mol./l.

It is clear from Figs. 7 and 8 that there is a considerable difference between experimental and calculated differential weight distributions. The shape of the corresponding curves up to the maximum weight fraction is very similar. However, beyond this, the experimental curves fall much less rapidly and unsymmetrically than do the calculated ones.

It may reasonably be assumed that the experimental molecular weight distribution consists of two parts, normal and abnormal distributions of molecular species. The part of the normal distribution may correspond to that which can be obtained from the initial stage of polymerization, while the part of the abnormal distribution may arise from the explosive polymerization. The kinetic treatment of such abnormal weight distribution may be complex. Nevertheless, it is of great interest that the result of explosive polymerization is reflected on such weight distribution.

From the study of the molecular weight distribution, it seems that the abnormal increase of the degree of polymerization at high conversion is not owing to the chain transfer to the already dead polymers, but is, probably, owing to the burying of the growing polymer radicals, because the produced polymer at high conversion involves a considerable part of low molecular weight.

Summary

The bulk polymerization of styrene initiated by 2, 2'-azobisisobutyronitrile was carried out up to high conversion at 60°C. The comparison of the experimental conversion~time data with calculated ones showed that there was a considerable deviation between them. The rate of the polymerization became explosively great toward the last.

Assuming the combination termination, the cumulative degree of polymerization was calculated and the values were compared with those obtained experimentally. The deviation at high conversion might be owing to the decrease in the catalyst efficiency as suggested by Robertson. However, the assumption that the polymer molecules have been produced only by combination is very doubtful.

The study of the molecular weight distribution suggested that the abnormal increase in the rate and the degree of polymerization seemed to be owing to the burying of the growing polymer radicals in themselves in the highly viscous solution.

The author wishes to express his thanks to Professor Shigeo Hasegawa and Professor Nishio Hirai for helpful suggestions and encouragement.

Department of Chemistry
Faculty of Science
Okayama University
Tsushima, Okayama

On the pd Hybridization of the Sulfur Atom in Thiothiophten. II. The Contraction of the d Orbital

By Kôgorô MAEDA

(Received December 27, 1960)

In the previous paper of this series[1], the pd hybridization was proposed on the central sulfur atom in thiothiophten to compose the full σ skeleton of condensed ring system of the molecule. It was shown that the above configuration of electrons on the central sulfur atom is favored in accounting for both the so-called abnormal length of the bond between two sulfur atoms and the right angle of S–S–C, and that the electronic structure of thiothiophten can be treated according to the usual LCAO π approximation without considering the σ skeleton, unlike the procedure proposed by Giacometti and Rigatti[2]. Further, the possibility of participation of the d orbital in the hybridization was examined from the standpoint of overlap criterion, giving the values of the overlap integrals. As the result of the inspection, however, it turned out that one might not except any participation of the d orbitals in bonding to occur through the hybridization. It was pointed out there that this may be due to the straightforward application of Slater's rule[3] to the estimation of the effective nuclear charges for the d orbitals. As already mentioned, since the maximum of the radial function of the d orbital with its effective nuclear charge required by Slater's rule lies at 9 atomic units, the orbital may be regarded as including the full σ skeleton of thiothiophten, so that it would be impossible to avoid the influence of the neighboring atoms in the molecule. The charges of the atoms may contract the d orbital and enlarge its nuclear charge, leading to a value of overlap integral comparable to that of 3p orbital. Contraction of this kind was once examined in the case of the d orbital in thiophene[4], where it might be expected that as the result of the contraction by the perturbation of neighboring carbon atoms, the participation of the d orbitals in bonding would take place to a greater extent than predicted by the direct application of free atom parameter by Slater's rule.

In the present paper, following the treatment about the d orbital of the sulfur atom in thiophene, the influence of neighboring atoms upon the d orbital will be examined on the central sulfur atom in thiothiophten and the possibility of the participation in the hybridization will be inquired into from the standpoint of overlap criterion, comparing the values of overlap integral.

Orbital Contraction.—A model is employed here, in which a single d electron on the central sulfur atom is supposed to move in the field of the nucleus of charge Z_S, and upon this hydrogen-like atom system a perturbation is superposed consisting of three positive charges of the neighboring atoms of thiothiophten. The positive charges come because the field of an atom capable of forming a covalent bond is substantially electron-attracting. The perturbing charges are composed of those of the two sulfur atoms of magnitude $Z_A(=Z_B)$ at the distance of S–S bond, 4.461 atomic units $(\sigma_A(=\sigma_B))$ and of the carbon atom of Z_C at the distance of central C–S, 3.440 atomic units (σ_C). These charges will be treated, not as three hydrogen-like atoms, but just as point charges of respective magnitudes. The actual potential of the perturbation is very intricate because it involves many factors, the attraction of the surrounding nuclei, the coulomb repulsions of their electrons, exchange terms, and others; hence the dependence on distance of the potential will not follow the r^{-1} law at all closely. The system being thus too complicated to be considered, the point charge model is employed as approximation in this paper. The magnitudes of the perturbing charges will be treated rather as parameters, values plausible in a wider range being involved.

Under this point charge approximation, the potential by the outlying charges may be expanded as a sum in the usual $1/r$ series[5] as follows:

For the two charges of sulfur atoms,

1) (a) K. Maeda, This Bulletin, **33**, 1466 (1960); (b) K. Maeda, ibid., **34**, 785 (1961).

2) G. Giacometti and G. Rigatti, *J. Chem. Phys.*, **30**, 1633 (1959).

3) J. C. Slater, *Phys. Rev.*, **36**, 57 (1930).

4) K. Maeda, This Bulletin, **33**, 303 (1960); The idea of orbital contraction was first given by D. P. Craig and E. A. Magnusson, *J. Chem., Soc.*, **1956**, 4895.

5) H. Eyring, J. Walter and G. E. Kimball, "Quantum Chemistry", John Wiley & Sons Inc., New York (1944), p. 369.

$$V_{A,B}(r>\sigma_A) = -(2Z_A/r)\{1+(1/2)(3\sin^2\vartheta \times\cos^2\varphi-1)(\sigma_A/r)^2+\cdots\cdots\}$$
$$V_{A,B}(r<\sigma_A) = -(2Z_A/\sigma_A)\{1+(1/2)(3\sin^2\vartheta \times\cos^2\varphi-1)(r/\sigma_A)^2+\cdots\cdots\}$$

and for the carbon atom,

$$V_C(r>\sigma_C) = -(Z_C/r)\{1+\sin\vartheta\sin\varphi\,(\sigma_C/r) +(1/2)(3\sin^2\vartheta\sin^2\varphi-1) \times(\sigma_C/r)^2+\cdots\cdots\}$$
$$V_C(r<\sigma_C) = -(Z_C/\sigma_C)\{1+\sin\vartheta\sin\varphi\,(r/\sigma_C) +(1/2)(3\sin^2\vartheta\sin^2\varphi-1) \times(r/\sigma_C)^2+\cdots\cdots\}$$

The perturbation energy due to the outlying potential is given by $\int\psi v\psi d\tau$, where ψ is the d electron wave function of the usual Slater type. As the wave function, two for the d orbital are taken, $3d_z$ and $3d_{xy}$ (notation of Pauling and Wilson[6]), which were discussed in the previous paper[2]. In integrating the two orbitals, one must pay some attention to the orientation of the $3d_z$ orbital, because in the present consideration the Z-axis is taken to be normal to the molecular plane, and the Y-axis goes along the central C–S bond. The oribital should be rotated by 90° about the Y-axis. After the rotation, the angular part of the orbital, $(3\cos^2\vartheta-1)$, turns into $(3\sin^2\vartheta\times\cos^2\varphi-1)$. Hereafter, the orbital is described as $3d_{x(z)}$ in this paper.

The total perturbation energy is given as the sum of the energies by the above three positive charges, and the terms higher than the 2nd of the potential may be neglected because of their small contributions to the energy. Hence, after the integration, the respective energies of the two orbitals are given as follows:

For $3d_{x(z)}$

$$E = -(2Z_A/\sigma_A)\{\sigma_A R^0_{33}(\alpha\sigma_A) +(2/7)\sigma_A R^2_{33}(\alpha\sigma_A)\} -(Z_C/\sigma_C)\{\sigma_C R^0_{33}(\alpha\sigma_C) -(1/7)\sigma_C R^2_{33}(\alpha\sigma_C)\}$$

and for $3d_{xy}$

$$E = -(2Z_A/\sigma_A)\{\sigma_A R^0_{33}(\alpha\sigma_A) +(1/7)\sigma_A R^2_{33}(\alpha\sigma_A)\} -(Z_C/\sigma_C)\{\sigma_C R^0_{33}(\alpha\sigma_C) +(1/7)\sigma_C R^2_{33}(\alpha\sigma_C)\}$$

where $R^p_{n'n}(\alpha\sigma)$ is the auxiliary function which was used in the case of thiophene[4], and its explicit form is

$$R^p_{n'n}(\alpha\sigma) = (1/\sigma)(2\alpha\sigma/n)^{2n+1}\{1/(2n)!\} \times\{(2n+p)!\times(n/2\alpha\sigma)^{2n+p+1} -A_{2n+p}(2\alpha\sigma/n)+A_{2n-p-1}(2\alpha\sigma/n)\}$$

where

$$A_n(\omega) = \int_1^\infty r^n\exp(-\omega r)dr$$

In the above expressions, α is a parameter to be determined to minimize the total energy which is the sum of the perturbation energy and the unperturbed given by

$$W = (\alpha/3^2)(\alpha/2-Z_s)$$

for the hydrogen-like orbital of free atom parameter Z_s; that is, the procedure to be performed now is to find the new value of effective nuclear charge for which the total energy is a minimum for given magnitudes of σ_A, σ_C, Z_A and Z_C. The new value of the charge will offer an appropriate basis for the discussion about the d orbital under the perturbation.

In conducting the procedure, it is necessary to set the values of Z_s, Z_A and Z_C. As the value of Z_s, 1 and 2 are chosen, and for Z_C three values are taken, 1, 2 and 3, which were used in the case of thiophene[4]. With respect to the value of $Z_A(=Z_B)$, four values are assigned, 1, 3, 5 and 6. All the above values are to be treated as tentative parameters. In the real system, it is difficult to determine the straightforward values of the parameters equivalent to the outlying potential, because, as mentioned above, the real field is not truly coulombic but much more complicated. Furthermore, there is, in general, a considerable difference between so-called potential- and field-determined nuclear charge on the same atom[7]. Hence, in this paper, some attention will be paid rather to a variation in α by adopting the values of the above parameters in wider range. In finding the minimum of the total energy, it is necessary to know the values of $\sigma R^p_{n'n}(\alpha\sigma)$, which are taken from the table in the previous paper[4].

In Table I are given the results. From this table it is found that the new values of the effective charges under perturbation are considerably greater compared with those of free atom parameters, without exception, and furthermore that there are only small variations between these values despite the adoption of a wider range of the parameters. In the case of thiophene, it was shown that the magnitude of the new value is more sensitive to the bond distance σ than to the parameters for the outlying potential, and that it is little altered

6) L. Pauling and E. B. Wilson, "Introduction to Quantum Mechanics", McGraw-Hill, New York (1935), p. 138.

7) For example, see: F. W. Brown, *Phys. Rev.*, **44**, 214 (1933).

TABLE I. EFFECTIVE NUCLEAR CHARGE α OF 3d ORBITAL UNDER THE PERTURBATION

I. $3d_{xy}$

Z_s	Z_c	$Z_A(=Z_B)$ 1	3	5	6
1	1	2.34	2.66	2.80	2.92
1	2	2.55	2.78	2.90	2.96
1	3	2.73	2.90	3.00	3.04
2	1	2.75	3.05	3.05	3.10
2	2	2.90	3.10	3.15	3.20
2	3	3.05	3.10	3.25	3.30

II. $3d_{x(z)}$

1	1	2.34	2.63	2.75	2.82
1	2	2.50	2.70	2.83	2.88
1	3	2.63	2.80	2.86	2.94
2	1	2.68	2.88	2.96	3.00
2	2	2.90	3.02	3.02	3.05
2	3	3.05	3.12	3.15	3.10

by the charges of neighboring atoms in the range 2~3 when $\sigma=3$ and 4. In the present consideration, with respect to the bond distance σ, the fixed values are assigned, $\sigma_A(=\sigma_B)$ and σ_C, which are taken from the actual distances in thiothiophten, obtained from the X-ray analysis study by Bezzi, Mammi and Garbuglio[8]. Considering the above situation in thiophene, therefore, the present results may be convincing in regard to making fast the values of σ. This fact is worthy of notice, because to obtain the same results through the different starting points of Z_s might indicate the existence of a self-consistent value of α appropriate for the perturbation in which the geometrical configuration of the outlying potential to the atom in question is settled. In fact, the values given in the Table would serve as the first steps of the procedure to the self-consistent value. The value would probably remain settled near 3~4. Of course, it must be emphasized that this discussion on the effective value for α is by all means of tentative character under the present point charge approximation. Furthermore, the value of α appropriate to the real system should be determined precisely with respect to the whole energy of the molecule. The values in the Table, however, may be used as useful clues to the studies about the behavior of the d orbital on the central sulfur atom in thiothiophten.

From these discussions, it might be inferred in any case that the effective nuclear charge for the d orbital on the central sulfur atom in thiothiophten would not bear the free atom parameter, but it should bear a greater value considering the influence by the surrounding nuclei, probably near 3~4. As suggested earlier in this paper, the value for the d orbital will furnish an appropriate basis of the discussion about the orbital.

Overlap Integral. — In the previous section, the influence of the surrounding nuclei upon the d orbital was examined, and the results were given in Table I. Using these results, the overlap integral with the 3p σ orbital of the neighboring sulfur atom were estimated for the corresponding values of Z_s, Z_A and Z_C. These are given in Table II. In calculating these values, the tables of the integrals given in the previous paper[1b] were used, and as the effective nuclear charge for the 3p orbital, the direct value through Slater's rule was assigned, because it was shown that the value for 3p is little affected by the outlying perturbing charges when $\sigma=3$ and 4, and moreover, because, although it was accurate in the case of thiophene[4], in general, the contraction of the orbital is great only when the orbital with high screened and loosely bound electrons lies under the perturbation.

TABLE II. OVERLAP INTEGRALS OF 3d ORBITALS WITH 3p ORBITALS OF NEIGHBORING S ATOM

I. $3d_{xy}$

Z_s	Z_c	$Z_A(=Z_B)$ 1	3	5	6
1	1	0.082	0.129	0.148	0.163
1	2	0.113	0.145	0.161	0.166
1	3	0.138	0.161	0.170	0.172
2	1	0.141	0.173	0.173	0.178
2	2	0.161	0.178	0.181	0.185
2	3	0.173	0.178	0.189	0.192

II. $3d_{x(z)}$

1	1	0.092	0.143	0.162	0.173
1	2	0.121	0.154	0.175	0.181
1	3	0.143	0.170	0.178	0.190
2	1	0.151	0.181	0.192	0.195
2	2	0.183	0.197	0.197	0.200
2	3	0.200	0.206	0.210	0.204

The values in Table II are all positive and of the order of 0.1~0.2. Craig et al.[9] once proposed that for significantly strong binding a value of the overlap integral of about 0.1 or greater is necessary. According to this proposition, one might expect some significant binding to take place between the 3d and the 3p orbitals. The participation of the d orbital to bonding is performed through the pd hybridization in the present problem, and whether the d orbital is to be used or not depends, amongst other factors, upon whether the overlap integral involving the d orbital is comparable

8) S. Bezzi, M. Mammi and G. Garbuglio, *Nature*, **182**, 247 (1958).

9) D. P. Craig and E. A. Magnusson, *J. Chem. Soc.*, **1956**, 4895.

TABLE III. OVERLAP INTEGRALS: $S(3p\sigma-3p\sigma)$

p/t	0.0	0.1	0.2	0.3	0.4	0.5
0.0	−1.000	−0.966	−0.867	−0.719	−0.543	−0.365
0.5	−0.965	−0.933	−0.840	−0.698	−0.531	−0.359
1.0	−0.866	−0.839	−0.761	−0.640	−0.494	−0.342
1.5	−0.715	−0.696	−0.639	−0.549	−0.436	−0.312
2.0	−0.531	−0.520	−0.488	−0.435	−0.361	−0.272
2.5	−0.333	−0.331	−0.324	−0.307	−0.275	−0.224
3.0	−0.140	−0.146	−0.161	−0.178	−0.183	−0.170
3.5	0.031	0.019	−0.013	−0.056	−0.094	−0.114
4.0	0.171	0.155	0.111	0.050	−0.013	−0.060
4.5	0.273	0.256	0.208	0.136	0.055	−0.011
5.0	0.342	0.324	0.275	0.200	0.114	0.033
5.5	0.377	0.361	0.314	0.243	0.155	0.068
6.0	0.385	0.371	0.331	0.266	0.184	0.096
6.5	0.373	0.362	0.328	0.273	0.199	0.116
7.0	0.346	0.338	0.312	0.268	0.205	0.129
7.5	0.311	0.306	0.287	0.253	0.202	0.136
8.0	0.273	0.269	0.257	0.233	0.194	0.138
8.5	0.233	0.231	0.225	0.210	0.181	0.136
9.0	0.195	0.195	0.193	0.185	0.166	0.130
9.5	0.161	0.162	0.163	0.160	0.149	0.123
10.0	0.130	0.132	0.135	0.137	0.132	0.114

to that of 3p in terms of overlap approximation employed here. Therefore, the integral between $3p\sigma$ orbitals of S–S bond in thiothiophten was estimated, for the sake of comparison, using free atom parameters, and it was obtained as 0.243. In estimating this value, Table III given in the present paper was used. The overlap integral $S(3p\sigma-3p\sigma)$ was once given by Mulliken et al. for $t=0$[10], and also by Craig et al., who evaluated the values with parameters p and t in the ranges of 2∼10 and 0∼0.5 at the respective intervals of 1.0 and 0.1[11]. In the present paper, the values with p in the wider range of 0∼10 at the intervals of 0.5 were calculated, and in Table III are given the results obtained.

From the above estimation of the overlap integrals, it is found that almost comarable values are obtained for both the integrals involving the 3p and the 3d orbitals. These values would become more close when the so-called self-consistent value above mentioned may be used as the effective nuclear charge for the d orbital. Then, it may be said that the participation of the d orbital in the hybridization is more favorable than predicted through the direct employment of free atom parameters by Slater's rule, and that the extent to which the d orbital participates in bonding through the hybridization will be of the order nearly the same as, or at least not much less than, that of the 3p orbital. These results may be somewhat deficient in precision under the present point charge and overlap approximations employed in this paper. However, they may be sufficiently valid for discussing semi-quantitatively how the d orbital behaves under the perturbation in the actual molecule.

It is of interest to notice that the values of the overlap integral for the 3d orbital lie very nearly at the corresponding maxima for the respective effective nuclear charges of the orbital (see Tables I and III in Ref. 2). These values approach more nearly to the maxima when the self-consistent values under the present perturbation, 3∼4, may be used, or when a larger value of the distance between the orbitals is adopted. This is because the parameter p in the calculation of overlap integral involves the distance between the orbitals. Hence the so-called abnormal length of S–S bond in thiothiophten may be rather consistent to give the greater possibility of participation of the d orbital in the hybridization.

Hybrid Orbitals. — From the above considerations, it is found that the d orbitals on the central sulfur atom in thiothiophten might be able to participate in the hybridization to the same as, or at least to an extent comparable to that of the 3p orbital. Then the hybrid orbitals may be written with the same mixing coefficient for the two d orbitals in question as follows:

For $3d_{xy}$,

$$(1/\sqrt{2})(\psi_{3d_{xy}}\pm\psi_{3p})$$

10) R. S. Mulliken, C. A. Rieke, D. Orloff and H. Orloff, *J. Chem. Phys.*, **17**, 1248 (1949).
11) D. P. Craig, A. Macoll, R. S. Nyholm, L. E. Orgel and L. E. Sutton, *J. Chem. Soc.*, **1954**, 332.

and for $3d_{x(z)}$,

$$(1/\sqrt{2})(\psi_{3d_{x(z)}} \pm \psi_{3p})$$

The mixing coefficient is fortunately compatible with the conditions required from the linear bond of S-S-S in thiothiophten and the symmetrical skeleton of the molecule[12]. The approximate forms of the hybrid orbitals were already shown in Fig. 2 of the previous paper[1b].

Of the two sets of hybrid orbitals, those involving the $3d_{x(z)}$ orbital may be more probable for participating in the hybridization to form the S-S-S bond in thiothiophten, because the values of the overlap integral are greater for the $3d_{x(z)}$ than for the $3d_{xy}$ with corresponding p and t values.

All the above discussions are those under the point charge approximation and within the framework of the overlap criterion. Therefore it is more or less inevitable that the results obtained in this paper should not be so readily sufficient for an accurate discussion of the formation of the possibe bond in thiothiophten. Furthermore, in fact, the accurate discussion dealing with the final determining factor in bonding, that is, on balancing of energy should be taken up for consideration with respect to the whole molecule of thiothiophten. Nevertheless, the results obtained above will be valuable enough for approximate and semi-quantitative discussion about the possibility of participation of the d orbital in the central sulfur atom in thiothiophten. Therefore it can now be said that the structure of thiothiophten is not one involving the no-bond resonance structure proposed by Bezzi et al.[8], but rather it may be the condensed ring system of the full σ skeleton involving the hybrid orbitals on the central sulfur atom of the molecule.

Electrotechnical Laboratory
Tanashi, Tokyo

12) C. A. Coulson, "Valence", Oxford University Press. London (1952), p. 195.

Studies on Organophosphorus Compounds. II. On Phosphite Cuprous Halide Complex Compounds[*1]

By Yoshihiko NISHIZAWA

(Received November 26, 1960)

Although many workers have studied complex compounds having phosphorus atom, many of them reported on phosphine[*2] complex compounds such as phosphine platinum halides[1], phosphine cuprous iodides[2] and phosphine chromium halides[3], while phosphite complex compounds were reported on only by Arbuzov[4] and others.

Arbuzov has reported that phosphites give phosphite cuprous halide complex compounds which have two experimental formulae, $(RO)_3PCuX$ (I) and $[(RO)_3P]_2CuX$ (II), and that *O,O*-dialkyl phosphonates give no complex compounds. Therefore, this reaction has been utilized as an identification of phosphite from phosphonate.

The present author separated two compounds having formulas I and II and measured their molecular weights in various organic solvents. It was made clear as a result, that these complex compounds showed an interesting behavior in organic solvents and reacted with pyridine, aniline and their analogues and produced new complex compounds having phosphites and amines.

Preparation of Phosphite Cuprous Halide Complex Compounds.—Phosphite cuprous halides were prepared by the reaction of phosphite with cuprous halide in a benzene solution. After cuprous halides were dissolved in benzene, the benzene was evaporated under reduced pressure, the complex compounds were obtained as white crystals or colorless oil.

Changing the mole ratio of phosphites to cuprous halides obtained two complex compounds, namely, phosphite cuprous halides I and bis-phosphite cuprous halides II. Triphosphite cuprous halide could not be prepared from three moles of phosphite and one mole

*1 Presented at the annual meeting of Chemistry of Coordination Compounds of Japan, Fukuoka, Oct., 1959.

*2 The phosphorus compounds in this paper were named according to the Drake Committee's Report (*Chem. Eng. News*, **30**, 4515 (1952).).

1) J. Chatt, *J. Chem. Soc.*, **1951**, 625.
2) F. G. Man, ibid., **1935**, 1503.
3) K. Issleib, *Z. anorg. u. allgem. Chem.*, **298**, 84 (1959).
4) A. Arbuzov, *Ber.*, **38**, 1171 (1905).

TABLE I. YIELDS, MELTING POINTS AND MICROANALYTICAL DATA OF PHOSPHITE CUPROUS HALIDES $(RO)_3PCuX$ (I)

No.	R	X	Yield %	M.p. °C	M.p. (°C) by A. Arbuzov[4]	Halogen, % Found	Halogen, % Calcd.	Phosphorus, % Found	Phosphorus, % Calcd.	Copper, % Found	Copper, % Calcd.
Ia	*iso*-C_3H_7	Cl	95.1	117	112 ~114	11.63	11.60	10.3	10.1	20.5	20.8
Ib	C_6H_5	Cl	98.1	88~ 89	95 ~ 96	8.55	8.68	7.7	7.6	15.2	15.5
Ic	*iso*-C_3H_7	Br	96.2	146~147	149 ~150	22.61	22.82	9.0	8.8	18.3	18.1
Id	C_6H_5	Br	97.7	91~ 92	90.5~ 91.5	17.51	17.64	6.8	6.8	14.3	14.0
Ie	C_2H_5	I	88.6	110~111	109 ~110	—	—	8.9	8.7	17.8	17.8
If	*n*-C_3H_7	I	90.2	61~ 63	—	—	—	7.7	7.8	16.4	16.0
Ig	*iso*-C_3H_7	I	93.5	199~200	184 ~185	—	—	7.7	7.8	16.2	16.0

TABLE II. YIELDS, MELTING POINTS AND MICROANALYTICAL DATA OF BIS-PHOSPHITE CUPROUS HALIDES $(RO)_3PCuXP(OR')_3$ (II)

No.	R	R'	X	Yield %	M.p. °C	M.p., °C by A. Arbuzov[4]	Halogen, % Found	Halogen, % Cald.	Phosphorus, % Found	Phosphorus, % Calcd.	Copper, % Found	Copper, % Calcd.
II a	*iso*-C_3H_7	*iso*-C_3H_7	Cl	93.1	69~70	—	6.75	6.89	11.9	12.0	12.8	12.3
II b	C_6H_5	C_6H_5	Cl	95.9	98~99	—	4.71	4.94	8.4	8.6	9.1	8.8
II c	*iso*-C_3H_7	*iso*-C_3H_7	Br	91.9	58~59	—	14.22	14.30	10.9	11.1	10.6	11.3
II d	C_6H_5	C_6H_5	Br	93.2	67~68	73~77	10.34	10.48	8.0	8.1	8.6	8.3
II e	*iso*-C_3H_7	*iso*-C_3H_7	I	95.6	94~95	—	—	—	10.3	10.2	10.6	10.5
II f	C_6H_5	C_6H_5	I	94.8	70~72	73~75	—	—	7.8	7.6	8.1	7.8
II g	C_2H_5	C_6H_5	Cl	97.8	75~76	—	6.15	6.17	11.2	10.9	10.8	11.0

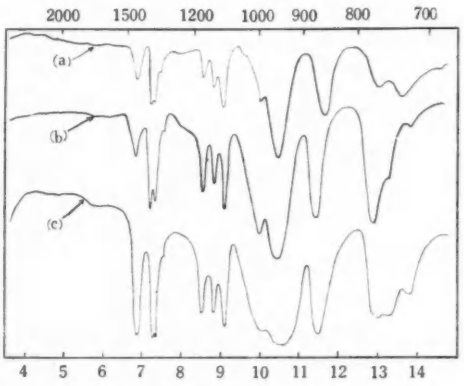

Fig. 1. Infrared absorption spectra (in Nujol) of (a) triisopropyl phosphite, (b) triisopropyl phosphite cuprous chloride (Ia) and (c) bis-(triisopropyl phosphite) cuprous chloride (IIa).

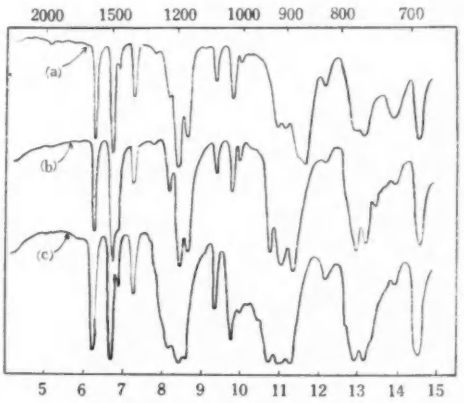

Fig. 2. Infrared absorption spectra (in Nujol) of (a) triphenyl phosphite, (b) triphenyl phosphite cuprous chloride (Ib) and (c) bis-(triphenyl phosphite) cuprous chloride (IIb).

of cuprous halides, but a product corresponding to one mole of bis-phosphite cuprous halides II and one mole of phosphite was obtained.

$$(RO)_3P + CuX \rightarrow \underset{(I)}{(RO)_3PCuX}$$

$$2(RO)_3P + CuX \rightarrow \underset{(II)}{[(RO)_3P]_2CuX}$$

Phosphite cuprous halides I gave bis-phosphite cuprous halides II by adding one mole ratio of phosphite and II gave also I by adding one mole ratio of cuprous halides.

Bis-phosphite cuprous halides II were converted to phosphite cuprous halides I by heating under reduced pressure.

$$\underset{(II)}{[(RO)_3P]_2CuX} \xrightarrow{heat} \underset{(I)}{(RO)_3PCuX} + (RO)_3P \uparrow$$

TABLE III. MOLECULAR WEIGHTS OF PHOSPHITE CUPROUS HALIDES $(RO)_3PCuX$ (I) IN VARIOUS SOLVENTS

No.	R	X	Cryoscopic solvent (*K*)	Concn. g./G%	*ΔT* °C	Molecular Weight: Experimental	Molecular Weight: Calcd. (monomeric)	Degree of association
				0	—	*1230*		
			Benzene (5120)	0.635	0.027	1204		4.02
				1.172	0.050	1200		
				2.005	0.088	1167		
I a	*iso*-C_3H_7	Cl					306	
				0	—	*1265*		
			Cyclohexane (20100)	0.636	0.103	1241		4.13
				1.201	0.200	1207		
				1.605	0.268	1204		
				0	—	*1555*		
			Benzene	0.639	0.021	1558		3.80
				1.333	0.044	1551		
				1.901	0.062	1569		
				0	—	*1230*		
I b	C_6H_5	Cl	Bromoform (14050)	0.532	0.061	1225	409	3.01
				1.426	0.168	1193		
				2.106	0.249	1188		
				0	—	*1565*		
			Cyclohexane	0.775	0.099	1573		3.83
				1.426	0.183	1566		
				2.221	0.283	1577		
				0	—	*1410*		
I c	*iso*-C_3H_7	Br	Benzene	0.436	0.016	1395	350.5	4.02
				1.326	0.049	1386		
				2.108	0.079	1366		
				0	—	*1730*		
			Benzene	0.476	0.014	1741		3.81
				1.181	0.036	1680		
				2.700	0.081	1707		
I d	C_6H_5	Br					453.5	
				0	—	*780*		
			Bromoform	0.663	0.123	757		1.72
				1.641	0.309	746		
				2.326	0.460	710		
				0	—	*1200*		
I e	C_2H_5	I	Benzene	0.536	0.023	1193	356.5	3.37
				1.487	0.070	1088		
				2.235	0.150	1090		
				0	—	*1135*		
I f	*n*-C_3H_7	I	Benzene	0.500	0.023	1113	397.5	2.86
				0.841	0.040	1076		
				2.011	0.100	1030		
				0	—	*1160*		
I g	*iso*-C_3H_7	I	Benzene	0.638	0.028	1167	397.5	2.92
				1.273	0.057	1143		
				2.081	0.092	1158		

It is clear from the following experimental facts that these complex compounds I and II have the phosphite group in their molecules. These compounds reacted with acetyl chloride in benzene solution to give *O,O*-dialkyl-acetyl phosphonates (A) and cuprous halides. The melting point of *p*-nitrophenylhydrazone of the phosphonate A coincided with that of *p*-nitrophenylhydrazone of the product prepared from trialkyl phosphite and acetyl chloride by Arbuzov's reaction[5].

$$[(RO)_3P]_nCuX \xrightarrow{n\cdot CH_3COCl} n\cdot(RO)_2P(O)-COCH_3 + CuX + n\cdot RCl$$

(A) → *p*-Nitrophenylhydrazone

$$(RO)_3P + CH_3COCl \rightarrow (RO)_2P(O)-COCH_3 + RCl$$

(*n* is 1 or 2 and R is alkyl group).

The infrared absorption spectra[*3] of these

5) M. I. Kabachnik, *Izvest. Akad. Nauk. SSSR.*, 1945, 364.

*3 Perkin Elmer 21 Spectrophostometer was used.

TABLE IV. MOLECULAR WEIGHTS OF BIS-PHOSPHITE CUPROUS HALIDES $[(RO)_3P]_2CuX$ (II) IN VARIOUS SOLVENTS

No.	R	X	Cryoscopic solvent (K)	Concn. (g./G%)	ΔT °C	Molecular Weight Experimental	Molecular Weight Calcd. (monomeric)	Degree of association
IIa	*iso*-C_3H_7	Cl	Benzene (5120)	*0*	—	*498*	515	0.97
				0.431	0.045	490		
				1.231	0.130	485		
				2.260	0.250	463		
			Bromoform (14050)	*0*	—	*513*		1.00
				0.251	0.070	504		
				1.449	0.400	509		
				2.396	0.685	491		
			Cyclohexane (20100)	*0*	—	*503*		0.98
				0.509	0.205	499		
				1.581	0.640	497		
				2.561	1.050	490		
IIb	C_6H_5	Cl	Benzene	*0*	—	*713*	719	0.99
				0.412	0.030	703		
				1.636	0.120	698		
				2.511	0.190	677		
IIc	*iso*-C_3H_7	Br	Benzene	*0*	—	*553*	559.5	0.99
				0.565	0.053	546		
				1.401	0.130	552		
				2.611	0.250	535		
			Bromoform	*0*	—	*530*		0.95
				0.395	0.105	529		
				1.405	0.390	506		
				2.793	0.770	510		
IId	C_6H_5	Br	Benzene	*0*	—	*782*	763.5	1.02
				0.599	0.040	767		
				1.315	0.090	748		
				2.461	0.175	720		
IIe	*iso*-C_3H_7	I	Benzene	*0*	—	*580*	606.5	0.96
				0.431	0.038	581		
				1.691	0.151	573		
				2.813	0.253	569		
			Bromoform	*0*	—	*598*		0.99
				0.813	0.192	594		
				1.906	0.461	581		
				2.741	0.661	583		
IIf	C_6H_5	I	Benzene	*0*	—	*802*	810.5	0.99
				0.685	0.044	797		
				1.801	0.117	788		
				2.589	0.170	780		

compounds I and II showed the absorption band of *P-O*-isopropyl group at 1010 cm^{-1} or *P-O*-phenyl group at 1200 cm^{-1} according to the kinds of phosphites in complex compounds I and II. (see Figs. 1 and 2).

However, the absorption bands of P-O stretching vibration[6] of phosphite at 857 and 769 cm^{-1} shift to 879 and 779 cm^{-1} respectively. Form this shift, it is considered that P-O bonds are shortened by the formation of the complex, namely, the bonding strength of P-O in these complex compounds becomes stronger than that of phosphite (see Figs. 1 and 2).

In the ultraviolet absorption spectra*4 of these complex compounds, absorption maximum λ_{max} of phosphite at 263.5 shifts to 265 and absorption bands became more broad by the formation of complex (see Fig. 3). This shift seems to show the usual correlation between the coordination compound and its donor[7].

Molecular Weights of Phosphite Cuprous Halide Complex Compounds.—The molecular weights of these complex compounds were measured by the cryoscopic method[8] in benzene, bromoform and cyclohexane, which are all prepared by purification of guaranteed reagents in the usual manner[9].

6) J. Bellamy, "The Infrared Spectra of Complex Molecules", John Wiley & Sons, New York (1958).

*4 Shimadzu QB-50 Spectrophotometer was used.

7) K. Sone, *J. Am. Chem. Soc.*, **75**, 5207 (1953).

8) J. Sameshima, "Buturikagaku-Zikken-Hô", Syokabo, Tokyo, (1959).

9) T. Kuwata, "Yôzai", Maruzen Pub. Co., Tokyo (1951).

Table V. Yields, melting points and microanalytical data of diisopropyl phenyl phosphonite cuprous halides $[(iso\text{-}PrO)_2PC_6H_5]_m$ CuX (III), (IV).

No.	X	m	Yield %	M.p., °C	Halogen, %		Phosphorus, %		Copper, %	
					Found	Calcd.	Found	Calcd.	Found	Calcd.
IIIa	Cl	1	98.5	141~142	10.88	10.92	9.4	9.5	19.8	19.5
IIIb	Br	1	97.9	143~144	21.91	21.64	8.1	8.4	17.3	17.2
IIIc	I	1	95.6	183~184	—	—	7.5	7.4	15.6	15.2
IVa	Cl	2	98.4	144~145	6.39	6.44	11.0	11.2	11.9	11.5
IVb	Br	2	99.0	148~149	13.18	13.43	10.3	10.4	10.5	10.7
IVc	I	2	98.0	187~189	—	—	9.8	9.6	9.6	9.9

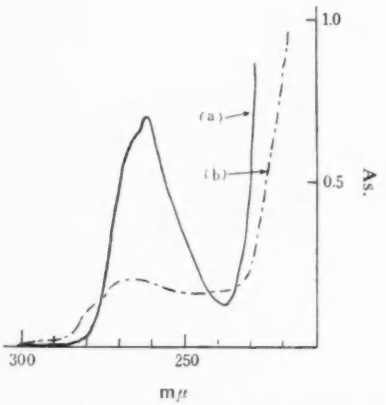

Fig. 3. Ultraviolet absorption spectra (in ethanol) of (a) triphenyl phosphite and (b) bis-(triphenyl phosphite) cuprous Chloride (IIb).

The results of these experiments are shown in Tables III and IV.

It is clear from Tables III and IV that the complex compounds I form associated molecules in organic solvents and that the degree of association are changed according to the kinds of halogens or solvents; on the contrary, the complex compounds II form simple molecules in organic solvents unconcerned with the kinds of halogens or solvents.

It seems to be possible that the apparent values of molecular weights will become smaller, if the associated molecules are dissociated in organic solvents. These possibilites are supported by the fact the degrees of association in nonpolar solvents are greater than that in polar solvent.

So, the present author prepared phenyl phosphonite, which is an analogue of phosphite but has the property of phosphine to a slight degree, and leads[10] to the complex compounds III and IV.

Preparation and Molecular Weight of *O, O*-Diisopropylphenyl Phosphoniten Cuprous Halides (III) and (IV).—Complex compounds III and IV were prepared from *O, O*-diisopropylphenyl phsophonite[11] and cuprous halide by the same method as phosphite I and II. The yield, the melting points and the microanalytical data of the complex compounds III and IV are shown in Table V.

As is clearly shown in Table VI, phenyl phosphonite cuprous halides (III) form tetramer and bis-(phenyl phosphonite) cuprous halides (IV) form dimer in organic solvents irrespectively of the kinds of halogens or solvents.

From the above results of Table VI and phosphine cuprous iodide which is reported as tetramer[2], it may be considered that complex compounds I will also be tetramer and complex compounds II dimer but these compounds I and II will be dissosiated in organic solvents.

But the real structures of these compounds must be determined by x-ray analysis.

Phosphite Cuprous Halide Amine Complex Compounds.—It was mentioned already that phosphite cuprous halides I reacted with more one mole ratio of phosphite and gave bis-phosphite cuprous halides II. In this reaction when aniline, pyridine and their derivatives are used instead of the phosphite, new complex compounds were prepared[12] on the contrary bis-phosphite cuprous halides II did not react with the above amines.

That is to say, to the acetone solution containing one mole of phosphite cuprous halides I, one mole of aniline, pyridine or their derivatives wasadded and thus, white crystals were obtained. These crystals had sharp melting points and showed the experimental formula of $(RO)_3PCuX\cdot$ Amine.

$$\underset{\text{(I)}}{(RO)_3PCuX} + \text{Amine} \rightarrow \underset{\text{(V), (VI)}}{(RO)_3PCuX\cdot \text{Amine}}$$

Changing the mole ratio of amines to phosphite cuprous halides I neither phosphite cuprous halide bis-amines $(RO)_3PCuX(Amine)_2$

10) Y. Nishizawa and Y. Suzuki, Japan. Pat. Applied No. 21678 (1959).

11) A. Arbuzov, *Chem. Abstr.*, **40**, 3411 (1946).

12) Y. Nishizawa and M. Nakagawa, Japan. Pat. Applied No. 21679 (1959).

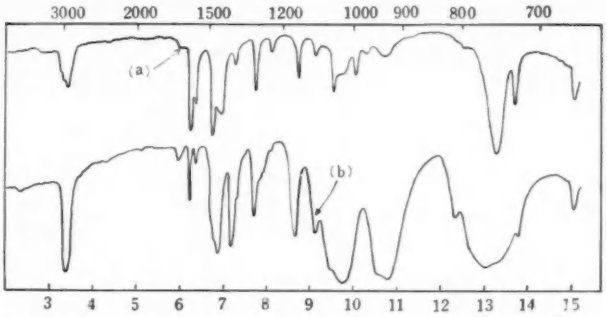

Fig. 4. Infrared absorption spectra of (a) α-picoline (liquid) and (b) triethyl phosphite cuprous iodide α-picoline complex compound (Ve) (in Nujol).

TABLE VI. MOLECULAR WEIGHTS OF PHENYL PHOSPHONITE CUPROUS HALIDES $[(iso\text{-}C_3H_7O)_2PC_6H_5]_mCuX$ (III) AND (IV) IN VARIOUS SOLVENTS

No.	X	m	Cryoscopic solvent (K)	Concn. (g./G%)	ΔT °C	Molecular weight: Experimental	Molecular weight: Calcd. (monomeric)	Degree of association
			Benzene (5120)	*0*	—	*1280*		
				0.593	0.024	1265		3.93
				1.911	0.086	1138		
				2.730	0.127	1101		
			Bromoform (14050)	*0*	—	*1220*		
IIIa	Cl	1		0.465	0.055	1188	325	3.75
				1.382	0.166	1170		
				2.655	0.322	1158		
			Cyclohexane (20100)	*0*	—	*1340*		
				0.298	0.046	1302		4.12
				0.951	0.147	1300		
				2.411	0.389	1261		
			Benzene	*0*	—	*1450*		
				0.675	0.025	1382		3.92
				1.715	0.069	1273		
				2.816	0.125	1153		
IIIb	Br	1					369.5	
			Bromoform	*0*	—	*1425*		
				0.593	0.059	1412		3.86
				1.491	0.151	1387		
				2.615	0.270	1361		
IIIc	I	1	Benzene	*0*	—	*1685*		
				0.427	0.013	1682	416.5	4.05
				1.793	0.054	1700		
				2.381	0.072	1693		
			Benzene	*0*	—	*1100*		
				0.298	0.014	1090		2.00
				1.613	0.076	1087		
				2.803	0.135	1063		
IVa	Cl	2					551	
			Bromoform	*0*	—	*1080*		
				0.445	0.058	1077		1.96
				1.412	0.187	1061		
				2.561	0.342	1052		
			Benzene	*0*	—	*1265*		
IVb	Br	2		0.343	0.014	1254	595.5	2.12
				1.612	0.065	1270		
				2.635	0.108	1249		
			Benzene	*0*	—	*1190*		
IVc	I	2		0.441	0.019	1188	642.5	1.85
				1.391	0.061	1181		
				2.546	0.111	1172		

TABLE VII. YIELDS, MELTING POINTS AND MICROANALYTICAL DATA OF PHOSPHITE CUPROUS HALIDE AMINE COMPLEX COMPOUNDS $(RO)_3PCuX \cdot Amine$ (V), (VI)

No.	R	X	Amine	Yield %	M.p. °C	Nitrogen, %		Halogen, %		Phosphorus, %		Copper, %	
						Found	Calcd.	Found	Calcd.	Found	Calcd.	Found	Calcd.
V a	C_2H_5	Cl	Pyridine	98.8	56～57	4.22	4.07	10.00	10.32	8.9	9.0	19.1	18.5
V b	C_2H_5	Br	Pyridine	97.2	105～106	3.81	3.60	20.38	20.59	7.9	8.0	15.8	16.3
V c	C_2H_5	I	Pyridine	97.9	72～73	3.50	3.21	—	—	6.8	7.1	14.6	14.6
V d	C_6H_5	Cl	Pyridine	93.5	126～127	2.76	2.87	7.55	7.27	6.6	6.4	13.3	13.0
V e	C_2H_5	I	α-Picoline	90.4	59～60	3.35	3.11	—	—	7.2	7.1	14.6	14.1
V f	C_2H_5	I	β-Picoline	96.2	84～85	3.08	3.11	—	—	6.9	7.1	14.0	14.1
V g	C_2H_5	I	γ-Picoline	88.2	76～77	3.31	3.11	—	—	7.3	7.1	13.8	14.1
V h	C_2H_5	I	2,4-Lutidine	77.5	97～99	3.15	3.02	—	—	6.7	6.9	14.1	13.7
V i	C_2H_5	I	2,6-Lutidine	82.8	70～71	3.31	3.02	—	—	6.8	6.9	13.6	13.7
V j	C_2H_5	Cl	α,α'-Dipyridyl	98.1	105～106	3.66	3.42	—	—	7.1	7.4	15.2	15.1
VI a	C_2H_5	I	Aniline	71.5	80～81	3.50	3.11	—	—	6.8	6.9	14.3	14.1
VI b	C_2H_5	I	*p*-Toluidine	97.2	60～61	3.15	3.01	—	—	6.5	6.7	13.9	13.7
VI c	C_2H_5	I	*p*-Anisidine	96.5	66～67	2.65	2.91	—	—	6.3	6.4	12.9	13.2
VI d	C_2H_5	I	*p*-Chloroaniline	95.5	72～73	2.65	2.83	—	—	6.5	6.3	12.6	12.8
VI e	C_2H_5	I	*m*-Chloroaniline	98.3	60～62	2.91	2.83	—	—	6.3	6.3	13.1	12.8

TABLE VIII. YIELDS, PHYSICAL CONSTANTS AND MICROANALYTICAL DATA OF PHOSPHITES $(RO)_3P$

R	Yield %	B. p. °C	B. p. mmHg	n_D (t°C)	Phosphorus, %		Carbon, %		Hydrogen, %	
					Found	Calcd.	Found	Calcd.	Found	Calcd.
C_2H_5	82	55～57	19	1.4135(20)	19.8	19.9	46.31	46.15	9.25	9.04
n-C_3H_7	85	82～83	10	1.4263(20)	15.1	14.9	52.06	51.92	10.09	10.10
iso-C_3H_7	80	60～61	9	1.4079(29)	15.0	14.9	51.88	51.92	10.41	10.10
C_6H_5	63	170	0.3	m.p.25°C	9.8	10.0	69.53	69.68	4.97	4.84

nor bis-amine cuprous halides $(Amine)_2CuX$ were obtained.

The yields, the melting points and the microanalytical data of these new complex compounds V and VI are shown in Table VII. The infrared absorption spectra of these complex compounds V and VI showed that these compounds V and VI have both the amine molecule and the phosphite molecule. Infrared absorption spectrum of triethyl phosphite cuprous iodide α-picoline (Ve) is shown in Fig. 4 as a representation.

It was interesting to see that ortho-substituted anilines, *O*-chloroaniline, *O*-toluidine, *O*-anisidine etc., did not give these complex compounds VI. The cause may be considered from models of complex molecules to be a steric hindrance owing to the ortho-substituent in aniline.

In the pyridine series, all derivatives gave new complex compound, irrespective of the position of substituents.

It was also made clear by the present author that all of the above mentioned compounds I, II, III, IV, V and VI had strong fungicidal activities[13], and the data of their biological activities will be reported in other paper.

13) J. Hattori and Y. Nishizawa, Japan. Pat. Applied No. 36382 (1958), 3506, 22572, 22573 (1959).

Experimental

Preparations of Phosphites.—Trialkyl or triphenyl phosphites were prepared by Ford-Moore's methods[14] and their yields, physical constants and microanalytical data are shown in Table VIII.

Preparation of Diisopropyl Phenyl Phosphonite.—This phosphonite was prepared from phenyl dichlorophosphine and isopropyl alcohol by Arbuzov's method[11]. The boiling point is 110°C/0.5 mmHg, the refractive index is n_D^{25} 1.5000 and the yield is 84%.

Found, P, 13.7; C, 63.59; H, 8.59. Calcd. for $C_{12}H_{19}O_2P$, P, 13.7; C, 63.72; H, 8.41%.

Preparation of Phosphite or Phosphonite Cuprous Halides I or III.—The following example illustrates the preparation of phosphite or phosphonite cuprous halides I or III. Other examples are shown in Tables I and V and their molecular weights are shown in Tables III and VI.

Preparation of Diisopropyl Phenyl Phosphonite Cuprous Chloride (IIIa).—To a solution of 14.3 g. (0.05 mol.) of diisopropyl phenyl phosphonite in 50 ml. of benzene was gradually added 4.95 g. (0.05 mol.) of cuprous chloride. The temperature rose gradually and cuprous chloride was dissolved in benzene. After one hour's stirring, the trace of insoluble matter was filtered off and concentrated under reduced pressure. White crystals (18.9 g,

14) A. H. Ford-Moore, "Organic Syntheses", Vol. 31, John Wiley & Sons, New York, (1951), p. 111.

98.5%) were obtained and recrystallized from petroleum ether, m. p. 141~142°C.

Found: Cl, 10.88; P, 9.4; Cu, 19.8. Calcd. for $C_{12}H_{19}O_2PCuCl$: Cl, 10.92; P, 9.5; Cu, 19.5%.

Preparation of Bis-phosphite or Bis-phosphonite Cuprous Halides II or IV.—The following example illustrates the preparation of bis-phosphite or bis-phosphonite cuprous halides II or IV. Other examples are shown in Tables II and V and their molecular weights are shown in Tables IV and VI.

Preparation of Bis-(diisopropyl Phenyl Phosphonite) Cuprous Chloride (IVa).—The compound was prepared from 28.5 g. (0.1 mol.) of diisopropyl phenyl phosphonite and 4.95 g. (0.05 mol.) of cuprous chloride in benzene solution as above mentioned. White crystals (32.9 g., 98.4%) were obtained and melted at 144~145°C (from ligroin).

Found: Cl, 6.39; P, 11.0; Cu, 11.9. Calcd. for $C_{24}H_{38}O_4P_2CuCl$: Cl, 6.44; P, 11.2; Cu, 11.5%.

Reaction of Triisopropyl Phosphite Cuprous Chloride (Ia) with Triisopropyl Phosphite.—To a solution of 15.3 g. (0.05 mol.) of triisopropyl phosphite cuprous chloride (Ia) in 50 ml. of benzene was added 10.4 g. (0.05 mol.) of triisopropyl phosphite. The temperature did not rise during this addition. The benzene was evaporated under reduced pressure, white crystals (23.8 g.) were obtained and melted at 69~70°C. A mixture of the crystals and the authentic bis-(triisopropyl phosphite) cuprous chloride which was prepared from two moles of triisopropyl phosphite and one mole of cuprous chloride, melted at 69~70°C.

Reaction of Triethyl Phosphite Cuprous Chloride[4] with Triphenyl Phosphite.—Triphenyl phosphite (15.5 g., 0.05 mol.) was added to a solution of 13.3 g. (0.05 mol.) of triethyl phosphite cuprous chloride in 50 ml. of benzene. After the benzene was evaporated off, white crystals of triethyl phosphite triphenyl phosphite cuprous chloride (IIg) (28.1 g, 97.8%) were obtained and melted at 75~76°C.

Found: Cl, 6.15; P, 11.2; Cu, 10.8. Calcd. for $C_{24}H_{30}O_6P_2CuCl$: Cl, 6.17; P, 10.9; Cu, 11.0%

Reaction of Bis-(triisopropyl phosphite) Cuprous Chloride (IIa) with Cuprous Chloride.—There was added 4.95 g. (0.05 mol.) of cuprous chloride to a solution of 25.7 g. (0.05 mol.) of bis-(triisopropyl phosphite) cuprous chloride (IIa) in 50 ml. of benzene. After cuprous chloride was dissolved in benzene, the reaction mixture was filtered off and concentrated. White crystals (29.6 g) were obtained and melted at 117°C.

This melting point coincides with that of the authentic triisopropyl phosphite cuprous chloride (Ia) prepared from one mole ratio of triisopropyl phosphite and one mole ratio of cuprous chloride, and the mixed melting point was not depressed.

Reaction of Triethyl Phosphite Cuprous Iodide (Ie) with Acetyl Chloride.—To a solution of 17.8 g. (0.05 mol.) of triethyl phosphite cuprous iodide (Ie) in 50 ml. of benzene, there was gradually added 3.9 g. of acetyl chloride. The temperature of the reaction mixture rose and white inorganic compounds were precipitated. After one hour's refluxing, the precipitates were filtered off and the filtrate was concentrated. The residual oil was fractionated under reduced pressure. The main product was distilled at 78~79°C/3 mmHg, and yielded 7.7 g.

n_D^{20} 1.4209. Found: P, 17.1; C, 39.81; H, 7.34. Calcd. for $C_6H_{13}O_4P$: P, 17.2; C, 40.00; H, 7.22%. *p*-Nitrophenylhydrazone of the aforesaid main product was prepared from *p*-nitrophenylhydrazine in the usual manner.

This hydrazone melted at 131~132°C (recryst. from ethanol) and the mixed melting point with authentic *p*-nitrophenylhydrazone of *O,O*-diethyl-acetyl phosphonate prepared from triethyl phosphite and acetyl chloride was not depressed.

Found: P, 9.6; C, 45.59; H, 5.89; N, 13.31. Calcd. for $C_{12}H_{18}N_3O_5P$: P, 9.8; C, 45.71; H, 5.71; N, 13.33%

Pyrolysis of Bis-(triisopropyl Phosphite) Cuprous Chloride (IIa).—The compound IIa (25.8 g., 0.05 mol.) was set in a distillation flask (50 ml.) which was combined with a trap cooled at −50°C and heated at 100°C under 0.3 mmHg for 6 hr.

The crystals IIa melted and then crystallized again. The product was recrystallized from petroleum ether and melted at 116~117°C. This melting point coincides with that of the authentic triisopropyl phosphite cuprous halide (Ia) prepared from one mole ratio of triisopropyl phosphite and one mole ratio of cuprous chloride and the mixed melting point was not depressed.

On the other hand, colorless oil which was captured in a trap, was distilled at 60~62°/9mmHg and yielded 7.7 g, n_D^{28} 1.4081.

Found: P, 14.6; C, 15.80; H, 10.35. Calcd. for $C_9H_{21}O_3P$: P, 14.9; C, 15.92; H, 10.10%

This oil was added to a benzene solution containing 5.3 g. of cuprous chloride and gave white crystals which melted at 116~117°C. The melting point of these crystals coincided with the authentic triisopropyl phosphite cuprous chloride (Ia) and the mixed melting point was not depressed.

Reaction of Phosphite Cuprous Halides I with Amines.—The following example illustrates the preparation of phosphite cuprous halide amine complex V or VI. Other examples are shown in Table VII.

Reaction of Triethyl Phosphite Cuprous Chloride with Pyridine.—To a solution of 26.5 g. (0.1 mol.) of triethyl phosphite cuprous chloride in 100 ml. of acetone was added 7.9 g. (0.1 mol.) of pyridine.

The acetone was evaporated off under reduced pressure and light green crystals (33.9 g.) were obtained. White needles were recrystallized from ligroin and melted at 56~57°C.

Found: N, 4.22; Cl, 10.00; P, 8.9; Cu, 19.1. Calcd. for $C_{11}H_{20}ClNO_3PCu$: N, 4.07; Cl, 10.32; P, 9.0; Cu, 18.5%

Summary

Phosphites or phosphonites react with cuprous halides in one to one or two to one mole ratio to give phosphite, phosphonite, bis-phosphite or bis-phosphonite cuprous halides complex compounds. Their molecular weights

in various organic solvents showed that these compounds formed polymer.

Phosphite cuprous halides react with pyridine, aniline or their derivatives and gave new complex compounds having phosphite, cuprous chloride and amine.

The author wishes to express his thanks to Professor Shinichiro Fujise and Professor Taro Yamazaki of Tohoku University and Professor Ryutaro Tsuchida of Osaka University for their helpful suggestions in the preparation of this manuscript. He also wishes to thank the Sumitomo Chem. Co., Ltd. for permission to publish this work. He is indebted to co-workers in the analytical section of this laboratory. He also wishes to express his thanks to Messrs. M. Nakagawa and Y. Suzuki for their never failing assistance.

Sumitomo Chem. Co., Ltd.
Osaka Works
Konohana-ku, Osaka

An Attempt to Discuss Reactivities of Excited Molecules by the Molecular Orbital Method

By Kenichi FUKUI, Keiji MOROKUMA and Teijiro YONEZAWA

(Received December 29, 1960)

In order to elucidate the mechanisms of reactions of conjugated or non-conjugated organic compounds which are in their ground state, a number of quantum mechanical, especially molecular orbital, studies have been performed and have achieved remarkable success in predicting theoretically their chemical reactivities[1-4]. In connection with the recent advance of techniques of photochemical investigation, chemical reactivities of electronically excited molecules have aroused our interest.

Because of the complicated characters and the multifariousness of reactions of excited molecules, only a few theoretical discussions have ever been made. As regards the problem of their self-dissociation, some qualitative discussions in terms of the potential energy curve have prevailed[5]. For discussing the energy transfer reaction between an excited molecule and an unexcited one, the collision theory has prevailed as a powerful tool[6]. On account of the lack in systematic experimental data and, in addition, because of the difficulties in the theoretical treatment, only a few quantum chemical studies have been presented on excited molecules involved in the addition reactions of large organic molecules. Photopolymerization of hydrocarbons has been discussed in terms of free valence of the molecules in their lowest excited state. The intramolecular orientation in the reaction of anthracene or naphthacene has been explained well[7]. But that of acenaphthylene has not been[8]; free valence of its lowest excited states is greatest at positions 5 and 6, and, on the contrary, the photodimer of the componud is produced through positions 1 and 2.

In the present paper, as was previously done with reference to the molecules in their ground state by the present authors[9,10] and by Brown[11], the reactivites of excited molecules are assumed to be parallel with the π stabilization energy at the transition state due to the interaction of the molecule with the reagent (molecule, ion or radical) through the position of attack. Under this assumption the reactivity indexes are derived by the use of the molecular orbital method.

1) G. W. Wheland, *J. Am. Chem. Soc.*, **64**, 900 (1942).
2) C. A. Coulson and H. C. Longuet-Higgins, *Proc. Roy. Soc.*, **A191**, 39 (1947).
3) F. H. Burkitt, C. A. Coulson and H. C. Longuet-Higgins, *Trans. Faraday Soc.*, **47**, 553 (1951).
4) K. Fukui, T. Yonezawa and C. Nagata, This Bulletin, **27**, 423 (1954); *J. Chem. Phys.*, **27**, 1247 (1957).
5) K. Yagi, Z. Yoshida and T. Tabata, "Fluorescence", Nanko-do, Tokyo (1958); and references cited there.
6) M. Shimizu, "Symposium on Molecular Structure and Chemical Reaction", held in Nov. 1960, Tokyo, p. 149; and references cited there.
7) C. Sandorfy, *Compt. rend.*, **230**, 961 (1950).
8) V. A. Crawford and C. A. Coulson, *J. Chem. Soc.*, **1948**, 1990.
9) K. Fukui, K. Morokuma, T. Yonezawa and C. Nagata, *J. Chem. Phys.*, **32**, 1743 (1960).
10) T. Yonezawa, K. Hayashi, C. Nagata, S. Okamura and K. Fukui, *J. Polymer Sci.*, **14**, 312 (1954).
11) R. D. Brown, *J. Chem. Soc.*, **1959**, 2224.

Formulation and Comparison with Experiments

Reactions of an excited molecule with an unexcited molecule are classified into several cases from the point of view of the spin multiplicity of reactants. The assumptions, the formulations and general considerations of the present molecular orbital treatments leading to the theoretical measures of reactivity will be described rather circumstantially in the first few cases, and in other cases only the indexes of reactivity derived will be given.

Reaction of an Excited Triplet Molecule with an Unexcited Radical.—First of all, attention is paid to the reaction of an excited triplet molecule (^{3}A) with an unexcited radical (^{2}B), where the numbers on the left shoulder refer to the multiplicity of the molecules. Here it would be rational for practical purposes in treating photochemical reactions to assume that the molecule ^{3}A has only one excited electron. Then the wave functions of these molecules are written as follows:

$$\Psi(^3\mathrm{A}) = \boldsymbol{A}\left[\cdots(\phi_1\alpha)^{m-3}(\phi_1\beta)^{m-2}(\phi_{01})^{m-1}(\phi_{02})^{m} \times \begin{Bmatrix} \alpha(m-1)\alpha(m) \\ \beta(m-1)\beta(m) \\ (1/\sqrt{2})\{\alpha(m-1)\beta(m)+\beta(m-1)\alpha(m)\} \end{Bmatrix}\right] \quad (1)$$

$$\Psi(^2\mathrm{B}) = \boldsymbol{A}\left[\cdots(\phi_1\alpha)^{n-2}(\phi_1\beta)^{n-1}\begin{Bmatrix}(\phi_0\alpha)^n \\ (\phi_0\beta)^n\end{Bmatrix}\right]$$

where ϕ_i and ϕ_j are the molecular orbitals of molecules A and B, respectively, whose numbering is schematically shown in Fig. 1, 01 and 02 denoting the lower and the higher half-occupied levels, of A, respectively, and (0) denoting the half-occupied level of the radical B; m, an even integer, is the number of electrons of the molecule A and n, an odd number, is that of the radical B; $\boldsymbol{A}$ is the antisymmetrizing operator including the normalization constant; and each line in braces may constitute one wave function.

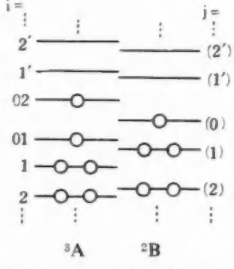

Fig. 1. Numbering of molecular orbitals.

The states of the total system consisting of the triplet A and the doublet B would be a quartet and a doublet. But the quartet, which would be proved later to be less significant in this discussion, is abandoned. The doublet wave function for $M_S=1/2$* is

$$^2\Psi_{1/2}[^2(\mathrm{AB})] \equiv \Psi[0] = \boldsymbol{A}[\cdots(\phi_1\alpha)^{m-3}(\phi_1\beta)^{m-2} \cdots(\phi_1\alpha)^{m+n-2}(\phi_1\beta)^{m+n-1}(\phi_{01})^{m-1}(\phi_{02})^{m} \times(\phi_0)^{m+n}\{(\alpha\beta+\beta\alpha)\alpha-2(\alpha\alpha)\beta\}/\sqrt{6}] \quad (2)$$

where, for example, $\alpha\beta\alpha$ means $\alpha(m-1)\beta(m)\alpha(m+n)$. That for $M_S=-1/2$ is not written because the energetical argument is similar. Thus the state $\Psi[0]$ is assumed to correspond to the initial system of the reaction in question. If A and B are far separated from each other, the energy of the state is the same as that of the product function $\Psi(^3\mathrm{A})\cdot\Psi(^2\mathrm{B})$. The molecular orbitals may include all π ones and σ ones, but in this paper we consider the reactions in company with only the π electron excitation, and hence σ orbitals will rationally be omitted as making an invariant framework.

At the transition state of the reaction the two molecules, ^{3}A and ^{2}B, will stay at a distance, making a weak interaction through the atoms at which the reaction takes place. This interaction is assumed to be a kind of $\pi-\pi$ conjugation and in this simple LCAO MO approach it will be represented by a small resonance integral $\gamma\beta$ between the atomic π orbitals r and s of the reactants, A and B, respectively, where β is the resonance integral of the C–C π bond in benzene. This perturbation makes the initial state $\Psi[0]$ come to the direct or indirect interaction with various electronic configurations of the combined system. Of these configurations only those, which have energy matrix elements with the initial state in scope of the simple LCAO MO approximation, are taken into account. This means that the configurations (of course, doublet and $M_S=1/2$) in which one electron transfers from ^{3}A to ^{2}B and vice versa have concern with the transition state of the reaction, whereas those which correspond to intramolecular one-electron transitions do not.

Under these assumptions the electron configurations to be taken into account are those corresponding to the following one-electron transfers, represented by $l\rightarrow m$, from an occupied or half-occupied orbital, l, to an unoccupied or half-occupied orbital, m:

$$\begin{aligned} &02\rightarrow(0),\ 02\rightarrow(j'),\ 01\rightarrow(0),\ 01\rightarrow(j') \\ &i\rightarrow(0),\ i\rightarrow(j'),\ (0)\rightarrow 01,\ (0)\rightarrow 02 \\ &(0)\rightarrow i',\ (j)\rightarrow 01,\ (j)\rightarrow 02,\ (j)\rightarrow i' \end{aligned} \quad (3)$$

* M_S denotes the eigenvalue of S_z, the z component of the spin momentum operator.

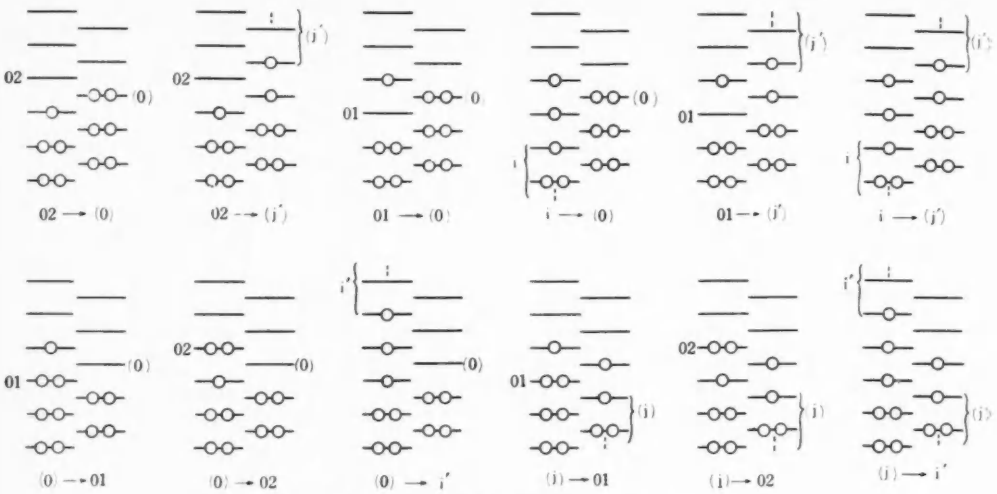

Fig. 2. Electronic configurations taken into account.

where

$i = 1, 2, \cdots$ (occupied orbitals of ^{3}A)

$i' = 1', 2', \cdots$ (unoccupied orbitals of ^{3}A)

$(j) = (1), (2), \cdots$ (occupied orbitals of ^{2}B)

$(j') = (1'), (2'), \cdots$ (unoccupied orbitals of ^{2}B)

They are schematically illustrated in Fig. 2. For an illustration, the configuration associated with the transfer $02 \rightarrow (0)$, will have the following wave function:

$$\Psi[02 \rightarrow (0)] = \boldsymbol{A}[\cdots(\phi_0\alpha)^{m+n-2}(\phi_0\beta)^{m+n-1}(\psi_0\alpha)^{m+n}] \quad (4)$$

The energy matrix element between these configurations and the initial state can be expressed in terms of the integral $\gamma\beta$. For example,

$$\left|\int \Psi^*[02 \rightarrow (0)]\, H\Psi(0)\mathrm{d}\tau\right| = |\, c_r^{02} d_s^{0} \gamma\beta \,| \quad (5)$$

where c_r^k and d_s^l are the coefficient of the atomic orbitals r and s in the molecular orbital k and l of the molecules A and B, respectively.

The transition state of the reaction is the lowest energy state resulting from the interaction mentioned above. The difference in π electronic energy, i. e. the stabilization energy, between the initial state and the transition state, was assumed in the preceding section to parallel the activation energy, of the reaction, and accordingly the reactivity of the excited molecule. This stabilization energy would be expanded in powers of γ by regarding it to be small. There arise three main subcases according to the mutual relation of the energy levels 01 and 02 of the molecule ^{3}A and (0) of the molecule ^{2}B*. In the following $Y_{k,l}$ denotes the energy in units of $(-\beta)$ turned out in one electron transfer from the molecular orbital k of the one molecule to the molecular orbital l of the other one. That is, $Y_{k,l}$ is positive if the level k is higher than the level l and vice veras. Thus we reach the final reactivity indexes of excited molecules.

(a) If $Y_{02,0} > Y_{0,01} > 0$, that is, if the half-occupied level of the molecule ^{2}B lies between the levels 01 and 02 of ^{3}A and is nearer to 01 than to 02, as is shown in Fig. 3 (a), the stabilization energy to the second order of γ is written in the following expression**:

$$\Delta E = \left[Y_{02,0} + \frac{(3/2)(c_r^{02})^2(d_s^0)^2}{Y_{02,0}}\gamma^2\right](-\beta) \quad (6)$$

From this formula some general conclusions on reactivities of excited molecules may be

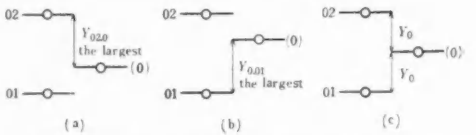

Fig. 3. Mutual relation of molecular levels.

* Some rare cases, for instance, $Y_{0,02} > 0$ or $Y_{01,0} > 0$, are not included for the sake of brevity.

** In general the stabilization energies for each M_S component may differ from each other. In the surroundings of reaction no magnetic field being applied, no specialization of the component is possible and the mean of all components would be significant as a real stabilization energy. In this case the energy for $M_S = 1/2$ is the same as that for $M_S = 1/2$; also the mean energy becomes the same.

TABLE I. RATE CONSTANT AND π STABILIZATION ENERGY OF POLYMERIZATION OF STYRENE

Reaction[a]	Rate constant[b] k (l. mol^{-1} sec^{-1})	π Stabilization energy (in units of $-\beta$)
R·+^{3}A→RA·	$\sim 10^{11}$	$0.414+0.801\gamma^2$ (position 9)
		$0.414+0.400\gamma^2$ (position 1)
		$0.414+0.200\gamma^2$ (position 2)
R·+A→RA·	3.4×10^2	$0.926\gamma^2$
R·+M→R·	1.2×10^2	$0.932\gamma^2$
RA·+M→R·	0.8	$0.739\gamma^2$

a) Abbreviations, R·: polymer radical of styrene; ^{3}A: triplet anthracene; A: anthracene; M: styrene.
b) Taken from Ref. 10.

derived. In most reactions between unexcited molecules, terms first appear in the second order of γ, whereas in Eq. 6 the term in zero order exists. The appearance of the zero order term is universal in all the following cases and subcases, making clear the reason why the reactions including excited molecules proceed so fast. The difference in reactivity of several excited molecules would thus dominantly be decided by this term. The intramolecular orientation, on the other hand, depends on the term in the second order. More minutely, so far as attention is paid to the lowest excitation of the molecule A as is expected in real photochemical reactions of conjugated molecules, the atom where $(c_r^{02})^2$, the frontier electron density for a nucleophilic attack in the ground state, is the greatest is the most reactive in an excited molecule. The coefficient (3/2) is characteristic to the triplet A molecule. If the molecule A is excited in the singlet state it amounts to (1/2), as will be mentioned in the next section. The difference would not necessarily mean the difference in reactivity of these two states, since the approximation is too simple to discuss at this point, on which there will be some discussion in a later section.

To the transition state the electron configuration corresponding to the one-electron transfer 02→(0) has the greatest contribution, since the other configurations have the first contribution to ΔE in the fourth order. Therefore, the direction of charge transfer is from molecule A to molecule B.

(b) If $Y_{0,01}>Y_{02,0}>0$, i.e., if the half-occupied level of ^{2}B lies between the levels 02 and 01, and nearer to 02 than to 01, as shown in Fig. 3 (b), then

$$\Delta E=\left[Y_{0,01}+\frac{(3/2)(c_r^{01})^2(d_s^0)^2}{Y_{0,01}}\gamma^2\right](-\beta) \quad (7)$$

In this subcase also the rate of reaction is great and the intramolecular orientation of the excited molecule is controlled by $(c_r^{01})^2$, the frontier electron density for an electrophilic attack in the ground state. The most contributive configuration in this subcase corresponds to the transition (0)→01, resulting in a charge transfer from B to A.

(c) If $Y_0\equiv Y_{02,0}=Y_{0,01}>0$, i.e., if the level (0) is just in the midst of the levels 01 and 02, as shown in Fig. 3 (c), then

$$\Delta E=\left[Y_0+\frac{(3/2)[(c_r^{01})^2+(c_r^{02})^2](d_s^0)^2}{Y_0}\gamma^2\right]\times(-\beta) \quad (8)$$

A large rate constant is confirmed also in this subcase, and $[(c_r^{01})^2+(c_r^{02})^2]$, the frontier electron density for a radical attack in the ground state, comes to the point.

So far as alternant hydrocarbons are concerned, however, the equality $(c_r^{01})^2=(c_r^{02})^2$ holds in the simple LCAO MO approximation, so that in all subcases and the following cases the most reactive position in a molecule in its lowest excited state is the same as that in the ground state. This explains the great reactivity of meso position of anthracene. Further experimental studies are anticipated with respect to the intramolecular orientation in nonalternant hydrocarbons and heterocyclic compounds where the equality mentioned above no more exists.

Here a comparison with experimental data may be given. Excited triplet anthracene was reported by Norrish et al.[12] to enter into the chain of polymerization of styrene in the following way:

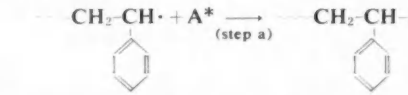

(9)

Observed rate constant, k_a, and calculated π stabilization energy ΔE are tabulated in Table I. The stabilization in the reaction a is calculated by using Eq. 8. Those of other reactions in which only molecules in their ground state participate are given by the usual formula for stabilization energy[10]:

12) V. S. Anderson and R. G. W. Norrish, *Proc. Roy. Soc.*, **A251**, 1 (1959); R. G. W. Norrish and J. P. Simons, ibid., **A251**, 4 (1959).

$$\Delta E=\left[\sum_{j}^{\text{unocc}}\sum_{i}^{\text{all}}\nu_i-\sum_{j}^{\text{occ}}\sum_{i}^{\text{all}}(2-\nu_i)\right]\times\underset{\gamma_{ji}}{(c_r{}^i)^2(d_s{}^j)^2}\gamma^2(-\beta) \qquad (10)$$

where ν_i is the number of electrons in the ith molecular orbital of A. The extraordinary great magnitude of rate constant of reaction a is well understood in connection with the presence of the zero order term. Further, the position 9 is the most active, at which anthracene would enter into the polymer chain. An appropriate choice of the value of γ ($=0.7$) makes the $\log k_a-\Delta E$ plots practically linear.

The wave functions (Eq. 1) of ^{3}A and ^{2}B may be combined so as to construct a quartet instead of the doublet (Eq. 2). The quartet state has matrix elements with some configurations in Eq. 3, only to give the stabilization energy in the second order. Because of the lack of the zero order terms and, accordingly, because of the instability of the transition state, reactions would not be considered to proceed by way of the quartet transition state.

Reaction of an Excited Singlet Molecule with an Unexcited Radical.—The reaction of an excited singlet molecule (^{1}A) with an unexcited radical (^{2}B) can be discussed in a way similar to that of a triplet molecule (^{3}A) mentioned in the preceding reaction. The doublet wave function for $M_S=1/2$ of the combined system is, in place of Eq. 2 in the triplet case,

$$\Psi[0]=\boldsymbol{A}[\cdots(\psi_{01})^{m+n-1}(\psi_{02})^{m}(\phi_0)^{m+n}\times\{(\alpha\beta-\beta\alpha)\alpha\}/\sqrt{2}] \qquad (11)$$

Also, we are led to the same equations as Eqs. 3, 4 and 5, excepting that the numerical coefficient in the second term should be read (1/2) in this case, instead of (3/2). The meanings of the frontier electron density and the direction of charge transfer in each subcase are entirely the same as in the last case; and therefore discussions may be omitted for brevity.

Reaction of an Excited Tripled Molecule with an Unexcited Molecule.—The reaction of an excited triplet molecule (^{3}A) with an unexcited singlet molecule (^{1}B)* now comes to our attention. Discussions are almost alike, so that the only important formulas would be summarized in this case and in the following case. The numbering of molecular orbitals is illustrated in Fig. 4. The states of the combined system at the initial stage of reaction are represented by a set of three triplet wave functions, one with $M_S=1$, one with $M_S=0$ and the other with $M_S=-1$, as follows:

* The singlet molecule ^{1}B may be an ion whose spin is singlet.

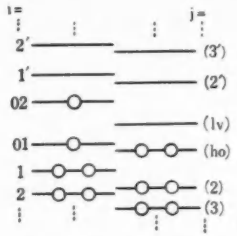

Fig. 4. Numbering of molecular orbitals. lv and ho mean the lowest unoccupied and the highest occupied orbitals, respectively.

$$\begin{aligned}
{}^3\Psi_1&=\boldsymbol{A}[\cdots(\psi_{01})^{m+n-1}(\psi_{02})^{m+n}\times\alpha(m+n-1)\alpha(m+n)]\\
{}^3\Psi_0&=\boldsymbol{A}[\cdots(\psi_{01})^{m+n-1}(\psi_{02})^{m+n}\times(\alpha(m+n-1)\beta(m+n)\\
&\quad+\beta(m+n-1)\alpha(m+n)\}/\sqrt{2}] \qquad (12)\\
{}^3\Psi_{-1}&=\boldsymbol{A}[\cdots(\psi_{01})^{m+n-1}(\psi_{02})^{m+n}\times\beta(m+n-1)\beta(m+n)]
\end{aligned}$$

Electronic configurations which are taken into account in the perturbation calculation are summarized in Fig. 5 with illustrations. Each M_S component of the functions 12 will have matrix elements with the same M_S component of the wave functions for the configurations

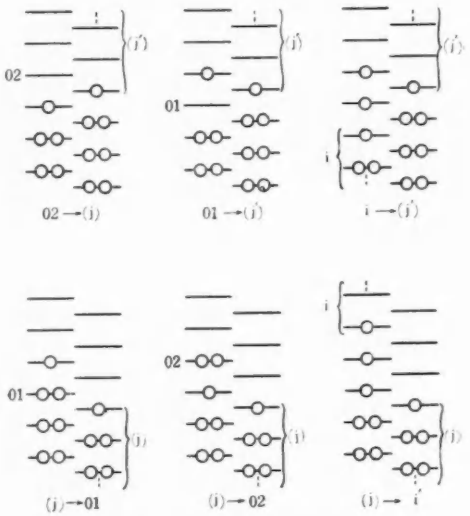

Fig. 5. Electronic configurations taken into account.
$i=1,2,\cdots$ (occupied orbitals of ^{3}A); $i'=1',2',\cdots$ (unoccupied orbitals of ^{3}A); $j=$ ho, 2, $\cdots$ (occupied orbitals of ^{1}B); and $j'=$lv, 2', $\cdots$ (unoccupied orbitals of ^{1}B).

TABLE II. π STABILIZATION ENERGY IN PHOTODIMERIZATION OF POLYACENES AND ACENAPHTHYLENE

Compound	Pairs of positions to react with	π Stabilization energy (in units of $-\beta$)
Anthracene	9-9, 10-10 (central)	0.547γ
	1-1, 4-4 (end)	0.273γ
Naphthacene	5-5, 12-12 (central)	0.417γ
	1-1, 4-4 (end)	0.159γ
Pentacene	6-6, 13-13 (central)	0.400γ
	5-5, 14-14	0.299γ
	1-1, 4-4 (end)	0.100γ
Acenaphthylene	1-1, 2-2	0.568γ
	5-5, 6-6	0.375γ

in Fig. 5. Then the stabilization energy* is obtained as follows, according to the mutual relation of energy levels:

(a) If $Y_{02,1v}$ is positive and the most positive of all Y's, then

$$\Delta E=\left[Y_{02,1v}+\frac{(c_r^{02})^2(d_s^{1v})^2\gamma^2}{Y_{02,1v}}\right](-\beta) \tag{13}$$

This is the case for most electrophilic reagents (cations) serving as ^{1}B.

(b) If $Y_{ho,01}$ is positive and the most positive of all Y's, then

$$\Delta E=\left[Y_{ho,01}+\frac{(c_r^{01})^2(d_s^{ho})^2\gamma^2}{Y_{ho,01}}\right](-\beta) \tag{14}$$

Most nucleophilic reagents (anions) as ^{1}B are included in this subcase.

(c) If $Y_{02,1v}=Y_{ho,01}$, and they are positive (then of course the most positive), then, putting them equal to Y_0,

$$\Delta E=\left[Y_0+\frac{\{(c_r^{02})^2(d_s^{1v})^2+(c_r^{01})^2(d_s^{ho})^2\}\gamma^2}{Y_0}\right]\times(-\beta) \tag{15}$$

Such a conjugated molecule as has its lowest excitation energy smaller than the excitation energy to the triplet of the molecule A would be classified in this subcase.

(d) If all Y's are negative, then

$$\Delta E=\left[\sum_j^{\text{unocc}}\sum_i^{\text{all}}\nu_i-\sum_j^{\text{occ}}\sum_i^{\text{all}}(2-\nu_i)\right]\frac{(c_r^i)^2(d_s^j)^2\gamma^2}{Y_{ji}}\times(-\beta) \tag{16}$$

In this subcase the stabilization energy begins in the second order terms, predicting a slow rate in the process of reaction.

(e) If $Y_{02,1v}=0$ and the others are negative, then

$$\Delta E=\left[|\ (c_r^{02})(d_s^{1v})\ |\gamma+\left\{\sum_j^{\text{unocc}}\sum_i^{\text{all}}\nu_i-\sum_j^{\text{occ}}\sum_i^{\text{all}}(2-\nu_i)\right\}'\frac{(c_r^i)^2(d_s^j)^2\gamma^2}{2Y_{ji}}\right](-\beta) \tag{17}$$

* Each M_S component gives the same stabilization energy, and the mean is, therefore, the same.

where the mark $'$ on the summation tells to omit the set $(j=1v,\ i=02)$.

(f) If $Y_{ho,01}=0$ and others are negative, then, similarly

$$\Delta E=\left[|\ (c_r^{01})(d_s^{ho})\ |\gamma+\left\{\sum_j^{\text{unocc}}\sum_i^{\text{all}}\nu_i-\sum_j^{\text{occ}}\sum_i^{\text{all}}(2-\nu_i)\right\}'\frac{(c_r^i)^2(d_s^j)^2\gamma^2}{2Y_{ji}}\right] \tag{18}$$

$'$ indicating the neglect of the set $(j=ho,\ i=01)$.

(g) If $Y_{02,1v}=Y_{ho,01}=0$ and others are negative, we obtain

$$\Delta E=\left[\sqrt{(c_r^{02})^2(d_s^{1v})^2+(c_r^{01})^2(d_s^{ho})^2}\gamma+\left\{\sum_j^{\text{unocc}}\sum_i^{\text{all}}\nu_i-\sum_j^{\text{occ}}\sum_i^{\text{all}}(2-\nu_i)\right\}'\times\frac{(c_r^i)^2(d_s^j)^2\gamma^2}{2Y_{ji}}\right](-\beta) \tag{19}$$

neglecting in the summation the sets $(j=ho,\ i=01)$ and $(j=1v,\ i=02)$. In the latter three subcases the stabilization is of the first order, and for the lowest excited molecule the frontier electron density controls a main part of the reactivity indexes. The subcase g includes reactions of an excited molecule with an unexcited molecule of the same kind.

The photodimerization of aromatic hydrocarbons has been considered to pass through the following mechanism:

$$A^*+A\underset{\text{(step b)}}{\longrightarrow}(AA^*)\underset{\text{(step c)}}{\longrightarrow}AA \tag{20}$$

Though the detail of the intermediate (AA*) is not clear, assuming the present type of complex for the transition state of step b, one can discuss the reactivity of this reaction as belonging to the subcase g. In Table II calculated values of the π stabilization energy are collected. In that table, reagents are assumed to make two weak bondings through two meso positions, as illustrated in Fig. 6; the assumption of one bonding would only need to divide the values by the factor 2.

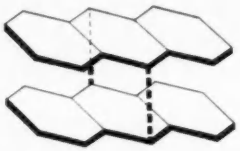

Fig. 6. Model of transition state of photodimerization of anthracene.

Anthracene is well known to make a photodimer at 9 and 10 positions, in accord with our calculation. Also in other polyacenes the most central meso-positions have the largest stabilization energy. This result is compatible with the experiment[13]. Bowen and Marsh[14] studied the photodimerization of acenaphthylene, finding that the structure of the photodimer was

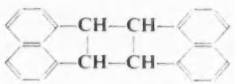

This finding was first theoretically discussed by Crawford and Coulson[8]. They calculated the free valence of this molecule in its lowest excited state and found that the values of positions 5 and 6 (0.62) are greater than those of positions 1 and 2 (0.57), which conflicted with the above experimental results. Thus they stated that the free valence is not a sufficient guide to reactivity. Recently this experiment has been interpreted successfully by the present authors in terms of the frontier electron density for a radical reaction[15]. The frontier electron density of positions 1 and 2 is greater than that of positions 5 and 6. In that paper the excited acenaphthylene was regarded as an ordinary radical reagent attacking an acenaphthylene molecule in the ground state. At this time it would be interesting to apply the present theory which involves an explicit consideration of the excitation. This belongs to the subcase g. As is seen in Table II the stabilization energy of the reaction through pairs of positions 1–1 and 2–2 is greater than that through 5–5 and 6–6, in accordance with the experiment.

In intermolecular comparison it is said that the ease of photodimerization is greater in pentacene than in anthracene[13]. But this is not a direct comparison of the rate constant k_b of the step b but a rough estimation from the amount of dimers produced. The total rate of dimer formation would be affected not only by the rate constant k_b but also by various competitive reactions such as the collisional or spontaneous degradation of the excited A molecule, dissociation of (AA*), and so forth. To measure and compare the rate constant with calculated stabilization energy would be interesting.

Reaction of an Excited Singlet Molecule with an Unexcited Molecule.—The method and the results of the treatment for this kind of reaction is exactly the same as that in the last case if only the wave function, Eq. 12, is replaced by the following equation:

$$^1\Psi_0 = \boldsymbol{A}[\cdots(\psi_{01})^{m+n-1}(\psi_{02})^{m+n}\{\alpha(m+n-1) \times \hat{\rho}(m+n) - \hat{\rho}(m+n-1)\alpha(m+n)\}/\sqrt{2}] \quad (21)$$

Eqs. 13 to 20 are also valid in this case.

Reaction of an Excited Molecule with Another Excited Molecule.—We derived also the equations giving the stabilization energy in a reaction of an excited molecule (singlet or triplet) with another excited molecule (singlet or triplet) in a similar way. But as they are less meaningful for practical purposes and rather intricate, we do not give their explicit forms. It would be noteworthy that in this case also the frontier electron densities decide the intramolecular orientation.

Discussion

We have derived formulas giving the π stabilization energy and the reactivity index, discussing the rate of reactions of excited molecules. But we do not, at all, regard this theory as complete but merely as a simple pioneering attempt in the molecular orbital method; the assumptions included may have to be subjected to some improvements in future. For discussing the difference in rate constant caused by the difference in multiplicity of states, interactions of electrons should be explicitly taken into account. For discussing various dissociation reactions, attention would have to be paid to σ electrons in the bond to be broken. Furthermore, in order to understand all the figures of reactions of an excited molecule, discussions on relations between various elementary steps involved in the reaction would be expected.

Faculty of Engineering
Kyoto University
Sakyo-ku, Kyoto

13) For example, M. Nakagawa, "Gendai Kagaku", III-D, Iwanami, Tokyo (1956); M. Koizumi and M. Shiba, ibid., I-E, (1956).
14) E. L. Bowen and J. D. F. Marsh, *J. Chem. Soc.*, **1947**, 109.
15) K. Fukui, T. Yonezawa and C. Nagata, This Bulletin, **34**, 37 (1961).

*Polarography of Narcotine-N-oxide**

By Yutaka ASAHI

(Received January 7, 1961)

It has been reported by Kirkpatrick[1] that narcotine, an opium alkaloid, shows a catalytic hydrogen wave as do the other alkaloids, and according to Holubeck[2], narcotine and hydrastin can be determined quantitatively with the the reduction wave of their oxidation product, opianic acid. It is known that *N*-oxides such as pyridine-*N*-oxide[3] and nitrogen mustard *N*-oxide[4] are reduced polarographically to the corresponding amines, but the polarography of narcotine-*N*-oxide has not been reported yet.

In this paper the polarographic determination of narcotine-*N*-oxide in the oxidation products of narcotine is attempted and further-more, the electrode reaction and behaviors of narcotine-*N*-oxide in aqueous solutions are examined by means of DC- and AC-polarography, electrocapillarity, potentiometric titration and ultraviolet absorption spectrometry. Narcotine-*N*-oxide shows 2-electron reduction waves of *N*-oxide, which are complicated by the adsorption on the electrode, the kinetic current of protonation and the reversible cleavage of lactone.

Experimental

The Yanagimoto pen-recording polarograph model PA 2, the Beckman pH meter model G and Beckman spectrophotometer model DU or DK 2 were used. The dropping mercury electrode has such characteristics as $m=0.817$ mg. sec^{-1}, $t=3.94$ sec., $m^{2/3}t^{1/6}=1.097$ and $h=70$ cm. Polarograms were taken in buffer solutions of acetate, phosphate,

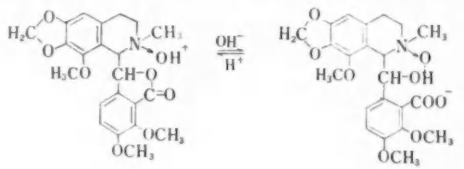

(I) (II)

borate, hydrochloric acid and sodium hydroxide at 25 ± 0.1°C after bubbling nitrogen gas, using N calomel electrode as the external reference electrode.

Narcotine hydrochloride and its *N*-oxide were given by Dr. H. Matsumaru of the Tokyo factory of our company.

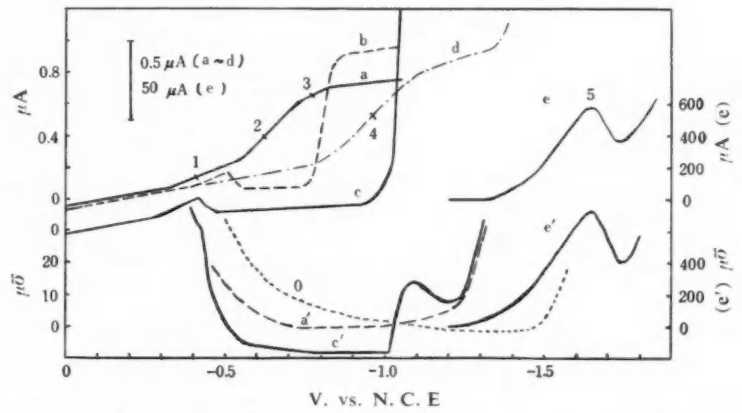

Fig. 1. D. C. (upper) and A. C. (lower) Polarograms of narcotine-*N*-oxide in pH 4. a, a, e, e', d: 0.2 mM, b: 0.3 mM, c, c': 1 mM, O: blank, d: hydroxycarboxylic acid form. 1~5: see Fig. 2.

* Polarographic studies of Pharmaceuticals. XXV. XXIV: *J. Pharm. Soc. Japan* (*Yakugaku Zasshi*), **80**, 1226 (1960).

1) H. F. W. Kirkpatrick, *Quart. J. Pharm. Pharmacol.*, **18**, 338 (1945).

2) J. Holubek, *Pharmazie*, **11**, 577 (1956).

3) A. Foffani and F. Fornasari, *Gazz. Chim. Ital.*, **83**, 1051, 1059 (1953).

4) I. Aiko, *Pharm. Bull.*, **1**, 335 (1953).

Results

Catalytic Hydrogen Wave. — Narcotin-*N*-oxide shows a great increase of current from about −1.2 V. and generally a maximum wave in a buffer solution of pH 1∼9. (Fig. 1e) The maximum wave height (i_m) is greatest at about pH 7 (Fig. 2 (5)) and tends to reach a limiting value at higher concentrations. The height (i_m) in a 0.2 mM solution of the *N*-oxide is supressed from 56 μamp. to 40 and 20 μamp. in the presence of 0.01 and 0.05% gelatin, respectively. The maximum potential (E_m), −1.4∼−2 V., becomes more negative in higher wave heights and higher concentrations: E_m −1.44 V., i_m 0.09 μamp. c 0.05 mM; E_m −1.55 V., i_m 7.6 μamp., c 0.2 mM; E_m −1.70 V., i_m 38.2 μamp., c 0.6 mM at pH 9.2. The temperature coefficient of i_m, 8% deg.$^{-1}$, is very high. The height decreases with the increase of mercury head (h): i_m in a 0.1 mM solution of pH 9.2 is 1.62, 1.19 and 0.89 μamp. at 48, 68 and 88 cm. of h respectively.

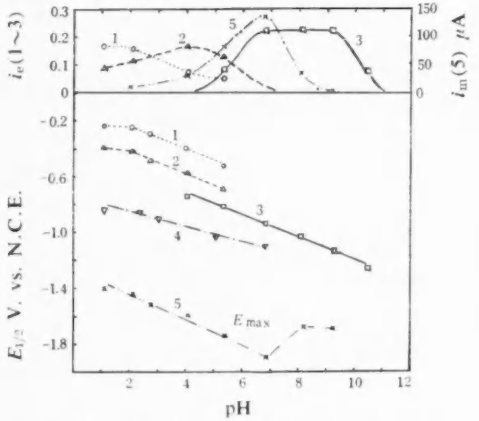

Fig. 2. $E_{1/2}$-pH curves (lower) and wave height-pH curves of narcotine-*N*-oxide (0.1 mM).
1) Absorption wave, 2) Reduction wave of cation, 3) Reduction wave of free base, 4) Reduction wave of hydroxy-carboxylic acid form, 5) Catalytic hydrogen wave.

Reduction Wave of Lactone type Narcotine-*N*-oxide (I). — 0.1 mM narcotine-*N*-oxide hydrochloride in a buffer solution of pH 1∼10 shows 1∼3 steps of reduction waves at the potential more positive than that of the catalytic hydrogen wave (Fig. 1a). The total wave height is independent of pH in a range of 1∼9, but decreases at above pH 9 (Fig. 2 (1∼3)). In 0.1 N hydrochloric acid, the total wave height (i_d) of 3 steps is proportional to the concentration (c) in a range of 0.1∼1 mM and the diffusion current constant (k_D) is calculated as 2.3 (μamp. mM^{-1} mg$^{-2/3}$ sec$^{1/2}$).

Their 1st step is considered as an adsorption wave since the relationships between the wave height (i_1) and the concentration (c) fulfil the equation $i_1 = a \cdot b \cdot c/(1+b \cdot c)$ with $a = 1.25$ $b = 2.67$ mM^{-1}.

In acetate buffer of pH 4, 3 steps of reduction waves are also obtained in low concentration (0.05∼0.23 mM), but in higher concentration (0.24∼1 mM) an anomalous minimum wave in some potential range is obtained (Fig. 1, b, c). Thus the current is strongly suppressed in the potential range of −0.42∼−1.04 V. at 1 mM and −0.6∼−0.7 V. at 0.24 mM. The limiting current at −1.1 V. corrected for the residual current is, however, proportional to the concentration.

At pH 6.8∼9.2, one reduction wave is observed near a catalytic hydrogen wave. Since the wave height tends to a limiting value (0.3 μamp.) at higher concentration (0.05∼0.6 mM) and its temperature coefficient is small (0.4% deg^{-1}), this wave is assumed to be an adsorption wave.

When the pH value increases from 4 to 7, the wave heights of the 1st and the 2nd steps decrease and that of the 3rd step increases (Fig. 2). The apparent pK of I is assumed to be 5.6 from the pH in which the 1st and 2nd wave height is equal to the 3rd one.

$E_{1/2}$-pH curves can be shown by the equation $E_{1/2} = E_0 + a$ pH, where E_0 are −0.08, −0.26 and −0.30 V. for 1st, 2nd and 3rd waves, respectively and a is about −0.08 V. (Fig. 2).

The slope of the reduction wave of narcotine-*N*-oxide at −0.2∼−0.9 V. in 0.25 mM solution of pH 3.7, becomes steep and the foot of the wave shifts toward the negative side in the presence of 0.1∼2 mM narcotine. The potential range of the anomalous wave observed at −0.47∼−0.89 V. in 0.5 mM at pH 4.1 becomes more negative and less wide (−0.63∼−0.92V.) in the presence of 2 mM narcotine. In both cases the total wave height is also proportional to the concentration of the *N*-oxide and is not altered with narcotine. Similar phenomena are observed in the coexistence of 0.01∼0.02% gelatin and 0.2∼1 mM the *N*-oxide.

Change of Polarograms of Narcotine-*N*-oxide by Alkali and Acid. — The reduction wave of narcotine-*N*-oxide hydrochloride (I) disappears gradually in alkali. From the current-time curve at a fixed potential, the reaction is estimated to be of the 1st order. Its velocity constant (k_1) is proportional to [OH$^-$] ion concentration. The reaction product II gives no wave above pH 9 but a reduction wave at more negative potential than that of I at pH

1~7 (Fig. 1d) and reverse to the original one I by acid. The velocity constant (k_2) of the reverse reaction is proportional to [H^+] ion concentration (Fig. 3).

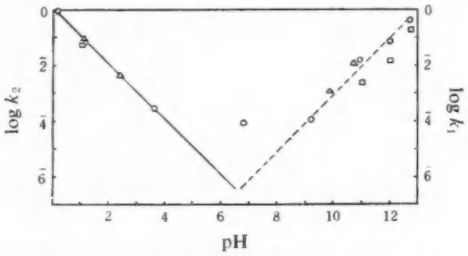

Fig. 3. Relationships between pH and reaction velocity constant of cleavage of the lactone (k_1) and of its formation (k_2) of narcotine (□) or its *N*-oxide (○, △) observed by reduction wave height (△) or $\varepsilon_{313m\mu}$ (○, □) at 25°C.

Change of Ultraviolet Absorption Spectra of Narcotine and its *N*-oxide by Alkali and Acid.—Narcotine hydrochloride gives a peak with λ_{max} 313 mμ (ε 4000) and a shoulder at 290 mμ in 20% ethanol solution (pH 5). The spectra change gradually to λ_{max} 282 mμ (ε 3200) in alkali.

Narcotine-*N*-oxide gives λ_{max} 313 mμ (ε 4000) and shoulders at 290 and 240 mμ in acid, and λ_{max} 278 mμ (ε 2800) in alkali. These changes occur reversibly and in measurable speed. The velocity constant of the 1st order reaction observed by absorbance at 313 mμ is proportional to [OH^-] in alkali and [H^+] in acid, and is in good agreement with that obtained by polarography (Fig. 3).

A. C. Polarography.—0.2 mM Narcotine-*N*-oxide in a buffer solution of pH 4 gives a large A. C. Polarogram (i_p 710 $\mu\bar{a}$) at the potential E_p −1.67 V. corresponding to the catalytic hydrogen wave but no wave at the potential of reduction of *N*-oxide. At higher concentration (1 mM) in the same buffer, the A. C. polarogram is suppressed in the potential range −0.5~−1 V. as D. C. polarogram.

Electrocapillary Curve.—The relationships between the applied potential and drop time of the mercury electrode in an acetate buffer of pH 4 is shown in the electrocapillary curve with a maximum at −0.6 V. (Fig. 4 ——). In the presence of 0.2 mM narcotine-*N*-oxide, the surface tension of the electrode is suppressed at −0.2~−1.4 V. and the curve extends to negative at −1.5~−1.7 V. because of the ohmic drop with the large catalytic current (Fig. 4------).

Potentiometric Titration.—Titration of 1 cc. of 10 mM narcotine-*N*-oxide·HCl with 0.1 cc. of

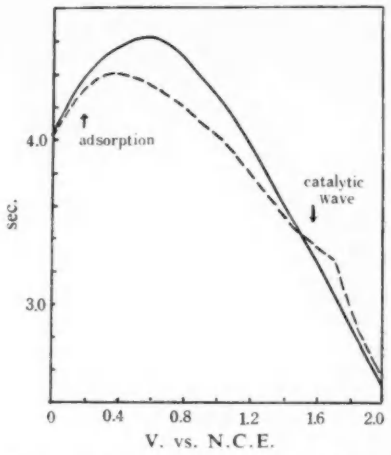

Fig. 4. Electrocapillary curves of acetate buffer (pH 4, ——) and with 0.2 mM narcotine-*N*-oxide (------).

0.1 N sodium hydroxide at 25°C reveals it to be an acid of pK 3.75. After an alkaline (5 mM the *N*-oxide, 0.02 N sodium hydroxide, 10 cc.) is heated at 100°C for 5 min., two acid groups of pK 6.0 and below 3 are observed by titration with 0.1 N hydrochloric acid or sodium hydroxide in nitrogen atmosphere and the product shows an absorption maximum at 280 mμ. When the solution of pH 2.7 is heated at 100°C for 30 min., an acid group of pK 3.7 and an absorption maximum at 313 mμ is obtained again. This alternation is ascribed to the reversible cleavage of the lactone. A similar phenomenon is also observed in narcotine, where the lactone type gives pK 6.1 and the hydroxycarboxyl type gives pK 9.4 and below 3.5 in 50% ethanol solution.

Discussion

The maximum wave of narcotine-*N*-oxide at about −1.4~−2 V. is considered to be a catalytic hydrogen wave as narcotine and other alkaloids. This is useful for a microdetermination of pure alkaloid because of its high sensitivity, but can not be used for the specific determination of each alkaloid.

The reduction wave of narcotine-*N*-oxide must be due to the *N*-oxide group as this wave is not observed in narcotine. The total wave height of the *N*-oxide in acetate buffer solution of pH about 4 can be utilized for its determination in the mixture of alkaloids. Applying Ilkovič's equation, $k_D = 607\ nD^{1/2} = i_d \cdot c^{-1} m^{-2/3} t^{-1/6}$, with $k_D = 2.3$ at pH 1~9 and $D = 4.1 \cdot 10^{-6}$ (cm^2 sec^{-1}) which is estimated from the molecular weight, $n = 1.88 \fallingdotseq 2$ is obtained.

As the wave is very flat and no A.C. polarogram is obtained at the corresponding potential, the electrode process may be irreversible. In strong acid solutions, narcotine (pK 6.1) and its N-oxide (pK 3.75) exist as proton adducts with lactone moiety I. Then the 1st and 2nd steps at pH 1~5 are assumed to be due to the following reaction.

$$\left(\rightarrow N-\!\!\rightarrow O\right)H^+ + 2e + 2H^+ \longrightarrow \rightarrow NH^+ + H_2O$$

The fact that the apparent pK 5.6 obtained from the wave height-pH curves is greater than pK 3.75, is explained by the kinetic current due to the protonation of the base on the electrode. The 3rd wave at pH 5~10 may be ascribed to the reduction of the N-oxide base to narcotine.

$$\rightarrow N-\!\!\rightarrow O + 2e + 2H^+ \longrightarrow \rightarrow N + H_2O$$

It is clear from the hysteresis of potentiometric titration curve and ultraviolet absorption spectra in acid and alkali that narcotine and its N-oxide change reversibly from lactone types I in acid to hydroxy-carboxylate types II in alkali. Because of this reaction, the wave height of the 3rd step decreases at pH above 10. The N-oxide with a hydroxy-carboxylate group II give more negative $E_{1/2}$ than that of lactone type I, perhaps because the N-oxide is stabilized by the formation of hydrogen bond $\left(\rightarrow N-\!\!\rightarrow O\cdots HO-\right)$.

The 1st step of the N-oxide with lactone ring has the character of an adsorption wave and disappears in the presence of narcotine or gelatin. Moreover the fact that the surface tension of the mercury electrode is suppressed in more negative potential than the 1st wave, confirms the adsorption of the reduction product, narcotine, on the electrode surface. Applying Brdička's equation[5], $z = i_a t / nF\Delta q$, with $i_a = 0.3\,\mu$amp. (pH 9.2), $t = 3.94$ sec. and $\Delta q = 0.85\ (mt)^{2/3} = 0.0185\,cm^2$, the maximum number of adsorbed molecule (z) is estimated to be 3.3×10^{-10} mol. cm^{-2} and the cross-sectional area of a narcotine molecule on the electrode surface (A) is calculated as 50 Å^2. From $i_a = 1.25\,\mu$amp. in 0.1 N hydrochloric acid, A is estimated to be 12 Å^2. These values are comparable to the minimum cross-sectional area of a molecule packing closely on the mercury surface.

The curious polarograms in higher concentration at pH about 4 are ascrided to the inactivation of the mercury electrode by the adsorption layer.

5) R. Brdička: *Z. Elektrochem.*, **48**, 778 (1942).

Summary

Narcotine-N-oxide shows a catalytic hydrogen wave as narcotine and other alkaloids. The reduction waves of narcotine-N-oxide are ascribed to the 2-electron reduction of the N-oxide to narcotine. Their 1st step is an adsorption wave of the reductant. The adsorped film disturbs the further electrode reaction, an anomalous minimum wave is observed in higher concentration. The 2nd step in pH 1~5 corresponds to the proton adduct of the N-oxide with lactone and the 3rd step in pH 5~10 to the base of the N-oxide.

Narcotine and its N-oxide change reversibly to hydroxycarboxylate type in alkali, which gives more negative reduction potential of the N-oxide and an absorption maximum in shorter wavelength. The velocity constants of cleavage of the lactone and of the reverse reaction are proportional to $[OH^-]$ and $[H^+]$, respectively.

The author express his sincre thanks to Dr. S. Kuwada, Dr. A. Watanabe and Dr. T. Kanzawa of this laboratory.

Research Laboratories
Takeda Pharmaceutical
Industries, Ltd.
Higashiyodogawa-ku, Osaka

A Novel Synthetic Route of 3,6-Dimethyl-2,3-dihydro-1H-cyclopent-[a]anthracene and 6-Methyl-2,3-dihydro-1H-cyclopent[a]anthracene

By Masao NAKAZAKI, Kikuo YAMAGAMI and Sachihiko ISOE

(Received December 26, 1960)

Tsuda and coworkers[1] reported the isolation of a hydrocarbon ($C_{19}H_{18}$, oil, melting point of the picrate, 133~134°C) among the products of selenium dehydrogenation of the phenol II which they obtained by the dienone-phenol rearrangement of 7-keto-5,8(9)-cholestadien-3β-yl acetate. The same compound was isolated by them[2] from the selenium dehydrogenation products of the anthrasteroid III from 5,8(9)-cholestadien-3β-ol.

Starting from 1-methyl-2-naphthoic acid (IV) we[3] succeeded in preparing 3,6-dimethyl-2,3-dihydro-1*H*-cyclopent[*a*]anthracene (I). This structure I was assigned by Tsuda and coworkers to their dehydrogenation product, but the comparison of the ultraviolet absorption spectra of synthetic I and the dehydrogenation product indicated that the latter was considerably contaminated with non-anthranoid impurities. Having established the structure of anthracholestatetraene, proposed by Mosettig[4], by an excellent method[5], Burgstahler and Mosettig[6] prepared *dl*-5,7,9,14-anthratetraen-17-one (V) to study a possible general synthetic route to anthrasteroids as well as to examine their carcinogenic properties. Sodium borohydride reduction of ketone V afforded alcohol VI, but the dehydrogenation which was expected to be accompanied by the migration of the 18-methyl group to 17-position to give I was found fruitless[7].

Since 3,6-dimethyl-2,3-dihydro-1*H*-cyclopent-[*a*]anthracene (I) is an analog of Diel's hydrocarbon usually obtained by the dehydrogenation of steroids, and since we happened to need a considerable amount of it for biological experiments, we explored a simpler route to compound I. In the present paper a new synthetic route to compound I and its nor-compound XIIIb is described.

Our synthesis, shown in Fig. 1, employs the

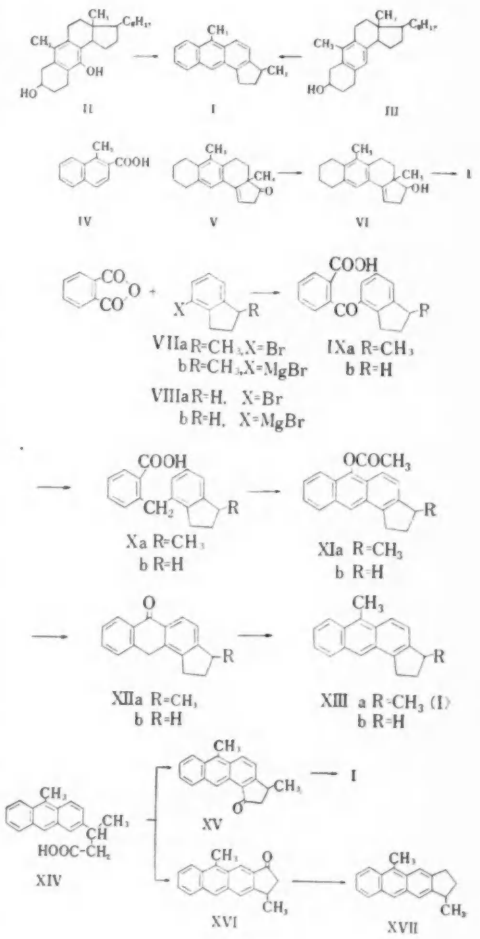

Fig. 1

method developed by Fieser and Hershberg[8] for the general synthesis of 9-alkylanthracene derivatives. Since the syntheses of I and XIIIb are similar, that of I is described at length. 4-Bromo-1-methylindan (VIIa), our starting substance, had been obtained by Hoyes[9] by

1) K. Tsuda, K. Arima and R. Hayatsu, *J. Am. Chem. Soc.*, **76**, 2933 (1954).
2) K. Tsuda and R. Hayatsu, ibid., **77**, 3089 (1955).
3) M. Nakazaki and S. Isoe., *Chem. & Ind.*, **1958**, 43; This Bulletin, **32**, 1202 (1959).
4) See Ref. 8 in our paper[3].
5) A. W. Burgstahler, *J. Am. Chem. Soc.*, **79**, 6047 (1957).
6) A. W. Burgstahler and E. Mosettig, ibid., **81**, 3697 (1959).
7) Private communication from Dr. Mosettig, National Institutes of Health, Bethesda, Maryland, U.S.A.
8) L. F. Fieser and E. B. Hershberg, *J. Am. Chem. Soc.*, **59**, 2331 (1937); **60**, 940 (1938).
9) H. Hoyes, *J. prakt. Chem.*, **139**, 242 (194).

reduction with hydriodic acid and phosphorus of 4-bromo-1-hydroxy-1-methylindan (b. p. 135~136°C/25 mmHg, m. p. 33~34°C), prepared from 4-bromo-1-indanone and methylmagnesium bromide. When we carried out the reaction of methylmagnesium bromide with the bromoketone, we obtained unsaturated 7-bromo-3-methylindene (b. p. 137~139°C/19 mmHg) which did not show an OH band in infrared spectrum but could be hydrogenated in a good yield to saturated 4-bromo-1-methylindan (VIIa) (b. p. 75~77°C/1.5 mmHg) in the presence of platinum oxide.

Although Kon and Woolman[10] observed that 4-bromoindan (VIIIa) could be converted with difficulty into a Grignard complex even under the condition elaborated by Fieser and Hershberg[5], bromide VIIa could be made to react smoothly with magnesium to afford Grignard compound VIIb, which gave 2-(1-methylindan-4-carbonyl)benzoic acid (IXa) (m. p. 123.5~124.4°C) with phthalic anhydride. The conversion into 2-(1-methylindan-4-ylmethyl)-benzoic acid (Xa) (m. p. 126~127°C) was effected by the high pressure catalytic hydrogenation with a copper chromite catalyst.

Heating with zinc chloride in acetic anhydride and acetic acid accomplished the ring closure of acid Xa to 6-acetoxy-3-methyl-2, 3-dihydro-1*H*-cyclopenta[*a*]anthracene (XIa) (m. p. 161~161.5°C), which, because of its instability toward acid and alkali, was hydrolyzed indirectly according to Fieser and Hershberg's method[5].

The reaction of methylmagnesium bromide with acetate XIa provided 3-methyl-6-oxo-2, 3, 6, 11-tetrahydro-1*H*-cyclopent[*a*]anthracene (XIIa) (m. p. 99~100°C), accompanied by a high melting compound (m. p. 221~223°C). The latter, in spite of its sparing solubility in benzene, always appeared in the mother liquor of recrystallization of even the purest sample of anthrone XIIa from benzene. From this behavior, together with other evidences (molecular weight, ultraviolet spectrum and infrared spectrum) it appears that the substance is a condensation product from two anthrone molecules, analogous to the high melting products obtained by Fieser and Hershberg[5] in their synthesis of 10-isopropyl-1′, 2′, 3′, 4′-tetrahydro-1, 2-benzanthracene.

The product from the Grignard reaction of anthrone XIIa with methylmagnesium bromide was decomposed with an acid and extraction with ether gave a highly blue-green fluorescent oil, which was purified by chromatography on alumina to afford pale yellow needles, m. p. 80.5~81°C. The substance was identified with 3,6-dimethyl-2,3-dihydro-1*H*-cyclopent[*a*]anthracene (I) prepared previously[3] by mixed melting point determination, comparison of infrared and ultraviolet spectra and mixed melting point determination of the trinitrobenzene complex.

In our previous synthesis of I, there remained a question whether the ring closure of acid XIV took place at 1-position to give XV or at 3-position to give XVI. Then, structure XVI was ruled out mainly on account of two observations, i. e. the 1-position of the anthracene nucleus is much more reactive toward electrophilic substitution, and the keto compound (XV) (m. p. 142~143.5°C) obtained showed a markedly similar ultraviolet spectrum with 1-acetylanthracene and exhibited an absorption at 12.2 μ in infrared spectrum which could be attributed to the presence of two adjacent hydrogen atoms in the anthracene nucleus[11]. The present synthesis with no such ambiguity can be taken as a support to the above view.

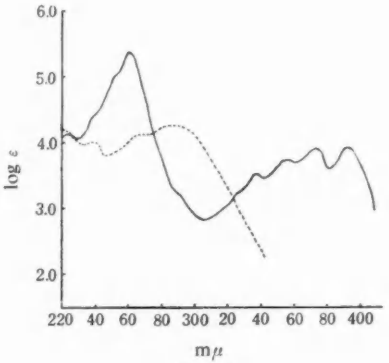

Fig. 2.

Solvent: 95% ethanol

TABLE I. ULTRAVIOLET ABSORPTION SPECTRA (in 95% ethanol)

I		XIIIb		XIa		XIb	
λ_{max}	log ε	λ_{max}	log ε	λ_{max}	log ε	λ_{max}	log ε
261	5.33	261	5.22	259	5.30	259	5.29
338	3.46	338	3.53				
354	3.73	354	3.79	353	3.81	356	3.40
372	3.90	372	3.95	371	3.95	375	3.55
392	3.89	392	3.95	391	3.94	396	3.55

10) G. A. Kon and A. M. Woolman *J. Chem. Soc.*, 1939, 796.

11) H. Dannenberg and D. D. Dannenberg, *Ann.*, 585, 1 (1954), see also W. West, "Chemical Applications of Spectroscopy", Interscience Pub. Inc., New York (1956), pp. 388—406.

The synthesis of 6-methyl-2,3-dihydro-1*H*-cyclopent[*a*]anthracene (XIIIb) was carried out in a way analogous to that described above, m. p. 127~128°C; melting point of the trinitrobenzene complex, 149.5~150.5°C; melting point of the picrate, 144~145°C, ultraviolet spectrum overlapping that of I (see Fig. 2 and Table I).

Experimental*

Ethyl *o*-Nitrocinnamate[12]. — Cinnamic acid was nitrated to give a mixture of *o*- and *p*-nitrocinnamic acids, which were esterified with ethanol and hydrogen chloride gas. From the mixture of ethyl *o*- and *p*-nitrocinnamates, the *o*-isomer was separated by virtue of its facile solution in m. p. 42°C, yield, 21.4%.

Hydrocarbostyril.—Ethyl *o*-nitrocinnamate (30 g.) was dissolved in 300 cc. of ethanol and hydrogenated in the presence of 4~5 g. of Raney nickel W-6 at 55~60°C and 47 atms. for 5~7 hr. Hydrocarbostyril was obtained in a yield of 79%, m. p. 163°C, (literature[13]: m. p. 165~166°C).

β-(2-Bromophenyl)propionic Acid (XVIII)[14].—*a. From Hydrocarbostyril*[15]. — A mixture of 30 g. of hydrocarbostyril, 97 g. of crystalline barium hydroxide and 400 cc. of water was refluxed for 20 hr. in a stream of nitrogen. The solution was diluted with 500 cc. of water and a stream of carbon dioxide was passed through it to precipitate barium carbonate.

After being freed from barium carbonate, the solution was made just alkaline to phenolphthalein with 10% sodium carbonate solution. The precipitated sodium salt, after being dried and washed with acetone, weighed 64.7 g. (yield, 84%), m. p. 155°C. A solution of 18.7 g. of this sodium salt and 6.9 g. of sodium nitrite in 100 cc. of water was added dropwise into 42 cc. of 48% hydrobromic acid chilled at 0~5°C in an ice bath. Cuprous bromide was precipitated by adding 6.3 g. of sodium sulfite to a mixture of 25 g. of cupric sulfate, 14.6 g. of sodium bromide and 100 cc. of water, and was dissolved by adding 6 cc. of 48% hydrobromic acid, and the solution was kept boiling. Onto this boiling solution, the above-mentioned diazonium bromide solution was added in four portions and the whole was refluxed for 30 min. The precipitated bromo acid was taken into ether, and the ethereal solution was washed with water and dried with anhydrous sodium sulfate. After removal of the solvent, the residue was recrystallized from aqueous acetic acid, m. p. 91~93°C, 5.6 g. The mother liquor was distilled and the fraction which boiled at 127~128°C/1 mmHg solidified on standing, m. p. 90°C, 1.2 g.

b. From o-Bromobenzyl Bromide.—*o*-Bromotoluene was brominated according to the procedure of Weizman and Patai[16], affording *o*-bromobenzyl bromide, m. p. 30°C (yield, 78%). To ethanolic sodium ethoxide prepared from 9.25 g. of sodium and 300 cc. of absolute ethanol, was added 28.5 g. of ethyl malonate and the mixture was heated for 15 min. on a water bath. After a solution of *o*-bromobenzyl bromide in 100 cc. of ethanol was added with stirring during 1 hr., the solution was stirred and refluxed for 3 hr.

The solvent was removed and the residue was diluted with ice water, and then concentrated hydrochloric acid was added to make the solution acidic to Congo red. After extraction with ether, the ether extract was washed with water and dried with anhydrous sodium sulfate. Removal of the solvent afforded a residue which was distilled to give ethyl *o*-bromobenzylmalonate boiling at 165~170°C/3 mmHg, 64.7 g. (yield, 82%)[10,14]. This malonate (64.5 g.) was hydrolyzed by boiling with 150 g. of potassium hydroxide, 175 cc. of ethanol and 300 cc. of water for 1 hr. After the ethanol was removed 250 cc. of concentrated hydrochloric acid was added to precipitate *o*-bromobenzylmalonic acid, which was collected and dried, 87 g. The malonic acid (87 g.) was decarboxylated by boiling with 400 cc. of water for 5 hr.

A heavy red oil which separated was extracted with ether and the ethereal solution was washed with water. After drying with anhydrous sodium sulfate, the solvent was removed to give β-(2-bromophenyl) propionic acid, m. p. 90°C. The yield was about 80% from the malonic ester.

4-Bromo-1-indanone (XIX).—Although Miersch[17] reported the formation of the bromoindanone XIX in a yield of 10% by the cyclization with concentrated sulfuric acid, XVIII did not give XIX with polyphosphoric acid[15] either under a rather mild condition (130°C, 20 min., recovery) or under a drastic condition (250°C, 20 min., polymerization). A mixture of 8.9 g. of crude XVIII and 15.6 g. of thionyl chloride was refluxed for 3 hr. After the excess of the thionyl chloride was removed, the residue, β-(2-bromophenyl)propionyl chloride, b. p. 120~123°C/2 mmHg, was dissolved in 240 cc. of carbon disulfide, and the solution was chilled at 5°C. To the stirred solution, 7.6 g. of aluminum chloride was added during 1.5 hr. After being allowed to stand at room temperature for 1.5 hr., the reaction mixture was refluxed for 15 min., and then a mixture of 100 cc. of concentrated hydrochloric acid and 300 cc. of water was added to decompose the reaction complex. The bromindanone was steam-distilled and recrystallized from ethanol, colorless needles, m. p. 95~96°C, (literature[15], m.p. 98~99°C), 6.2 g. (yield, 85%).

* All melting points are uncorrected. All ultraviolet spectra were measured with an EPS-2 Hitachi autorecording spectrophotometer and infrared spectra with a Perkin Elmer Model 12C. The analyses were performed in the microanalytical laboratory of the Institute of Polytechnics, Osaka City University.

12) L. Müller, *Ann.*, **212**, 124 (1882); L. Vanino, "Handbuch der Präparativen Chemie", Band II, Ferdinand Enke, Stuttgart (1937), p. 599.

13) E. R. Blout and D. C. Silverman, *J. Am. Chem. Soc.*, **66**, 1442 (1944).

14) For detailed discussion on the preparation of XVIII, see L. F. Fieser and A. M. Seligman, ibid., **57**, 2175 (1935).

15) F. Mayer, H. Phillips, F. W. Ruppert and A. T. Schmidt, *Ber.*, **61**, 1966 (1928).

16) M. Weizman and S. Patai, *J. Am. Chem. Soc.*, **68**, 151 (1946).

17) W. Miersch, *Ber.*, **25**, 2109 (1892).

18) F. D. Popp and W. E. Ewen, *Chem. Revs.*, **58**, 321 (1958).

4-Bromoindan (VIIIa)[10,14].—To a solution of 11.0 g. of XIX and 110 cc. of ethanol, 99 g. of amalgamated zinc was added with 70 cc. of concentrated hydrochloric acid. While the mixture was refluxed for 3 hr., 60 cc. of concentrated hydrochloric acid was added in three portions, and refluxing was further continued for 2 hr. The reaction mixture was diluted with water and, after the excess of zinc was removed, was extracted with ether. After drying with anhydrous sodium sulfate, the solvent was removed to give a liquid, which was distilled in vacuo, b. p. 75~77°C/2 mmHg, 8.7 g. (yield 85%), (literature, b. p. 118°C/18 mmHg[14], 100°C/1.5 mmHg[10]).

7-Bromo-3-methylindene (XX)[9].—Methyl bromide-gas was introduced into a stirred mixture of 6.1 g. of magnesium and 200 cc. of ether until the magnesium disappeared. To the Grignard reagent, a solution of 2.5 g. of XIX in 500 cc. of ether was added during 1 hr., and the mixture was refluxed for 2 hr. While the solution was cooled in an ice bath, a mixture of 100 cc. of concentrated hydrochloric acid and 500 cc. of ice water was added, and the solution was extracted with ether. After the extract was washed with water and dried with anhydrous sodium sulfate, the solvent was removed to give an oil, which was distilled in vacuo, b. p. 137~139°C/19 mmHg, 11.1 g. (yield, 45%).

4-Bromo-1-methylindan (VIIa).—To a solution of 11.1 g. of XX in 50 cc. of ethanol, 0.2 g. of platinum oxide was added and the mixture was shaken in an atmosphere of hydrogen. Hydrogen was absorbed rapidly, and after 2 hr. the solution was freed from the catalyst. Removal of the solvent gave an oil, which was distilled in vacuo, b. p. 75~77°C/1.5 mmHg, 9.4 g. (yield, 84%), (literature[9], b. p. 245°C).

2-(1-Methylindan-4-carbonyl)benzoic Acid (IXa).—When a mixture of 5 drops of ethyl iodide and 10 drops of VIIa was added to a stirred mixture of 2.16 g. of magnesium and 5 cc. of ether, ebullition of ether was observed to indicate the start of the Grignard reaction. With stirring and heating on a water bath, a solution of 9.4 g. of VIIa in 80 cc. of ether was added during 3 hr., and the mixture was refluxed for 15 hr. in an atmosphere of nitrogen.

The Grignard solution was transferred into a dropping funnel with the aid of the pressure of nitrogen from a tank; then the reaction flask was washed with 100 cc. of ether, and the washing was transferred again into the funnel.

To a solution of 11.4 g. of phthalic anhydride in 200 cc. of benzene, the above Grignard solution was added during 1.5 hr. with stirring and refluxing, and the mixture was stirred and refluxed for 2 hr. in an atmosphere of nitrogen. Dilute hydrochloric acid was added to decompose the Grignard complex, and the solution was steam-distilled. The precipitate which separated from the distillated was dissolved in 10% sodium carbonate solution, and the resulting solution was again steam-distille. The turbid solution was filtered through a layer of Hyflo and was made acidic with dilute hydrochloric acid to precipitate IXa, which was recrystallized from benzene, m. p. 114~120°C. Recrystallization from benzene-ligroin yielded pure carboxylic acid, m. p. 123.5~124.5°C, 4.5 g. (yield, 36%). IR spectrum: 5.95 and 6.0 μ.

Found: C, 77.15; H, 5.89. Calcd. for $C_{15}H_{16}O_3$: C, 77.12; H, 5.75%.

2-(1-Methylindan-4-ylmethyl)benzoic Acid (Xa).—A mixture of 3.5 g. of IXa and 140 cc. of ethanol was refluxed with a small amount of Raney nickel. The Raney nickel was filtered off, and the solution was hydrogenated with 0.5 g. of a copper chromite catalyst in a steel bomb at 149~155 atms. and 210~220°C for 4 hr. After the bluish green solution was freed from the catalyst, hydrogen sulfide was introduced to remove copper and chromium ions, and precipitated sulfides were filtered off through a layer of Hyflo. Removal of the solvent from the filtrate gave crystals, which were recrystallized from ethanol, m. p. 126~127°C, 3.2 g. IR spectrum: 5.9 μ.

6-Acetoxy-3-methyl-2,3-dihydro-1*H*-cyclopent[α]anthracene (XIa).—To a mixture of 3.2 g. of Xa, 30 cc. of acetic anhydride and 20 cc. of acetic acid, was added 0.27 g. of fused zinc chloride. After the brown mixture was refluxed for 1 hr., 50 cc. of water was added and the precipitated crystals were recrystallized from ethanol, m. p. 137~138°C, 2.5 g. (yield, 72%). IR spectrum: 5.7 μ. UV spectrum: see Table I.

Found: C, 82.87; H, 6.64. Calcd. for $C_{20}H_{18}O_2$: C, 82.73; H, 6.25%.

3-Methyl-6-oxo-2,3,6,11-tetrahydro-1*H*-cyclopent-[α]anthracene (XIIa).—To a Grignard reagent, prepared from 0.755 g. of magnesium, 30 cc. of ether and methyl bromide gas, 2.3 g. of XIa was added with 90 cc. of benzene. After the ether was removed, 90 cc. of benzene was added and the mixture was refluxed for 30 min. To the yellow solution, 100 cc. of diluted hydrochloric acid was added and the product was extracted with ether. After the ether extract was washed with water and dried with anhydrous sodium sulfate, the solvent was removed and the crystals were recrystallized from ethanol-ligroin, m. p. 86~93°C. For the preparation of an analytical sample, the product was recrystallized from methanol, m. p. 99~100°C.

Found: C, 86.11; H, 6.26. Calcd. for $C_{15}H_{16}O$: C, 87.06; H, 6.50%.

The mother liquor gave sparingly soluble crystals which were recrystallized from benzene-ethanol, m. p. 221~223°C.

3,6-Dimethyl-2,3-dihydro-1*H*-cyclopent[α]anthracene (I).—To the Grignard reagent, prepared from 0.252 g. of magnesium, 30 cc. of ether and methyl bromide, 427 mg. of XIIa was added with 50 cc. of benzene. After the ether was removed, the reaction mixture was refluxed on a water bath for 30 min. While the solution was chilled in an ice bath, 50 cc. of 2 N hydrochloric acid was added and the product was extracted with ether. The greenish blue fluorescent ether extract was washed with water and dried with anhydrous sodium sulfate. Removal of the solvent gave an oil which was chromatographed on 10 g. of alumina. Elution with benzine-benzene gave crystals which were recrystallized from methanol, pale yellow crystals, m. p. 80.5~81°C, 177 mg. (yield, 42%). The substance was found identical with I previously

prepared[3] by the comparison of the infrared spectra and the mixed melting point determination. UV spectrum: see Table I.

Found: C, 92.14; H, 7.60. Calcd. for $C_{19}H_{18}$: C, 92.63; H, 7.37%.

The trinitrobenzene complex was prepared from 35 mg. of I and 30 mg. of trinitrobenzene in benzene, and recrystallized twice from ethanol, reddish scarlet needles, m. p. 141.5~142°C. The mixed melting point determination (m. p. 140.5~142.5°C) confirmed the identity with the trinitrobenzene complex previously prepared[3] (m. p. 142~142.5°C).

Found: C, 65.37; H, 4.60; N, 9.15. Calcd. for $C_{25}H_{21}O_6N_3$: C, 65.35; H, 4.61; N, 9.15%.

2-(4-Indancarbonyl)benzoic Acid (IXb). — To a suspension of 2.05 g. of magnesium in 5 cc. of ether, was added a mixture of 2 drops of ethyl iodide and 10 drops of VIIIa to start the Grignard reaction. When ebullition of ether was observed, a mixture of 8.7 g. of VIIIa and 60 cc. of ether was added dropwise during 4 hr. After the solution was refluxed and stirred for 20 hr., the solution was transferred into a dropping funnel by means of the pressure of nitrogen from a tank, then the flask was washed with 100 cc. of ether and the washing was also transferred into the dropping funnel. To a solution of 11.3 g. of phthalic anhydride in 120 cc. of benzene, was added the above Grignard solution during 1.5 hr., and the mixture was refluxed for 30 min. A mixture of concentrated hydrochloric acid and 300 cc. of ice water was added to the reaction mixture and the whole was steam-distilled to remove volatile by-products. Ketoacid IXb was separated and dissolved in 150 cc. of a 10% sodium carbonate solution and the solution was steam-distilled for 2 hr. Fifty cubic centimeters of concentrated hydrochloric acid was added to the solution to give IXb, which was collected and recrystallized from benzene, m. p. 174~175°C. For the preparation of an analytical sample, the substance was recrystallized from benzene, m. p. 175~176°C, 6.8 g. (yield, 58%). IR spectrum: 6.01 and 5.94 μ.

Found: C, 76.29; H, 5.54. Calcd. for $C_{17}H_{14}O_3$: C, 76.67; H, 5.30%.

2-(4-Indanylmethyl)benzoic Acid (Xb).—A solution of 6.2 g. of IXb in 125 cc. of ethanol was refluxed with a small amount of Raney nickel. The solution, after the catalyst was filtered off, was hydrogenated in a steel bomb with 0.3 g. of a copper chromite catalyst at 199~202 atoms. and 215°C for 4 hr. The solution was separated from the catalyst and treated with hydrogen sulfide to remove copper and chromium ions as the sulfides. The solution was filtered through a layer of Hyflo and the filtrate was concentrated under reduced pressure to afford crystals, which were recrystallized from benzene, m. p. 146~146.5°C, 5.42 g. (yield, 72%). IR spectrum: 6.01 μ.

Found: C, 81.00; H, 6.24. Calcd. for $C_{17}H_{16}O_2$: C, 80.92; H, 6.39%.

6-Acetoxy-2, 3-dihydro-1*H*-cyclopent[*a*]anthracene (XIb).—To a mixture of 4.2 g. of Xb, 30 cc. of acetic acid and 20 cc. of acetic anhydride, was added 0.35 g. of zinc chloride and the solution was refluxed for 1 hr. To the brown solution, 200 cc. of water was added to precipitate a dark brown solid mass, which was continuously extracted with benzene to remove a brown insoluble by-product. The benzene extract was concentrated to afford yellow crystals, which were recrystallized from benzene, yellow prisms, m. p. 161~161.5°C, 3.4 g. (yield, 74%). IR spectrum: 5.70 and 12.35 μ. UV spectrum: see Fig. 1 and Table I.

Found: C, 82.69; H, 6.12. Calcd. for $C_{19}H_{16}O_2$: C, 82.58; H, 5.84%.

6-Oxo-2,3,6,11-tetrahydro-1*H*-cyclopent[*a*]anthracene (XIIb). — To the Grignard reagent, prepared from 1.15 g. of magnesium, 60 cc. of ether and methyl bromide, was added 3.4 g. of XIb in three portions, which was followed by 40 cc. of benzene and then the ether was distilled off. The yellow reaction complex was decomposed with 100 cc. of water, while the solution was chilled in an ice bath, and the product was extracted with ether. After the ether extract was washed with water and dried with anhydrous sodium sulfate, the solvent was removed to give crystals, m. p. 115~140°C, which were recrystallized from benzene, m. p. 160~163°C. For the preparation of an analytical sample, the substance was recrystallized from benzene, m. p. 165~166°C, 0.981 g. (yield, 34%). IR spectrum: 6.10 μ. UV spectrum: see Fig. 1.

Found: C, 86.68; H, 6.25. Calcd. for $C_{17}H_{14}O$: C, 87.15; H, 6.02%.

The mother liquor gave pale yellow needles, which were sparingly soluble in benzene, m. p. 222~223.5°C.

Found: C, 86.40; H, 5.63%.

6-Methyl-2,3-dihydro-1*H*-cyclopent[*a*]anthracene (XIIIb).—To the Grignard solution, prepared from 0.488 g. of magnesium, 30 cc. of ether and methyl bromide, was added 0.98 g. of XIIb, which was followed by 50 cc. of benzene. After the ether was distilled off, the benzene solution was refluxed for 30 min. After diluted hydrochloric acid was added to decompose the Grignard complex, the solution was extracted with ether. The bluish green fluorescent ether extract was washed with water and dried with anhydrous sodium sulfate. Removal of the solvent gave orange yellow needles, which were recrystallized from benzene to give pale yellow needles, m. p. 127~128°C. The mother liquor was concentrated and the residue was chromatographed on 10 g. of alumina affording an additional crop, with made the total yield of XIIIb 434 mg. (yield, 56%). UV spectrum: see Fig. 1 and Table I.

Found: C, 92.83; H, 6.85. Calcd. for $C_{19}H_{16}$: C, 93.06; H, 6.94%.

The trinitrobenzene complex was prepared from 20 mg. of XIIIb and 20 mg. of trinitrobenzene, and was recrystallized from ethanol, reddish scarlet needles, m. p. 149.5~150.5°C.

Found: C, 64.92; H, 4.35; N, 9.59. Calcd. for $C_{24}H_{19}O_6N_3$: C, 64.71; H, 4.30; N, 9.34%.

The picrate was recrystallized from benzene, brownish black needles, m. p. 144~145°C.

Found: C, 62.87; H, 4.19; N, 8.88. Calcd. for $C_{24}H_{19}O_7N_3$: C, 62.47; H, 4.15; N, 9.11%.

The authors are indebted to Mr. Yoshio Ota for his technical assistance, and also to

Mr. Eiichi Togashi, the Vice President of Shiono Koryo Kaisha, for a generous gift of cinnamic acid and to Kotobukiya Distillery and Nitto Kasei Co. for financial support.

Department of Chemistry
Institute of Polytechnics
Osaka City University
Kita-ku, Osaka

SHORT COMMUNICATIONS

Manganese(III) Complexes with Ethylenediaminetetraacetic Acid

By Yukichi Yoshino, Yoshikazu Tsunoda and Akira Ouchi

(Received June 1, 1961)

Although there have been some papers[1-3] on the analytical use of maganese(III) complexes with ethylenediaminetetraacetic acid (EDTA), little is known of the nature of the complex compounds. The authors had studied the critical condition of their formation in solution and could isolate the crystalline solid.

Three methods of the preparation of Mn-(III)-EDTA complexes from compounds of manganese in higher valency states have been examined. (1) Manganese dioxide suspended in water was mixed with solid ethylenediaminetetraacetic acid (H_4Y) under vigorous stirring. (2) In place of the free acid, a mixture of disodium salt of EDTA ($Na_2H_2Y \cdot 2H_2O$) and acetic acid was added to manganese dioxide. (3) Mn(II)-EDTA complex solution and manganese dioxide were mixed. Of these methods, the first was found to be the most suitable.

The relation between the mole ratio of manganese dioxide to EDTA and that of manganese dioxide to the produced Mn(III)-EDTA was shown in Fig. 1. Through the reaction a little of EDTA was lost and this may be due to its oxidation by manganese dioxide. However the mole ratio of Mn(III) to EDTA in the complex was approximately 1 : 1. Of course permanganate can also be used in place of manganese dioxide in all of these three methods.

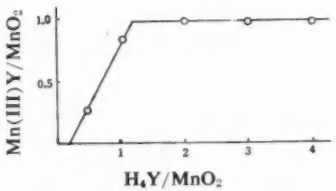

Fig. 1. Relation between the mole ratio of EDTA (H_4Y) : MnO_2 and the mole ratio of Mn(III)-EDTA : MnO_2 (MnO_2 : 2.69×10^{-4} mol.).

The general method used to prepare the solid complex was as follows: to manganese dioxide precipitated by reducing potassium permanganate with ethanol, EDTA (in the acid form) was added in a ratio of little less than 1 : 1. On vigorous stirring reaction took place, evolving carbon dioxide, and a deep red solution was obtained. Filtering off the excess manganese dioxide, an equal volume of cold ethanol was added to the filtrate. The solution was allowed to stand for 1~2 hr. Deep red crystals thus obtained were washed with 90% ethanol and then with ethyl ether. Finally it was dried in the air in cold dark place; yield: 45~55%.

The crystal is deep red in color and decomposes easily in the light or on heating, giving carbon dioxide. The decomposition rate seems to be increased by the presence of Mn-(II) ion. The oxidation equivalent of the complex was evaluted as 435±3 by iodometric titration. It is very soluble in water but insoluble in most of organic solvents. When a sample was heated with gradual elevation of temperature, 12~13% of weight loss took place at 25~130°C. This value may correspond to the sum of the weight of the water of crystallization and of EDTA partially decomposed. The remaining EDTA was completely

1) R. Přibil and J. Horacek, *Collection Czechoslov. Chem. Communs.*, **14**, 626 (1949).
2) R. Přibil and V. Sumon, ibid., **14**, 454 (1949).
3) R. Přibil and E. Hornychova, *Chem. Listy*, **40**, 101 (1950).

decomposed at 260~300°C. The solid gave the analysis: K, 9.50; Mn, 12.52; C, 28.56; H, 3.57; N, 6.53%. From these results the formula $K[Mn(EDTA)(OH_2)_2]\cdot H_2O$ was tentatively given as in the case of Cr(III)-EDTA complex[4].

Visible absorption spectra of the complex in acetic acid-sodium acetate buffer solutions of various pH were illustrated in Fig. 2. In the solution of pH 2.5~4.0 the maximum absorption was observed at 500 mμ, while in the higher pH region the color turned yellow and the maximum shifted to 450 mμ. By plotting the extinction against pH of the solution, the pK value between the red and the yellow species was evaluated as 5.3. It was also found that the red complex was strongly adsorbed on an anion-exchange resin in the chloride form. On titrating the complex with sodium hydroxide the curve in Fig. 3 was obtained. This curve has a single inflection at a neutralization point with approximately 1 mol. of sodium hydroxide per 1 mol. of the chelate. The pH of the half-neutralized solution is 5.5; which agrees fairly well with the pK value obtained from spectral data.

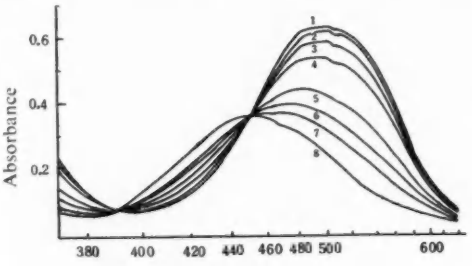

Fig. 2. The absorption spectra of Mn(III)-EDTA in CH_3COOH-CH_3COONa buffer solutions of various pH ($\mu=0.1$) (Mn(III): 9.34×10^{-4} mol./l.).

1: pH=2.50 2: pH=4.09 3: pH=4.54
4: pH=4.98 5: pH=5.40 6: pH=6.00
7: pH=6.28 8: pH=8.70

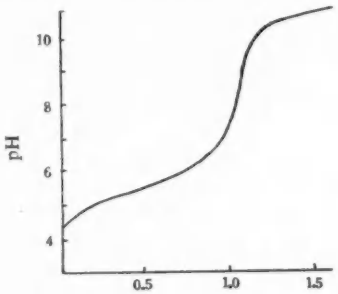

Fig. 3. Potentiometric titration of Mn(III)-EDTA with NaOH. (Concentration of Mn(III): 0.21×10^{-2} mol./50 ml., NaOH: 9.89×10^{-2} mol./l.).

4) C. Furlain, G. Morpurgo and C. Sartori, *Z. anorg. u. allgem. Chem.*, **303**, 1 (1960).

The authors thank to Dr. Masuo Kojima for the spectral measurements, to Mr. Shozo Masuda for the elementary analysis and to their colleagues in the laboratory for their helpful discussions.

College of General Education
The University of Tokyo
Meguro-ku, Tokyo

The Electron Spin Resonance Absorption of Vanadium Pentoxide Catalysts

By Kimio Tarama, Shiichiro Teranishi, Satohiro Yoshida and Hiroshi Yoshida

(Received June 2, 1961)

Kozyrev[1] and Pecherskaya et al.[2] studied the electron spin resonance (ESR) absorption of VO^{2+} in organic solvents at room temperature and observed that its spectrum consisted of eight hyperfine components, while Sands[3] reported the ESR absorption of V^{4+} ions in glass, and Faber et al.[4] observed the hyperfine structures of VO^{2+} ions on the ion exchangers. But no one has ever reported the ESR absorption of vanadium pentoxide.

The ESR method was used in order to study the magnetic properties of vanadium pentoxide and the binary system of vanadium pentoxide-potassium pyrosulfate.

Vanandium pentoxide was prepared by calcining ammonium metavanadate at 450°C, and vanadium pentoxide-potassium pyrosulfate

1) B. M. Kozyrev, *Discussions Faraday Soc.*, **19**, 135 (1955).
2) Y. I. Pecherskaya et al., International Congress on Catalysis, Paris, 1960.
3) R. H. Sands, *Phys. Rev.*, **99**, 1222 (1955).
4) R. Faber and M. Rogers, *J. Am. Chem. Soc.*, **81**, 1849 (1959).

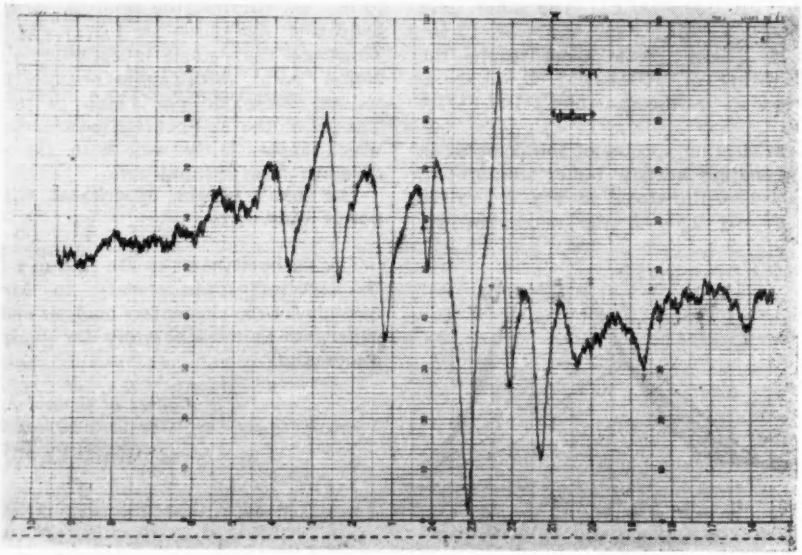

Fig. 1. ESR spectrum of the solid solution of vanadium pentoxide and potassium pyrosulfate.

samples were prepared by calcination of the mixture vanadium pentoxide and potassium pyrosulfate which contained vanadium pentoxide 10, 15, 25, 40, 50 and 70 mol. % respectively at 450°C, in closed glass vessels. Vanadium pentoxide-potassium pyrosulfate samples containing vanadium pentoxide less than 40 mol. % melted completely, and changed into amorphous substances of dark brownish color.

The spectrometer used in this research was of reflecting-type, and its resonance frequency was 9410 Mc. The observation were carried out at room temperature and also at liquid oxygen temperature.

In the case of vanadium pentoxide, an asymmetric ESR signal was observed and the *g*-value was 1.96. The line width ($\Delta Hmsl$) was 89 gauss at 16°C and 173 gauss at −183°C.

ESR signals of vanadium pentoxide-potassium pyrosulfate samples containing vanadium pentoxide less than 25 mol. %, showed the well-resolved hyperfine structures at room temperature. Fig. 1 shows the hyperfine structure of the sample consisting of vanadium pentoxide 15 mol. % and potassium pyrosulfate 85 mol. %. Eleven components are observed and its central eight components are stronger than the others.

In the case of the samples containing vanadium pentoxide more than 25 mol. %, the spectrum was not so well-resolved as Fig. 1.

The analysis of this spectrum according to Kozyrev's method shows that the *g*-value and the coupling constant for the central eight components are 1.98 and 98 gauss, and for the other three components are 1.92 and 320 gauss respectively.

The spectrum of vanadium pentoxide-potassium pyrosulfate is quite similar to that of VO^{2+} ions on the ion exchangers observed by Faber et al.[4] and this fact shows that the observed paramagnetic absorption results from VO^{2+} ions.

The authors wish to thank Professor Seizo Okamura, Kyoto University, for allowing one of the authors to use the ESR absorption apparatus.

Faculty of Engineering
Kyoto University
Sakyo-ku, Kyoto

Synthesis of D-*Threosamine and* D-*Erythrosamine*[1]

By Juji Yoshimura, Yoshiaki Ohgo and Tetsuo Sato

(Received June 27, 1961)

In the course of studies on the glycosylation of aminosugars[2], the requirement of a lower 2-aminosugar had arisen, so we attempted to synthesize 2-amino-D-tetroses. Recently, the synthesis of them was reported by Kuhn et al.[3], in which the hydrochlorides of D-threosamine and D-erythrosamine were obtained by catalytic half reduction of *N*-benzyl-D-tetrosaminonitriles (III_b and IV_b) prepared by acidic hydrolysis of corresponding acetone derivatives (I_b and II_b).

It prompts us to record further observations related to their work. To obtain *N*-substituted-D-tetrosaminonitriles (III and IV) two paths shown in Fig. 1 were examined. By treatment of D-glyceraldehyde[4] with amines (aniline, benzylamine and isopropylamine respectively) and hydrogen cyanide, *N*-phenyl-D-threosaminonitrile (IV_a), m. p. 114~116°C, $[\alpha]_D$ −247.2° (*c* 0.72, ethanol), Found: C, 62.38; H, 6.30; N, 14.5, Calcd. for $C_{10}H_{12}O_2N_2$: C, 62.48; H, 6.29; N, 14.58%, and *N*-isopropyl-D-erythrosaminonitrile (III_c), m. p. 103~104°C, $[\alpha]_D$ + 48.1° (*c* 0.21, methanol), Found: C, 53.43; H, 8.90; N, 17.48. Calcd. for $C_7H_{14}O_2N_2$: C, 53.14; H, 8.92; N, 17.71%, were obtained as colorless needles.

On the other hand, when acetone-D-glyceraldehyde[5] was treated in the same manner, two epimeric pairs of the corresponding acetone-aminonitriles (I_a, II_a, I_b and II_b) were separated in crystalline forms (acetone-*N*-phenyl-D-erythrosaminonitrile (I_a), m. p. 124°C, $[\alpha]_D$ +157.9° (*c* 0.69, methanol), yield 7.4%, Found: C, 66.30, H, 6.85; N, 12.06, Calcd. for $C_{13}H_{16}O_2N_2$: C, 67.22; H, 6.94; N, 12.06%, acetone-*N*-phenyl-D-threosaminonitrile (IIa), m. p. 100~102°C, $[\alpha]_D$ −149.4° (*c* 0.86, methanol), yield 30%, Found: C, 67.40; H, 7.04; N, 11.94. Calcd. for $C_{13}H_{16}O_2N_2$: C, 67.22; H, 6.94; N, 12.06%. The physical properties of *N*-benzyl derivatives, I_b and II_b, are entirely consistent with those of the substances reported by Kuhn et al.[3] respectively.

In addition to them, a trace of rhombic colorless crystal, m. p. 115~116°C, $[\alpha]_D$ +15° (*c* 0.77, methanol), having the same analytical values as the epimeric pair (Found: C, 67.06; H, 7.02; N, 11.92%) in the case of *N*-phenyl derivatives and a small amount of crystals corresponding to $C_{13}H_{18}O_4N_2$, m. p. 255~256°C, and $C_{16}H_{16}O_2N_2$, m. p. 216~218°C in the case of *N*-benzyl derivatives were obtained.

To prepare *N*-substituted D-tetrosaminonitriles the above acetone derivatives were subjected to hydrolysis in a mineral acid, to which *N*-benzyl derivatives (I_b and II_b) showed such an extraordinary resistance that it was impracticable to obtain hydrolyzates of I_b and II_b even in 2 N hydrochloric acid solution of 80% ethanol at room temperature for 24 hr., although Kuhn et al. carried out successfully by exsiccating the 2 N hydrochloric acid solution of I_b or II_b on phosphorus pentoxide at room temperature. *N*-Phenyl derivatives (I_a and II_a) changed gradually in their optical rotation in a 1 N mineral acid solution of 80% ethanol at room temperature [I_a: $[\alpha]_D$ +107° (5 min.)→ +156° (3 hr.)→+165° (22 hr. approximately const.), II_a: $[\alpha]_D$ −164° (3 min.)→−177° (1 hr.) →−220° (20 hr.)→−222° (41 hr.)→−228° (92 hr. const.)]. Colorless needles, m. p. 114~116°C, obtained from the reaction mixture of II_a, was agreed with IV_a described above.

The presumption whether these aminonitrile derivatives belong to the threo-type or the erythro-type was deduced from the general survey on their yields and their optical rotational data. In general, an epimer in which –NHR group has trans configuration to the hydroxyl gronp attached to the adjacent carbon precedes the cis isomer in their yield[6]. Moreover, the one having –NHR group on the right hand in the Fischer projection shows generally more positive optical rotation than the other, when they are measured in an inert solvent. This relationship seems to be closely akin to the acid-amide rule[7] in the sugar series. Fortunately, Kuhn et al. established the configurations of I_b and II_b by converting them into the configurationally known α-amino-β, γ-dihydroxybutyric acid[8], and the result coincides with the above mentioned presumption.

To obtain pure epimeric pair of aminosugars,

1) This work was presented at the 14th Annual Meeting of the Chemical Society of Japan, Tokyo, April, 1961.
2) J. Yoshimura, N. Muramatsu and T. Sato, *J. Chem. Soc. Japan, Pure Chem. Sec.* (*Nippon Kagaku Zasshi*), **79**, 1503 (1958); ibid., **80**, 1472 (1959).
3) R. Kuhn and H. Fischer, *Ann.*, **641**, 152 (1961).
4) E. Baer and H. O. L. Fischer, *J. Am. Chem. Soc.*, **61**, 761 (1939).
5) E. Bear and H. O. L. Fischer, *J. Biol. Chem.*, **128**, 463 (1939).
6) R. Kuhn, W. Bister and H. Fischer, *Ann.*, **617**, 109 (1958); ibid., **628**, 193 (1959).
7) C. S. Hudson and S. Komatsu, *J. Am. Chem. Soc.*, **40**, 813 (1918); ibid., **41**, 1141 (1919).
8) E. E. Hamel and E. P. Painter, ibid., **75**, 1362 (1953).

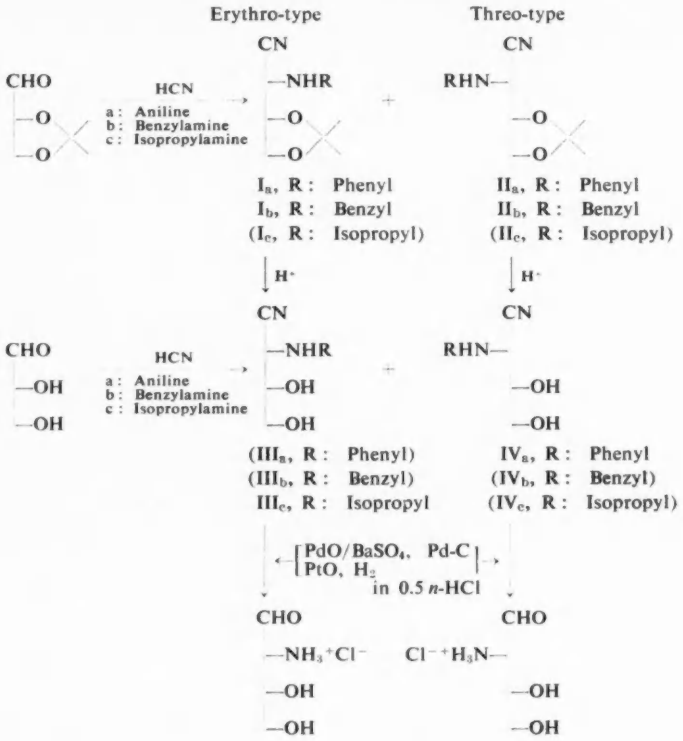

Fig. 1. Substances in parentheses could not be isolated as crystals.

N-phenyl-D-threosaminonitrile IV_a and *N*-phenyl-D-erythrosaminonitrile III_a which was derived by hydrolysis of I_a were subjected to catalytic half reduction in hydrochloric acid solution to afford D-threosamine hydrochloride and D-erythrosamine hydrochloride which showed the same behavior as depicted by Kuhn et al.[3]

The authors gratefully thank Mr. Hiroichi Ono for his help throughout this work and Dr. Asaji Kondo for microanalyses.

Laboratory of Organic Chemistry
Tokyo Institute of Technology
Meguro-ku, Tokyo

The Preparation of Carrier-free $^{234}Th(UX_1)$ by Anion Exchange from Nitric Acid-Alcohol Mixed Solution of Uranyl Nitrate

By Jun AKAISHI

(Received June 15, 1961)

The preparation of thorium-234 by solvent extraction[1-6] and ion exchange[7-10] from uranyl nitrate have been reported by many

1) O. Erbacher, W. Herr and M. Wiedmann, *Z. anorg. Chem.*, **252**, 282 (1944).
2) A. Norström and L. G. Sillén, *Svensk Kem. Tidskr.*, **60**, 227 (1948).
3) J. B. Th. Aten and F. Barendregt, *Physica*, **16**, 760 (1950).
4) G. A. Cowan, *US AEC Report*, LA-1721, 227 (1954).
5) L. Kosta, *J. Stefan Inst. Repts. (Ljubligna)*, **3**, 157 (1956).
6) R. Muxart, *Bull. soc. chim. France*, No. 5, 803 (1960).
7) D. Dyrssen, *Svensk Kem. Tidskr.*, **62**, 153 (1950).
8) B. G. Harvey, Brit. Pat. 704602 (1954).
9) R. Lumbroso and J. Petit, *Compt. rend.*, **243**, 145 (1956).
10) S. S. Berman, L. E. Mackinney and M. E. Bednas, *Talanta*, **4**, 153 (1960).

workers. In nitric acid medium, thorium-234 was separated by anion exchanger Amberlite IRA-400[11]. Recently, Korkisch et al.[12] reported that the adsorption of thorium onto anion-exchange resin is very strong, but that of uranium is rather weak, in a nitric acid-alcohol mixed solution.

The author studied the procedure of the preparation of carrier-free thorium-234 using an anion exchanger Dowex 1-X8. The preparation procedure is as follows. One gram of commercial reagent grade uranyl nitrate hexahydrate crystal was dissolved without further purification in 5~6 ml. of 0.2 N nitric acid-ethyl alcohol 80%, mixed solution*, and the solution was passed through Dowex 1-X8 resin column (100~200 mesh, 1.0 g., 0.70 cm^2 ×2.8 cm., pretreated with a few milliliters of the nitric acid-alcohol mixed solution) at a flow rate 0.7 ml. per min., and then the column was washed with 30~40 ml. of the nitric acid-alcohol mixed solution. The elution of thorium from the resin column could be attained with a small amount of 0.2 N nitric acid or water. When the elution was carried out with 0.2 N nitric acid, thorium was almost completely eluted with 4~5 column volumes of the nitric acid solution at a flow rate 1.0 ml. per min.

The result shown in Fig. 1 was obtained using the procedure described above. The activity measurement of the solution was as follows; an aliquot of the solution was transferred to a glass counting dish, and evaporated to dryness. The α and β activities were counted using a gas flow proportional counter and G-M counter respectively. In Fig. 2, decay curve of the eluate is shown.

The yield of thorium-234 from one gram of uranyl nitrate crystal was 4.6×10^5 d.p.m. (^{234}Th $+^{234}$Pa), and the radiochemical impurities were not observed by β and γ energy measurements.

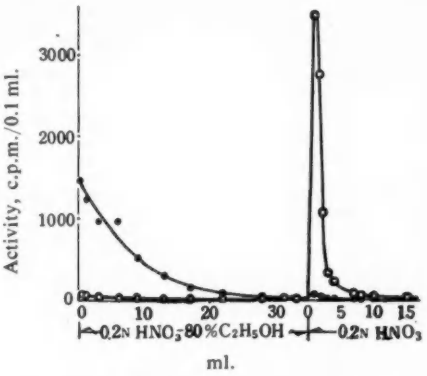

Fig. 1. Elution curve of thorium-234.
•—•: α-activity, ○—○: β-activity

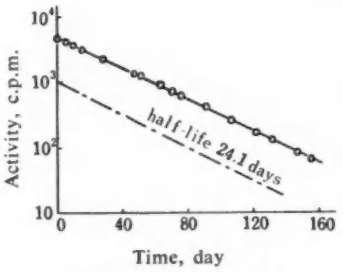

Fig. 2. Decay curve.

The author wishes to express his thanks to Mrs. Junko Iwamoto and Mr. Toshio Okamoto of the Division of Health Physics, JAERI for their kind assistance.

Japan Atomic Energy Research Institute
Tokai-mura, Ibaraki-ken

11) Y. M. Chen, *J. Chinese Chem. Soc.* (*Taiwan*), [2], **4**, 47 (1957).
12) F. Tera, J. Korkisch and F. Hecht, *J. Inorg. Nucl. Chem.*, **16**, 345 (1961).
* For example, 2 ml. 1 N HNO_3+8 ml. 99.5 vol. % C_2H_5OH.